CONJUGATION OF VANCOMYCIN AND ANTIBACTERIAL POLYMERS TO INVESTIGATE THE SYNERGISTIC ANTIBACTERIAL ACTIVITY

by
İlayda Acaroğlu Degitz

Submitted to Graduate School of Natural and Applied Sciences
in Partial Fulfillment of the Requirements
for the Degree of Doctor of Philosophy in
Chemical Engineering

Yeditepe University
2019

CONJUGATION OF VANCOMYCIN AND ANTIBACTERIAL POLYMERS TO INVESTIGATE THE SYNERGISTIC ANTIBACTERIAL ACTIVITY

APPROVED BY:

Prof. Dr. Seyda Malta .....
(Thesis Supervisor)
(Yeditepe University)

Prof. Dr. Tarık Eren .....
(Yıldız Technical University)

Assoc. Prof. Dr. Erde Can .....
(Yeditepe University)

Assoc. Prof. Dr. Nihan Çelebi Ölçüm .....
(Yeditepe University)

Assist. Prof. Dr. Mehmet Burak Aksu .....
(Marmara University)

DATE OF APPROVAL: ..../..../2019

ACKNOWLEDGEMENTS

To my advisor, Professor Dr. Seyda Malta, I express my deepest appreciation. It has been a great pleasure to being a part of her research group for me. She was always there when I needed her consultancy and she has supported me throughout this challenging route. One of the best parts of being supervised by her is that she has great analytical skills while facing problems and her being a result-oriented and very positive person which made this journey easier, instructive and joyful for me. Working with her developed me in scientific manners as well as personally. I am also very thankful to her that she introduced me to Prof. Dr. Tarık Eren involved me in their TUBITAK project, which has been a great experience in my carrier.

Also, I further thank Professor Dr. Tarık Eren, for his endless support through my dissertation. It has been a great chance to work in his project, which gave me opportunity to spend time with him and his research group. He always had time to answer my endless questions, shared his knowledge with me and he was there to guide me throughout this project. He also opened his laboratory's doors for me and I got to experience working in another environment. In pursuing this project, his great help has broadened my mind and presented me with unlimited sources of learning.

I would like to thank The Scientific and Technical Council of Turkey (TUBITAK) for their support of this study under the research grant no: 215Z330.

I greatly thankful to Assoc. Prof. Dr. Ali Demir Sezer and to Dr. Mehmet Burak Aksu for their support and help during my thesis. Assoc. Prof. Dr. Ali Demir Sezer provided one of the key material for this project which is vancomycin and Dr. Burak Aksu conducted MIC analyses and hemolytic concentration assay for this project.

I thank Assoc. Prof. Dr. Nihan Çelebi Ölçüm for her support as being one of the juries of progress meeting of my dissertation. I also owe thanks to all of my instructors in Yeditepe University, Professor Dr. Mustafa Özilgen, Professor Dr. Süheyla Uzman, Assoc. Prof. Dr. Tuğba Candan Davran, Assoc. Prof. Dr. Erde Can, Assoc. Prof. Dr. Betül Ünlüsu, Assist. Prof. Dr. Funda Oğuz, Assist. Prof. Dr. Cem Levent Altan and Assist. Prof. Dr. Oluş Özbek

for their support during my education and teaching assistantship term. They had no hesitations to share their knowledge with me. I also would like to thank our department secretary Mrs. Ezgi Baran İlhan.

I further thank Prof. Dr. Mustafa Çulha who opened his laboratory so I could be able to pursue cell proliferation assay in his cell culture laboratory. I also am thankful to Deniz Uzunoğlu for her support and help during cell proliferation experiments.

One of the best parts of having my PhD in Yeditepe University which allowed me to meet such great people inside and out and gain their friendships forever. I am forever thankful to Şelale Gülyuva, for her being one of my lifetime friends that would never change wherever we would be. She thought me the physical distances does not affect true friendship. I am grateful to Berk Gazioğlu, he helped and supported me during my experiments. Beyond his help in the laboratory, he was there for me when I was down and gave me the courage to keep going. He is one of the most golden hearted people that I have ever met. I want to thank Öykü Gizem Zaloğlu due to her friendship and emotional support. She was always there when I needed, she has been a really good friend and I know she always will be. She has a beautiful heart. I am thankful to Sera Erkeçoğlu for her lovely friendship during this journey, she was always nice and helpful. I am also very thankful to Elçin Yenigül, she shared her knowledge on some laboratory instruments and also cell proliferation assay. She had never turned me down when I needed her support. I have been so lucky to be surrounded by such a great people.

Last but not least, I am very appretiative to my husband Brian John Degitz, without his support it would have been a harder journey. He was always there when I needed motivation to continue. I am forever indebted to my sister Alara Acaroğlu, my mother Rengin Acaroğlu, and my father Engin Acaroğlu, they have supported me in all circumstances and have given me the courage to move forward in my academic carrier. I became who I am thanks to their endless love and support throughout my life. I am grateful to my in-laws Sherry Belcher and William Belcher. I thank all of my family members including my two furry sons Chubs and Leo for their endless love, which makes everything more beautiful.

ABSTRACT

CONJUGATION OF VANCOMYCIN AND ANTIBACTERIAL POLYMERS TO INVESTIGATE THE SYNERGISTIC ANTIBACTERIAL ACTIVITY

In global healthcare infectious diseases are of critical importance. For example, annually, ~2 million nosocomial infections occur in US hospitals, of which, ninety-nine thousand of the infections result in death, adding an additional 20 billion dollars to healthcare costs. The rate of resistance of bacteria, against even the most powerful antibiotics, has increased at an alarming rate. In Turkey, as the number of people dying from infectious diseases has been on the rise, it has been emphasized in a declaration against infection based diseases by the Ministry of Health, that R&D funding should be increased for the development of antibacterial and antiviral medicine.

Especially in the newest generation of antibiotic studies, natural and synthetic peptides are now frequently encountered. In the synthesis of synthetic derivatives, there are some desired features such as: having a wide spectrum, to be resistant towards environmental conditions, low cost, and low toxicity with specificity. Vancomycin is a widely used antibiotic all around the world. The FDA approved Vancomycin is active against Gram (+) bacteria, however, it is completely inactive against Gram (-) bacteria. In order to make vancomycin to also be effective against Gram (-) bacteria, a conjugate of vancomycin with an antibacterial cationic polymer is being designed. The amphiphilic structure of synthetic polymers disrupts cell membranes that causes a breakdown of the transmembrane potential which leads to the leakage of cytoplasmic contents and ultimately cell death. When the mechanism of cell death was investigated apart from the hydrophobic interactions, the interaction between the positively charged polymers and negatively charged bacterial cell walls also resulted in cell death. Therefore, in literature, hydrophobic antibacterial polymers with cationic groups such as pyridine, and primary amine salts are frequently encountered. In this project, highly active, well-designed cationic polymers are planned to be used in conjugation with vancomycin, exploiting their synergistic effects on antibacterial activity.

ÖZET

VANKOMİSİN İLE ANTİBAKTERİYEL POLİMERLERİN KONJUGASYONU İLE SİNERJİSTİK ANTİBAKTERİYEL ETKİNLİĞİNİN İNCELENMESİ

Bulaşıcı hastalıklar küresel sağlık bakımından kritik öneme sahiptir. Örneğin, Amerika Birleşik Devletleri'ndeki hastanelerde yılda yaklaşık iki milyon hasta hastane enfeksiyonuna yakalanmakta olup, bu hastaların doksan dokuz bini ölmektedir ve bu durum sağlık harcamalarına 20 milyar dolar daha eklemektedir. En güçlü antibiyotiklere bile bakteriyel direnç endişe verici bir oranda artmaktadır. Türkiye'de bulaşıcı hastalıklardan ölen insanların sayısı giderek artmakta ve Sağlık Bakanlığı'nca enfeksiyona bağlı hastalıklara karşı savaşta; antibakteriyel ve antiviral ilaçların geliştirilmesi için Ar-Ge fonlarının artırılmasının gerekliliği vurgulanmıştır.

Özellikle yeni nesil antibiyotik araştırmalarında, doğal ve sentetik peptitlerin kullanımına sıklıkla rastlanmaktadır. Sentetik türevlerin sentezinde, geniş bir spektruma sahip olma, çevre koşullarına karşı dirençli olma, düşük maliyetli olma, toksik olmama ancak seçicilik özelliğine sahip olma gibi istenen bazı unsurlar vardır. Vankomisin, dünyanın her yerinde yaygın olarak kullanılan bir antibiyotiktir. Amerikan Gıda ve İlaç Dairesi (FDA) onaylı olan Vankomisin, gram pozitif bakterilere karşı etkili bir antibiyotik olmasına karşın, gram negatif bakterilere karşı tamamen etkisizdir. Bu çalışmada, vankomisinin gram negatif bakterilere de karşı etkili olmasını sağlamak için, bir antibakteriyel katyonik polimer ile konjugasyonunun yapılması tasarlanmaktadır. Sentetik polimerlerin amfifilik yapısı, hücre zarlarını bozarak; transmembran potansiyelinin bozulmasına, sitoplazmik içeriklerinin sızmasına ve sonuçta hücre ölümüne neden olur. Hidrofobik etkileşimlerden ayrı olarak hücre ölüm mekanizması incelendiğinde, pozitif yüklü polimerler ve negatif yüklü bakteriyel hücre duvarları arasındaki etkileşim de hücre ölümüne neden olur. Bundan dolayı, literatürde piridin gibi katyonik gruplara ve birincil amin tuzlarına sahip olan hidrofobik antibakteriyel polimerlere sıklıkla rastlanmaktadır. Bu projede, yüksek aktifliğe sahip, iyi tasarlanmış katyonik polimerlerin antibiyotik aktivitesi üzerindeki sinerjistik etkilerinden yararlanmak için, bu polimerler ile vankomisinin konjugasyonunun yapılması planlanmaktadır.

TABLE OF CONTENTS

LIST OF FIGURES

LIST OF TABLES

LIST OF SYMBOLS/ABBREVIATIONS

ACN	Acetonitrile
ADMET	Acyclic diene metathesis polymerization
AMP	Antimicrobial peptides
ATCC	American type culture collection
ATR	Attenuated total reflection
ATRP	Atom transfer radical polymerization
CAUTI	Catheter-associated urinary tract infections
CCP	Cationic conjugated copolymers
CDC	Centers for Disease Control and Prevention
CFU	Colony forming unit
CLABSI	Central line associated bloodstream infections
CM	Cross metathesis
CRP	Controlled radical polymerization
CPF	Ciprofloxacin
DABCO	1,4-Diazabicyclo[2.2.2]Octane
DE	Diethyl ether
DCM	Dichloromethanol
DMEM	Dulbecco modified Eagle's medium
DMF	N,N-dimethyl formamide
DMSO	Dimethyl sulfoxide
DNA	Deoxyribonucleic acid
DP	Degree of polymerization
DPBS	Dulbecco's phosphate buffer saline solution
EtOAc	Ethyl acetate
EU	European Union
EVE	Ethyl vinyl ether
FBS	Fetal bovine serum
FDA	Food and Drug Administration
FTIR	Fourier transform infrared spectroscopy
HAI	Health care-associated infection
HC_{50}	Hemolytic concentration

HEX	Hexane
HIV	Human immunodeficiency viruses
HPLC	High pressure liquid chromatography
HUVEC	Human umbilical vein endothelial cells
ICU	Intensive care units
IMS	Intercontinental marketing services
IR	Infrared
MDR	Multi-drug resistant
MeOH	Methanol
MIC	Minimum inhibitory concentration
MRSA	Methicillin-resistant *Staphylococcus aureus*
MW	Molecular weight
MWCO	Molecular weight cut off
NC	Negative control cell
NMR	Nuclear magnetic resonance spectroscopy
PBF	Polyfluorene
PBS	Phosphate buffer saline solution
PEG	Polyethyleneglycol
PLA	Poly(D,L-lactide)
PLB	Polymyxin B
PLGA	Poly(lactide-co-glycolide)
PSA	Streptomycin-Penicillin
PT	Polythiophene
RAFT	Reversible addition-fragmentation chain transfer
RBC	Red blood cell
RCM	Ring closing metathesis
ROMP	Ring opening metathesis polymerization
SEM	Scanning electron microscope
SM	Self-metathesis
SSI	Surgical site infections
TEA	Triethylamine
TFE	Triflouroethanol
THF	Tetrahydrofuran
USA	United States of America

UV	Ultra violet
VAP	Ventilator associated pneumonia
VP	Vancomycin-PEG
VRE	Vancomycin-resistant *Enterococcus*
VRSA	Vancomycin-resistant *S.aureus*
WHO	World Health Organization

1. INTRODUCTION

Infections can be treated through the use of proper antimicrobial treatments, which are important for the mortality of the patients as well as for the prevention of complications and/or a worsening of the conditions, which can become chronic. In particular, the usage of the incorrect antibiotic and/or the incorrect treatments results in antibiotic resistance [1]. Antibiotic resistance refers to the antibiotic no longer having effectiveness and that there is an ongoing continuous demand for new generations of antibiotics. In spite of a myriad of recent advances in the medical sciences, infections acquired in hospitals continue to cause a substantial number of illnesses and mortalities. Nosocomial infections are the more common name of health care-associated infections (HAIs), which occur in patients under medical care, and antibiotic resistance are major health-care problems all over the world [2–4]. In developed countries, seven out of every one hundred hospitalized patients (ten out of every one hundred in developing countries) are acquiring health care-associated infections [3]. Each year, 648 thousand to 1.7 million hospitalized patients are infected with HAIs in the United States (USA) alone [5].

According to IMS (Intercontinental Marketing Services) data, the rate of producing antibiotics has been increasing dramatically over the last few decades, and in the meantime, antibiotic usage in the treatment of infectious diseases, has increased as well [6]. Due to the misuse and/or excessive use of antibiotics, increases in the selective pressure encourages the appearance, duplication, and spread of resistant strains [6–8]. The severity and the global spread of the phenomenon have prompted the attention of the World Health Organization (WHO) and European Union (EU) [8]. Increasing rate of bacterial resistance in health care facilities, particularly in intensive care units (ICUs) are associated with poorer recovery and worsening conditions. These include: multi-drug resistant (MDR) Gram (-) bacteria, vancomycin-resistant *Enterococci* (VRE) and methicillin-resistant *Staphylococcus aureus* (MRSA) [1, 9].

MRSA causes infections across different parts of body. Vancomycin and its derivatives are extensively used in MRSA treatments. In particular, MRSA acquired in hospitals may cause very serious infections such as: blood infections and pneumonia [10–12]. Vancomycin is a glycopeptide structured antibiotic [13], which is produced by the fermentation of

Amycolatopsis orientalis and it is used in the treatment of the infections caused by Gram (+) bacteria [14, 15]. The cell membrane of bacteria are essential for survival, they keep foreign substances from entry into the cell and retain the contents of the cell from leakage. The cell wall of bacteria is reinforced by peptidoglycans. Prohibiting the formation of the peptidoglycans is how vancomycin is effective [16], and vancomycin further weakens the cell walls, thus resulting with the death of the bacteria. Nevertheless, vancomycin is not effective on Gram (-) bacteria [13, 14, 17], because Gram (-) bacteria's cell membrane is impermeable for the larger molecule size of vancomycin. Furthermore, vancomycin has ototoxic and nephrotoxic effects [18] if it is not combined with a polymer or carrier system. Thus, patients with a renal function disorder cannot use vancomycin, but if it must be used, a dosage adjustment is imperative. In addition, the short half-life and the labile structure of the antibiotic cause severe problems on formulation [19, 20]. These disadvantages of vancomycin limit its usage for wider spectrum of infectious diseases.

Bacterial infection, as a global problem, became more important especially in the last decades due to rising death rates. The new generation antibiotics are quite important for fighting against the bacteria [21]. This study focuses on the novel construction of a new generation of antibiotic, where vancomycin (active towards Gram (+) bacteria) is conjugated with a synthesized antibacterial polymer (active towards Gram (-) bacteria) with well-defined architecture and the synergistic antibacterial activity is explored in quest of a labile, wide-spectrum antibiotic.

2. THEORETICAL BACKROUND

2.1. LITERATURE SURVEY

The antibiotic resistance of bacteria has become a significant problem all over the globe. In 2013, The American Center for Disease Control and Prevention (CDC) has reported that 2 million patients have developed resistance to antibiotics and 23 thousands of the cases resulted with death [22]. In order to find a solution to this problem, scientists have made much effort to develop new antimicrobial agents that can inhibit bacteria without causing bacterial resistance [22–26].

Two main groups are present in the world for production of newer generations of antibiotics in order to combat the bacterial resistance in the fight against bacteria. The first group deals with isolating the natural peptides from natural sources and/or synthetization of their analogs in laboratories [27–32]. Although peptides are very promising materials with their facially amphiphilic structures indicating selectivity, exhibit very low hemolytic activity toward human red blood cells while possessing high antibacterial potency [33, 34], their stability in physiological condition and the production costs present a major problem to their use [35]. They have been developed against the disease-causing bacteria that cannot evolve to become resistant to the membrane-disruption mode of action [35, 36]. The second group involves with the synthetic mimics of peptides using a polymer or oligomer via the control of the balance of hydrophobicity/hydrophilicity of their structure. Therefore, the cationic polymers are designed and developed inspired by the structure of natural peptides [37–45]. Synthesizing polymers in a laboratory environment is relatively low cost, easy and quick to produce, and also provides an additional advantage in that the activities can be adjusted with the modifications in polymers' structures. Moreover, those polymers are more stable in the physiological environment. New studies on antimicrobial polymers aim to synthesize polymers economically yet expediously in laboratory environments, highly effective at low concentrations, and with a wide spectrum of effectivity while being non-toxic.

Recently, scientists are attracted by the new strategies and materials for efficient, rapid killing of bacteria. Taking into consideration the lesser killing of small doses of individual antibiotics, antibiotic mergers are utilized to treat bacteria, particularly drug-resistant

bacteria [46, 47]. The combinations of antibiotics could enlarge the antibacterial spectrum and create synergistic effects. Indeed, there has been limited scope for finding effective antibiotic combinations due to lack of targeting moieties and poor pharmacokinetic properties [46, 48]. There have been several attempts to combine antibiotics with non-antibiotic molecules and the antibacterial activity increase of new systems have been reported [46, 49]. In this respect, chemical conjugation of antibiotic with polymers, proteins or antibodies have been under consideration. Among the other materials, drug conjugation with polymers can display unique properties such as: controlled and sustained release, vary in antibiotic class types, synthetic methods, carrier composition, bond liability and antibacterial activity [48, 50].

In literature, there are synthetic peptides with high activity and selectivity that have been synthesized by different polymerization methods. Yang *et al.* [52], synthesized biodegradable cationic antimicrobial polycarbonates, which are bearing hexyl and propyl side groups, with ring-opening metathesis using the amine groups that were quaternized with various nitrogen compounds. They have reported in their activity and toxicity studies that the increasing of the hydrophobicity of the quaternary group, the activity was also increased.

Takahashi *et al.* [44], synthesized cationic amphiphilic methacrylate homo- and co-polymers by Reversible Addition-Fragmentation Chain Transfer (RAFT) polymerization method against *S. mutans* bacteria to prevent their biofilm formation which is causing dental decay. They investigated the bactericidal kinetics of the synthesized polymers, and found that at a concentration above the MIC values; 99.8 percent of bacteria were killed by PE_{31} and PE_0, in 180 minutes and 120 minutes, respectively.

İlker *et al*. [27], synthesized water soluble, amphiphilic and antimicrobial polymers and they studies to determine the effects of the different hydrophobic groups and molecular weights upon the activity of the synthesized polymers. İlker *et al.*, synthesized four different homopolymers via Ring Opening Metathesis Polymerization (ROMP). When they examined the activities of homopolymers, they observed that the activity increased upon increasing hydrophobicity until a threshold value, and above that value the activity of the polymers started decreasing. When they examined the effects of the molecular weight, decreasing molecular weights of Poly3, leads to increasing of the activity; however, the molecular weight was not found to have any significant effect on the hemolytic concentration nor the antimicrobial activity of these polymers.

Tew and coworkers have published many studies about antimicrobial polymers. Tew *et al*. investigated highly selective polymers with their study named "Molecular Structure Kit" [53]. They synthesized polymers which contained both hydrophilic and hydrophobic groups. They maintained the hydrophilic groups of the polymers and investigated the effect of the varying hydrophobic groups (such as; ethyl, butyl, hexyl, methyl, etc.) on the antimicrobial activity. They reported that while the activity was increasing within increasing molecular weight against *E.coli*, however, it was decreasing against *S.aureus*. Tew *et al*., also studied on the effects of charge density on the activity and toxicity by polymerizing three different norbornene monomers with an increased amine group by the ROMP method [54]. It was observed that an escalation in the total count of cationic groups in polymers which were the most hydrophobic, decreased the toxicity, however, there were not any critical differences in the activity against *E.coli*. In spite of this, an increase in the quaternary amine groups in the oxirane functional polymer significantly increases the activity against *S.aureus* with a MIC from >200 μg/mL to 15 μg/mL.

Eren and coworkers [55] synthesized amphiphilic polyoxanorbornenes containing various quaternary alkyl pyridinium side chains and investigated their biological efficiencies against bacteria and human red blood cells. Furthermore, they reported that, although alkyl chain lengths of six or more carbons bearing polymers had increases in their antibacterial activity, they became hemolytic. Eren *et al.*, also investigated the activity on the surface of pyridinium salt bearing oxabornene derivative ROMP polymers [56]. The activity study was conducted for liquid and solid surfaces, and it was found that the polymer bearing octyl unit (p(OPyOct)) has the highest activity in liquid phase, however activity dropped on the solid surface. In spite of this, hexyl polymer with a 3000 g/mol has the highest activity on solid phase and activity did not diverge from the solution phase and it was reported that 99 percent of the bacteria (*E.coli*) died in 5 minutes above the threshold concentration for the polymer used to coat the surface. Besides the quaternary amine or pyridine functionality, phosphonium containing ROMP type polymers were also investigated in solution [57]. MIC analyses of the different alkyl and aromatic phosphonium side chains bearing polymers were performed against Gram (-) and Gram (+) bacteria, the homopolymers containing aromatic groups had a much higher activity with a value of 8 μg/ mL against *S.aureus* and 16 μg/ mL against *E.coli*.

Cheng *et al*. [47], combined several cationic conjugated polymers (CCP) with polypeptide antibiotics and investigate their bactericidal activity against drug resistant *E.coli*. Cheng *et al*. reported that CCP-antibiotic combination was exceptionally potent and synergistically killed the drug resistant bacteria. CCPs without antibiotic combination showed low toxicity towards bacteria, however, when bacteria's cell membrane was treated with CCPs it became loose due to the strong coating of CCPs. Cheng et al. synthesized polyfluorene (PBF) and polythiophene (PT) derivatives as CCPs in their work. They conducted MIC analysis to CCPs, antibiotics and their combinations, and reported that the combination of Polymyxin B (PLB) with PBF enhanced antimicrobial activity (MIC: 2.3 μg/mL) 98.6 percent at low PLB concentration (2.5 μg/mL) while PLB's antimicrobial efficiency was 25 percent alone. They have suggested that antimicrobial efficiency improves due to the synergistic antibacterial mechanism of CCPs and antibiotics, through their study.

He *et al*. [23], synthesized copolymers using ciprofloxacin (CPF), which have water soluble amphiphilic structures. They used primary amine salt and methacrylate monomer containing CPF by copolymerization of protonated primary amine monomer with methyl acrylate. They investigated the antimicrobial activity using MIC analysis, and they reported that all copolymers that exhibited high activities towards *E.coli* (MIC: 5-40 ppm) with an increasing hydrophobic methyl acrylate content and decreased MIC values.

Lawson *et al*. [58], synthesized various polymerizable vancomycin derivatives containing arylamide or poly ethylene glycol (PEG)-acrylates. The PEG chain which has 5000 Da molecular weight showed an excellent decrease in activity comparing the ones with 3400 Da molecular weight.

In this study, the synthesized polymers were designed as the carrier system are completely original and has not been used as a drug carrier before. The originality of this project is that the synthesized polymers themselves exhibit antimicrobial properties against both Gram (-) and Gram (+) bacteria, and they can covalently bind to vancomycin which is already effective against Gram (+) bacteria. It is also expected that the newly designed macromolecules can release vancomycin, the remaining cationic polymers maintain their antibacterial property and a dual effect is achieved.

2.2. NOSOCOMIAL INFECTIONS

Viruses, bacteria, fungi and parasites are the pathogenic microorganisms which are the crucial reasons of infectious diseases. Infections could be spread from one person to another, either directly or indirectly. HAIs are serious universal health problems. The World Health Organization (WHO) defined HAIs as any infection obtained in a hospital or health care facility by a person being treated for a medical problem other than that infection. Or as an infection arising in a patient in a health care facility in whom it was not previously found or was incubating during admission. The WHO further includes infections that were not present beforehand but presented itself after the patients discharge from the facility which was obtained while in care, and also includes infections among facility personnel obtained during their occupation. Even though there are many recent studies and advances in medical science, nosocomial infections continue to cause a substantial number of illnesses, mortalities and morbidities [4].

In 2017, CDC reported that, even though a considerable progress had been done in preventing HAIs, there is still more to be done. Every day, about one in every 25 patients has faced at least one HAI type infections [59]. In the USA ~1.7 million patients are infected with all types of microorganisms. The patients are at a higher risk in ICUs, burn units, while undergoing organ transplants, and neonates. The USA hospitals registered: 417946 HAIs among adults and children in ICUs, 19059 among newborns in well-baby nurseries , 33269 among newborns in high-risk nurseries, and over 1 million among adults and children outside of ICUs in 2018 [60]. The approximated number of fatalities attributed to HAIs in hospital in the USA were 98987: of these, 36 percent were for pneumonia, 31 percent for bloodstream infections, and 13 percent for urinary tract infections, 8 percent for surgical site infections, and 11 percent for infections of other sites [61]. Vincent *et al*. [62] reported that 7087 of 13796 patients (51 percent) were considered to be infected while 9084 (71 percent) of them were taking antibiotics. The infections were of respiratory in origin 64 percent, and in 70 percent of the infected patients the microbiological culture results were positive. Patients with prolonged ICU stays, also had higher infection rates, the infections were particularly due to resistant *staphylococci*, *Acinetobacter*, *Pseudomonas species*, and *Candida species*. The fatality rates of infected patients in the ICU and in the hospital were more than double that of non-infected patients (25 percent versus 11 percent and 33 percent

versus 15 percent, respectively). HAI incidence density ranged from 13.0 to 20.3 episodes per thousand patient days, according to comprehensive studies across the USA and across Europe. [10].

2.2.1. Nosocomial Pathogens

The liable pathogens for HAIs are fungi, viruses, and bacteria. These microorganisms alter according to different population of patients, care/medical facilities, and the differences in the care environments. [63].

The most common pathogens causing HAIs are bacteria. Some of these bacteria belong to the patient's natural flora and only cause infections once immune system of the patient has become susceptible to infection. *Acinetobacter* is a genus of pathogenic bacteria that causes ICU infections [64]. The most frequent bacteria that causes HAIs are: *S.aureus*, *Acinetobacter spp*., *Coagulase-negative staphylococci*, *Streptococcus spp*., *B.cereus*, *Enterococci*, *Legionella*, *P.aeruginosa*, and members of *Enterobacteriaceae* like *E.coli*, *Salmonella spp.*, *P.mirabilis*, *K.pneumoniae* and *S.marcescens* [63]. *Bacteroides fragilis* is a commensal bacteria located in the colon and intestinal tract, causing infections by combining with other bacteria. *C.difficile* causes inflammation of the colon, which leads to antibiotic-associated diarrhea and colitis, predominantly due to the eradication of salubrious bacteria. *C.difficile* is generally spread from an infected patient to other patients through health care staff via improperly sanitized hands [64, 65]. Carbapenem resistant *Enterobacteriaceae* include *Klebsiella* species and *E.coli*, usually populate in the gut, and if transport occurs to other body parts, it causes infection. The high resistance of *Enterobacteriaceae*, *Klebsiella* and *E.coli* against carbapenems causes the counteractions against them to be more difficult [3]. MRSA is transmitted through immediate contact, contaminated hands, and by open lesions. MRSA causes sepsis, pneumonia, and surgical site infections by travelling through organs or the bloodstream. MRSA is exceptionally resistant against beta-lactam antibiotics [3].

Viruses also have an important role causing HAIs, it has been revealed that 5 percent of all HAIs are caused by viruses [67]. Transmission of viruses can be from hand-to-mouth, by respiration, or fecal-oral routes [68]. Hepatitis is a chronical viral disease, and hepatitis viruses can transmit to patients and to workers during the healthcare provision. The most

common Hepatitis viruses are Hepatitis B and C, which are generally communicated during unsafe injection proceedings [67]. Influenza, HIV, rotavirus, and the herpes-simplex virus are some examples of other common virus types [68].

Fungal pathogens cause HAIs in immunocompromised people. *Aspergillus spp*. can cause infections by the inhalation of fungal spores from contaminated air during periods of construction or renovation of health care facilities, and *Cryptococcus neoformans* and *Candida albicans* are also can cause infections during hospital stay [3, 67].

2.2.2. Environmental Factors

The environmental factors in the hospital for patients include: hygiene of equipment, surroundings, healthcare workers, etc. Hospitalized patients are highly susceptible to infection due to their weakened immune systems and medical applications such as intubation, surgery or use of antibiotics, as well as exposure to microorganisms which have spread from other sources including but not limited to the hospital/healthcare environment, staff and personnel, or other patients. However, it seems that the primary mode of transport for the pathogens and germs that cause the infections is from the medical or nursing staff, but there are other ways of contamination such as the direct contact of the patients with contaminated devices, objects, materials, and air [4, 68]. Thus, the usage of antimicrobial surfaces within the healthcare facilities has a potential of further reduce contamination in the environment [5].

2.2.3. Patients at Risk of Nosocomial Infection

Although all of the patients are potentially at a risk for infection, certain patients or conditions carry a much higher risk. The following conditions are the highest risk groups.

- Patients who are over 70 years of age are more likely to become infected. Also newborns, especially premature newborns whose birth weight is under 2 kg are potential candidates for infections [62, 69].
- Patients who have been admitted for or have experienced shock, major trauma, or acute renal failure [71].

- Comatose patients.
- Patients who have priority used antibiotics or are using drugs that affect the immune system (steroids, chemotherapy, etc.).
- Patients who are reliant on life support systems such as ventilation machines or have indwelling catheters.
- Patients who have had a prolonged ICU stay of more than 3 days [62, 70].

2.2.4. Types of Nosocomial Infections

Common HAIs are: “Central Line Associated Bloodstream Infections” (CLABSI), “Catheter-Associated Urinary Tract Infections” (CAUTI), “Surgical Site Infections” (SSI), “Ventilator Associated Pneumonia” (VAP), lower respiratory tract infections, gastroenteritis, other soft tissue infections, etc. [3, 63].

CAUTI: CAUTI is caused by the endogenous native microflora in the patient, which is the most common type of HAIs. Catheters placed inside the patient’s body act as a channel for the access of bacteria. Furthermore, flawed drainage of catheters retain urine traces from the bladder and provide a stable residence for bacteria [65]. Some complications might be developed in the presence of CAUTI within patients such as: pyelonephritis, cystitis, and meningitis, as well as orchitis, epididymitis and prostatitis in males. In 2011, more than 12 percent of CAUTIs were accounted of reported infections by acute care hospital stats [3].

SSI: 2 percent-5 percent of patients who have surgery, end up having a SSI, which is the second most common type of HAIs. The main reason for SSIs is *S.aureus*, which causes a prolongation in hospitalization and an increased risk of fatality. The pathogens causing SSI emerge from internal microflora in the patient. The rate may increase up to 20 percent which depends upon the criteria operation and surveillance [71, 72].

CLABSI: CLABSIs are lethal HAIs with a mortality rate of 12–25 percent. Catheters are placed in the central line to deliver fluids and medicine, however extended usage may cause serious infections in the bloodstream which results in compromised health and an increased cost of care. Although there has been a 46 percent decrease in CLABSI from 2008 to 2013 in hospitals in the USA, approximately 30100 CLABSI transpire in ICU and acute facility wards in the USA each year [3].

VAP: 9-27 percent of patients on mechanically assisted ventilators are developed VAP. Occasionally, it occurs within a 48 hour window after tracheal incubation. The common symptoms of VAP are fever, leucopenia, and bronchial sounds, and 86 percent of VAP is associated with mechanical ventilation [3, 73].

2.2.5. Treatment of Bacterial Infectious Diseases

Antibodies have been used for over a century in the treatment and prevention of infectious diseases. Antibodies neutralize toxins in bacterial infections, that facilitate opsonization and in addition promote bacteriolysis. In viral diseases, antibodies block against viral access into healthy cells, promote antibody-directed cell-mediated cytotoxicity by natural killer cells, and further neutralize viruses alone or in corporation with a complement [70]. Nevertheless, the overuse and/or misuse of antibodies and antibiotics lead to the pathogens evolving multidrug resistance to all divisions of commercially available medications [75]. In the 21st century, previously considered extinct or non-threatening infectious diseases may once again become serious issues in western countries which creates an urgency to find safer and more effective antimicrobial agents with higher efficacy in order to circumvent resistances that have developed. Current drugs may be categorized due to their method of effectiveness such as: inhibiting the synthesis of bacterial cell walls, proteins, nucleic acid, and folic acid, or disorganizing membranes or other enzyme catalyzed reactions. Certain types of bacteria are generally more resistant to certain types of antibiotics as is the case with Gram (-) bacteria to antibiotics designed against Gram (+) bacteria due to their outer membrane containing a lipopolysaccharide layer which impedes the usage of these antibiotics [76].

2.3. BACTERIA

Bacteria are the smallest living structures, which are prokaryotes that consist of a single cell with a simple internal structure (1-5 μm) [77]. They contain inorganic materials, water and organic materials such as: protein, carbohydrate, lipid and nucleic acid. There are two main groups of bacteria which are the beneficial bacteria and the disease-causing “pathogens”. [65, 77]. It is also possible to classify the bacteria due to their different characteristics. The

most common classification for bacteria in medical field is according to their reaction to the gram stain (Figure 2.1).

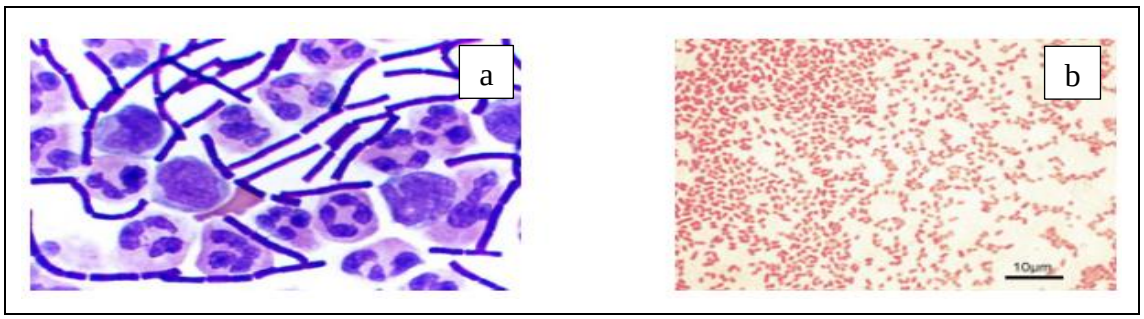

Figure 2.1. Gram stained bacterial cells: a) Gram (+) bacteria, b) Gram (-) bacteria [79]

2.3.1. Classification of Bacteria in Medicine

In medicine, there are typically two main classifications of bacteria, Gram (-) and Gram (+) bacteria. The classifications are determined using the gram staining method due to the differences in physical and chemical properties of the bacteria [76, 79]. One of the significant differences between Gram (-) and Gram (+) bacteria is that they have some differences in the structures of their cell walls, with Gram (+) bacteria having a thick mesh-like cell wall made of peptidoglycan while Gram (-) bacteria has a thinner peptidoglycan layer and thinner cell walls (Figure 2.2). Due to this difference, when the gram staining method is conducted; Gram (+) bacteria is stained purple with crystal violet whereas Gram (-) bacteria is stained pink with safranin [80].

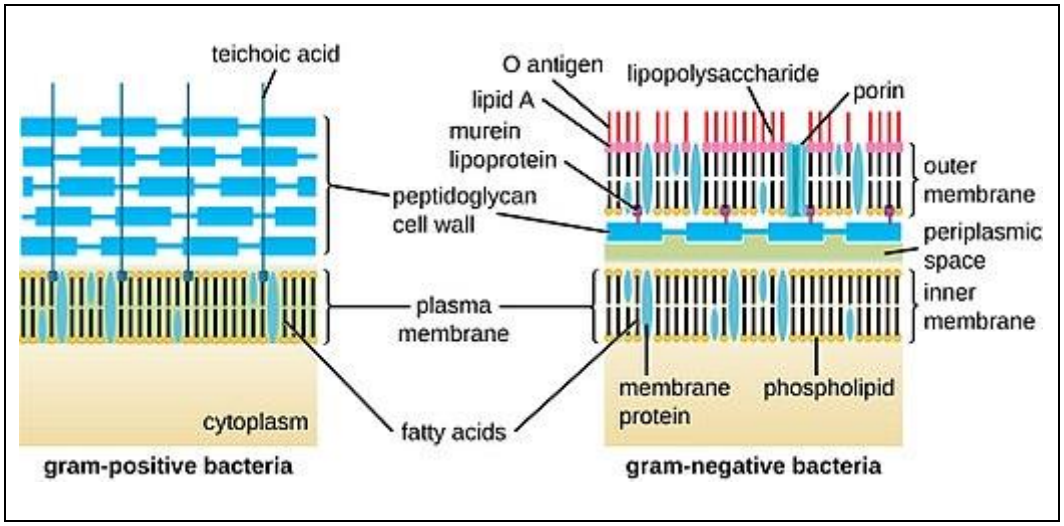

Figure 2.2. Cell membrane differences of the Gram (+) and the Gram (-) bacteria [79]

The gram staining method consists of four basic steps (Figure 2.3). (i) The first step is applying the primary stain -crystal violet, which stains all of the cells either blue or purple. (ii) The second step is applying the mordant -iodine solution, which forms a complex with crystal violet and and all cells remain blue or purple. (iii) The third step is the decolorization. In this step the Gram (+) bacteria differ from Gram (-) bacteria due to the cell wall differences between them. An organic solvent such as ethanol or acetone, extracts the blue dye complex from the Gram (-) bacteria due to its lipid-rich, thin cell wall to a greater degree than from the Gram (+) bacteria which has lipid poor, thick cell wall. Gram (-) bacteria become colorless and Gram (+) bacteria keep their blue/purple color. (iv) The last step is applying the counter stain -safranin. Safranin colors the decolorized Gram (-) cells red or pink, while the Gram (+) bacteria cells remain blue [80].

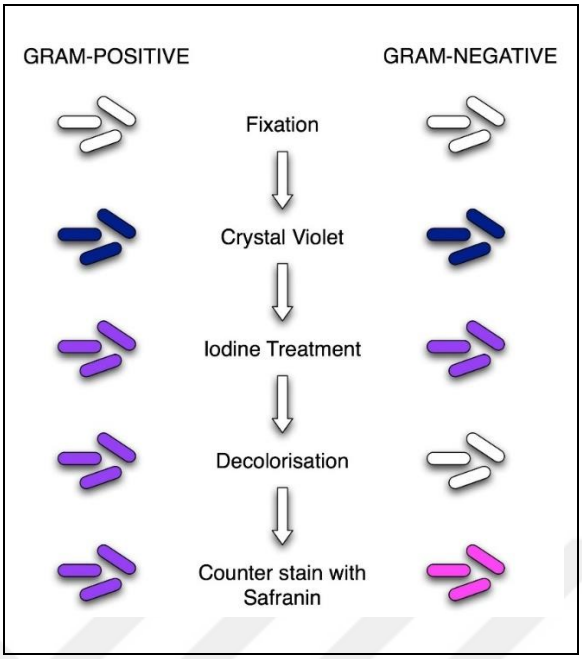

Figure 2.3. Procedure of Gram Staining Method [81]

2.3.1.1. Gram Positive (+) Bacteria

Gram (+) bacteria appear blue or purple under an optical microscope, after the gram staining method application. This color is due to their thick cell wall structure which does not allow the crystal violet to leave cell walls. The peptidoglycan cell walls of the Gram (+) bacteria contains many layers of teichoic acid, lipoteichoic acid and polysaccharide complexes. Teichoic acid and lipoteichoic acid have significant roles in Gram (+) bacteria cell determination of shape, regulation of cell division, and other essential aspects. *S.aureus*, *S.epidermidis*, *S.pneumoniae*, *M.tuberculosis* are some examples for Gram (+) bacteria. [82].

2.3.1.2. Gram Negative (-) Bacteria

Gram (-) bacteria appears pink or red beneath an optical microscope, after the gram staining method application. On the contrary to Gram (+) bacteria, Gram (-) bacteria possess thinner peptidoglycan cell walls which contain lipopolysaccharides. Lipopolysaccharide is a toxic material and its presence cause sepsis especially for infants and children [82].

2.4. ANTIMICROBIAL RESISTANCE

The continuous development in resistance to antibiotics has been a profound problem for pharmaceutical industries and doctors, since as many microorganisms have acquired resistance to multiple-antibiotics. Drugs that had once cured a broad range of infections became less useful, mostly due to the abuse of drugs and the continuous development of multi-drug resistances, that leads the treatments could potentially be exceedingly difficult, and significantly associated mortality [4, 76, 83, 84]. The growing prevalence of antibiotic resistance by a broad range of microorganisms has led to increased research studies into traditional medicinal plants as alternatives.

Presently, nearly all antimicrobial agents, including both widely used and some of the newest ones, are exposed to bacterial resistance. A resistance to drugs and their effectiveness occurs from changes in the genes or in the adaptation of the genes to inhibit the antibiotics' delivery [85]. Organisms, including bacteria, naturally have many defense mechanisms that allow for structural changes, both internally and externally, and resistance development that may prevent molecules from being able to bind with it, which may decrease the permeability of the cell membrane which is a primary method of entry for antibiotics, may actively force the drug out of the cell, or furthermore, may produce enzymes which can deactivate the drug after it has already been absorbed. Initially, resistance to drugs begins as a mutation of existing genes which upon being transferred through cell reproduction or bacterial genetic exchanges, to members of both the same and other species, contributes to the spread of the resistance which may be expedited by the overuse of antibiotics obtained from the community due to over-the-counter availability in some countries or increased migration/travel/health tourism, obtained from hospitals, or may be further obtained through the food chain as veterinarians may also use them in livestock [4].

In 1944 only two years after the introduction of penicillin, the first instances penicillin resistant *S.aureus* were reported. It was determined that this isolate produced a penicillinase enzyme (a type of ß-lactamase) that hydrolyzes the beta-lactam ring of penicillin. Today, in many geographic regions over 90 percent of the incidences of penicillin resistance are due to beta-lactamase production [86]. In 1948, the spread of resistant strains had tremendously decreased the beneficial value of benzyl penicillin in the treatment of infections caused by *S.aureus*, and towards the end of the following decade, *S.aureus* had become resistant to

almost all available drugs at that time, including: erythromycin, streptomycin, and the tetracycline.

In 1961, Strains of MRSA first appeared, although only occurring sporadically and only resistant to β-lactam antibiotics, reappear at the end of nineteen-seventies in a very different form than the previous strains, as they were resistant to multiple other drugs as well as the β-lactam compounds which then disseminated to health care institutions throughout the world. MRSA is currently among the most frequent causation of HAIs and is a significant healthcare problem, responsible for 40-70 percent of *S.aureus* infections in ICUs [76].

2.4.1. Mechanism of Resistance

Gram (-) bacteria generally have the ability to transfer extrachromosomal genetic material, "plasmids", through direct cell-to-cell contact or through a bridge-like connection between two cells using a process of bacterial conjugation. One large class of plasmids is referred to as resistance plasmids because of their genes that produce drug resistant properties, most of which have genes responsible for resistances to multiple antibiotics. Some species of bacteria can also absorb DNA fragments from their surroundings through their cell membranes in a process called transformation. If they absorb DNA that has drug resistant genes, a drug resistance is then gained by the bacteria. Genetic exchanges may also occur by transduction, a process of bacterial recombination mediated by bacteriophages (injection of foreign DNA by a bacteriophage virus into the host bacterium). Transposons, which are sequences of bacterial DNA that can insert themselves randomly into other genomes might also carry drug resistance genes [4, 75].

2.4.2. Vancomycin Resistance

Vancomycin works by inhibiting the polymerization of essential component of the cell wall of the bacteria -peptidoglycan [11, 12, 87]. MRSA first appeared as a hospital acquired infection, then has developed into limited endemic status and currently is community acquired. MRSA bacteria are more likely to evolve when antibiotics are overused or misused and the use of more powerful drugs than needed for mild infections, can be reasons for the development of MRSA. Given enough time, bacteria can modify and mutate so that these

antibiotics are no longer effective against the bacteria [76]. Over the last decade, newer strains of MRSA have appeared in society and the spread of community acquired MRSA is rapidly increasing. MRSA bacteremia is significantly associated with a higher death rate and becomes more expensive to treat [88]. While Vancomycin is commonly prescribed to combat infections caused by multiple drug resistant *S.aureus*, isolates with a decreased sensitivity to vancomycin have been recorded in a plethora of countries [13, 89].

Enteroccoci are very strong bacteria towards environmental effects. They are capable of living in temperatures from 10 ^{o}C to 45 ^{o}C and pH from 4.8 to 9.6. Most *Enterococci* are intrinsically resistant to many kinds of antibiotics, therefore, therapeutic drugs for *enterococcal* infectious disease are very limited to a few antibiotics such as vancomycin, ampicillin and gentamicin. However, therapeutic complications caused by *Enterococci* were identified in the beginning of the nineteen-fifties, as most *Enterococci* became resistant to the bactericidal effect of β-lactam and glycopeptide drugs. High level vancomycin resistant strains of *Enterococcus* were first isolated in England in 1986. Only four years later, vancomycin-resistant *Enterococcus* (VRE) had spread all the world, especially, multi-antibiotic resistant strains, which were resistant to high concentrations of ampicillin, gentamicin and vancomycin [87]. *Entorococcus* strains are capable of transferring vancomycin resistance genes to unrelated bacteria such as *S.aureus* which are renamed Vancomycin-resistant *S.aureus* (VRSA). One of the main reasons for these pathogens to survive within a hospital or healthcare environment, is their high resistance towards the most frequently utilized drugs and due to their ability to obtain resistance to all of the antibiotics that are available in the market, either through mutation or by the receipt of foreign genetic material during the transfer of plasmids and transposons. An increase in the cases of VRE infections have been reported from health care facilities in the past 10 years. This increase causes several problems, which includes: a) lack of efficient antibiotics for VRE infections, since most VRE are already resistant to multiple antibiotics, e.g. aminoglycosides and ampicillin, and b) vancomycin resistance genes in VRE chances to transferred to other Gram (+) pathogens, e.g. *S.aureus*. Until recently, vancomycin was the only antibiotic that could be depended upon for the therapy of multi-antibiotic resistant *Enterococci* infections [90, 91].

2.5. POLYMERS

Polymers have a molecular structure constructed of a large number of similar monomers bonded together. In Figure 2.4, a schematic of polymerization is shown.

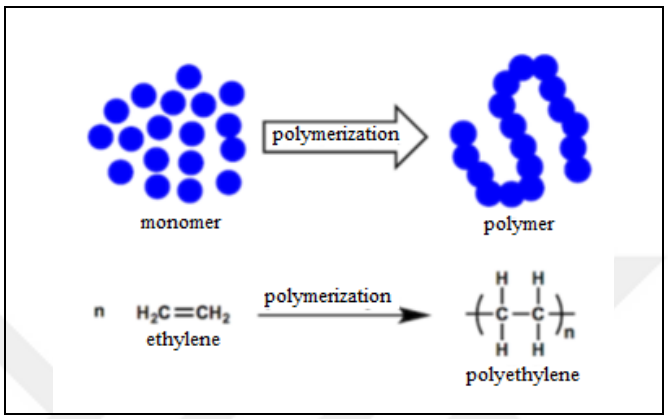

Figure 2.4. Schematic of polymerization

Polymers are widely used in medical field, as implants, surgical sutures and drug carrier systems and as a framework for tissue engineering. Polymers are preferred instead of ceramics and metals due to some of their features; such ease of shaping, low molecular weight controllable synthesis mechanisms and low production costs [92].

2.5.1. Classification of Polymers

It is possible to classify polymer in variable ways. There are two classes, homopolymers and copolymers depending on polymers' monomer contents. Homopolymers are synthesized due to covalent bonding of one type of monomer subunit. In contrast, copolymers are composed linking of at least two types of monomer subunits. According to Figure 2.5, copolymers can be classified as block, random and alternate copolymers with respect to the order of monomer subunits. Blocked polymers are formed of linking two larger chains, while random polymers are formed by linking of monomer subunits randomly. Third type, the alternate copolymers are formed by linking of monomer subunits in an alternative way [93]. Another classification of polymers are due to their existence in nature: natural or synthetic polymers. The natural polymers are identified and harvested from nature, while synthetic polymers are

synthesized industrially [94]. Natural polymers which are used for these purposes are chitosan, alginate, hyaluronic acid, agarose, methylcellulose, collagen and fibrin. On the other hand, poly alpha-hydroxyl acids, polyhydroxyalkanoates, polyacrylates, polycaprolactones, polyanhydrides, polyorthoesters, polyvinyl alcohols and polymethylmethacrylates are all synthetic polymers used in the manufacture of drug release systems, implants and scaffolds [95].

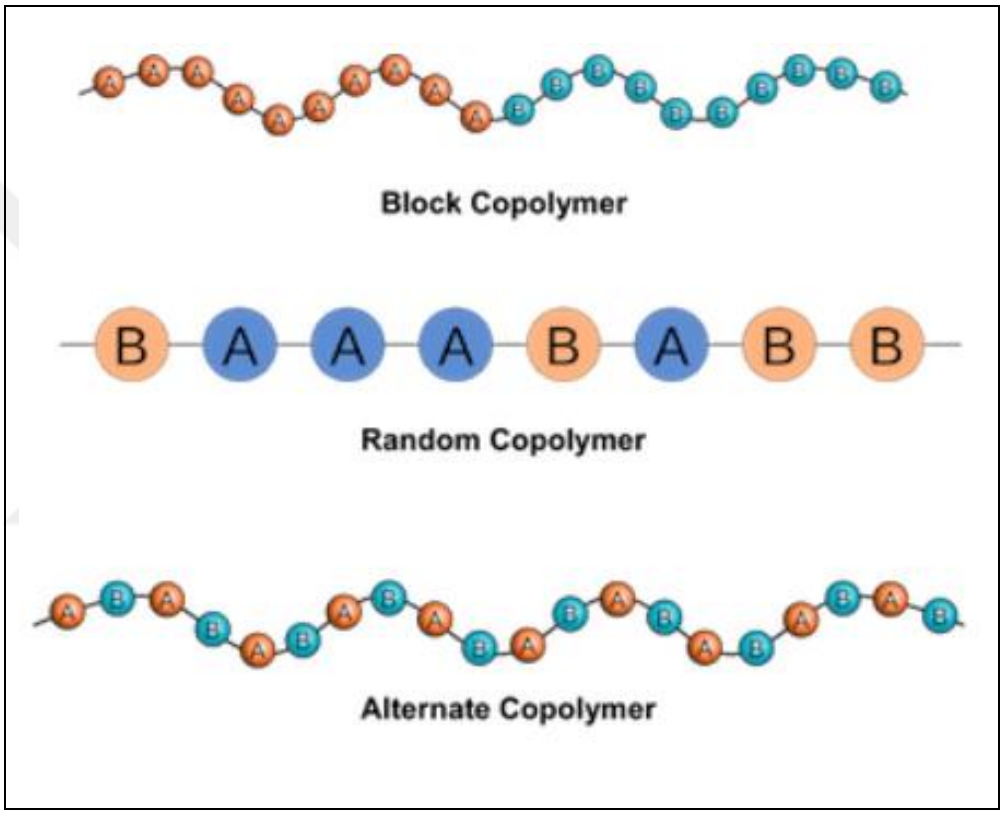

Figure 2.5. Types of copolymers

2.5.2. Classification of Polymers in Accordance with Methods of Synthesis

Classification of the synthesis of polymers can be divided into two groups as Step-growth and Chain-growth polymerization.

2.5.2.1. Step-growth Polymerization

During Step-growth polymerization, polymer's molecular weight is consistently increasing. Monomers are forming dimers, and dimers are forming trimers, thus the polymer chain keep continue growing, which is resulting with high molecular weight macromolecules. Step-growth polymerization can be classified as: poly-condensations whereas polyesters, polyamids etc. form by elimination of a small molecule such as water e.g., and poly-addition whereas polyurethanes and polyurea form without any elimination of small molecules. Step-growth polymerization is an expensive method due to high pressure and temperature requirement compared to Chain-growth polymerization. Thus, many synthetic polymers are synthesized by Chain-growth method [93, 95, 96].

2.5.2.2. Chain-growth Polymerization

Chain-growth polymerization (Figure 2.6) is faster compared to the Step-growth polymerization method. Chain-growth polymerization has three main steps in contrast to Step-growth polymerization, which are initiation, propagation, and termination. In this polymerization an anion, a cation, or a free radical may be used as an initiator. The chain reactions start at initiation step, the initiated species continue building at propagation step this step is the main step where the product was developed, finally the chain reactions end at termination step. During Chain-growth polymerization greatest number of monomers are subjected to free radical polymerization, while less number of monomers are subjected to ionic polymerization.

Free radical Chain-growth polymerization in which polymerization occur in three step as explained above, is started using a radical initiator such as: peroxides etc. Radical initiators stabilized oxygen or other impurities. This polymerization is very common in the chemical industry. A small amount of initiator is required and various monomers could be polymerized. Ionic polymerizations are less well defined compared to free radical polymerizations.

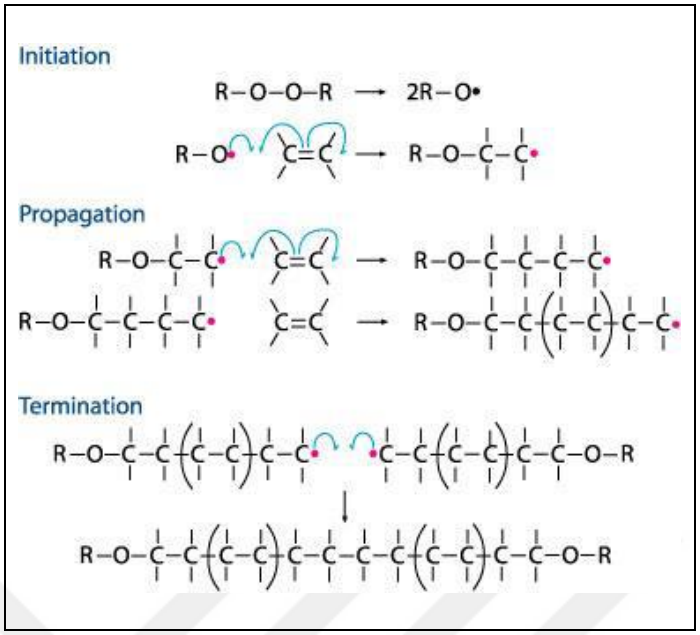

Figure 2.6. Chain-growth polymerization mechanisms [98]

In ionic polymerization, heterogeneous initiators can be used, thus the polymer formation rates are more rapid, however, these initiators are very sensitive to impurities being present most of the time that leads to the difficulties in kinetic studies due to the results are being sensitive to specific reaction conditions [99]. Ionic polymerization occurs as cationic or anionic polymerizations. The formation and propagation of ionic species are involved in both cationic and anionic polymerizations. The low stable and high energy involving ions are more expected to react with most double bonds. The ionic species stable enough to propagate, however they are difficult to form and easy to destroy. The `energetic window` which allows these charged species to form, is slim. The main difference between cationic and anionic polymerization is that cationic polymerization requires monomers have an electron releasing group (e.g. phenyl, vinyl or alkoxy group), while anionic polymerization requires monomers to have an electron withdrawing groups (e.g. nitrile, carboxyl or halide). This selectivity is due to strict regulations for the stabilization of cationic and anionic species [97–99].

2.5.3. Controlled Polymer Synthesis

The mechanical properties of polymers have significant role on their area of utilization. Mechanical properties of polymers are changing depending on the processing and synthesizing methods. In 1956, Swarzc defined a polymerization method which is living/controlled polymerization that does not require chain transfer or termination step [102].

Controlled polymerization method provides specifying the polymerization degree in advance and also attaining polymers with narrow range of molecular weight. In addition, using controlled polymerization method leads producing monodisperse polymers with equal chain lengths. [101, 102]. Controllable polymerization method ensures the reaction continuing until all the monomers within the reaction medium will be consumed, thus, polymers with desired molecular weights can be synthesized. “Controlled Radical Polymerization” (CRP), “Reversible-Addition Fragmentation Transfer” (RAFT), “Atom Transfer Radical Polymerization” (ATRP), and nitroxide mediated polymerizations are some important examples for controlled/living polymerization [104].

2.5.3.1. Olefin Metathesis

Olefin metathesis is widely used for polymer syntheses. Metathesis mechanism consist of breaking carbon-carbon double bond to form a new carbon bond (Figure 2.7) [105].

Olefin metathesis method provides an easy and fast route in production of difficultly synthesized olefins. Additionally, using olefin metathesis provides high yield due to the easy removal of the by product which is ethylene [106]. The metathesis methods are used in double bonded molecules syntheses vary as: “Acyclic Diene Metathesis Polymerization” (ADMET), “Ring Closing Metathesis” (RCM), “Cross-Metathesis” (CM), “Self-Metathesis” (SM) and “Ring Opening Metathesis Polymerization” (ROMP) [106, 107].

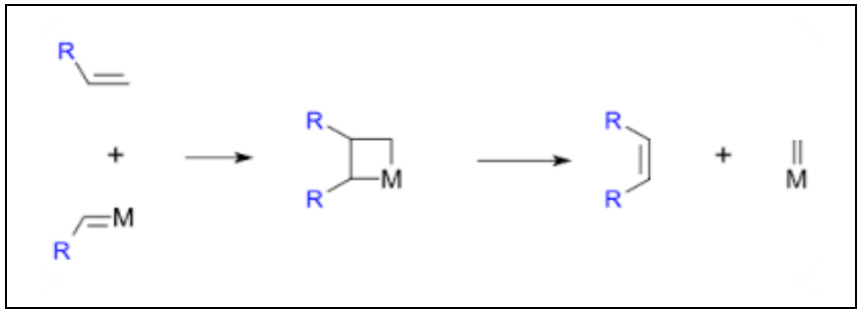

Figure 2.7. Schematic view of olefin metathesis

2.5.3.2. Ring Opening Metathesis Polymerization (ROMP)

ROMP has a great importance in the conversion of cyclic compounds to linear polymers via ring-opening reactions. The significance of ROMP method is that carbon-carbon double bonds are preserved during the polymerization process [109].There is a variety of cyclic monomers that undergo ROMP polymerization such as: lactones, lactams, alkanes, alkenes, heterocyclic compounds containing multiple heteroatoms in the ring, cyclic olefins (e.g. norbornenes, cyclooctenes, cyclobutadienes) [98, 108, 109]. The ROMP method is a type of ionic Chain-growth polymerization where the opened structures are added to the polymer successively [97, 98]. There are two equally important factors in order to polymerize a cyclic monomer via ROMP that the conversion of monomers must be kinetically and thermodynamically possible. In practice, this infers that: (i) the monomer-macromolecule balance has to be shifted to the macromolecule side; and (ii) the corresponding polymerization mechanism need to exist, which can allow the monomer molecules to be converted into polymer repeating units during the operable polymerization period [110]. Cyclic olefins are the most common monomers used in ROMP such as: cis-cyclooctene, cyclopentene, cyclobutene and norbornene [103].

Mechanism of the ROMP polymerization (Figure 2.8) is a unique metal mediated carbon-carbon double bond excess process based on olefin metathesis [103]. During ROMP the unsaturation associated of the monomer is conserved while a polymer is forming. This conservation is an important feature of ROMP which distinguish it from the typical olefin addition polymerizations.

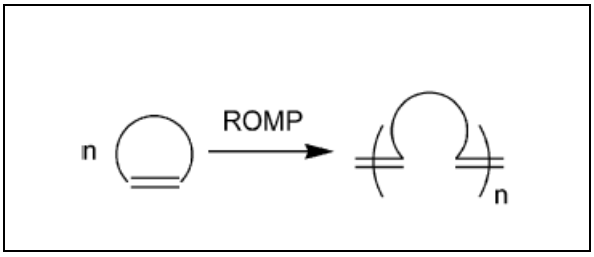

Figure 2.8. ROMP reaction

Figure 2.9 represents the general ROMP mechanism based on the proposal of Chauvin. The initiation starts with the coordination of a cyclic olefin with a transition metal alkylidene complex. The following [2+2]-cycloaddition provides a four-member intermediate, metallacyclobutane, that forms the beginning of a continuous polymer chain. Then, with the cycloreversion reaction of this intermediate a new metal alkylidene is formed. Even though the final compound has an increasement in the size, the reactivity to cyclic olefins remain similar as the initiator due to the incorporated monomer. The polymerization is continued during the propagation step by the repeatation of the analogous steps; until 100 percent conversion of monomers is achieved, or the reaction reached to an equilibrium, or the reaction is terminated. ROMPs are most frequently terminated intentionally by adding a specialized reagent. This reagent has two functions, which are (i) to remove and deactivate selectively the transition metal from the end of the growing polymer chain, and (ii) to shift the metal group with a known functional group [97, 98].

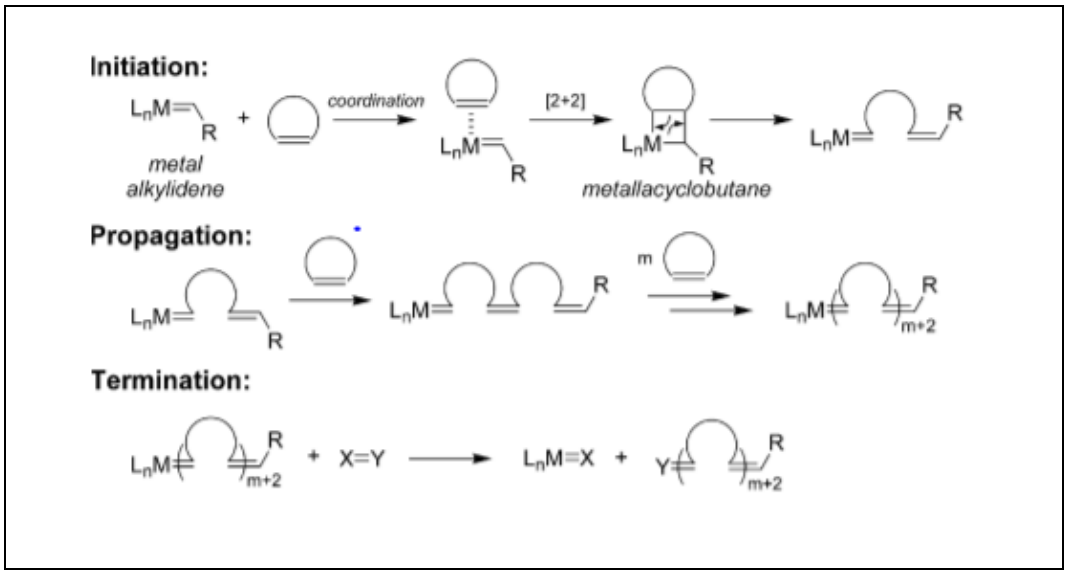

Figure 2.9. General mechanism for ROMP polymerization

Even though, the ROMP reactions are generally reversible, as well as the most olefin metathesis reactions, they are equilibrium-controlled reactions, by considering the polymerization thermodynamics the position of the equilibrium (monomer vs. polymer) can be predicted. As other ROMP polymerizations are driven from monomer to polymer by the releasing strain associated with the cyclic olefin balanced by entropic penalties [103].

ROMP provides intended molecular weights, uniformity of the chain lengths, and balance of the hydrophobic/hydrophilic groups in the synthesis of the polymers, due to its being a well-controlled method. Many studies on synthetic mimic host defense peptides with high activity and selectivity synthesized with ROMP have been reported in literature [21].

2.5.3.3. Catalysts for ROMP Polymerization

ROMP catalysts have essential role on polymerization where precise control over polymerization kinetics are critical. The catalysts for olefin metathesis reactions are transition metals. Chauvin used a specific metathesis mechanism to prove that in order to form a metathesis reaction a metal complex is required (Figure 2.10) [111]. After the achievement of a successful mechanism by Chauvin, the studies on the catalyst have increased. In literature the most efficient catalysts known are molybdenum complexes, which were developed by Schrock *et al*., and the rubidium complexes, which were developed by Grubbs *et al*. (Figure 2.11) [111].

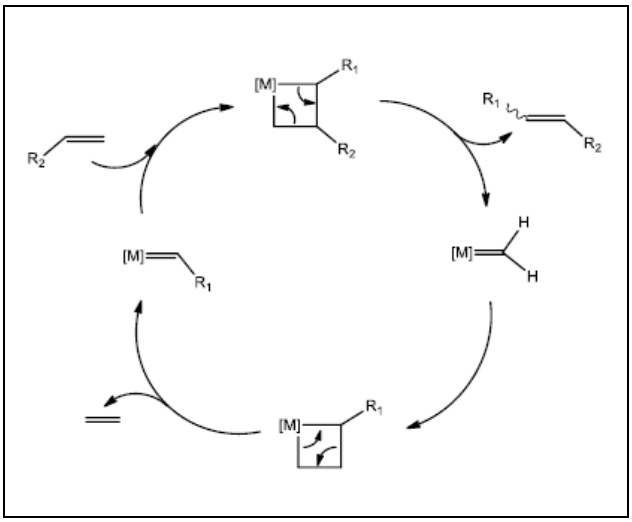

Figure 2.10. Chauvin's mechanism

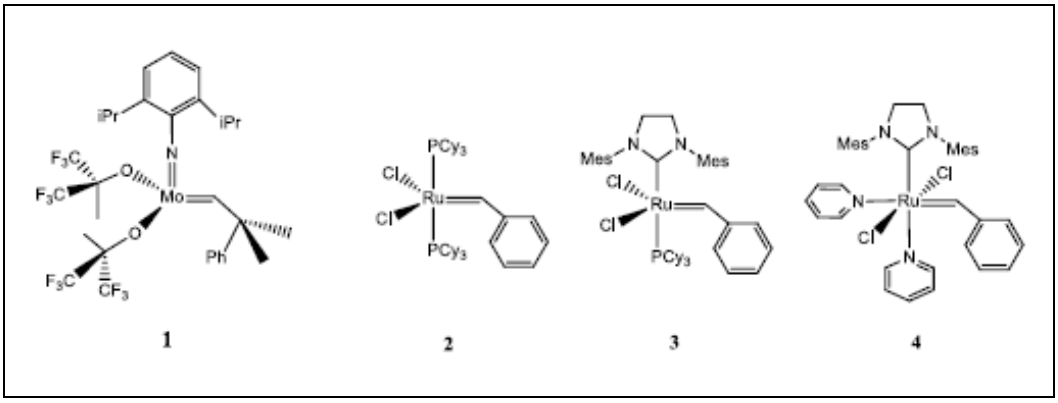

Figure 2.11. Examples of active catalyst for metathesis reaction

The catalysts used for olefin metathesis reactions contain molybdenum, tungsten, and ruthenium. The selectivity of Grubbs catalysts for the olefinic group, their resistance to humidity and atmospheric conditions, and their concordance to variety of solvents lead them to be widely used for olefin metathesis reactions [112].

2.6. NEW TRENDS IN ANTIBIOTIC DESIGN

2.6.1. Antibiotics

Today, there are many commercially available antibiotics such as: amoxicillin, doxycycline, ciprofloxacin, levofloxacin, vancomycin etc. However, bacterial resistance towards these antibiotics have been increasing over the recent few decades. Nowadays, host defence peptides and their synthetic analogous are being studied in the scope of newest trends in antibiotics. In this study, a natural glycopeptide antibiotic, vancomycin was cross metathesized with newly synthesized cationic polymers within the scope of new trends in antibiotics, thus, vancomycin and host defense natural peptides and their synthetic analogous will be described in this section.

2.6.1.1. Vancomycin

Vancomycin (Figure 2.12), is a natural antibiotic which was isolated from *Streptomyces orientalis*, and has a tricyclic glycopeptide structure. Vancomycin binds to the terminal D-

ala-D-ala sequence which is a cell wall precursor and inhibits the cell wall biosynthesis [13, 19, 113]. The bactericidal effect of vancomycin leads to the safe and successful treatments of severe infections caused by MRSA since early 1980s [114]. Vancomycin was first approved by the FDA in 1958 due to its bactericidal activity against Gram (+) bacteria as mentioned previously, however, resistance against coagulase negative *staphylococci* appeared for the first time in 1987. In 1996, the lesser sensitive *S.aureus* was isolated clinically in Japan, and in 2002 a vancomycin resistant strain was isolated from a patient in the US [76,95].

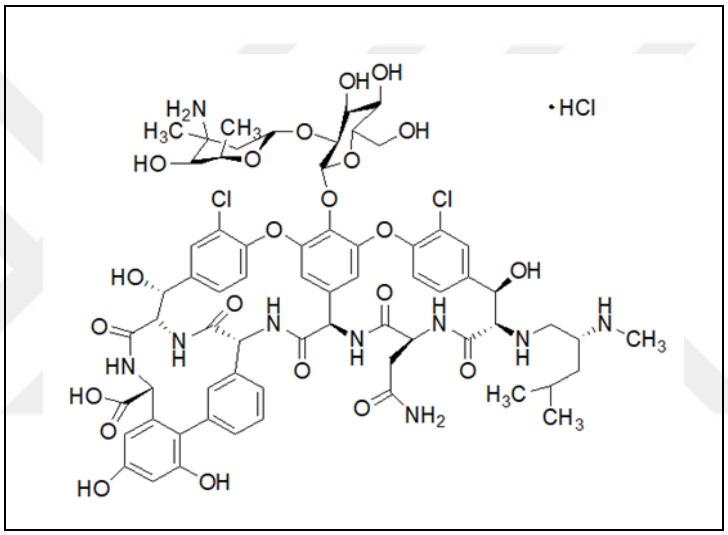

Figure 2.12. Structure of Vancomycin-HCl

Vancomycin is preferred mostly in the treatment of infections caused by MRSA and *Staphylacoccus epidermis.* The minimum inhibitory concentration (MIC) of vancomycin for MRSA and *S. epidermis* were in the range of 1-5 μg/mL and with sufficient concentration it was used successfully fighting against these strains for very long time, however over the time these strains become resistant towards vancomycin and even 10-20 μg/mL of concentration was not sufficient to inhibit these bacteria [91]. In the later years, it was observed that *Staphilacoccus* strains, especially *S. epidermis*, adhere to surfaces such as prothesis and form biofilms, thus decreased the efficacy of vancomycin via blocking the passage through the cell walls, leading to unsucccesful clinical treatments. However, *Streptococcus pneumoniae*, *Streptococcus pyogenes*, B type *streptococci*, *Clostridium difficile* and *Corynebacterium jeikeium* strains continue to be sensitive to vancomycin with

very low MIC levels, since the first usage of vancomycin in clinics. In addition to those problems, the essential drawbacks of treatment with vancomycin are the Gram (-) *Enterococcus* strains. Vancomycin does not exhibit activity towards Gram (-) bacteria due to its inability to pass through the double layered cell wall of Gram (-) bacteria. *Enterococcus faecalis* strains are often inhibited by the achievable concentrations of vancomycin in the serum, however, the vancomycin concentration should be higher than 100 μg/mL in order to exhibit a bactericidal activity. Another disadvantage of vancomycin, it is extracted from body renally and thus it might exhibit nephrotoxic effects on patients while high doses (>20 mg/L or >4 g/day) are induced and/or patients were exposure vancomycin with prolonged treatment times (>7 days) [115]. Minejima *et al.* pursued a study about early identification of vancomycin's nephrotoxicity, in 2011. They reported that, 19 percent of the patients who were received vancomycin treatment for 8 days developed acute kidney injury, and this rate was even higher in ICUs [116]. Systemic administration of vancomycin is limited due to its side effects of nephrotoxicity, ototoxicity, and poor venous tolerance, as well as it is being inactive against Gram (-) and increasing resistance rate [18]. Furthermore, short half life and labile structure are other disadvantages of its use.

2.6.2. Antimicrobial Natural Peptides

The antimicrobial peptides (AMPs) are the part of the immune systems of biological organisms which fight against bacteria and other pathogens, and even cancer cells [117]. AMPs are natural antibiotics, that multicellular microorganisms produce them as a first line of defense [30, 117]. They are promising candidates to combat antibiotic resistance compared to traditional antibiotics, with their facially amphiphilic structures that indicate selectivity i.e. possess high antibacterial activity while exhibiting low hemolytic activity towards human red blood cells. They have been developed against the disease-causing bacteria and are promising candidates for the therapeutic potential because it is speculated that bacteria cannot evolve to become resistant to the membrane-disruption mode of action [35, 36]. Nonetheless, there are some major disadvantages of AMPs such as: they are being salt-sensitive, and susceptible to proteolysis making them unstable in philological environments. Currently, AMPs are producing using recombinant technology in milligram scale and producing them in larger scales is very expensive. In order to overcome these limitations, scientists are focusing on the synthesis of their synthetic mimics [21, 45].

2.6.2.1. Structures of AMPs

In general, the AMPs are classified primer and seconder AMPs according to their structures. Yet, both types share some similarities in their structures, that are the length of the amino acids (<60), their wide spectrum of antimicrobial activity at physiological conditions, and an overall positive charge [118]. Primer structured AMPs have relatively short amino acid chains ranging from 12 to 50 and 50 percent of amino acids are hydrophobic. In addition they carry arginine and lysine amino acids in their structure which lead them to be charged generally +2, and +4, +6 or +7. Secondary AMP has a three dimensional amphipathic structure formed by folding of the peptides on themselves by the help of disulfide bond or by contact with the bacterial membrane. Seconder structure consists of two parts that are the hydrophilic part which is because of the presence of positively charged polar amino acids; and the hydrophobic part which is because of the presence of apolar natural amino-acids. This structure provides strong interactions between the bacterial membrane and the peptide. The seconder structures of antimicrobial cationic peptides may be divided into four classifications: β-sheet peptides (A: β-defensin), α-helical peptides (B: magainin), cyclic peptides (C) and long peptides (D) (Figure 2.13) [31].

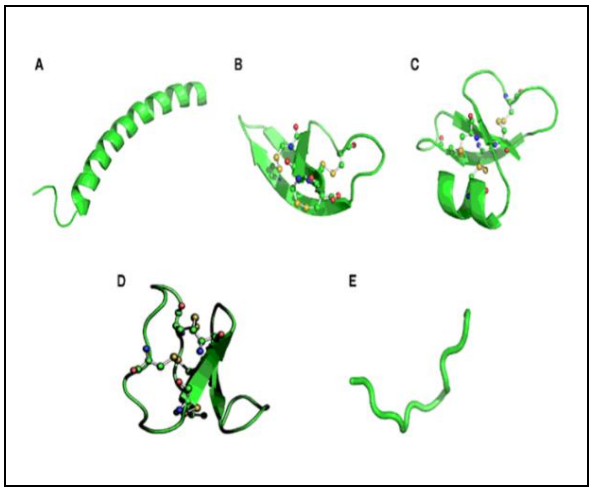

Figure 2.13. Antimicrobial effective cationic peptides structures: A: magainin, B: α-defensin, C: β-defensin, D: bactenecin, E: indolicidin [119]

2.6.2.2. Mechanism of Action of AMPs

The cationic charge and hydrophobic structure of AMPs contribute a considerable role in the interaction with bacteria. Many cationic peptides are able to interact directly with negatively charged cell walls of bacteria. The negative charges of the Gram (-) bacteria are caused by lipopolysaccharides in their outer membranes while Gram (+) bacteria's negative charge is due to lipoteichoic acid in their membranes. Additionally, the phospholipid structured inner membranes of Gram (-) bacteria facilitate the antimicrobial interactions [120].

Toxicity of peptides is another parameter which is as important as antimicrobial activity. AMPs are believed to show cell selectivity, in other words, they kill microorganisms selectively while not being inevitably toxic to host cells. The selectivity of AMPs stands for the difference between mammalian eukaryotic cell membranes and the bacterial cell membrane. While the membranes of eukaryotic cells in mammalians formed by electrically neutral, zwitterionic phospholipids such as sphingomyelin and phosphatidylcholine; the bacterial membrane is formed by neutral phosphatidylglycerol and cardiolipin. In addition, another difference between the cell membranes is while bacterial membrane does not contain cholesterol, but mammalian cell membranes do. Due to these differences AMPs are selective towards bacterial cell membrane [121, 122].

Figure 2.14 represents the AMPs have amphipathic structures with a hydrophobic part (brown) and positively charged part (blue). The electrostatic interaction is the main driving force for cellular association. This interaction occurs on the bacterial surface and mammalian cell surface, between their negatively charged components and the positive charges of AMPs. Glycoproteins' negatively charged sugar chains can also help as binding sites for AMPs. Moreover, the hydrophobic interaction between hydrophobic part of AMPs and lipidic parts of cell membrane also leads peptides to bind to cell [121].

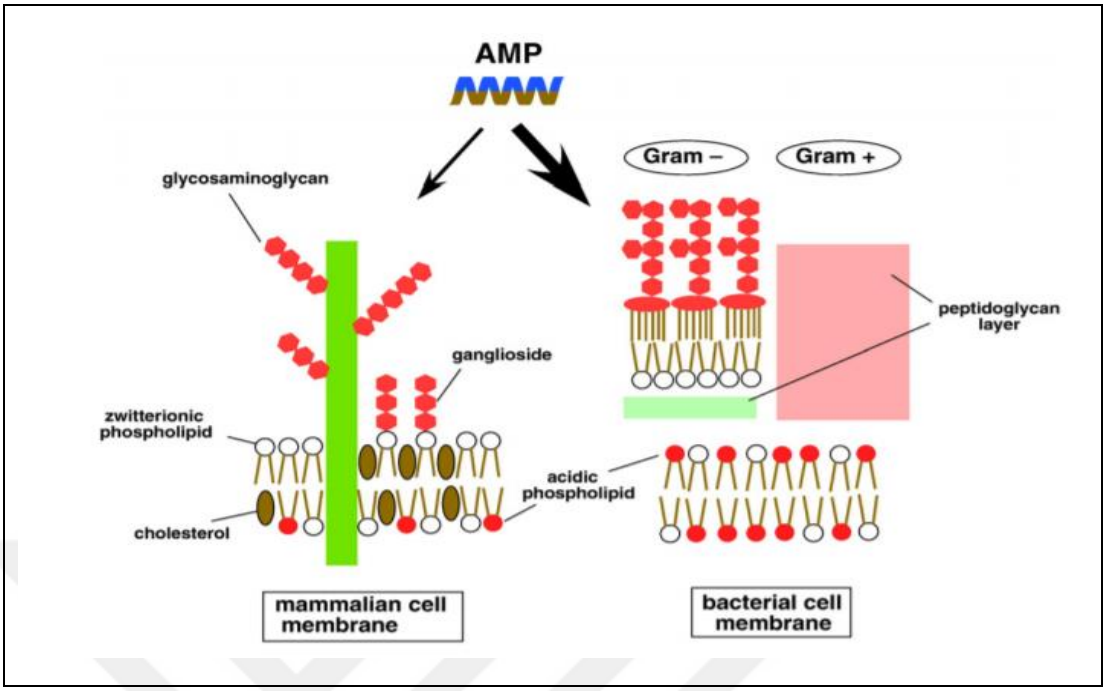

Figure 2.14. Selectivity of AMPs on molecular basis [121]

Many studies have been done to explain the killing mechanism of AMPs, different mechanisms were defined. The electrostatic interaction between the cell membrane of the Gram (+) and Gram (-) bacteria, and the peptide provides the actual lethal effect. During this interaction, the hydrophilic groups of the cationic peptides and the hydrophobic chains of the membrane phospholipids are confronted, the peptides come into a position parallel to the membrane and cause the formation of channels that disrupt membrane integrity [123] (Figure 2.15).

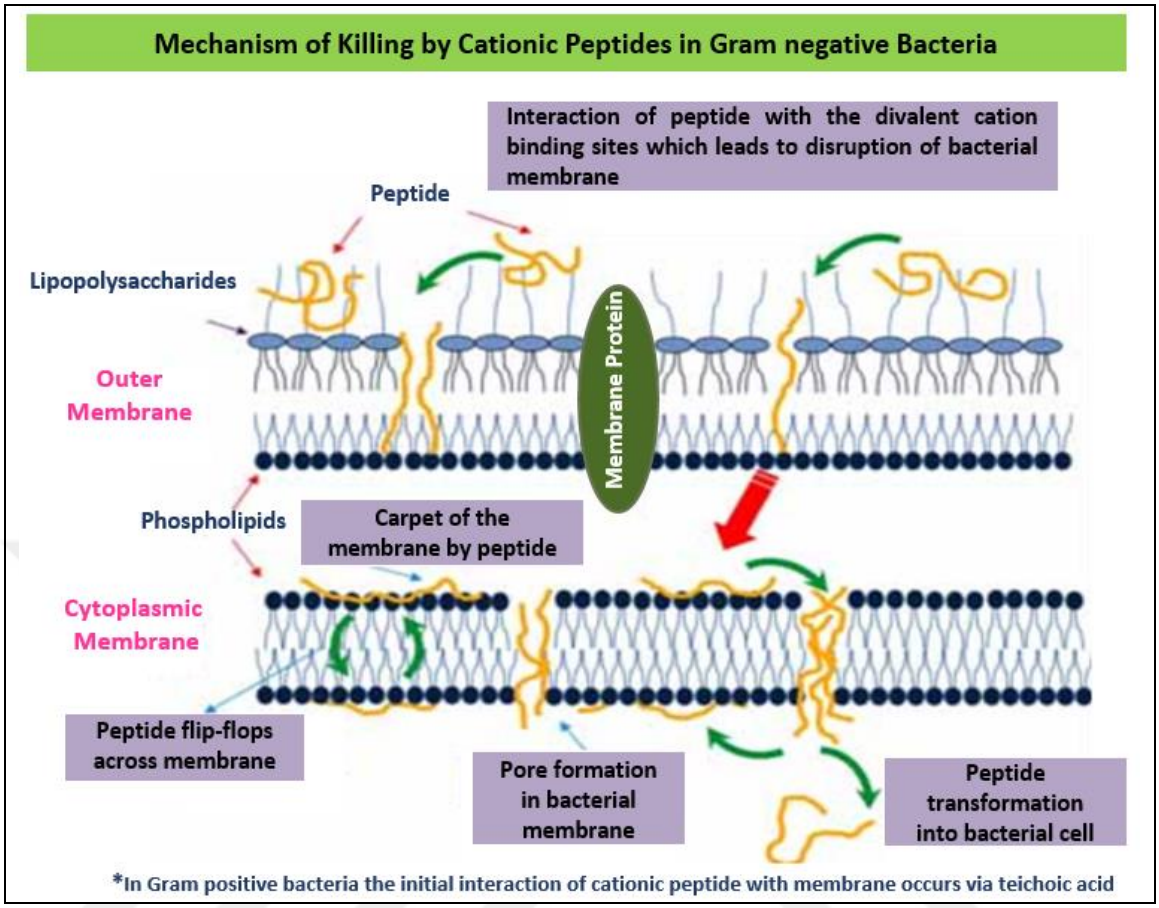

Figure 2.15. Killing mechanism of cationic peptides in Gram (-) bacteria [124]

Antibacterial mechanism occurs differently in solution and on surface [39, 120]. The antibacterial mechanism disrupts cell membranes instead of targeting specific receptors which are on the cellular surface or on the interior of the cell. Simply, cationic peptides and their synthetic analogs form facially amphiphilic structure in aqueous solution. Both electrostatic interaction and hydrophobic interaction between the phospholipid bilayer cause disruption of membrane via several mechanisms [121, 122]. Common proposed mechanisms are toroidal pore barrel-stave pore, and carpet model (Table 2.1).

Table 2.1. Membrane models for Antimicrobial Peptide Killing Mechanisms [128]

Model	Synonym	Examples of peptides
Barrel-Stave	Helical-bundle model	Alamethicin
Carpet-like	-	Dermaseptin S, cecropin, melittin, caerin, ovispirin
Toroidal pore	Wormhole, disk	Magainin, protegrin, melittin, LL-37, MSI-78

In the barrel-stave model, the peptide helices are positioned as a ring in the cell wall of bacteria, forming a bundle with a central lumen in the cell wall which resembles a barrel of peptides as the staves [128]. The α-helical or β-sheet peptides' hydrophobic surfaces face the membrane's acyl chains, meantime the hydrophilic surfaces form the porous lining. The initial step in the formation of barrel-staves pores involve peptide binding on the surface of the cell wall, predominantly as monomers do. When the peptide is binding, it can be subjected to a conformational phase transition, that forces polar-phospholipid head groups to induce localized cell wall thinning [129] (Figure 2.16-A).

The toroidal model (Figure 2.16-B) differs from barrel-stave model as in the toroidal model, peptides are only associated with the lipid head groups, and peptides are inserted in the lipid layer perpendicularly [130]. The aggregation and induction of peptides to the lipid monolayers. A toroidal pore, which is lined by the lipid head groups and the peptides, form due to the continues bending through the pore [123, 125].

According to carpet-like model (Figure 2.16-C), the first interaction between bacteria and peptide occurs electrostatically. In the carpet-like model, accumulation of a high density of peptides on the cell wall of bacteria and a disruption of the cell wall by alignment being parallel to the lipid bilayer surface forms a large surface-like carpet [124, 125].

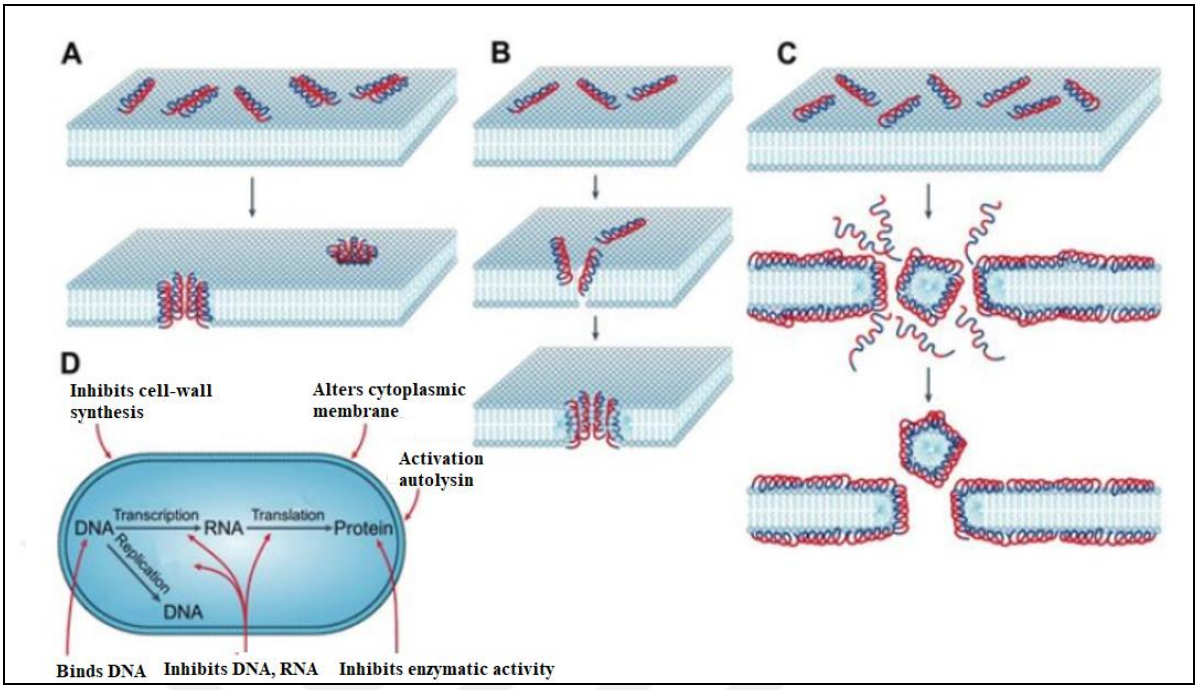

Figure 2.16. Illustration of membrane models of antimicrobial peptide killing mechanisms. A: Barrel-stave model, B: Toroidal model, C: Carpet-like model, D: Mode of action for intracellular antimicrobial peptide activity [132].

2.6.3. Mimicry of Antimicrobial Peptides: Antimicrobial Polymers

Eventhough the antimicrobial natural peptides have many beneficial antimicrobial characteristics, the important obstacles at the large-scale applications of their clinical setting are present [28, 30, 44, 128, 129]. One of the main problems with the application of AMPs as therapeutics is that their functionality and activity are generally identifed in controlled laboratory environments by revealing them to a complex serum medium which leads to a decrease in their functional activity [30, 44, 130, 131]. Another obstacle is that the oral availability of AMPs is low due to the efficient digestion of peptide/protein material by the gastrointestinal tract. Therefore, the additional carriers or additives are required to increase the oral availability and the half-life. As an alternative, it is possible to deliver peptides intravascularly, but it limits the applicability of the peptides and yet the small molecule antibiotics are currently available instead. Another major problem is that the producing peptides as therapeutics in large amounts is highly expensive [30, 128]. According to their antibacterial nature, large-scale fermentations and organic production are unsuitable for

these molecules. Antimicrobial polymers were inspired by natural antimicrobial peptides, and designed according to natural antimicrobial peptides' cationic and amphiphillic natural structures. These polymers are more active, and have low toxicity relative to the AMPs. These polymers have significant advantages over AMPs that they may be produced cost-effectively in much larger amounts, they allow a flexible framework for chemical modifications and adaptations, and are more compatible with the drug delivery systems [45]. In general, the antimicrobial polymers are designed with low molecular weights compared to AMPs [43]. According to the net positive charge of the antimicrobial polymers they may be classified as polycations, however, their low molecular weights, primary ammonium side chains, and hydrophobic components supply new functionalities and characteristics such as: polymer-lipid intractions and altered biological activity. Figure 2.17 shows a few examples of antimicrobial polymers [45].

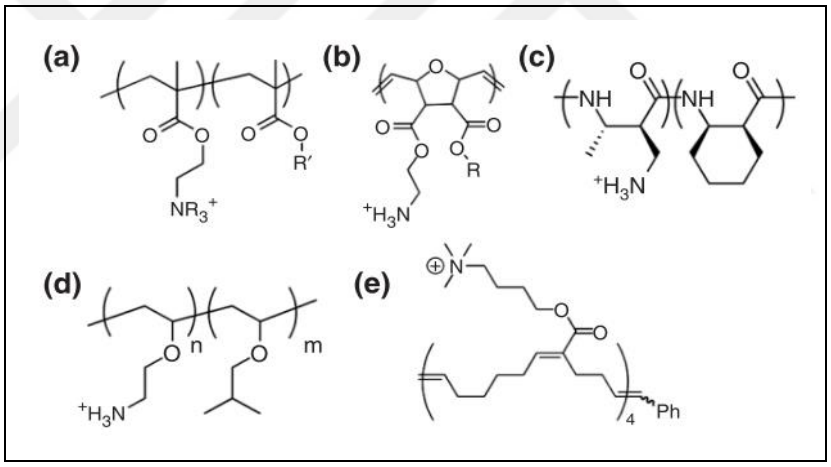

Figure 2.17. Some examples of antimicrobial polymers. (a) methacrylate, (b)norbornene, (c) nylon, (d) vinyl ether, (e) ROMP copolymers. [45]

2.6.3.1. Antimicrobial Activity of Antimicrobial Polymers

The antimicrobial activity of the polymers against bacteria is assessed as an inhibition effect on bacterial growth and bactericidal effect. In general, antimicrobial polymers exhibit wide-spectrum activity towards both Gram (-) and Gram (+) bacteria, conversely, common antibiotics are often more specific due to their cellular targets. Polymers show almost similar

activity with antibiotics against bacteria, but, there appears to not be general trend in Gram positive and Gram (-) strains of preference [45].

Polymers' antimicrobial activity generally increases proportional to the hydropohic content in the side chains, due to increasing hydrophobicity improves the insertation of polymers into the hydrophobic part of bacterial membrane. Also, the elongated cationic side chains in the spacer arms lead deeper insertation due to the cationic ammonium groups bound to the anionic phosphate lipid headgroups and allow the polymer chains to separate from the membrane surface and insert the lipid bilayer deeper, which is known as snorkelling effect [39, 44].

2.6.4. Polymer-Drug Conjugates

Polymers have been getting much attention being used as therapeutic agents for half a century. The polymeric carrier systems such as: conjugation of polymers with drugs or proteins has gained their places in the literature as polymer therapeutics [137]. In 1960s, researchers utilized polymers to use as wound dressing, injectable or implantable depots and blood plasma expanders [138]. In 1975, Ringsdorf suggested a rational model for pharmacologically active polymers for the first time [139]. The Ringsdorf Model suggested that using polymers in therapeutics as polymer-drug conjugates have some remarkable advantages: (i) increase in the aqeous solubility of drugs when the drug conjugated with an water soluable polymer, (ii) controllable drug delivery, which is a very important parameter that provides reducing the amount of drug usage and concordantly reducing the adverse effects of the drug, (iii) altering the pharmacokinetic, and the biodistribution of drugs, which is useful for drugs that have short half-life, or high toxicities, (iv) bring drugs the targetting moieties [137–139].

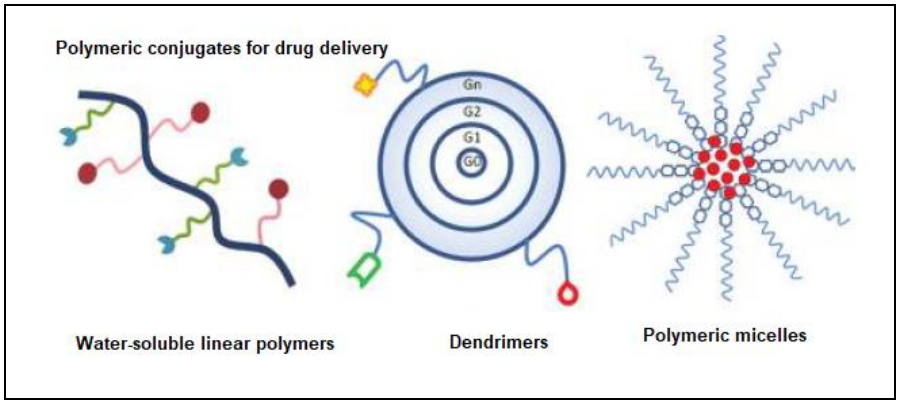

Figure 2.18. Polymeric conjugates for drug delivery [138]

Arimoto *et al*., synthesized vancomycin based multivalent polymer via ROMP polymerization and they reported a significant enhancement of antibacterial activity against VRE [140]. They have used a fast growing multivalent effect in order to enhace the weak non-bonding interactions. Vancomycin binds to the terminal D-ala-D-ala sequence of the bacteria through five hydrogen bonds, thus, Arimoto *et al,* reported that enhancing this association can be enhance the antibacterial activity. They synthesized a vancomycin and norbornene based monomer using ROMP polymerization and using this monomer they synthesized two polymers with two different conditions: (i) polymerization in aqueous emulsion condition (Polymer2), (ii) polymerization in MeOH (Polymer3). The polymerization in aqueous emulsion was slow and had low yield (4 percent), however, they reported a significant improvement with the polymerization in MeOH. They conducted MIC analysis to the monomer and the polymers in order to investigate the antibacterial activity towards *S.aureus, Enterococcus* and VREs. The activity of vancomycin did not changed in the presence of norbornene unit in the monomer, however, after polymerization (Polymer2 and Polymer3) the antibacterial activity significantly enhanced 8 to 60 fold against *S.aureus* and *Enterococcus.* Arimoto *et al*., suggested with this study that polyvalent polymers might be promising in fighting against multi-resistant bacteria.

Lawson *et al*. [58], synthesized acrylamide or PEG acrylate bearing vancomycin derivatives and polymerized them via a surface-mediated reaction. All the vancomycin derivatives were exposed to a 10^4 CFU/mL of *S.epidermis* solution for 20 hours. They have reported that the vancomycin derivatives bearing acrylamide had almost the same antibacterial activity with the control, however, when the activities of the vancomycin derivatives bearing PEG-

acrylate were investigated, the activities were decreased with greater PEG chain length. The activities of the polymers of PEG-acrylate derivatives with longer chain reduced 8-log in CFU compared to the control, while the shorter one showed a 10^7-log reduction. Despite of these results, they suggested that tethering the antibiotic with PEG might be convenient to separate the antibiotic from the camouflaging polymer architecture and allow spatially desired biochemical interactions.

3. MATERIALS AND METHODS

3.1. MATERIALS

3.1.1. Materials for Polymers Synthesis

Furan, tetrahydrofuran (THF), diethyl ether (DE), chloroform, ethyl acetate (EtOAc), hexane (HEX), petroleum ether, methanol (MeOH), methyl iodide (CH_3I), acetonitrile (ACN), pridine, pentane, N,N-dimethyl form amide (DMF), dichloromethane (DCM), ethyl vinyl ether (EVE), triflouroethanol (TFE), dimethyl sulfoxide (DMSO) were received from Sigma Aldrich and utilized without any additional purification. Maleic anhydride, 3-bromopropyl amine hydro bromide, sodium sulfate (Na_2SO_4), sodium chloride (NaCl), sodium bicarbonate ($NaHCO_3$), DABCO, Grubbs catalysts first and second generation, 3-bromopyridine, silica gel were also obtained from Sigma Aldrich. HEX and EtOAc were distilled before using for the reactions.

3.1.2. Materials for Conjugation Process

Vancomycin hydrochloride was obtained from Marmara University, complimentary from Koçak Pharma. PEG-diacrylate (MW: 575 mol/g) and Triethylamine (TEA, 99.5 percent purity) were received from Sigma Aldrich. Dimethyl sulfoxide (DMSO) was received from Fisher Chemical (HPLC grade).

All of the chemicals were purchased in analytical purity and utilized as such, without additional purification. Dialysis cassettes were used for the purification of the vancomycin-PEG conjugate 2000 MWCO which were purchased from Thermo Scientific (Slide-A-Lyzer Dialysis). Additionally, 3500 MWCO dialysis cassettes were purchased from Thermo Scientific (Slide-A-Lyzer Dialysis) and used for purification of vancomycin-PEG-polymer conjugates.

3.1.3. Materials for Cytotoxicity Study

The “Human Umbilical Vein Endothelial Cells” (HUVEC) were supplied from “American type Culture Corporation” (ATCC-CRL-1730, Virginia, USA). DMEM (glucose: 4,5 g/L, PAN Biotech GmbH) was used as cell medium and the cell medium was prepared with addition of 1 percent (volume) of streptomycin-penicillin (Anti-Anti (100X), Gibco), and 10 percent (volume) Fetal Bovine Serum (FBS, PAN Biotech GmbH), for the MTS study. Dulbecco’s Phosphate Buffer Saline Solution (w/o: Ca^{2+}, w/o: Mg^{2+}) was supplied from PAN Biotech GmbH. Trypsin-EDTA (0.25 percent, 1X) was supplied from Gibco.

3.2. METHODS

3.2.1. Nuclear Magnetic Resonance Spectroscopy (NMR)

NMR spectroscopy is a method that is upon the absorption of electromagnetic rays by the nuclei of the molecules. All nuclei are electrically charged. Thus, with the application of an external magnetic field, an energy transfer transpires from the base energy to a higher energy at a wavelength that corresponds to radio frequency. NMR absorption bands are named as peaks, and the plot obtained by marking frequencies against the peaks that are formed as a result of absorption is called the "NMR spectrum". NMR spectroscopy is a widely used method in order to determine molecular structure of compounds. Using this method together with other instrumental methods like infrared and mass spectrometry, allows scientist to characterize the entire structure of a molecule [132, 133, 134]. NMR spectroscopy differs from other spectroscopic methods such IR and UV. NMR spectroscopy gives information on the skeleton of the molecule, depending on the magnetic character of the atomic nuclei of the related compound, while IR and UV provides information about the functional groups of the molecules and percentage of the C, H, O, N, S atoms in the molecules. NMR spectroscopy requires strong electromagnetic field and radio waves, which are very long wavelengths of the electromagnetic spectrum.

In this study, Bruker Avance III 500 MHz spectrometer was used to obtain ^{13}C NMR and ^{1}H NMR spectra. For the analysis of NMR data, the appropriate frequencies were applied using either residual $CDCl_3$, D_2O or DMSO-d_6 as internal reference (for ^{1}H and ^{13}C).The

structures of the synthesized polymers and conjugates were determined using NMR techniques.

3.2.2. Fourier Transform Infrared Spectroscopy (FTIR)

FTIR spectroscopy is one of very common methods used in the characterization of organic compounds qualitatively and quantitatively. FTIR provides information on molecular structure, chemical bonding, and functional groups in the molecules [144]. FTIR has the ability of collecting spectra from a very wide range of materials in solid, liquid and gaseous phases [145]. In this study Attenuated total reflection (ATR) technique, which is a sampling tool of FTIR was used. In recent years, ATR has reformed for solid and liquid sample analyses through challenging the most difficult aspects of infrared analysis, that are the spectral reproduction and the preparation of sample and [143]. ATR provides non-destructive measurement of samples without any extra performance for preparing the samples, which increases the speed of the analysis [146].

ATR imposes single or multiple reflections on an optical beam at the interface between a sample and a material. It is important that the material must be transparent in the chosen wavelength region and possess a high refractive index (n). The IR beam with a certain angle is channeled into a visually impenetrable crystal, high in the refractive index. Thus the internal reflection creates an evanescent wave and this wave extends beyond the surface of the crystal into the sample positioned in the immediate vicinity of the crystal. The resulting strength for the evanescent wave is typical of the proximity to the sample, which is the basic idea behind the ATR method [147]. In this study, ATR method of FTIR (Thermo Fischer Scientific, Nicolet™ iS50) was used additional to the NMR techniques to characterized the synthesized polymers and the conjugates.

3.2.3. High Pressure Liquid Chromatography (HPLC)

In the analytical chemistry, HPLC might be one of the most common tools among all of the chromatographic techniques which use liquid mobile phase [143]. HPLC has become the preferred method of analyzing a wide range of compounds over the last decade. The essential advantages of the HPLC compared to gas chromatography (GC), is that the analytes are not

supposed to be volatile, thus, allowing analysis of the macromolecules. In the HPLC analysis, a minute amount of the sample in liquid form is injected into the moving fluid stream -a mobile phase which passes through a column packed with stationary phase particles [148] A high pressure must be everted on the mobile phase for continuous flow, thus, the stationary phases have porous monolithic material or spherical micro-particles to lead a significant drop in pressure in the column [143]. HPLC is widely used in many fields including the pharmaceutical, biotechnology, food, cosmetics, environmental and polymer industries [149].

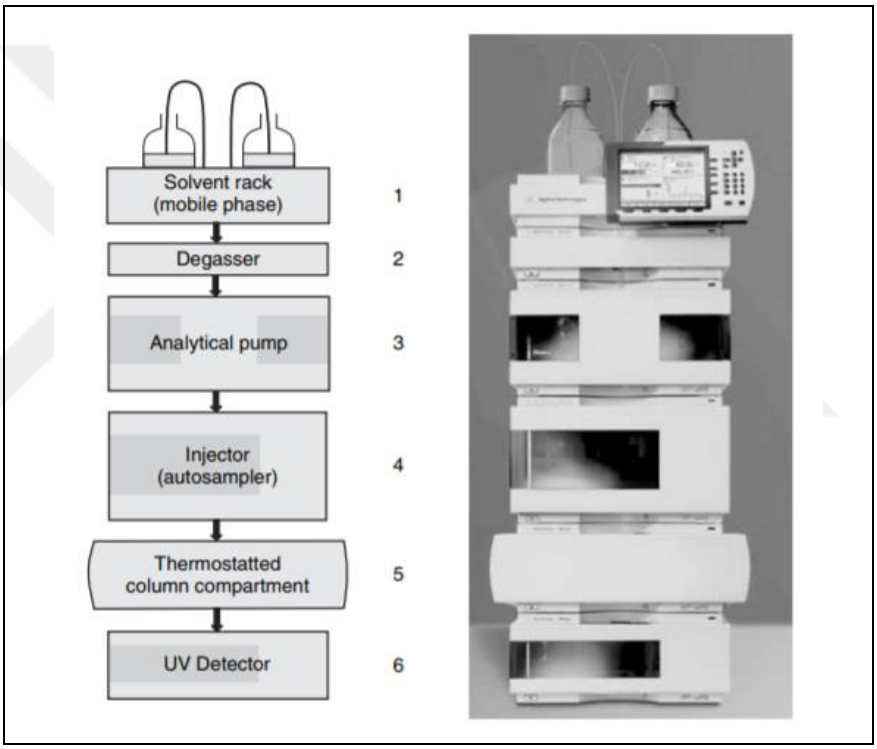

Figure 3.1. Schematic demonstration of HPLC instrument [143]

The HPLC instrument consists of various specialized units that can be either separated entities or integrated into a common framework (Figure 3.1). Miniscule internal diameter tubing system (0.1 mm) ensures the movement of the mobile phase between modules. The tubing system is produced using stainless steel or polyether-ether ketone, which is a colored and flexible polymer, that the system can withstand common solvents under high pressure (up to 350 bars) [143].

The HPLC analysis is performed using a small amount of sample, that must be in the liquid phase, is injected into the mobile phase which is pumped to the column contains the stationary phase at a constant rate. When the sample reaches the column, it separates into its components depending on different degrees of retention of the individual component within the column. The sample component that is retained within the column is determined by its division between the liquid and the stationary phases. The characteristic retention time of the eluted components is provided with this detection technique. The effecting parameters of the retention time are the strength of the interactions between the components and the stationary phase, the solvent ratio and/or composition, and the flow rate of the mobile phase [149].

In this study HPLC was used for characterization of vancomycin-PEG conjugate, vancomycin-PEG-polymer conjugates. The release of vancomycin from VP-PEG-polymer conjugates was also monitored using HPLC. The method and information about the HPLC is given in Table 3.1.

Table 3.1. HPLC information and conditions

HPLC conditions	**Information**
System	Waters 717 Autosampler, Waters 2487 UV detector, Waters 1525 Pump, Empower software
Detector	UV detector, 236 nm
Mobile Phase	25 mM K_2HPO_4 (91 percent), ACN (9 percent)
Flow rate	1.2 mL/min
Injection volume	50 μL
Elution	Isocritic
Furnace Temperature	Room Temperature
Solvents for standards	diH_2O

3.2.4. Scanning Electron Microscop (SEM)

SEM microscopy uses a high-energy electrons' focused beam and generates multitude of signals on to the surface of solid specimens. This technique gives information about orientation of the material, the chemical composition of the material, crystalline structure and surface morphology of the material according to the signals derived from electron-sample interactions [150]. In the majority of applications, a two-dimensional image is generated that shows the spatial variations of a specific area on the sample surface.

A basic construction of SEM microscopy requires an electron gun which produces electron beam, a condenser and objective lenses which control the beam diameter, a specimen where the beam scanned over, a sample stage and a software which collects data (Figure 3.2). The penetration of the electron beam into the sample leads to the acceleration of the voltage, and density of the specimen produces the signals of secondary electrons, back-scattered electrons and characteristic X-rays which are collected by detectors. Finally the images are created according to these signals and monitored from a computer [151].

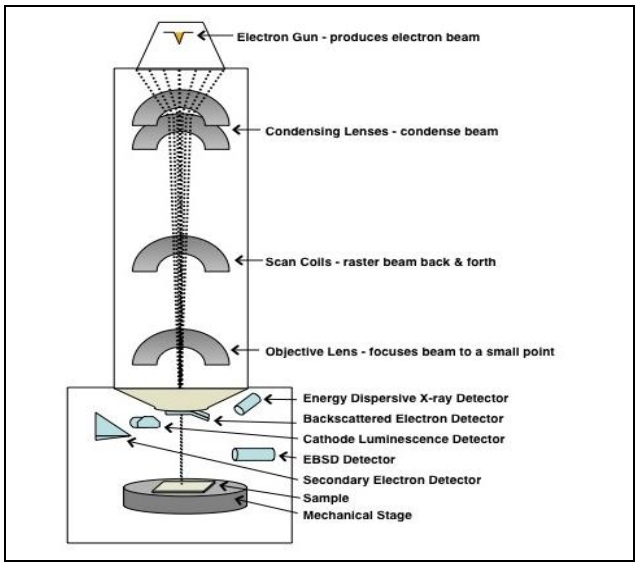

Figure 3.2. Schematic diagram of the Scanning Electron Microscopy

In this study, SEM (EVO/MA10, Zeiss) analysis was used to monitor the morphological damage of *S.aureus* in the presence of vancomycin-polymer conjugates.

4. EXPRIMENTAL STUDY

4.1. SYNTHESIS OF COMPOUNDS AND MONOMERS

4.1.1. Synthesis of 4,10-Dioxa-tricyclo [5.2.1.$0^{2,6}$] dec-8-ene-3,5-dion (Compound 1) via Diels Alder Reaction between Maleic Anhydride and Furan

63 grams (0.66 mol) of maleic anhydride was dissolved in 200 mL of THF in an erlenmeyer flask and 49 mL (0.63 mol) of furan was added, then $N_{2(g)}$ was purged into the flask for 5 minutes. Due to the photo sensitivity of the product, the erlenmeyer flask was covered with aluminum foil and the reaction was held in a dark room for four days. Then, the crystal product was formed. The product was washed using 200 mL of cold THF (100 mLx2) and filtered. The obtained crystals were dried under vacuum at room temperature (Compound 1, Figure 5.1).

4.1.2. Synthesis of Bromooxanorbornene (4-(3-bromopropyl)-10-oxa-4-azatricyclo [5.2.1.$0^{2,6}$] dec-8-ene-3,5-dione) (Compound 2)

The synthesis of bromooxanorbornene was altered from Bazzi and Sleiman's (2002) study [152]. 5.44 grams (0.065 mol) of $NaHCO_3$ was dissolved in 50 mL of diH_2O, 14.24 grams (0.065 mol) of 3-bromo propyl amine hydrogen bromide was added, and stirred rapidly at room temperature, under $N_{2(g)}$ atmosphere. 10 grams (0.06 mol) of the pulverized Compound 1 was added to the reaction and continued stirring for 45 minutes. After 45 minutes, the reaction mixture was filtered and washed with diH_2O (20 mL x 1), and DE (20 mL x 3). The washed product was dried in a vacuum oven and white powder product was collected.

For the second step of the procedure an oil bath was heated to 90 ^{o}C. A two neck round-bottomed flask was used for this procedure, a condenser was placed on to the main neck to prevent the solvent loss caused by the high temperature, and the second neck was used for $N_{2(g)}$ purging of the system. 0.72 grams (0.0082 mole) of sodium acetate was stirred with 16 mL of acid anhydride for 15 minutes in the round-bottomed flask. After 15 minutes, 4 grams of (0.013 mol) of white product that was collected from the first step, was added to the round-

bottomed flask and continued stirring at 90 ºC for 4 hours, then, the reaction mixture was poured on 20 grams of ice, and extracted using $CHCl_3$ (50 mL). Further extractions were conducted using 10 percent $NaHCO_3$ (3x50 mL) and 10 percent NaOH (1x50 mL) solutions. After extractions, $Na_2SO_{4(s)}$ was added to the product phase, in order to remove the aqueous phase from the solution and filtered. The residual solvent was removed under vacuum. The dried product was purified using column chromatography technique. In this technique, EtOAc:HEX (1:1, v/v) mixture was used as mobile phase. After column chromatography, the remained solvent was removed using rotary evaporator, and white solid product (Compound 2, Figure 5.1) was obtained.

4.1.3. Synthesis of Pyridinium Salt Bearing Oxanorbornene (Monomer 1)

0.6 gram (0.002 mol) of Compound 2 was dissolved in 5 mL of ACN and 0.40 mL (0.005 mole) of pyridine was added dropwise. The reaction was stirred at 60 ºC under $N_{2(g)}$ atmosphere, overnight. The product was washed with THF (20 mLx4) and dried using a vacuum oven. The pure light pink solid product (Monomer 1, Figure 5.1) was obtained.

4.1.4. Synthesis of DABCO Salt Bearing Oxanorbornene

The DABCO double-charged salt bearing Monomer 2 was synthesized in two steps. First mono charge was formed (Compound 3) then the additional charge was obtained using either methyl iodate or propyl bromide to the Compound 3.

4.1.4.1. Mono-charged Salt Bearing Oxanorbornene (Compound 3)

0.85 grams (0.003 mol) of Compound 2 was dissolved in EtOAc (8 mL) in a vial, meantime 0.46 grams (0.005 mole) of DABCO was dissolved in10 mL of EtOAc and added a drop at a time into the vial and the mixture was stirred for 2 days under $N_{2(g)}$ atmosphere at room temperature. The vial was blanketed using aluminum foil. After 2 days, the precipitated product was collected and washed with EtOAc (20 mL x 3) and DE (20 mL x 1). The pure white solid product (Compound 3, Figure 5.1) was obtained.

4.1.4.2. Synthesis of DABCO Double-charged Salt (via methyl iodate) Bearing Oxanorbornene (Monomer 2)

0.1 grams (0.00025 mol) of Compound 3 was dissolved in THF:MeOH (3:10, v/v) mixture in a vial. 1.83 grams (0.014 mol) of methyl iodine (CH_3I) was dissolved in 1 mL of MeOH and added to the vial a drop at a time within 10 minutes and stirred for 2 days at room temperature under $N_{2(g)}$ atmosphere. Then, the precipitated product was collected and washed with THF:MeOH (8:12 v/v, 3:7 v/v) mixture for 6 times and DE for 2 times, then dried under vacuum. The final yellow solid product (Monomer 2, Figure 5.1) was obtained.

4.1.4.3. Synthesis of DABCO Double-charged Salt (via Propyl Bromide) Bearing Oxanorbornene (Monomer 3)

2 grams (0.005 mol) of Compound 3 and 2.28 mL (0.025 mol) of propyl bromide was dissolved in 15 mL of MeOH in a round-bottomed flask. The round-bottomed flask was placed into an oil bath at 50 ^oC. The reaction was stirred for 48 hours with a reflux setup, under $N_{2(g)}$ atmosphere. 48 hours later, the reaction mixture was placed in an evaporating flask and the excess MeOH was evaporated with rotary evaporator at 40 ^oC, 400 mbar, until 2-3 mL of the reaction solution is left. After evaporation process, the reaction mixture was added drop by drop into 25 mL of DE in a 50 mL of falcon tube, and centrifuged for 2 minutes at 2000 rpm. Viscous, yellow colored product was obtained and washed with dietyl ether for 3 more times. Then, the product (Monomer 3, Figure 5.1) was dried under vacuum.

4.1.5. Synthesis of Trimethoxyphenyl Phosphonium Bearing Oxanorbornene (Monomer 4)

0.5 grams (0.00175 mol) of Compound 2 and excess amount 1.8487grams (0.00525 mol) Tris(4-methoxyphenyl)phosphine were dissolved in 15 mL of EtOAc in a round-bottomed flask. The reaction was held at 50 ^oC using an oil bath, and stirred for 24 hours under $N_{2(g)}$ atmosphere. The product was precipitated using DE and washed with THF:DE (1:1, v,v) mixture and dried in a vacuum oven. The final white colored product (Monomer 4, Figure 5.2) was obtained.

4.1.6. Synthesis of Triphenyl Phosphonium Bearing Oxanorbornene (Monomer 5)

0.5 grams (0.00175 mol) of Compound 2 and excess amount 1.376 grams (0.00525 mol) of triphenylphospine were dissolved in 11 mL of EtOAc in a round-bottomed flask. The round-bottomed flask was then placed into a 50 ^{o}C oil bath. The reaction was stirred for three days at room temperature under $N_{2(g)}$ atmosphere. The precipitated product was collected and washed with EtOAc and THF. Then, the product was dried using a vacuum oven. Beige colored Monomer 5 was obtained (Figure 5.2).

4.2. SYNTHESIS OF 3RD GENERATION GRUBBS CATALYSTS

Grubbs catalyst 3rd generation (Grubbs 3) was synthesized from Grubbs catalyst 2nd generation according to Love *et al.*'s (2002) study [153]. The structures of Grubbs Catalyst are shown in Figure 4.1. 0.5 mL of 3-bromopyridine was reacted with 0.2 g of Grubbs 2 for 10 minutes in an aluminum covered vial, under $N_{2(g)}$ atmosphere. The obtained Grubbs-3 was precipitated and washed with pentane, and then dried under vacuum. The Grubbs 3 was kept in an aluminum covered vial in order to protect from light, at +4 ^{o}C (MW: 884.48 g/mol).

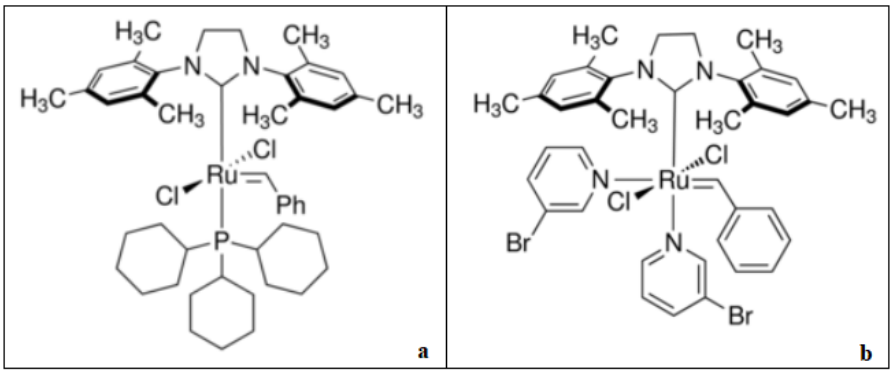

Figure 4.1. Structures of Grubbs Catalysts: a) Grubbs Catalyst 2nd Generation, b) Grubbs Catalyst 3rd Generation

4.3. SYNTHESIS OF POLYMERS

4.3.1. Homopolymerization of DABCO Double-charged Salt Bearing Oxanorbornene via ROMP

The homopolymers were synthesized with two different molecular weights, 3000 g/mol and 10000 g/mol. The molecular weight of the polymers were adjusted using a required amount of Grubbs catalyst. The required amount of Grubbs catalyst for the synthesis of 3000 g/mol of DABCO double charged monomer was calculated as below.

$$mol\ of\ monomer = \frac{mass\ of\ monomer\ (g)}{Molecular\ Weight\ of\ monomer\ (g\ mol^{-1})} \tag{4.1}$$

$$[Mol\ of\ monomer] = \frac{0.1\ g}{539.94\ {}^{g}/_{mol}}$$

$$[Mol\ of\ monomer] = 0.0001852\ mol$$

$$DP = \frac{Molecular\ Weight\ of\ Polymer\ (g\ mol^{-1})}{Molecular\ Weight\ of\ Monomer\ (g\ mol^{-1})} \tag{4.2}$$

$$DP^{*} = \frac{3000}{539.94}$$

$$DP = 5.55$$

$$DP = \frac{mol\ of\ monomer(mol)}{mol\ of\ catalys\ (mol)} \tag{4.3}$$

$$5.55 = \frac{0.0001852}{[\ mol\ of\ catalyst\ (mol)]}$$

$$Mass\ of\ catalyst\ (g) = Mole\ of\ catalyst\ (mol)\ x\ Molecular\ Weight\ of\ Catalyst\ (g.mol^{-1}) \tag{4.4}$$

$$[Mass\ of\ catalyst\ (g)] = 0.000033\ mol\ x\ 884.48\ g.mol^{-1}$$

$$[catalyst] = 0.0295\ g$$

Where, DP is degree of polymerization. This calculation was used for all the polymers that where synthesized within this project.

4.3.1.1. Synthesis of DABCO Double-charged (via methyl iodate) Cationic Homopolymer (D-3)

0.1 g of Monomer 2 was dissolved in DMF in a vial. 0.0295 grams of Grubbs 3 catalyst was dissolved in 0.5 mL of DCM and added to the vial in one rapid shot. Grubbs 3 catalyst is a photo sensitive catalyst, thus, in order to prevent the reaction from the light, the vial was covered with aluminum foil for all the polymer synthesis which include Grubbs catalysts. The polymerization was continued at room temperature under $N_{2(g)}$ atmosphere, overnight. The polymerization was terminated with the addition of 0.5 mL of 30 percent EVE in DCM. Then, D-3 (Figure 5.18) was precipitated with DE, and washed with THF. The polymer was dried under $N_{2(g)}$.

4.3.1.2. Synthesis of DABCO Double-charged Cationic (via methyl iodate Homopolymer (D-10)

0.1 g of Monomer 2 was dissolved in 4 mL of TFE and 0.0088 grams of Grubbs 3 catalyst dissolved in 0.5 mL of DCM was in one rapid shot, and the reaction was stirred for 3.5 hours. Then 0.5 mL of 30 percent EVE in DCM was added in order to inhibit the catalyst, and continued stirring for 30 minutes. The following day, the polymer (D-10, Figure 5.18) was precipitated with DE and washed with THF for 3 times, and dried using $N_{2(g)}$.

4.3.1.3. Synthesis of DABCO Double-charged (via Propyl Promide) Cationic Homopolymers (ID-3, ID-10)

0.1 g of Monomer 3 was dissolved in 4 mL of MeOH:DCM (1:1, v,v) mixture and 0.0294 grams of Grubbs 3 catalyst dissolved in 0.5 mL of DCM was added in one rapid shot, and continued stirring for 6 hours at room temperature. After 6 hours, 0.5 mL of 30 percent EVE in DCM was added in order to inhibit the catalyst. The polymer was precipitated with DE and washed with DE:THF (2:1, v,v) mixture for 3 times. The polymer (ID-3) was dried using a vacuum oven at room temperature for 3 hours. On the purpose of synthesis of ID-10, the same procedure was followed using 0.0088 grams of Grubbs 3 catalyst.

4.3.2. Homopolymerization of Pyridinium Salt Bearing Oxanorbornene via ROMP (P-3, P-10)

The pyridinium salt bearing homopolymers were also synthesized with two different molecular weights as 3000 g/mol and 10000 g/mol.

For the synthesis of the pyridine based polymer with the molecular weight of 3000 g/mol (P-3, Figure 5.18); 0.1 g of Monomer 1 was dissolved in 2.5 mL of MeOH:DMF (0.5:2, v/v) mixture and the 0.0294 grams of Grubbs 3 catalyst in 0.5 mL of DCM was added in one rapid shot, and the reaction was stirred overnight. The next day the polymerization terminated with 0.5 mL of 30 percent Eve in DCM. The polymer was precipitated with DE and washed with THF for 3 times and dried using $N_{2(g)}$. P-10 (Figure 5.18) was synthesized using 0.0088 grams of Grubbs 3 catalyst with the same procedure.

4.3.3. Copolymerization of Pyridinium Monomer (Monomer 1) and DABCO Double-charge Monomer (Monomer 2) via ROMP

Three different random copolymers were synthesized using DABCO and pyridinium salt bearing monomers with different weight ratios. For this purpose Monomer 1 and Monomer 2 were used with different ratios as 1:1 (D1-P1), 1:2 (D1:P2), and 2:1, (D2:P1), respectively (Figure 5.25). The desired molecular weight for the copolymers was 5000 g/mol. The required monomer amounts, the degree of polymerizations, and the required amount of Grubbs 3 catalyst were calculated using the same equations (Equation 4.1-4.4) used for the homopolymerization.

For the synthesis of D1-P1 (1:1 weight ratio of monomers), 0.1 grams of Monomer 2 and 0.099 grams of Monomer 1 were dissolved in TFE (3 mL) and 0.0353 grams of Grubbs 3 added to the reaction in one rapid shot, and continued stirring overnight, under $N_{2(g)}$ atmosphere. The next day, the reaction was trminated with the addition of 0.5 mL of percent30 EVE in DCM . The copolymer was precipitated with DE, and washed with THF and DE, then dried using $N_{2(g)}$. D1-P2 (1:2, weight ratio of monomers) and D2:P1 (2:1 weight ratio of monomers) were synthesized with following the same procedures using required amount of Grubbs-3 catalysts.

4.3.4. Homopolymerization of Trimethoxy Phosponium Bearing Oxanorbornene via ROMP (M-3, M-10)

The trimethoxy posphonium bearing homopolymers were synthesized with two different molecular weight as 3000 g/mol and 10000 g/mol.

For the synthesis of the polymer with 10000 g/mol molecular weight (M-10); 0.1 g of Monomer 4 was dissolved in 2 mL of dry DCM. 0.0088 grams of Grubbs 3 catalyst were dissolved in 0.5 mL of dry DCM and added to the mixture in one rapid shot. The reaction was held under $N_{2(g)}$ atmosphere overnight. The polymerization was terminated with the addition of 0.5 mL of 30 percent EVE in DCM. The polymer was precipitated with DE and washed with DE and THF, then dried in a vacuum oven. M-3 (MW: 3000 g/mol, Figure 5.19) was synthesized following the same procedure using 0.0294 grams of Grubbs 3 and shortening the reaction time to 2 hours.

4.3.5. Homopolymerization of Triphenyl Phosphonium Bearing Oxanorbornene via ROMP (Phe-3, Phe-10)

The phenyl based homopolymers were synthesized with two different molecular weight as 3000 g/mol and 10000 g/mol.

For the synthesis of the polymer with 10000 g/mol molecular weight (Phe-10); 0.1 g of Monomer 5 was dissolved in 2 mL of dry DCM. 0.0088 grams of Grubbs 3 catalyst were dissolved in 0.5 mL of dry DCM and added to the mixture with one rapid shot. The reaction was held under $N_{2(g)}$ atmosphere overnight. The polymerization was terminated with the addition of 0.5 mL of 30 percent EVE in DCM. The polymer was precipitated with DE and washed with DE and THF, then dried using a vacuum oven. Phe-3 (3000 g/mol, Figure 5.19) was synthesized according to the same procedure explained above, using 0.0294 grams of Grubbs 3 with the same reaction time.

4.4. CONJUGATION OF VANCOMYCIN AND PEG-DIACRYLATE VIA MICHAEL ADDITION REACTION

Conjugation of vancomycin and PEG diacrylate was conducted via michael addition (Figure 5.39) which is also known as 1, 4 addition or conjugate addition [154].

The excess amount of PEG-diacrylate (4.2 g, 7.30 mmol), vancomycin (0.2 g, 0.14 mmol) were weighed and transferred into a round bottom flask. 15 mL of DMSO was added as a solvent and they were stirred for 30 minutes at room temperature. Then, 0.18 g TEA (1.78 mmol) was added as a catalyst in order to neutralize free HCl. After the addition of TEA, $N_{2(g)}$ was purged to mixture for 5 minutes, and the system was sealed. The reaction mixture was stirred magnetically for 5 days under $N_{2(g)}$ atmosphere.

4.4.1. Purification of the Conjugate

The reaction mixture, which was obtained after 5 days of mixing, was transferred into dialysis cassettes. The molecular weight of vancomycin-PEG (VP) conjugate was calculated as 2061 g/mol, while vancomycin and PEG-diacrylate had 1485.723 g/mol and 575 g/mol respectively. In order to purify the VP conjugate and remove the unreacted reactants 2000 MWCO dialyses cassettes were used. The dialysis cassettes which were filled with the reaction medium were placed into a beaker filled with diH_2O for 15 days, and the diH_2O was renewed twice daily, once every 12 hours. DMSO is a water soluble solvent, thus, during the dialysis, DMSO was replaced with diH_2O, and the conjugate is collected into diH_2O in the dialysis membrane.

4.5. CROSS METATHESIS REACTIONS OF VANCOMYCIN-PEG CONJUGATE WITH ANTIMICROBIAL POLYMERS

According to the MIC analyses results, among all the DABCO double-charged and pyridinium salt bearing polymers, D-10 exhibit the highest antimicrobial activity towards *S.aureus* with a MIC of 8 μg/mL, thus D-10 was used for the conjugation with vancomycin, as well as ID-3 and ID-10. Additionally, the polymers which were active against both

S.aureus and *E.coli* (Table 5.1) M-3, M-10, Phe-3, and Phe-10 were used for conjugation with vancomycin.

The vancomycin-PEG-polymer conjugates were synthesized via cross metathesis reactions between VP conjugate and the polymers (Figure 5.48 and Figure 5.49). The general procedure for cross metathesis is as explained in following. All the cross metathesis reactions were performed in a septum top glass vial under $N_{2(g)}$ atmosphere. Required amount of the polymers and VP conjugate were dissolved in 1 mL of DMF, when the mixture became homogeneous, required amount of Grubbs catalyst (Figure 4.2), which was dissolved in 0.5 mL of DCM, was added in one rapid shot. The reaction mixture was stirred under $N_{2(g)}$ atmosphere. The reaction was ended with the addition of 0.5 mL of EVE 30 percent, in DCM. The obtained conjugates were washed with DE for 5 times and dried using $N_{2(g)}$. The parameters and the reaction conditions are shown in Table 4.1.

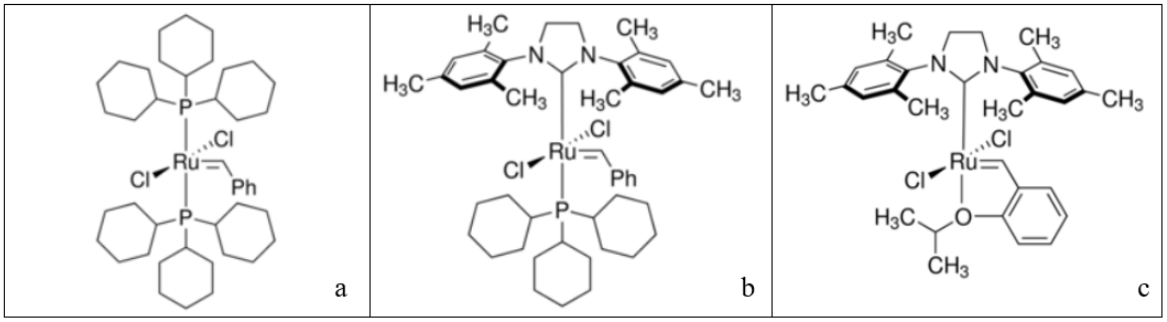

Figure 4.2. Structures of Grubbs Catalyst that were used in cross metathesis reactions: a) Grubbs Catalyst 1st Generation, b) Grubbs Catalyst 2nd Generation, c) Hoveyda-Grubbs Catalyst 2nd Generation

4.5.1. Purification of Cross Metathesis Products

All the samples were dissolved in diH_2O and transferred into dialysis cassettes (3500 MWCO). Purification process was applied to the reaction mixture for 48 hours using diH_2O, in order to eliminate unreacted components. During the purification process diH_2O was renewed three times daily, once every 8 hours.

Table 4.1. Changed parameters and reaction conditions for Cross metathesis reactions

No	Sample Code	Polymer	VP:Polymer ratio	Solvent	Catalyst (5 percent over all reactant moles)	Temperature (ºC)	Time (hours)
1	D10-M1	D-10	1:1	DMF	Hoveyda 2nd generation Grubbs	40	4
2	D10(DMF)-M1	D-10(DMF)	1:1	DMF	Hoveyda 2nd generation Grubbs	40	24
3	D10-M2	D-10	5:1	DMF	Hoveyda 2nd generation Grubbs	40	24
4	D10-M3	D-10	1:1	DMF	Grubbs-2	40	24
5	D10-M4	D-10	5:1	DMF	Grubbs-2	40	24
6	D10-M5	D-10	1:1	o-xylene	Hoveyda 2nd generation Grubbs	100	4
7	D10-M6	D-10	5:1	DMF	Hoveyda 2nd generation Grubbs	100	4
8	D10-M7	D-10	1:1	DMF	Grubbs-1	40	24
9	D10-M8	D-10	5:1	DMF	Hoveyda 2nd generation Grubbs	100	24
10	D10-M9	D-10	10:1	DMF	Hoveyda 2nd generation Grubbs	40	24
11	D10-M10	D-10	10:1	DMF	Hoveyda 2nd generation Grubbs	100	4
12	D10-M11	D-10	20:1	DMF	Hoveyda 2nd generation Grubbs	40	24
13	D10-M12	D-10	20:1	DMF	Hoveyda 2nd generation Grubbs	100	4
14	ID3-M1	ID-3	10:1	DMF	Hoveyda 2nd generation Grubbs	100	4

Table 4.1. Changed parameters and reaction conditions for Cross Metathesis reactions-Cont'd

No	Sample Code	Polymer	Vancomycin-PEG:Polymer ratio	Solvent	Catalyst (5 percent over all reactant moles)	Temperature (°C)	Time (hours)
15	ID3-M2	ID-3	20:1	DMF	Hoveyda 2nd generation Grubbs	100	4
16	ID10-M1	ID-10	10:1	DMF	Hoveyda 2nd generation Grubbs	100	4
17	ID10-M2	ID-10	20:1	DMF	Hoveyda 2nd generation Grubbs	100	4
18	M3-M1	M-3	5:1	DMF	Hoveyda 2nd generation Grubbs	100	4
19	M10-M1	M-10	5:1	DMF	Hoveyda 2nd generation Grubbs	100	4
20	Phe3-M1	Phe-3	5:1	DMF	Hoveyda 2nd generation Grubbs	100	4
21	Phe10-M1	Phe-10	10:1	DMF	Hoveyda 2nd generation Grubbs	100	4
22	Phe10-M2	Phe-10	20:1	DMF	Hoveyda 2nd generation Grubbs	100	4

4.6. ANTIMICROBIAL ACTIVITY (MIC ANALYSIS)

The dilution methods are used in order to identify the MIC of the antimicrobial polymers, which are the references for the antimicrobial susceptibility tests. These tests evaluate the observable growth on agar surfaces or on well plates which contain antimicrobial polymers. The MIC of the sample is identified as the concentration where no visible growth is observed [155]. MIC values can be obtained with *in vivo* and *in vitro* studies. There are some methods formic studies such as: optical density, diffusion, impedance and dilution methods. More quantitative results are provided by the dilution method [156]. In this study, microdilution method was used in order to determine the MIC of the synthesized polymers (Figure 4.3).

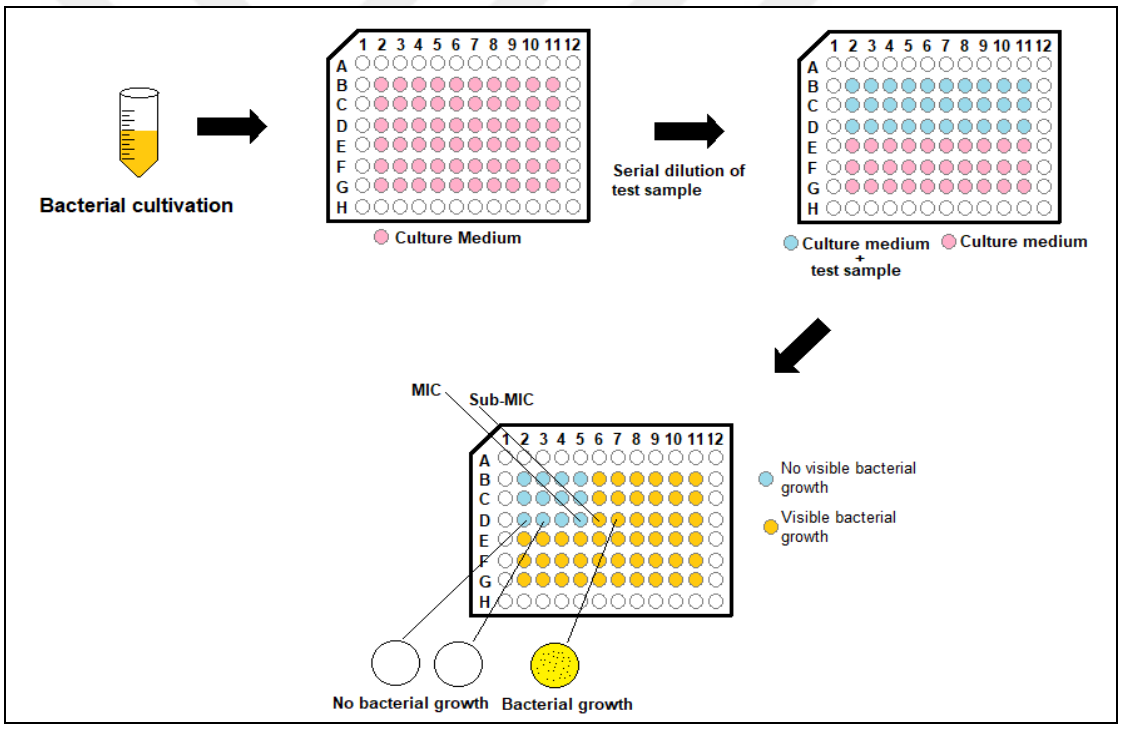

Figure 4.3. An illustration of microdilution method

In this study, MIC of the synthesized polymers and conjugates were determined against Gram (+) *S.aureus* and Gram (-) *E.coli*, as representative microorganisms. Stock solutions of each samples were prepared as 2 mg/mL using a proper solvent. 1×10^8 CFU/mL (0.5 McFarland) of cultivated bacterial solutions were prepared and diluted in 5×10^5 CFU/mL. 110 µL bacterial solution (10 µL cultivated bacterial solution in 100 µL of LB broth) was seeded into each well of 96-well plates. LB broth alone was used as negative control and

microorganisms in LB broth was used as positive control. The stock solutions of the samples were prepared and serial dilutions were made in ½ ratios and placed into 10 wells. The 96-well plate was gently vortexed, then incubated overnight at 37 °C. The next day, the turbidity in wells signifies the presence of bacteria, that were observed for each sample solution. The minimum concentrations at which no turbidity was observed were chosen as the MIC of the sample.

4.7. CYTOTOXICITY STUDIES

4.7.1. Hemolytic Concentration (HC_{50})

Hemolytic concentration (HC_{50}) signifies the toxicity of an antimicrobial polymer towards human red blood cells (RBCs) [27]. Hemolysis can be defined as the destruction of the RBCs which is resulting as the release of hemoglobin within the RBCs into the medium.

In this study, hemolytic concentrations were tested against fresh human O Rh(-) RBCs. 50 μL of RBCs were suspended in 10 mL of sterile PBS (0.05 M, pH 7.4) and washed thrice by centrifugation (1500 rpm, 5 min, 4 °C) and then resuspended in PBS to yield a 0.5 percent (v/v) final RBC concentration.

8 mg/mL of sample solutions were prepared as in 1x PBS and low DMSO concentration (PBS was used for further dilutions when necessary). 100 μL of the sample solutions with various concentrations were added to a 96-well plate. 100 μL of the 0.5 percent erythrocyte suspension was added to the polymer solutions in the wells (final volume 200 μL/well). Triton-X 100 (20 percent in DMSO), which is a strong surfactant, was used as a positive control. RBCs suspension in PBS was used as a negative control. 96-well plate was incubated 30 minutes at 37 °C, then centrifuged at 1500 rpm (4 °C) for 10 minutes. The supernatant in each well was transferred into a new plate, and the absorbance of released hemoglobin in each well was measured at 405 nm using a plate reader (Synergy H1, BioTek Instruments, Winooski, VT, USA). HC_{50} value was determined as the mean concentration of the polymer causing 50 percent hemolysis compared to the positive control. Triplicate runs were performed for all experiments.

4.7.2. MTS Assay

In vitro cytotoxicity study of polymers were investigated using tetrazolium salt based [3-(4,5-dimethylthiazol-2-yl)-5-(3-carboxymethoxyphenyl)-2-(4-ulphophenyl)-2H-tetrazolium, inner salt (MTS)], which is a colorimetric technique for the investigation of cell viability [157]. Viable cells consume of MTS tetrazolium and generate a colored formazan product which is soluble in cell media. The colored formazan product is quantified by measuring the absorbance at 490 nm.

HUVEC cell line was used to investigate the cytotoxicity of the synthesized polymers and vancomycin-polymer conjugates. The frozen HUVEC cells were incubated at T75 wells in medium at 37 ºC in an incubator (95 percent air, 5 percent CO_2) for the growth for approximately for a week in order to obtain sufficient amount of cells. The cell medium was prepared using 10 percent FBS, 1 percent antibiotic (Penicillin-Streptomycin/Antimycotic) and phenol red containing DMEM-high glucose concentration (4.5 g/L, 1x and pH 7.4).

For each experiments, 5000 cells per well were seeded into 96-well plates and the cells were incubated at 37 °C (95 percent air, 5 percent CO_2) for 24 hours. Then the stock solutions of the samples were prepared using 1 percent DMSO in DMEM. Each sample was prepared with 5 different concentrations (2048, 1024, 512, 256 and 128 μg/mL). The negative control was prepared as 1 percent DMSO in DMEM to be able eliminate the toxic effect of DMSO on the cell viability, and the positive control was prepared as 20 percent DMSO in DMEM. The sample solutions and the controls were placed into 96-well plates as 110 μL per well and incubated at 37 °C for 24 hours. This study was pursued for four replicates of each compound. After 24 hours, the sample solutions were removed and MTS reagent in DMEM (100 μL DMEM:20 μL MTS reagent) was added into each well again incubated at 37 °C for 2 hours. 2 hours later the absorbance was measured in a microtiter plate reader (BIOTEK, ELx800) at 490 nm. In this study, cell viability was determined for 24, 48 and 72 hours.

4.8. INVESTIGATION OF THE INTERACTION BETWEEN BACTERIA AND VP-CONJUGATES USING BIOPHYSICAL TECHNIQUES

The cationic ends of the cationic polymers interact with the negatively (-) charged cell wall of bacteria. This interaction allows the polymers to be adsorbed into the bacterial cell and this electrostatic interaction results in the death of bacteria. The hydrophobic interactions plays a key role as well as the cationic groups, in bacterial death. Long-chain fatty acids in the wall of the bacteria interact with the hydrophobic groups in the polymer and resulting in the destruction of the existing order in the cell membrane. This irregularity causes the internal pressure-external pressure difference and consequently breaks the membrane.

There are two main antibacterial mechanisms proposed for polycationic surfaces. Although many studies have been executed in this context, the antibacterial mechanism of polymer coated surfaces is still being investigated [158]. One of the proposed mechanisms is the interaction between polycation with the biomembrane, and the other one is cation exchange (Ca^{+2} and Mg^{+2}). According to the second mechanism; the positively charged cationic polymer interacts with lipopolysaccharide (LPS) layer which is an anionic surface. The affinity of the cationic polymers is three times higher than divalent cations; Ca^{+2} and Mg^{+2} which keeps LPS together, these ions are displaced competitively in antibacterial polymers. As a result, cationic polymers accumulate on the cell surface to partially neutralize LPS and disrupt the normal barrier integrity of the outer membrane. Thus, the outer membrane becomes permeable for hydrophobic structures, small proteins, antimicrobial agents and most importantly cationic polymers, and consequently, the cationic polymers pass through the outer membrane, reaching the cytoplasm membrane of the phospholipid structure. The important second stage is the passing through the cytoplasm membrane. In other words, eventhough it is necessary for antimicrobial cationic polymers pass through the outer membrane of the bacteria, it is not sufficient for the lethal effects of these substances. The main lethal effect of the antimicrobial cationic polymers is the electrostatic interaction with negatively charged cytoplasm membrane. During this action, the cationic polymers confront the hydrophilic groups with the hydrophobic chains of the membrane phospholipids, causing the polymers to form a membrane parallel to the membrane to form channels that disrupt the integrity of the membrane [159, 160]. It was observed that the antimicrobial ROMP polymers generally follow the carpet model, which was explained in Chapter 2 (2.6.2.2.

Mechanism of Action of the Antimicrobial Peptides). In this mechanism, due to the formation of pore in the cell wall, the molecules pass through the cell wall, and interact with DNA in the cell causes the death of bacteria.

In this study, morphostructural damage analysis was performed using SEM in order to understand the bacterial killing mechanism of the vancomycin-polymer conjugates.

4.8.1. Morphostructural Damage Analysis (SEM Analysis)

The morphostructural damage analysis of D10(DMF)-M1 and Phe3-M1 were investigated utilizing scanning electron microscopy (SEM, EVO/MA10, Zeiss). The microdilution method which was mentioned in "MIC Analysis" section for *S.aureus* ATCC 29213 was studied in glass tube for MIC, sub-MIC, supra-MIC concentrations of the samples (D10-M1 and Phe3-M1). Untreated *S.aureus* was used as control group. 1.5 mL of each solutions were transferred into Eppendorf tubes, then the samples were centrifuged at 3000 rpm for 5 minutes and supernatants were removed. The remaining pellets in the Eppendorf tubes were washed twice using approximately 1.5 mL of PBS (0.05 M, pH: 7.4). The collected pellets were smeared on glass slides using pipette tips, and covered with 2 mL of 2.5 percent glutaraldehyde, then incubated for 2 hours at room temperature. The glass slides were washed with 1 mL of PBS (0.05 M, pH: 7.4) for 1 minute, then the dehydration treatment was applied using 50 percent ethanol, 70 percent ethanol, 80 percent ethanol, 90 percent ethanol, 95 percent ethanol, and 100 percent ethanol, respectively, the samples were treated with each solution for 10 minutes. Then, the slides were incubated for 2 hours at room temperature. Control cells and and treated bacteria cells were subsequently analyzed at different magnifications by SEM.

5. RESULTS AND DISCUSSION

5.1. CHARACTERIZATION OF MONOMERS

The synthesis steps of the monomers, which were synthesized within this study, are shown in Figure 5.1 and Figure 5.2. The synthesis of oxanorbornene via the Diels Alder reaction between maleic anhydride and furan was the first step. The ^{1}H NMR and the ^{13}C NMR spectra of Compound 1 are shown in Figure 5.3 and Figure 5.4, respectively. Compound 1 was shown to be 100 percent exo structure; the characteristic peaks of the exo stereoisomer structure was observed at 6.5 ppm on ^{1}H NMR spectrum for olefinic hydrogen and at 137 ppm on ^{13}C NMR spectrum for olefinic carbon.

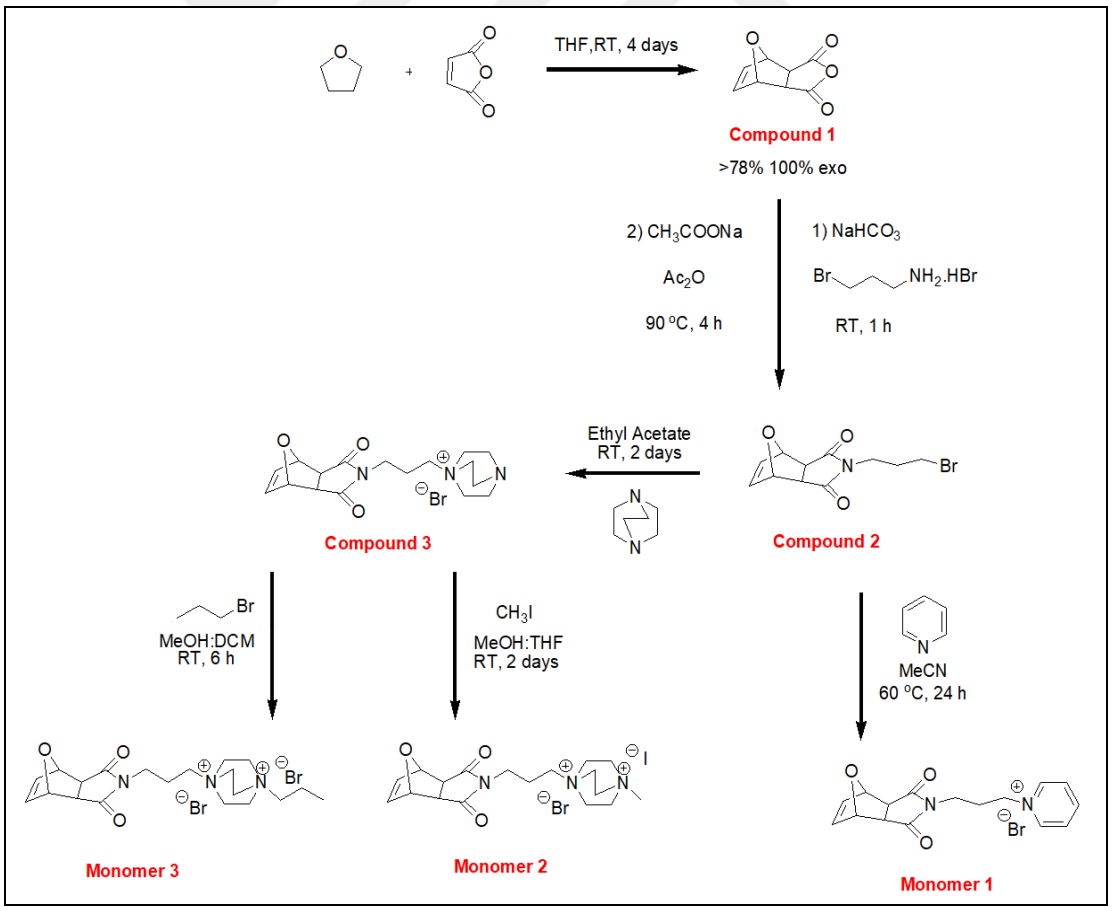

Figure 5.1. Synthesis scheme of the DABCO and Pyridinium salt bearing Oxanorbornenes

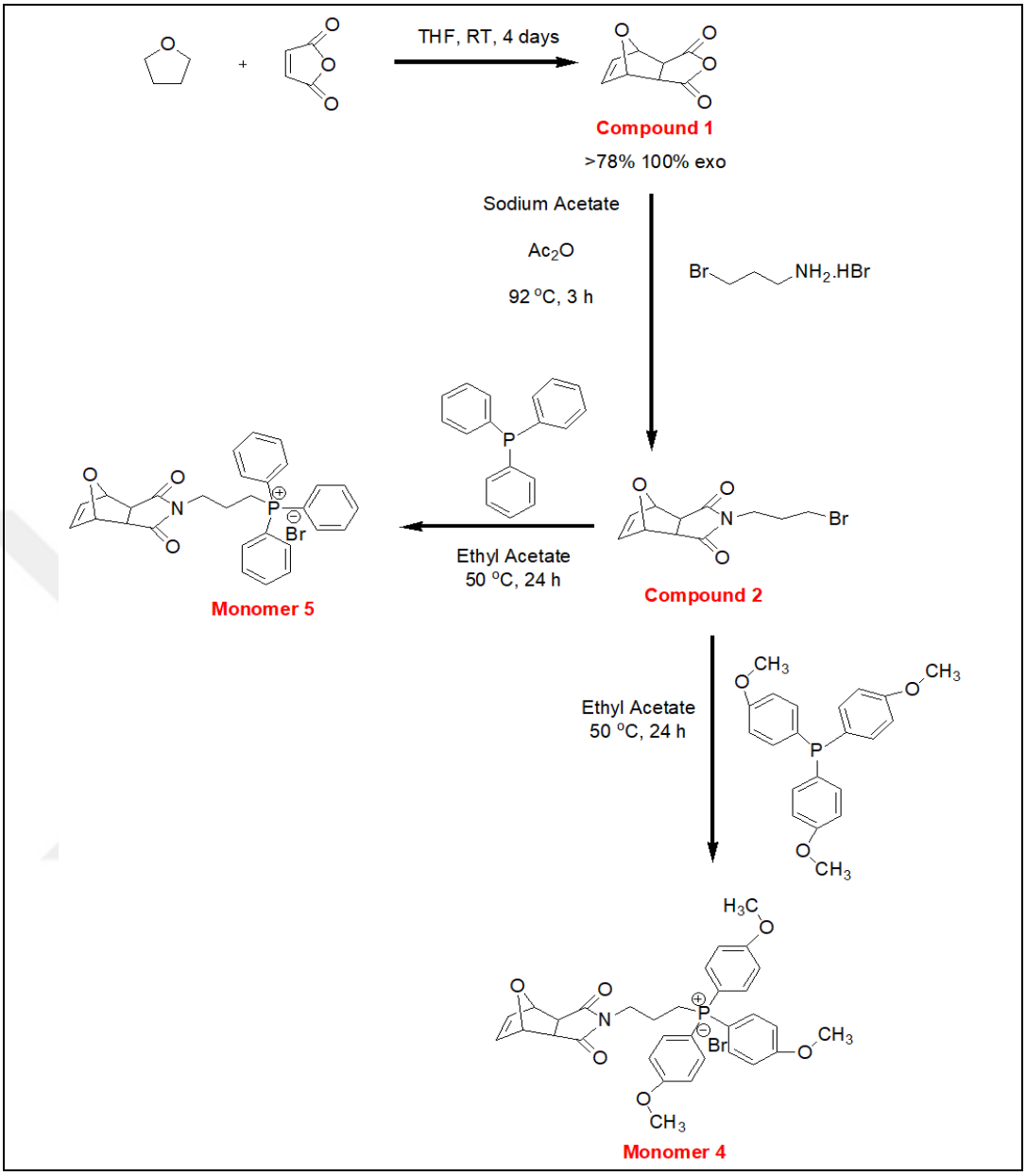

Figure 5.2. Synthesis scheme of the Trimethoxyphenyl Phosphonium and Triphenyl Phosphonium bearing Oxanorbornenes

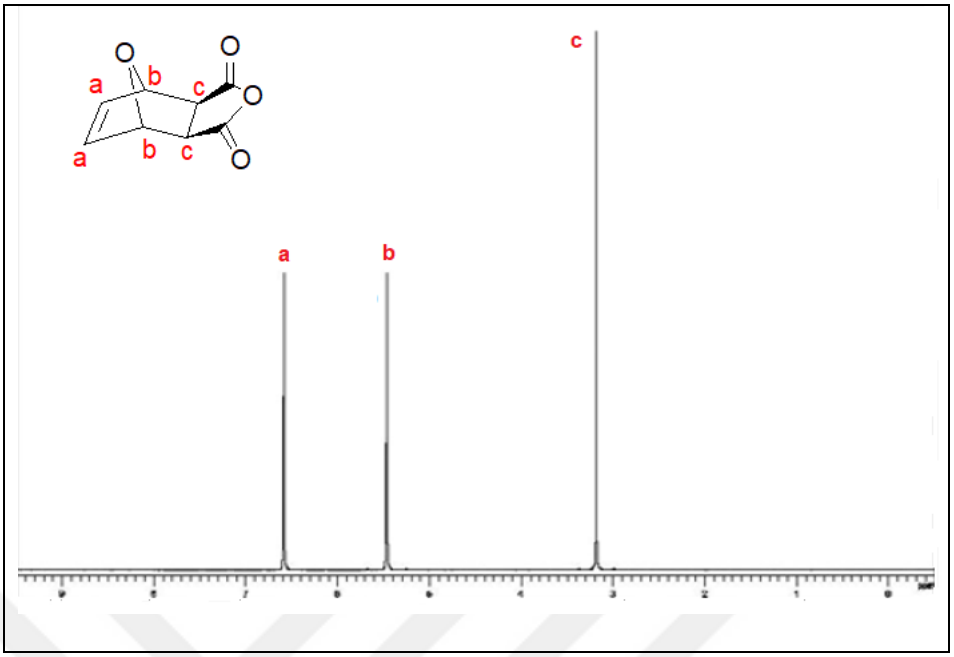

Figure 5.3. ^{1}H NMR spectrum of Compound 1

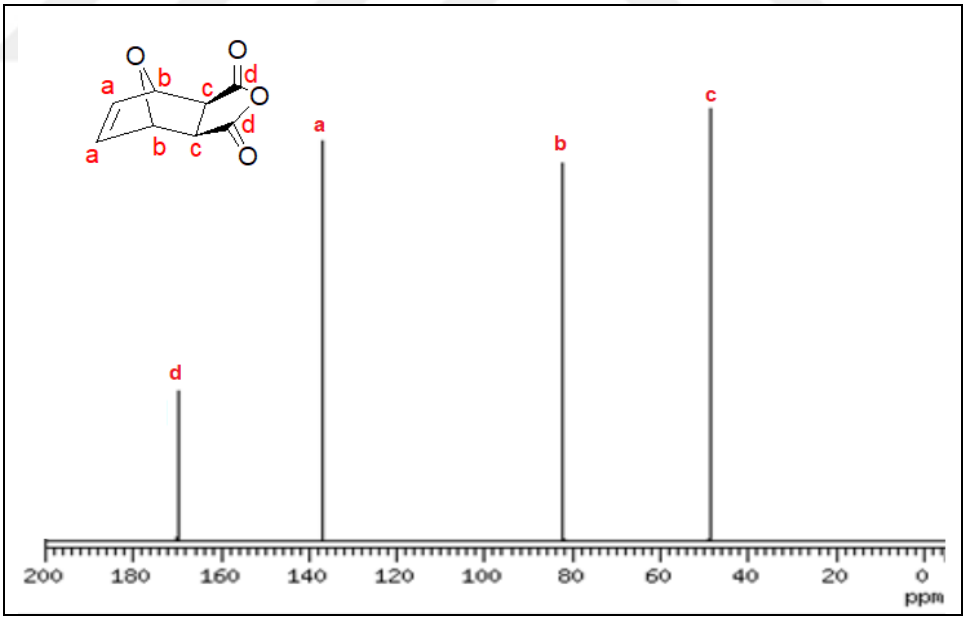

Figure 5.4. ^{13}C NMR spectrum of Compound 1

Compound 2 was synthesized via Imide mechanism. The reaction between 3-bromo propylamine hydrogen bromide and Compound 1 was catalyzed by sodium acetate, and from this reaction Compound 2 was obtained. Column chromatography method was used

for purification process. HEX:EtOAc (1:1, v/v) was used as mobile phase for the column chromatography, and pure Compound 2 was collected with yield of 46 percent. ^{1}H NMR and ^{13}C NMR spectra of Compound 2 are shown in Figure 5.5 and Figure 5.6, respectively. The characteristic peaks of Compound 2, N-CH_2 and CH_2-Br were seen at 3.5 ppm and at 3.2 ppm, respectively on ^{1}H NMR spectrum. The peak regarding to N-CH_2 is seen on ^{13}C NMR spectrum at around 137 ppm.

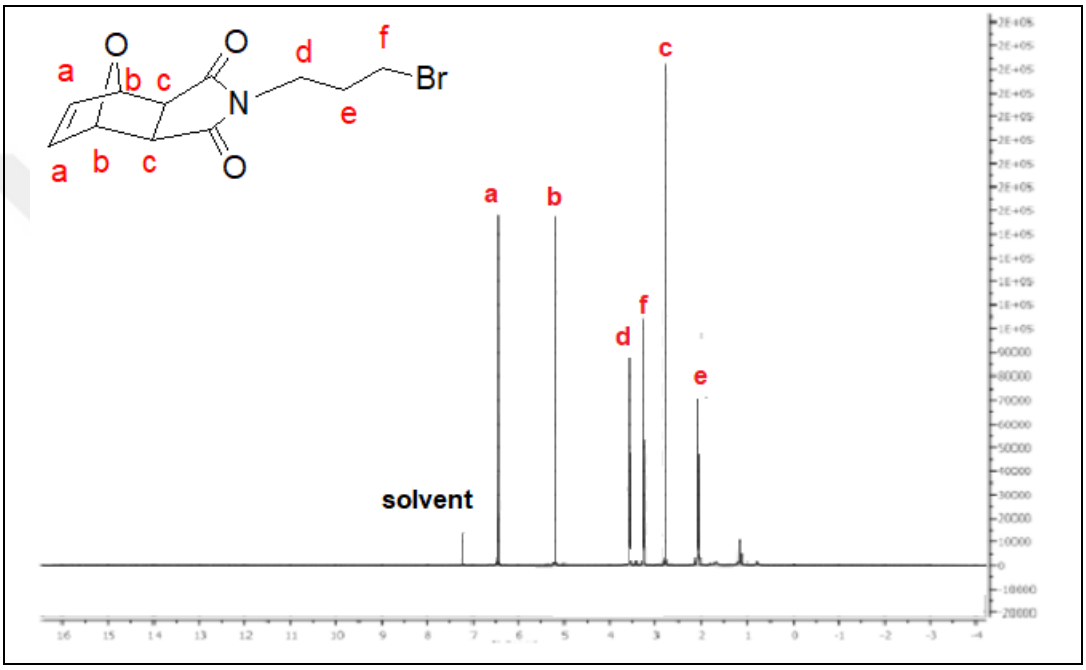

Figure 5.5. ^{1}H NMR spectrum of Compound 2

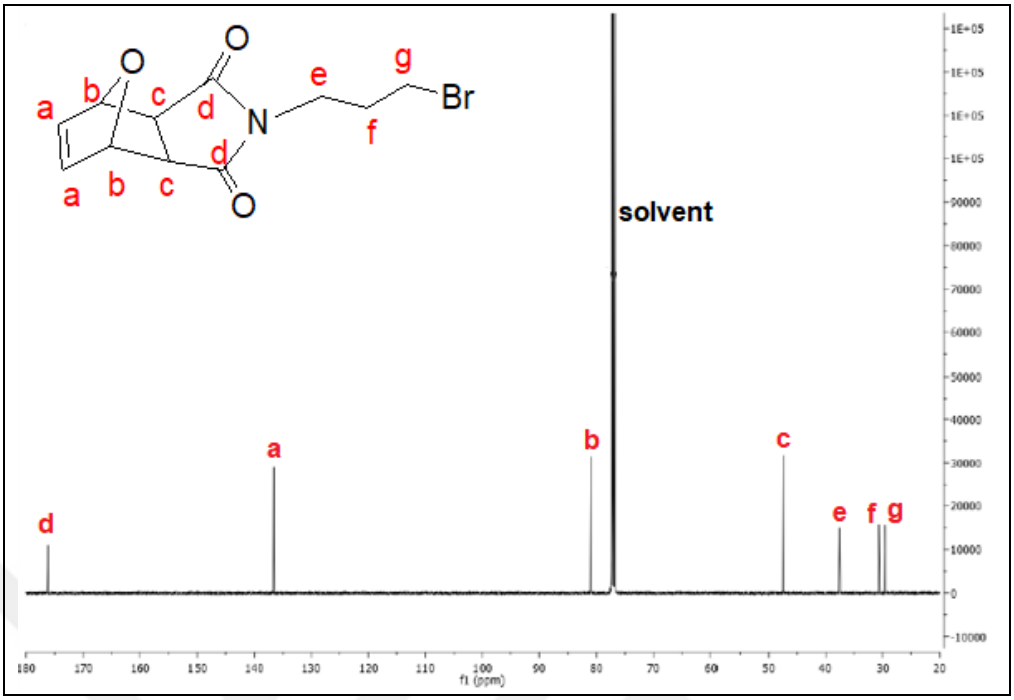

Figure 5.6. ^{13}C NMR spectrum of Compound 2

Monomer 1 is a pyridinium functional monomer, which was synthesized via S_N2 reaction between the pyridine and the Compound 2. The quaternization was conducted at 60 ^oC in the presence of ACN under N_2 atmosphere. Light pink colored Monomer 1 was obtain with yield of 84 percent. The ^{1}H NMR and ^{13}C NMR spectra of the pyridinium salt bearing monomer are given in the Figure 5.7 and Figure 5.8, respectively. On the ^{1}H NMR spectrum, the peaks regarding to the protons of CH_2-Br and CH_2-N, which were formed due to the addition of pyridinium ring to the structure, occurred at 3.33 ppm and 4.56 ppm, respectively. The peaks corresponding to the carbon atoms of CH_2-Br and CH_2-N were seen around 8.0-9.5 ppm as the result of presence of the pyridinium ring in the structure (Figure 5.7). On ^{13}C NMR spectrum, the peaks regarding the pyrdinium ring occurred between 125-150 ppm (Figure 5.8).

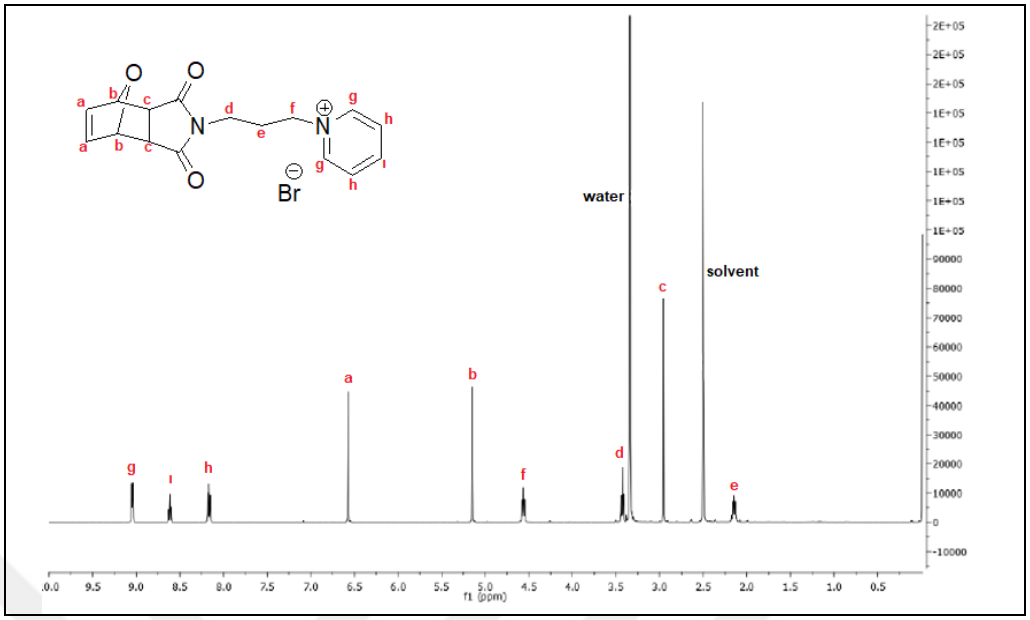

Figure 5.7. ^{1}H NMR spectrum of Monomer 1

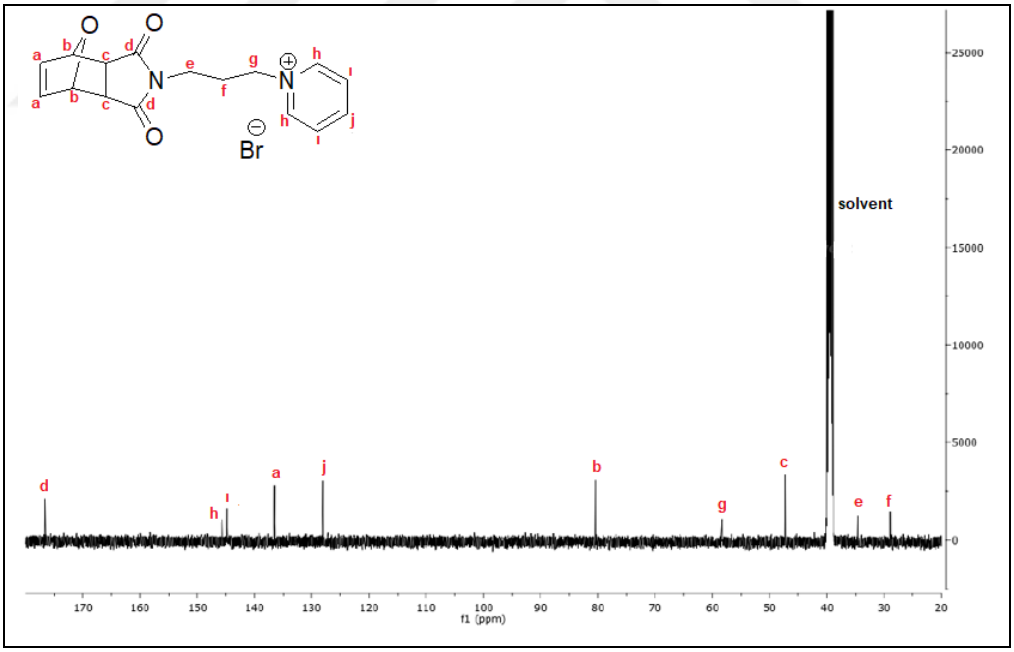

Figure 5.8. ^{13}C NMR spectrum of Monomer 1

Monomer 2 is a DABCO double-charge bearing monomer, which was synthesized in two steps. At first step, mono-charged compound (Compound 3) was synthesized from the S_N2 reaction between the Compound 2 and DABCO. The reaction was held at room temperature

for 2 days, and the mono-charged compound was precipitated in EtOAc. After washing the product with DE, it was characterized using NMR techniques. The ^{1}H NMR spectrum of Compound 3 is given in Figure 5.9, it was seen from the spectrum that the characteristic peak of Compound 2 at 3.33 ppm which corresponds to CH_2-Br disappeared and the peak regarding to CH_2-N shifted to 3.44 ppm (compared to Figure 5.5), and the peaks corresponding to DABCO were seen at 3.0-3.26 ppm. In the ^{13}C NMR spectrum of Compound 2 (Figure 5.6), DABCO had one type protons and these protons are seen at 47 ppm, however, in the ^{13}C NMR of Compound 3 (Figure 5.10), DABCO had two different types of protons and the peaks regarding to those protons were seen at 44.6 ppm and 60.5 ppm.

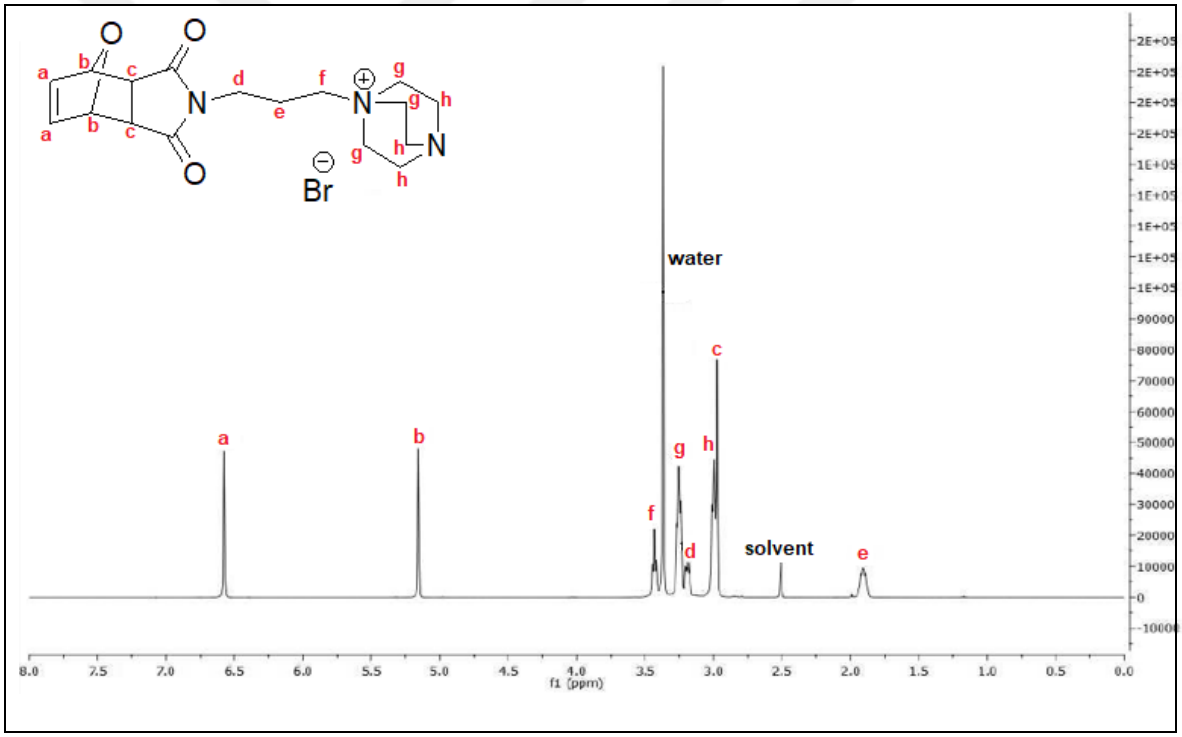

Figure 5.9. ^{1}H NMR spectrum of Compound 3

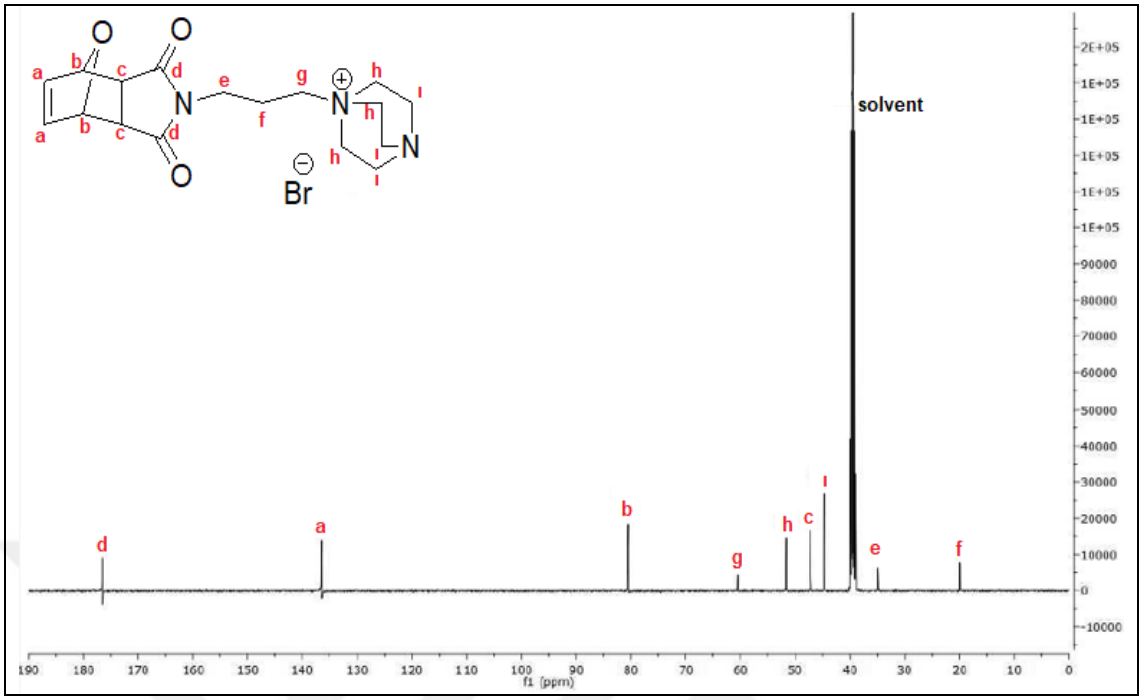

Figure 5.10. ^{13}C NMR spectrum of Compound 3

After the formation of DABCO mono-charged monomer, the second step provided an additional charge from the S_N2 reaction between Compound 3 and methyl iodide, thus the Monomer 2 was obtained as double-charged monomer. This reaction was held in room temperature for 2 days and MeOH:THF (10:3, v/v) mixture was used as solvent. After purification of the product (Monomer 2), the structural analysis was conducted using NMR techniques. Secondary positive charge of the structure was due to protons of methyl group, and to point this protons on the spectrum, a model composite was synthesized via a reaction between DABCO and CH_3I, and ^1H NMR analysis was applied. According to ^1H NMR spectrum the characteristic peak (N^+-CH_3) was observed at 3.26 ppm. The ^1H NMR and ^{13}C NMR spectra of Monomer 2 are given in the Figure 5.11 and Figure 5.12, respectively. The peaks correspond to N^+-CH_3 are seen at 3.26 ppm on ^1H NMR spectrum and at 50.42 ppm on the ^{13}C NMR spectrum.

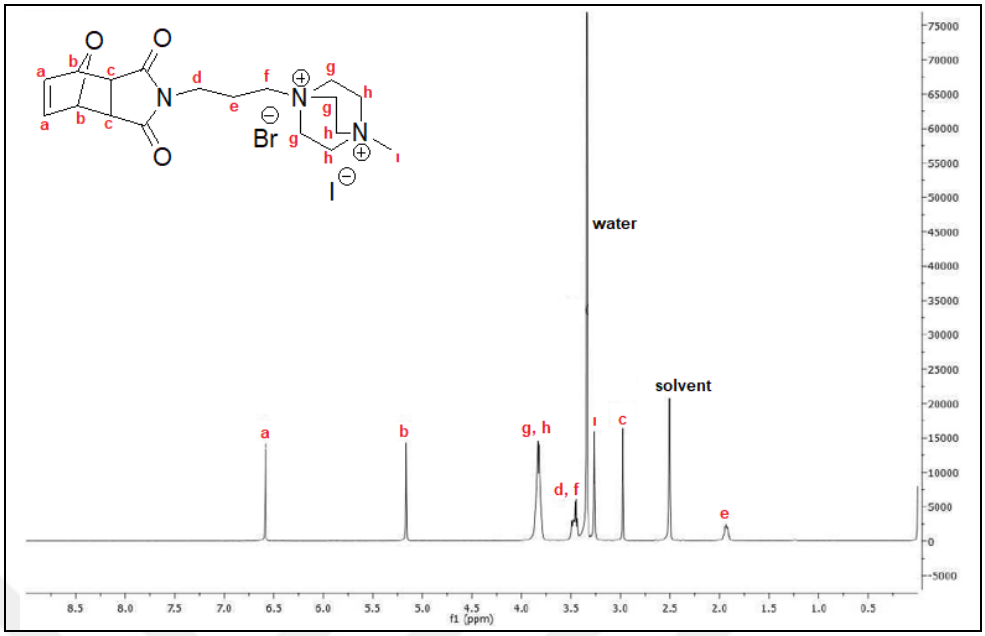

Figure 5.11. ^{1}H NMR spectrum of Monomer 2

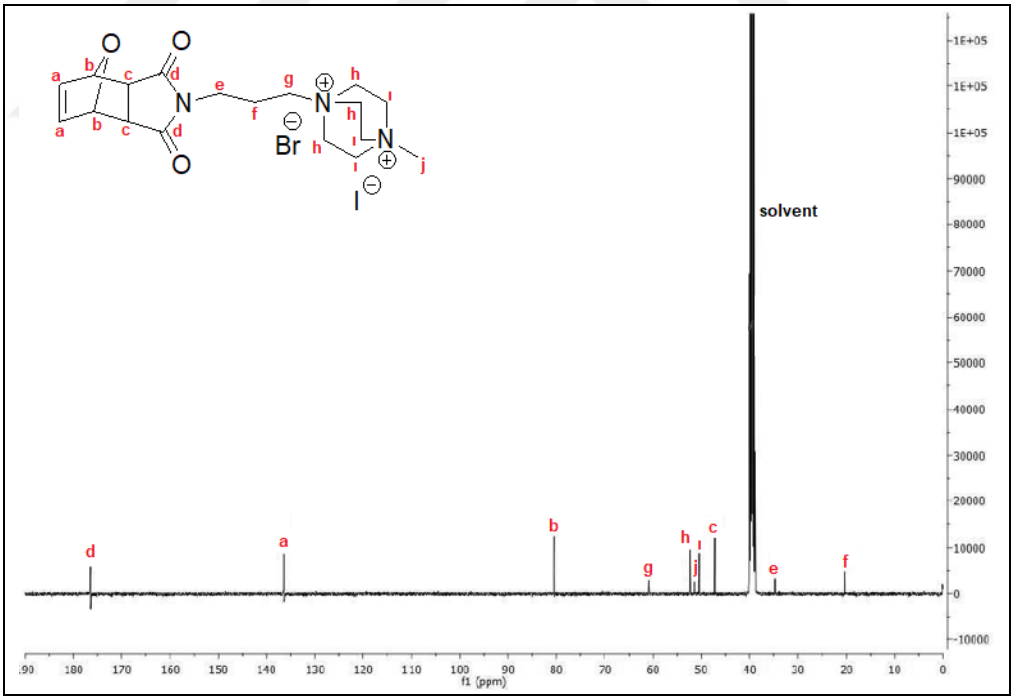

Figure 5.12. ^{13}C NMR spectrum of Monomer 2

Monomer 3 is also a double-charged monomer and the additional charge for this monomer was formed due to the S_N2 reaction between Compound 3 and propyl bromide. The

characteristic peak of the structure was occurred at 3.26 ppm on the ^{1}H NMR spectrum which is due to the protons of the N^{+}-CH_3 (Figure 5.13).

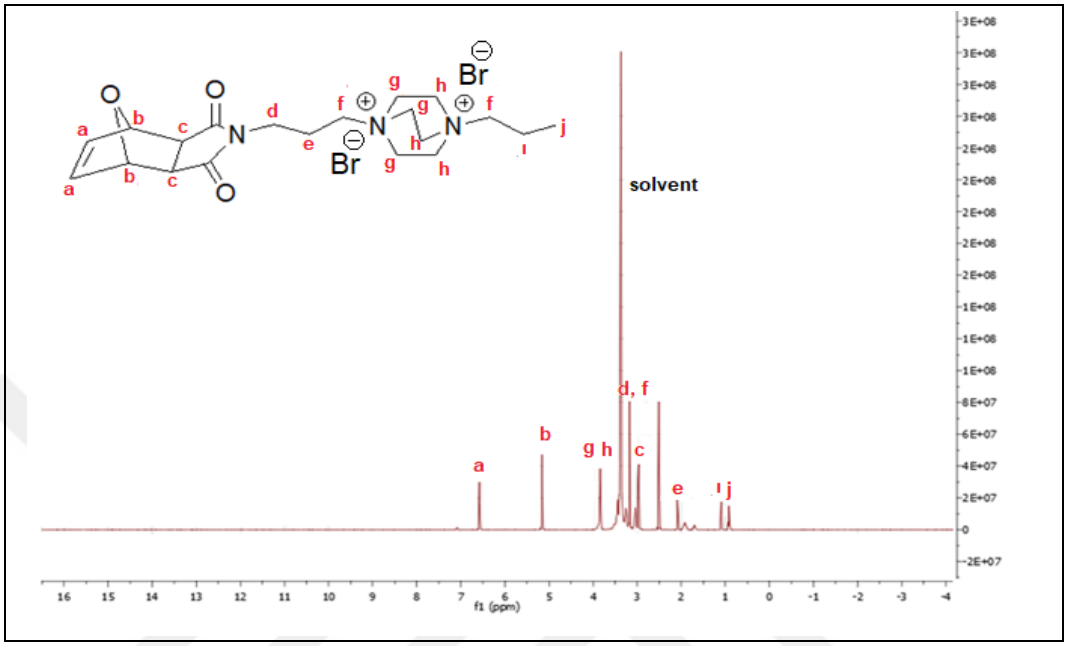

Figure 5.13. ^{1}H NMR spectrum of Monomer 3

Monomer 4 is a trimethoxyphenyl phosphonium bearing monomer and Monomer 5 is a triphenyl phosphonium bearing monomer. The ^{1}H NMR and ^{13}C NMR spectra of Monomer 4 are given in Figure 5.14 and Figure 5.15, respectively. The spectra for Monomer 5 are shown in Figure 5.16 and Figure 5.17. For Monomer 4, the peaks corresponding to phenyl rings were observed between 8.00-7.0 ppm on ^{1}H NMR, and between 140-110 ppm on ^{13}C NMR. The characteristic oxanorbornene protons and carbons were occurred at 6.57 ppm, 5.15 ppm and 2.98 ppm on ^{1}H NMR spectra, and 176.65 ppm, 136.41 ppm, 80.45 ppm and 47.21 ppm on ^{13}C NMR spectra. For Monomer 5, the peaks corresponding to phenyl rings were observed between 8.00-7.5 ppm on ^{1}H NMR, and at around 130 ppm on ^{13}C NMR.

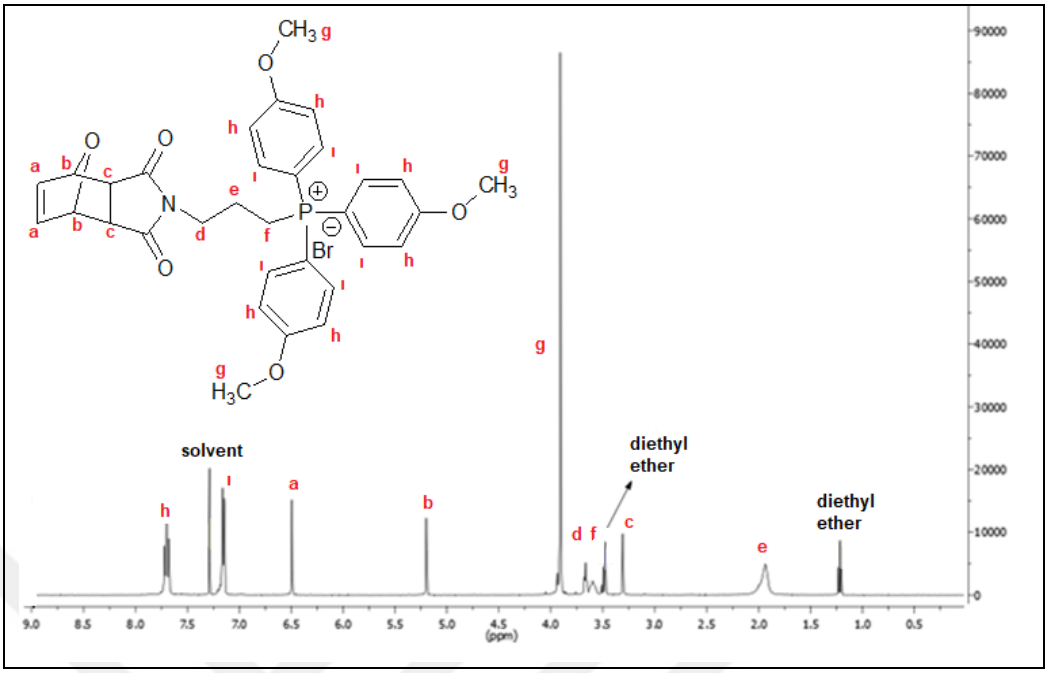

Figure 5.14. ^{1}H NMR spectrum of Monomer 4

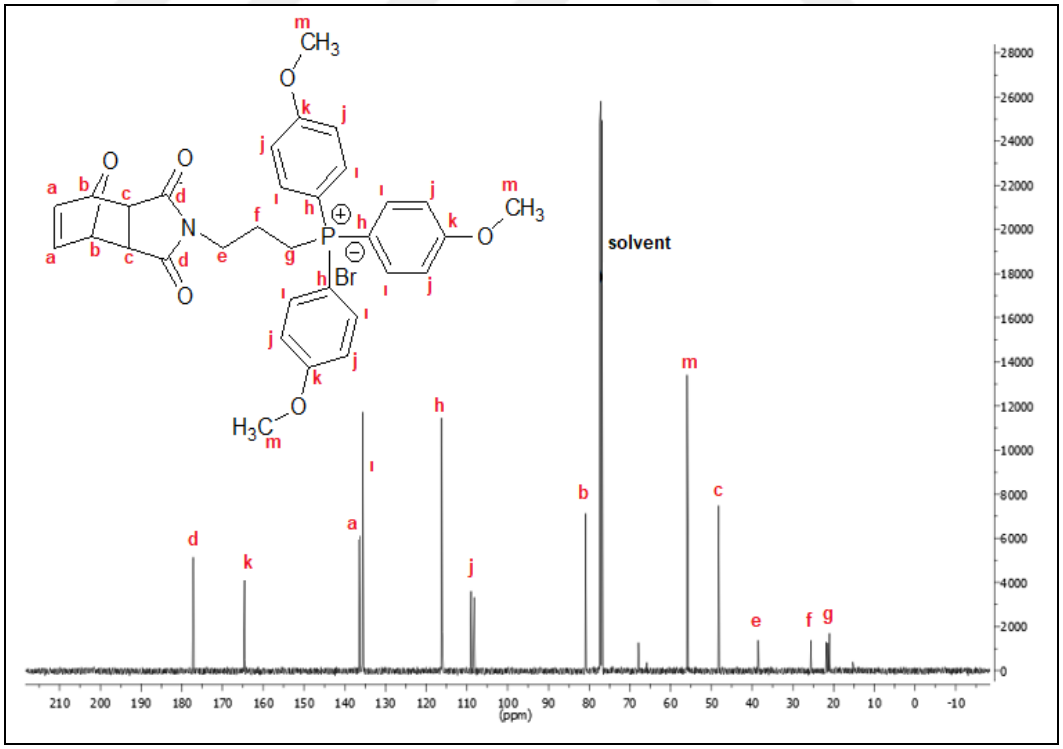

Figure 5.15. ^{13}C NMR spectrum of Monomer 4

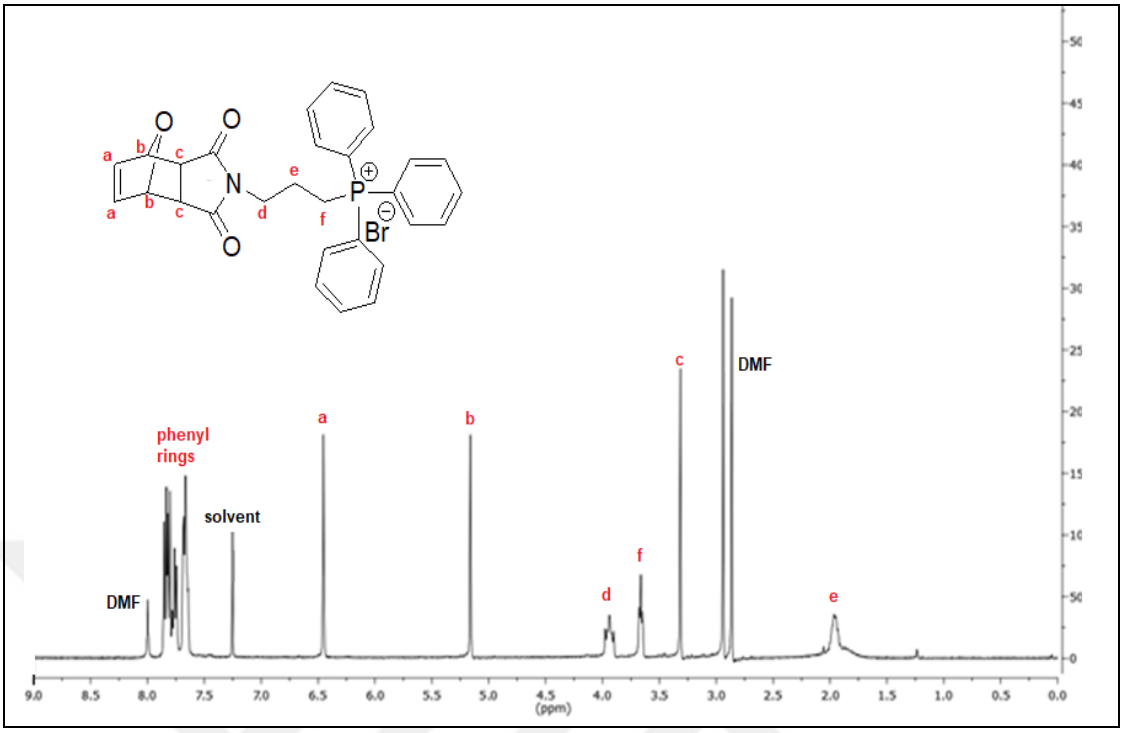

Figure 5.16. ^{1}H NMR spectrum of Monomer 5

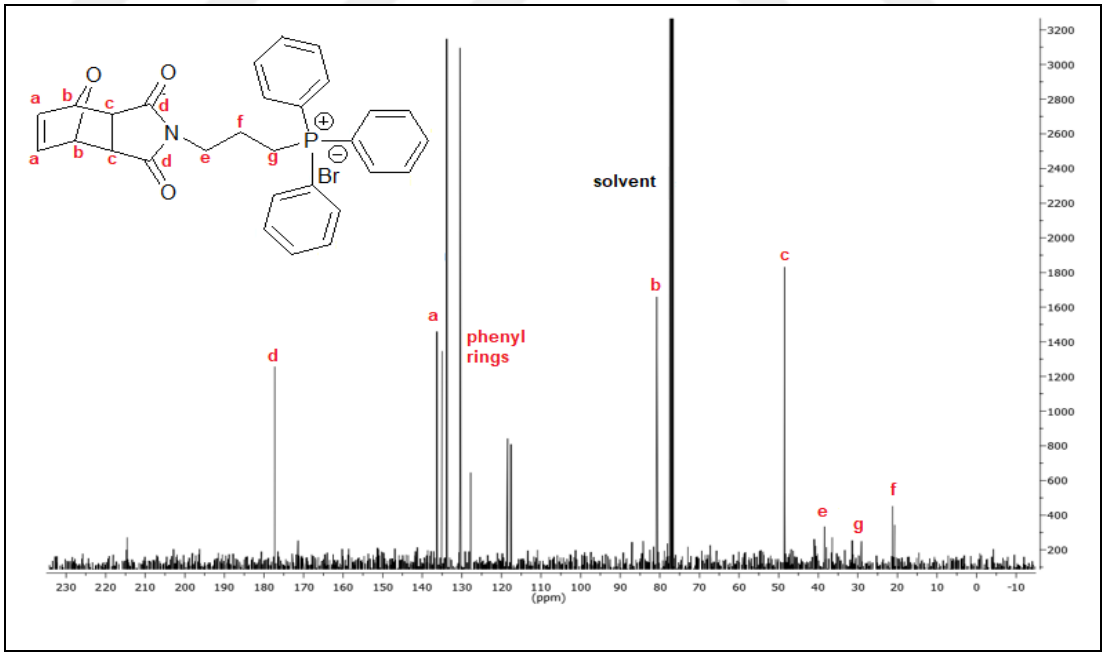

Figure 5.17. ^{13}C NMR spectrum of Monomer 5

5.2. CHARACTERIZATION OF POLYMERS

ROMP polymerization is an effective method in the syntheses of the cyclic olefins such as norbornenes [109, 161]. The selection of a convenient catalyst is one of the key steps to synthesize a well-defined polymerization system with regard to effectivity of initiation, and propagation control [162]. The effective catalyst systems for ROMP method are molybdenum based Schrock [163] and ruthenium based Grubbs [105] catalyst. In this study, we used less-oxygen sensitive [162] Grubbs catalysts (Grubbs catalyst 3rd generation). The synthesis schema of the pyridinium and DABCO Salt bearing polymers homopolymers is shown in Figure 5.18 and the triphenylmethoxy phosponinium and triphenyl phosponium bearing homopolymers is shown in Figure 5.19.

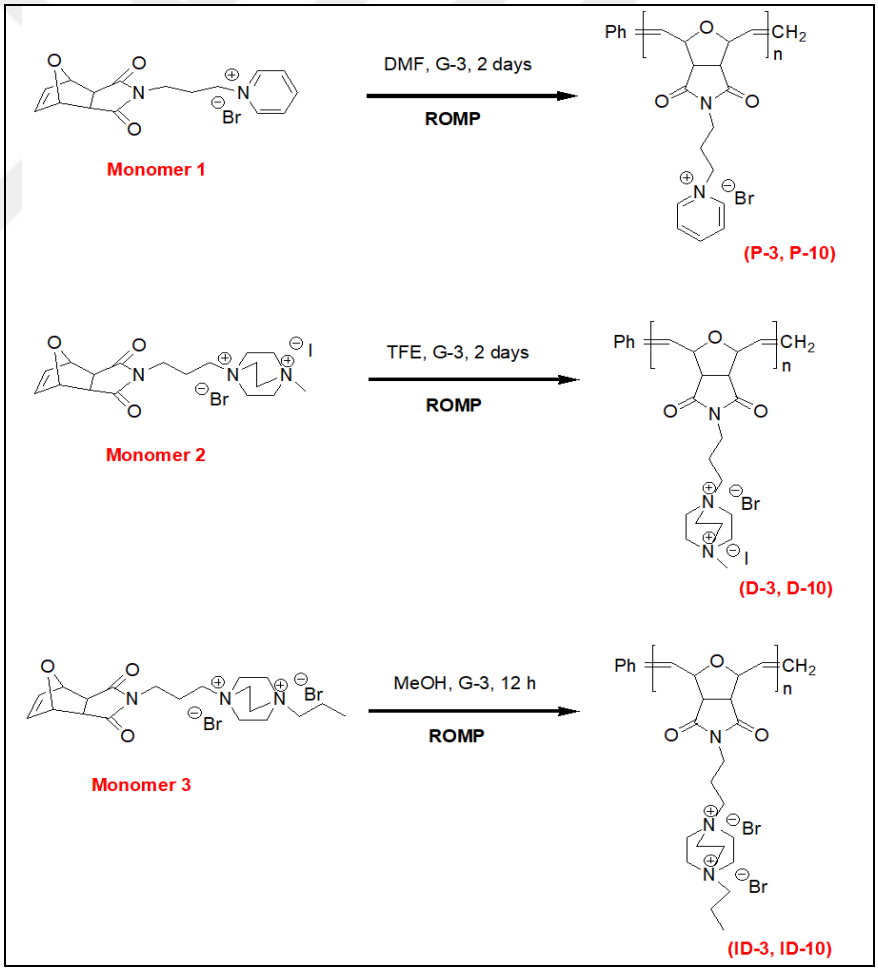

Figure 5.18. The synthetic schema of the Pyridinium and DABCO salt bearing polymers

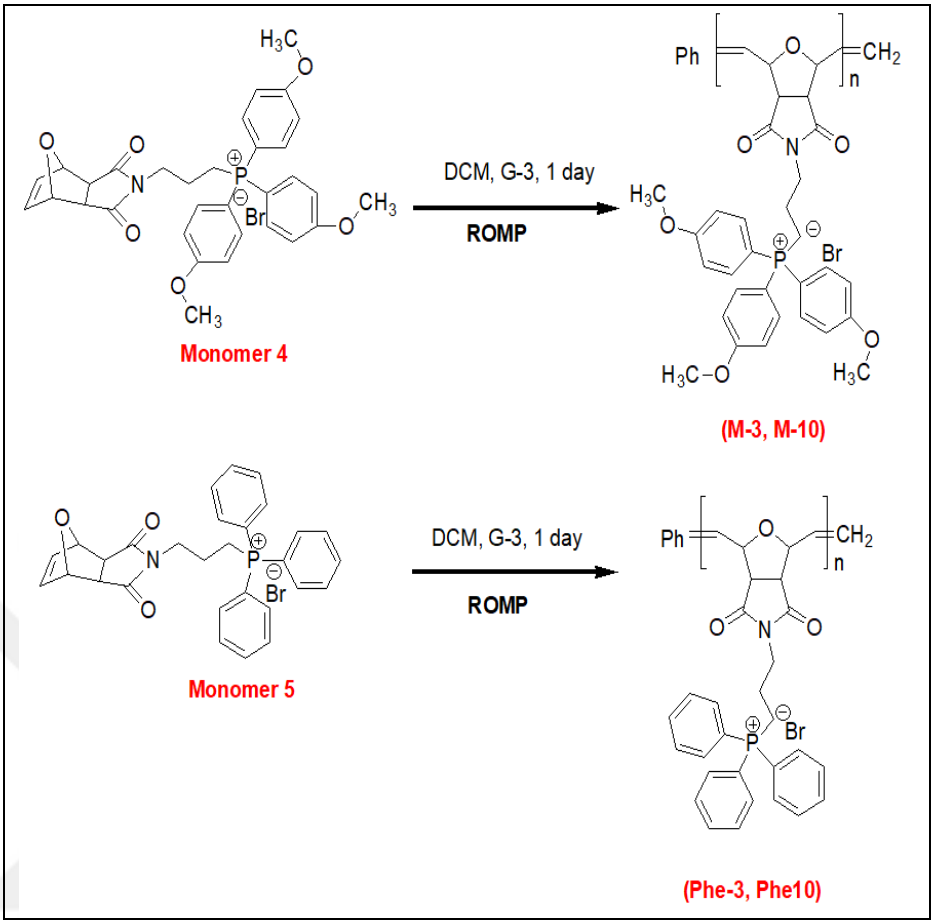

Figure 5.19. The synthetic schema of the Triphenylmethoxy Phosponinium and Triphenyl Phosponium bearing homopolymers

5.2.1. NMR Analysis of Homopolymers

All the homopolymers were synthesized with two different molecular weights as 3000 and 1000 g/mol, and the required catalyst amount (Grubbs 3) were calculated from the equations (4.1)-(4.4). The ^{1}H NMR spectra of the homopolymers are found in Figure 5.20 to Figure 5.24. In this section, the ^{1}H NMR spectrum of each polymer were given for only one molecular weight as representative, the other ^{1}H NMR spectra can be found in Appendix A (Figures A.1-5).

In the figures (Figure 5.20-Figure 5.24) it was observed that the peaks regarding to norbornene ring (6.5 ppm) disappeared due to the ring opening polymerization and peaks corresponding to olefinic protons appeared at around 5.1 ppm-5.6 ppm (c_{cis}), and 6.00 ppm

(c_{trans}). The cis and trans protons of the polymers were integrated and the cis/trans ratio was found to be 58/48. In Figure 5.23 and Figure 5.24, the peaks around 7.20 ppm- 7.50 ppm were observed due to the phenyl end group connection to the structures.

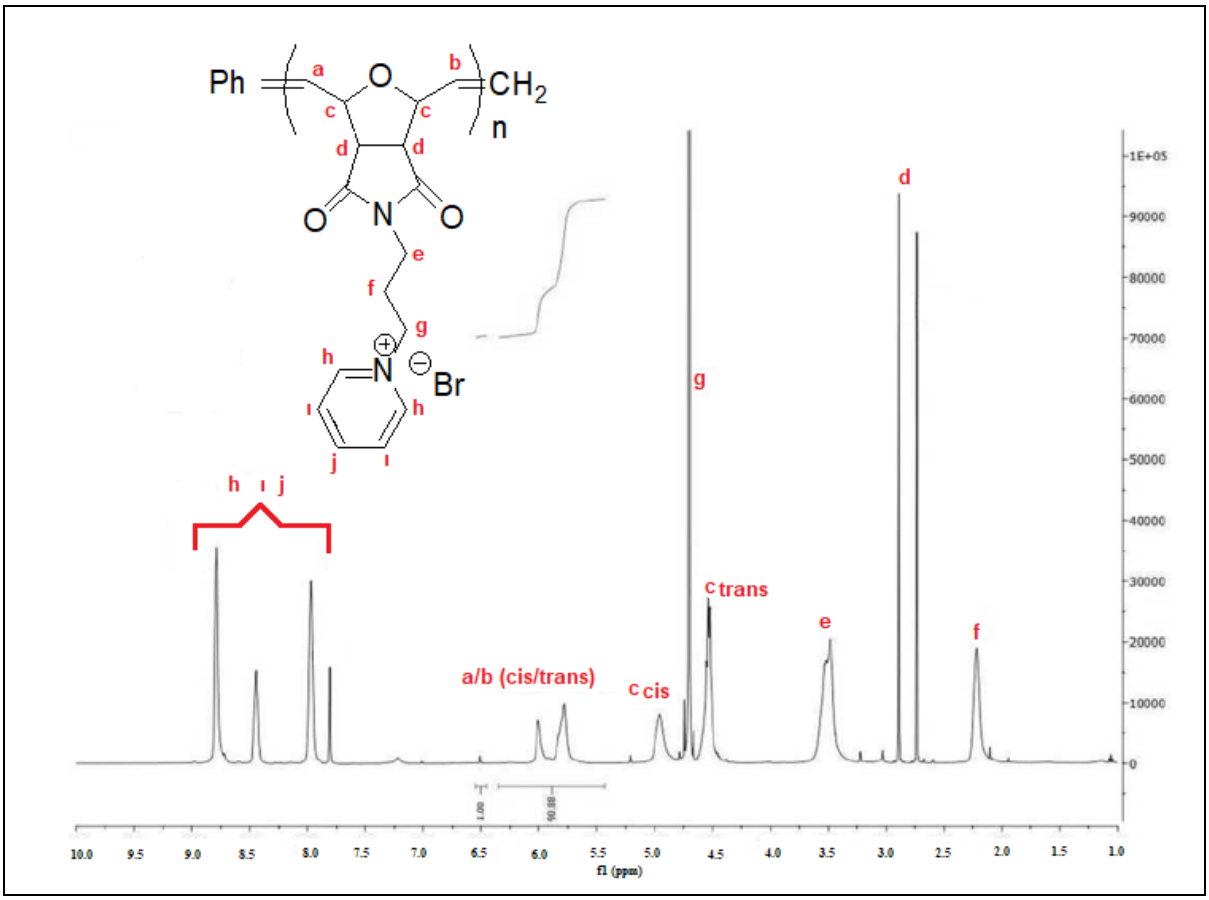

Figure 5.20. ^{1}H NMR spectrum of P-10

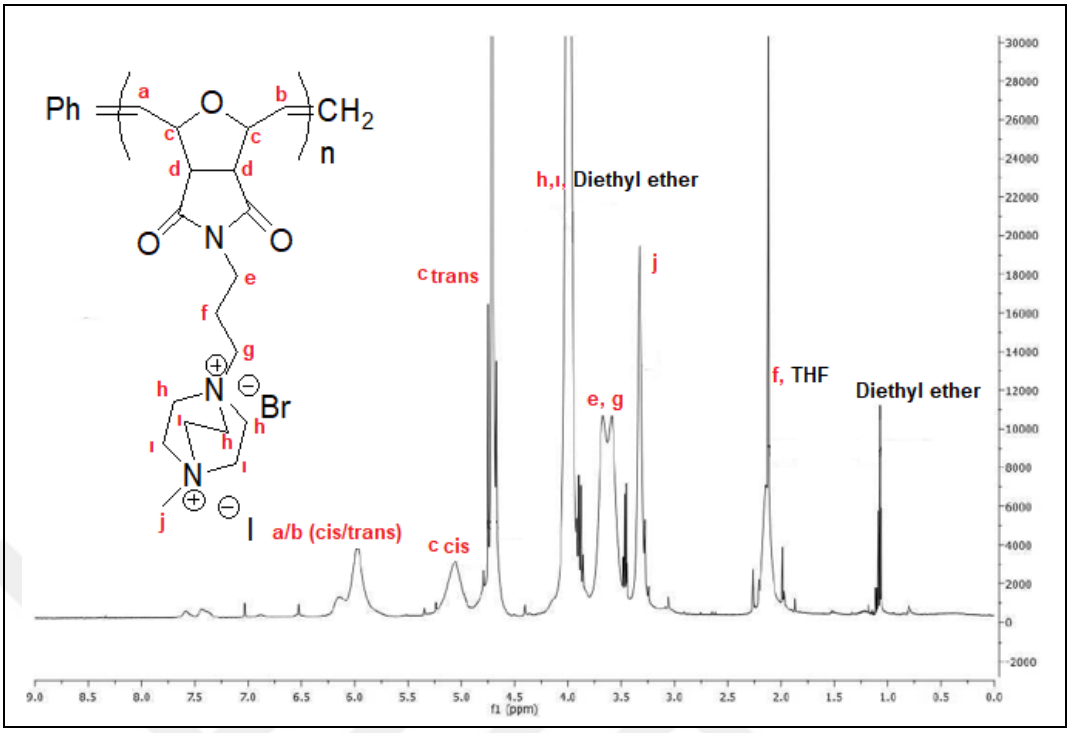

Figure 5.21. ^{1}H NMR spectrum of D-10

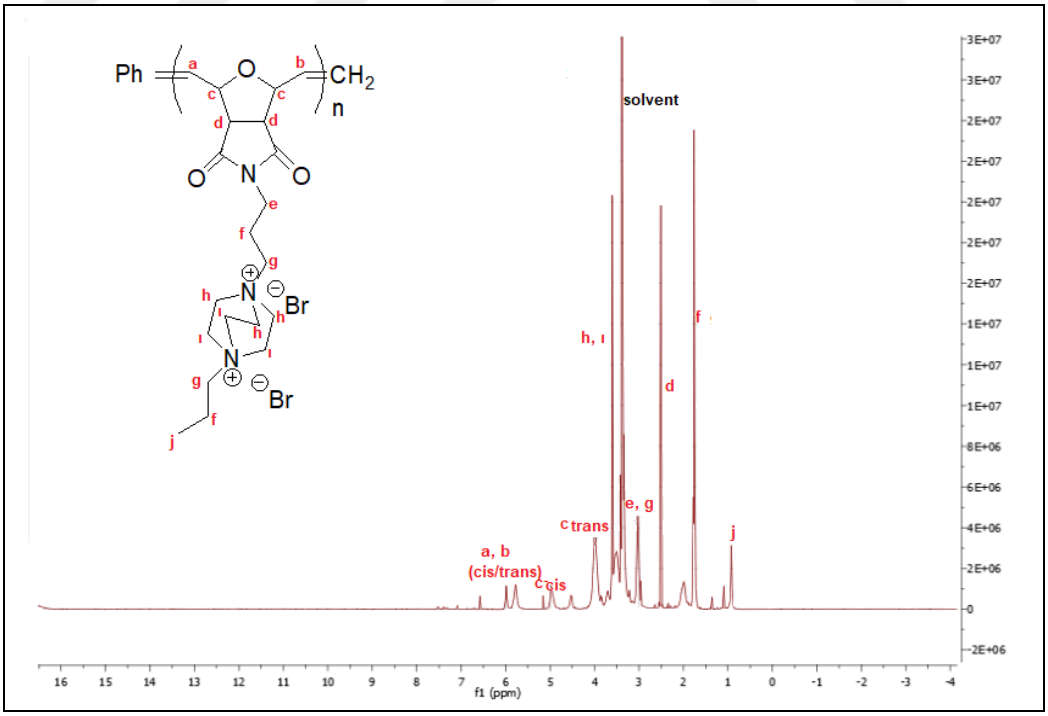

Figure 5.22. ^{1}H NMR spectrum of ID-10

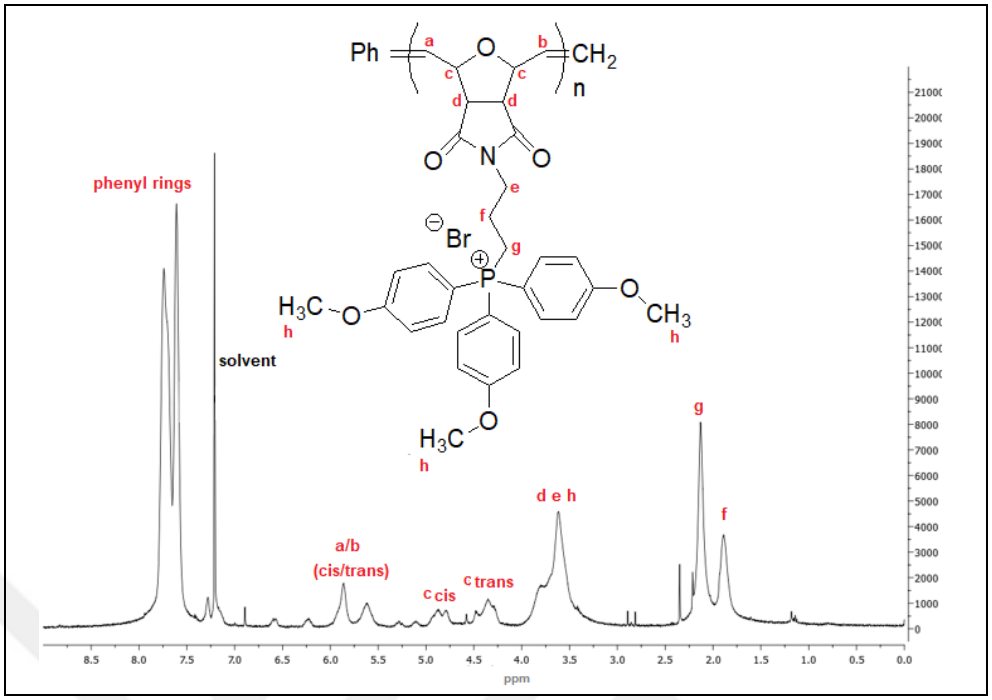

Figure 5.23. ^{1}H NMR spectrum of M-3

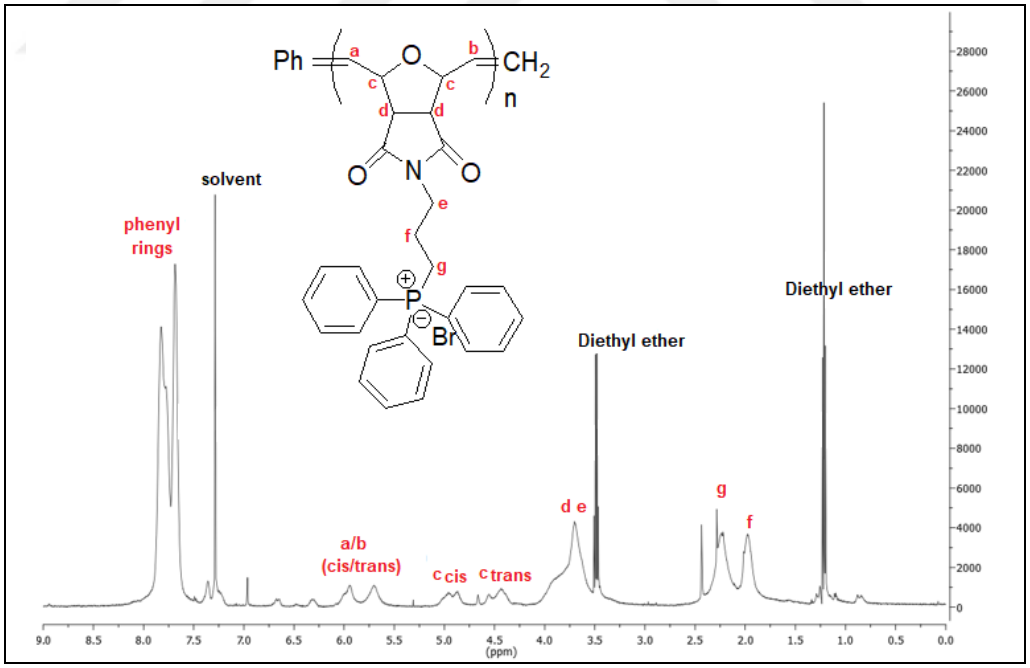

Figure 5.24. ^{1}H NMR spectrum of Phe-3

5.2.2. NMR Analysis of Copolymers

In this study, copolymers were also synthesized using different weight ratios (1:1, 1:2, 2:1) of pyridinium and DABCO double-charge bearing monomers (Monomer 1 and Monomer 2, respectively), while keeping the molecular weight constant at 5000 g/mol. The synthetic schema of the copolymers are given in Figure 5.25.

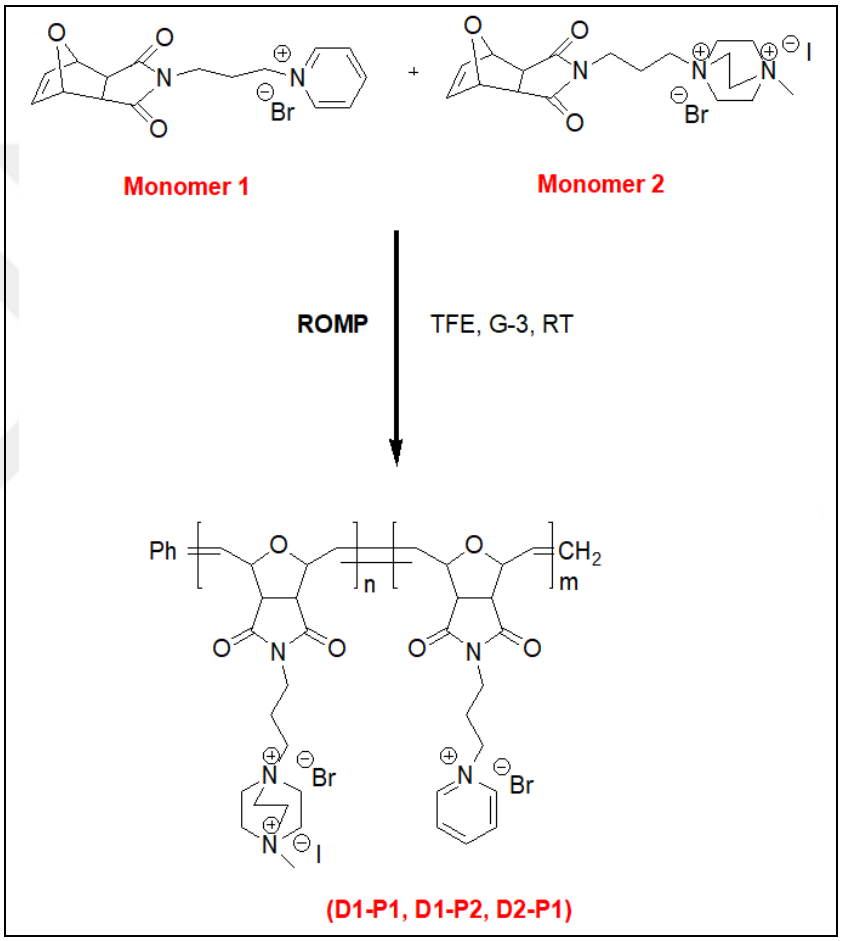

Figure 5.25. The synthetic schema of the copolymers

The ^{1}H NMR spectrum of the copolymer D1-P1 is given in Figure 5.26 as representative. The ^{1}H NMR spectra of D1-P2 and D2-P1 can be seen in Appendix A (Figure A.6 and Figure A.7, respectively). The double bond protons (6.5 ppm) of norbornene rings are disappeared due to ring opening polymerization, and the peaks correspond to cis and trans protons of the structures were occurred at 5.6 ppm (C_{cis}) and 6 ppm (C_{trans}), respectively.

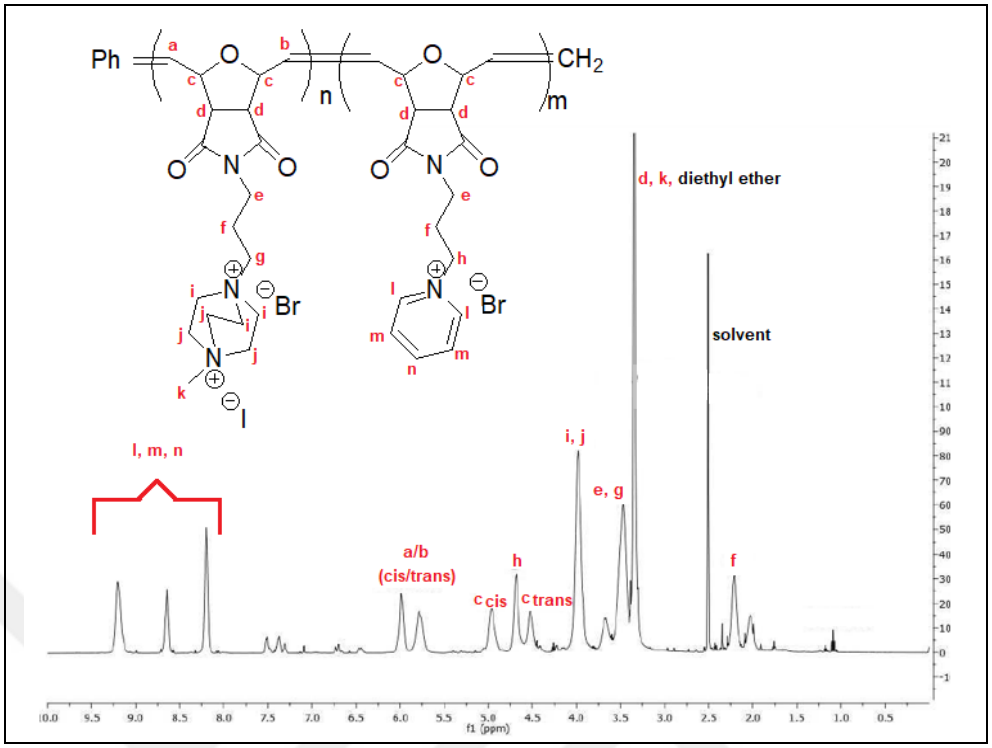

Figure 5.26. ^{1}H NMR spectrum of D1-P1 copolymer

5.2.3. FTIR Analysis of the Polymers

FTIR spectrum of each polymer was given only for one molecular weight as representative from Figure 5.27 to Figure 5.32, the other FTIR spectra can be found in Appendix B (Figure B.1 to Figure B.7).

The FTIR spectra of pyridinium bearing P-10, DABCO double charge bearing (via CH_3I) homopolymers D-10, and their copolymer D1-P1 are given in Figure 5.27, Figure 5.26 and Figure 5.28, respectively. Figure 5.30 shows DABCO double charge bearing (via propyl bromide) homopolymer ID-10. The synthesized polymers were hygroscopic, thus the peaks around 3400-3446 cm^{-1} are attributed to the retained moisture from the environment during analysis. The peaks around 3052-2960 cm^{-1} are regarding to the stretching of C-H bonds in the aliphatic and aromatic groups. The strong peaks around 1773-1770 cm^{-1} represents the symmetric and asymmetric stretching vibrations of imide carbonyl groups. The peaks around 1690-1700 cm^{-1} are attributed to the stretching of C=C and C=N of aromatic groups. The bands at 1495-1397 cm^{-1} are due to the stretching of C-C bonds in aromatic groups. The

bands around 1399-1362 cm^{-1} are attibuted to the stretching of C-N bonds. The peaks around 1100 cm^{-1} represent the stretching of C-O-C bonds. The bands around 1054-1028 cm^{-1} are due to the stretching of C-N bonds. The bands around 912-660 cm^{-1} are corresponding to aliphatic C-H bending. The bands at around 860-790 cm^{-1} in Figure 5.28 to Figure 5.30 represent the para disubstituted aromatic groups.

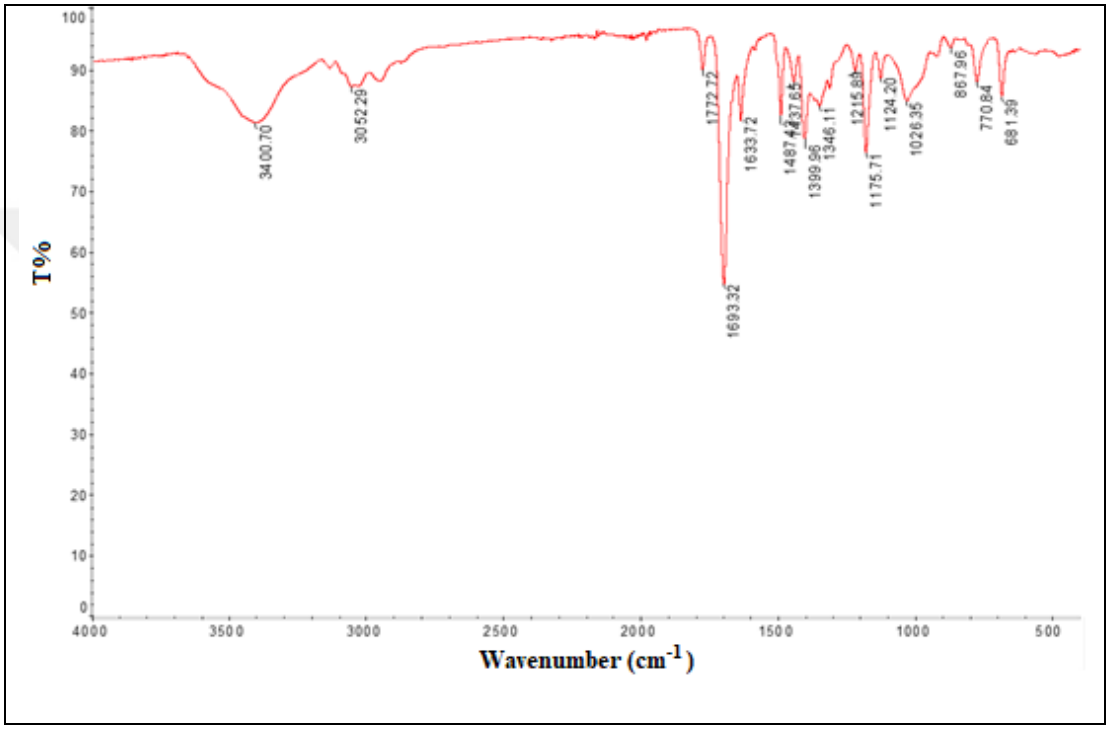

Figure 5.27. FTIR spectrum of P-10

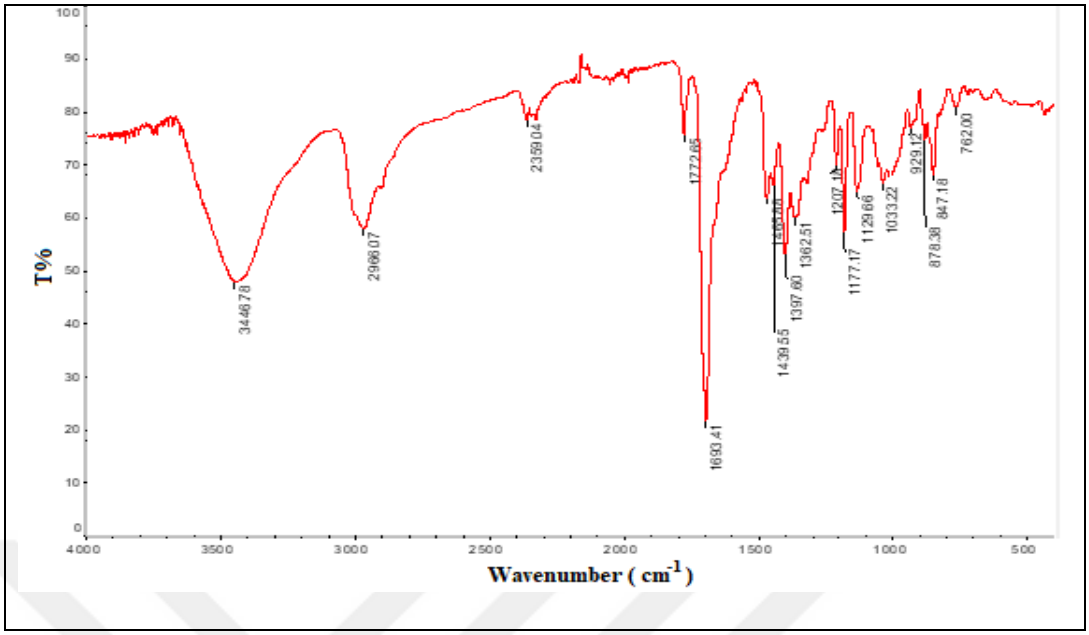

Figure 5.28. FTIR spectrum of D-10

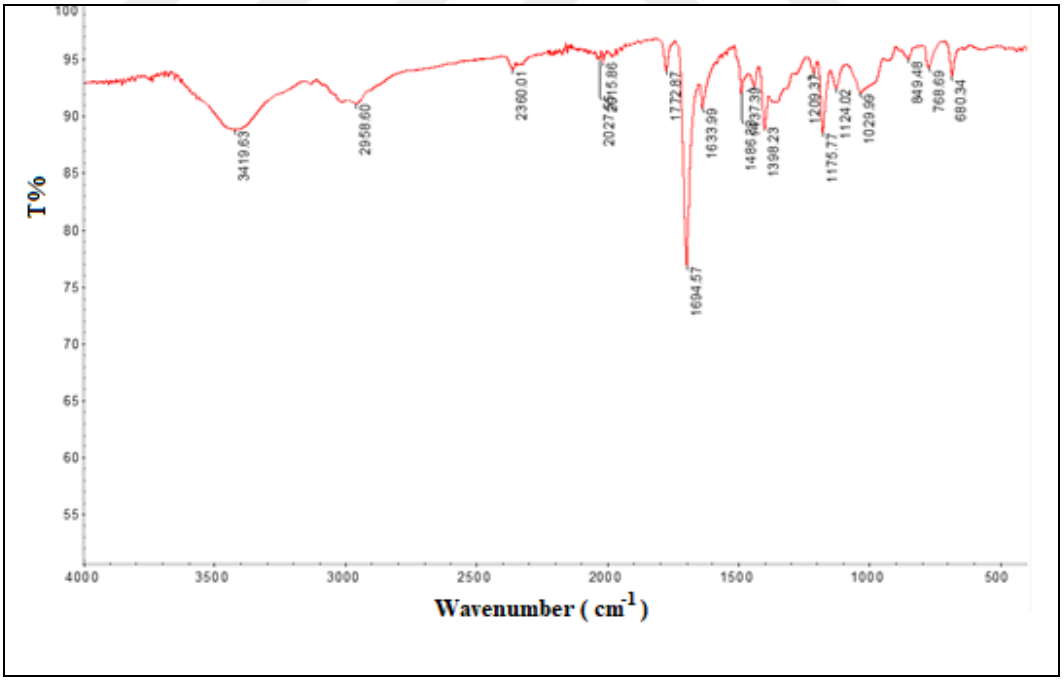

Figure 5.29. FTIR spectrum of D1-P1

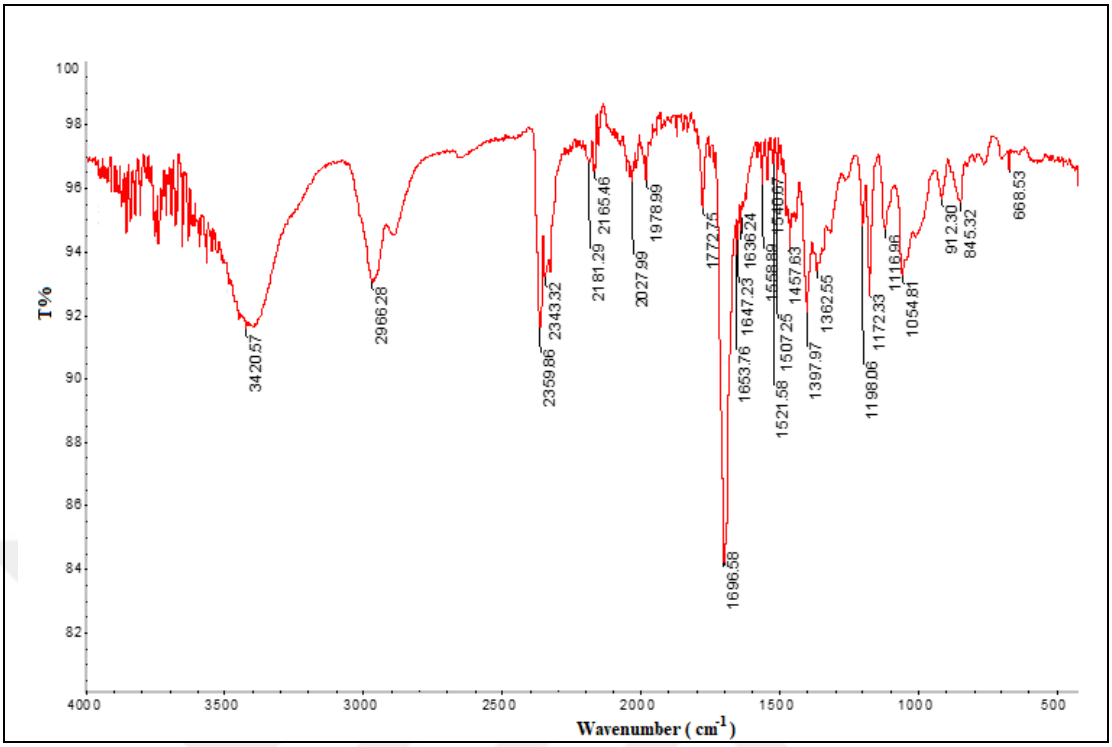

Figure 5.30. FTIR spectrum of ID-10

The FTIR spectra of trimethoxyphenyl phosphonium bearing homopolymer M-10 and triphenyl phosphonium bearing homopolymer Phe-3 are given in Figure 5.31 and Figure 5.32, respectively. The peaks around 3390-3385 cm^{-1} are attributed to the retained moisture from the environment during analysis. The peaks around 3052-2906 cm^{-1} are regarding to the stretching of C-H bonds of phenyl rings. The bands around 2841 cm^{-1} in Figure 5.31 are attributed to the bending of C-H bonds of methoxy groups (CH_3-O-). The peaks around 1774-1773 cm^{-1} are regarding to the stretching of the imide groups. The peaks around 1698 cm^{-1} are attributed to the stretching of C=C and C=N bonds of aromatic groups. The peaks at 1503-1399 cm^{-1} are due to the C-C stretching in aromatic groups. The bands around 1200-1296 cm^{-1} are due to the stretching of P-C bonds. The peaks around 1153 cm^{-1} represent the stretching of C-O-C bonds. The bands around 1015-1025 cm^{-1} are due to the stretching of C-N bonds. The several peaks between 830-689 cm^{-1} represents the bending of C-H bonds of aromatic groups.

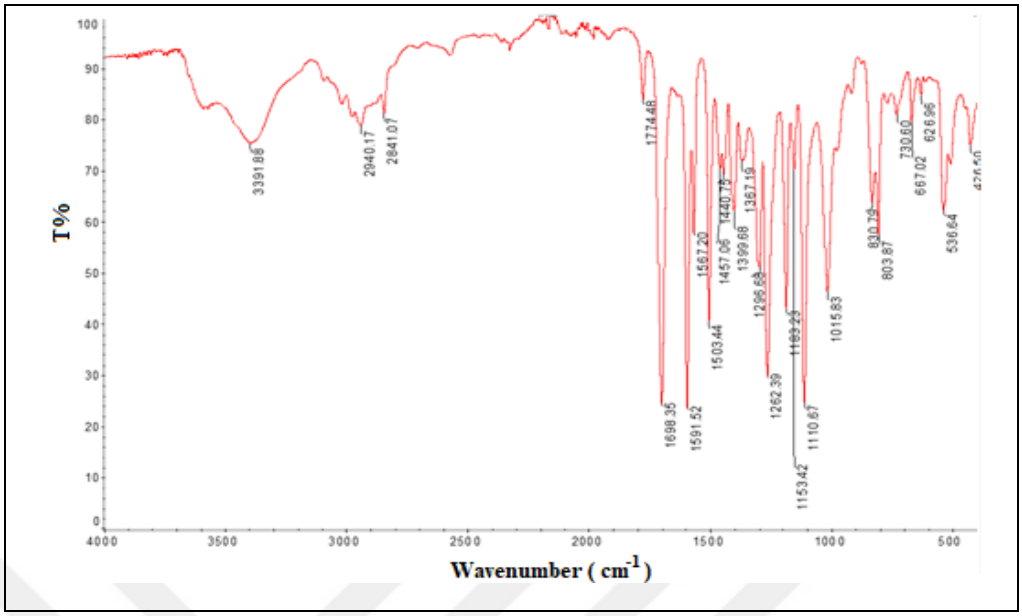

Figure 5.31. FTIR spectrum of M-10

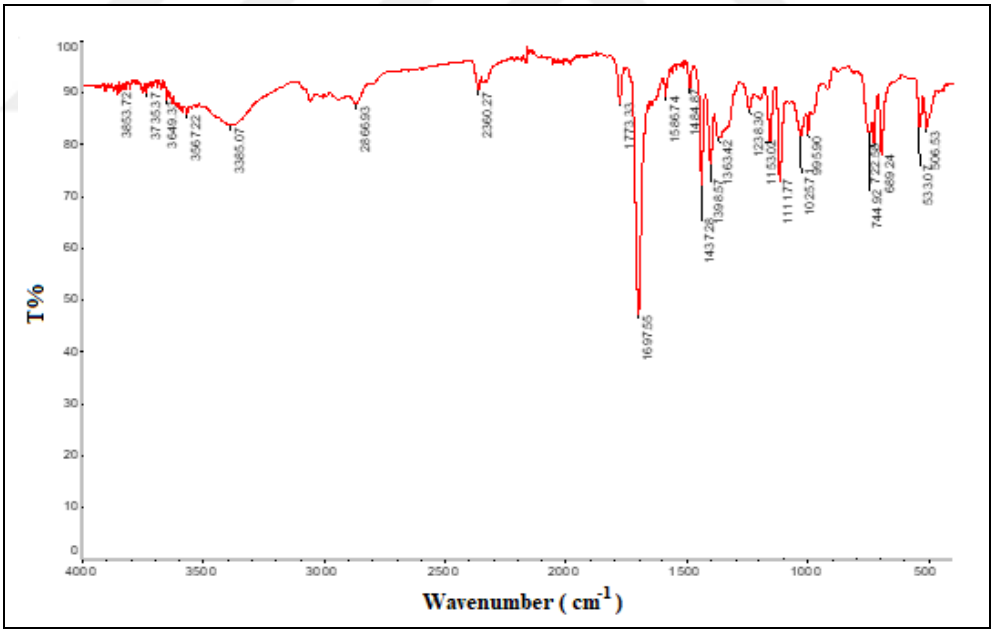

Figure 5.32. FTIR spectrum of Phe-3

In this section, the charcterization of the synthesized compounds, monomers and polymers were done using NMR techniques. The structures of the compunds were determined using NMR techniques. For further analysis FTIR was applied and FTIR analyses supported the

^{1}H NMR results. The desired polymers were synthesized succesfully via ROMP polymerization.

5.3. ANTIMICROBIAL ACTIVITY OF THE POLYMERS

The determined MICs of the synthesized polymers are shown in Table 5.1. Concentrations tabulated in the Table 5.1 are the minimum concentrations of polymer required to inhibit the growth of the bacteria. The polymers with MIC >512 μg/mL were accepted as inactive against bacteria. The pyridinium and DABCO double-charged salt bearing polymers generally exhibit low activity against *E.coli*, compared to the triphenyl phosphonium and the tirmetoxhyphenyl phosphonium salt bearing polymers. According to the test results, DABCO double charge salt bearing homopolymers are more active against Gram (+) *S.auerus* than the pyridinium based homopolymers. Among all the DABCO double-charged and pyridinium salt bearing polymers, increasing from mono charged to double charged in each repeating unit highly enchanced the activity towards *S.aureus*, yet they had low activity against *E.coli* either way. Additionaly, there is a relation between the antimicrobial activity and the molecular weight for DABCO double-charge and pyrdinium salt bearing homopolymers, that can be seen from Table 5.1, the increasing molecular weight lead to enhancement in the antimicrobial activity towards *S.aureus* from 16 μg/mL to 8 μg/mL for DABCO double-charged bearing polymers, and from >256 μg/mL to 128 μg/mL for pyridinium salt bearing polymers. However, the copolymers (D1-P1, D1-P2 and D2-P1, MW: 5000 g/mol), which are the combination of DABCO doulbe-charge and pyrdidinium salt bearing monomers did not exhibit any significant enhancement. Overall, D-10 (MW: 10000 g/mol) exhibit the highest activity towards *S.aureus* with a MIC of 8 μg/mL.

Table 5.1. MICs of the synthesized polymers

Polymer	**$M_{n(theoretical)}$ (g/mol)**	***S.aureus* (μg/mL)**	***E.coli* (μg/mL)**
P-3	3000	>256	>256
P-10	10000	128	128
D-3	3000	16	128
D-10	10000	8	128
D1-P1	5000	32	>256
D1-P2	5000	16	>256
D2-P1	5000	16	>256
ID-3	3000	512	>512
ID-10	10000	512	>512
Phe-3	3000	8	16
Phe-10	10000	16	32
M-3	3000	8	64
M-10	10000	8	32

The reason for the DABCO double-charge and pyridinium salt bearing polymers having low activity against *E.coli* might be due to the cell membrane structure of the Gram (-) bacteria, which might block the interaction between the phospholipid layers and polymers [53]. Gram (+) bacteria have a 20-80 nm thick peptidoglycan layers, while Gram (-) bacteria have much thinner (2 nm), however, Gram (-) bacteria have double plasma membrane, which increases the resistance and obstructs the entrance of the polymers to the inner membrane [57]. Thus, the polymers are supposed to break two membranes in order to kill *E.coli.* Additionally, hydrophobicity is also an important parameter on antimicrobial activity [164]. The interactions between polymers and bacteria's phospholipid bilayer enhance with increasing hydrophobicity [57]. It was thought that, the hydrophobicity of the mono-charged DABCO and pyridinium salt bearing polymers were not sufficient to destabilize the outer membrane, however double-charged polymers were able to disrupt the membrane of *S.aureus* while they were not able to disintegrate the double membrane of the *E.coli*. The polymers might aggregate on the outer layer of *E.coli* but the inner membrane lead to the bacterial survival.

ID-3 and ID-10 polymers are also DABCO double-charged salt bearing polymers, they were synthesized using propyl bromide in order to have longer alkyl chain which enhance hydrophobicity. However these polymers were found inactive towards both *S.aureus* and *E.coli* with MIC of >512 μg/mL.

On the other hand, the triphenyl phosphonium and trimethoxyphenyl phosphonium bearing polymers were highly active towards both *S.aureus* and *E.coli*. Phenyl rings bearing substantially hydrophobic rigid structure might lead to a better interaction between the polymers and the bacterial cell wall.

5.4. CYTOTOXICITY STUDY OF THE POLYMERS

5.4.1. Hemolytic Activity (HC_{50})

Toxicity has a great importance for polymers as well as antimicrobial activity. The concentration of the polymer whereas the 50 percent of the RBCs are lysed gives the HC_{50} value of the related polymer [165]. HC_{50} values of all the synthesized polymers were determined and are given in Table 5.2.

It is seen from the Table 5.2 that the DABCO double charge and pyridinium salt bearing polymers have high HC_{50} values (HC_{50}>1000 μg/mL), thus, it can be concluded that they are not toxic. Among all the copolymers, the increasing amount of double-charged monomer presence leads to a drop in the HC_{50} value from 2000 μg/mL to 1000 μg/mL. The selectivity values shows that D-10 (HC_{50}< 2000 μg/mL) has 250 times more selective towards *S.aureus* than the RBCs. However, triphenyl phosphonium (Phe-3 and Phe-10) and trimethoxy phosphonium (M-3 and M-10) salt bearing polymers are very hemolytic (HC_{50}< 250 μg/mL) and they exhibit low selectivity towards bacteria (Table 5.2). Süer *et. al*, reported that the low hemolytic concentrations of Phe-3, Phe-10, M-3 and M-10 might be due to the overly aromatic structure of the polymers, that enhance the membrane interactions and as a result they are hemolytic [57].

Table 5.2. The Hemolytic concentration (HC_{50}) and selectivity values of the synthesized polymers

Polymer	**HC_{50} (μg/mL)**	**Selectivity (SI) (HC_{50}/MIC*)**	
		S.aureus	***E.coli***
P-3	>2000	7.81	7.81
P-10	>2000	15.62	15.62
D-3	1000	62.5	7.81
D-10	>2000	250	15.62
D1-P1	>2000	62.5	7.81
D1-P2	2000	125	7.81
D2-P1	1000	62.5	3.9
Phe-3	99	12.38	6.19
Phe-10	>100	6.25	3.13
M-3	85	10.63	1.33
M-10	46	5.75	1.44

*MIC values of the polymers were taken from Table 5.1 for calculation.

5.4.2. MTS Assay

MTS assay provides information about the toxic effect of the samples on the cell viability that it can be determined if the sample is cytotoxic or non-cytotoxic. *In vitro* cytotoxicity of all the polymers at varying concentrations were tested. The cell viability results of the polymers are given in the figures from Figure 5.33 to Figure 5.37. The MTS results for DABCO double charge and pyridinium salt bearing homo- and copolymer are given in the Appendix C (Figure C.1- Figure C.8).

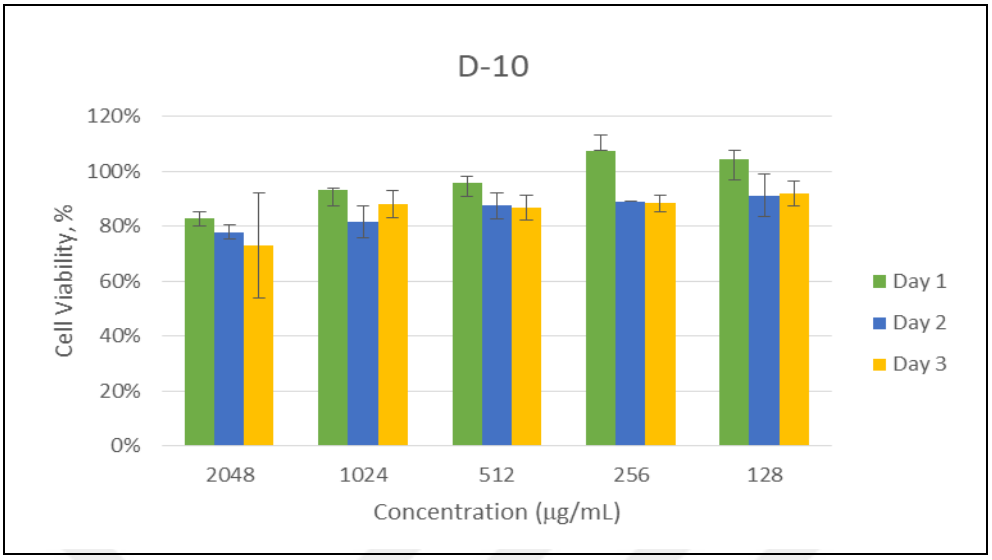

Figure 5.33. MTS results of D-10

Figure 5.33 represents the MTS assay results of DABCO double-charge bearing homopolymer, D-10. According to the Figure 5.33, D-10 homopolymer didn't exhibit any toxic effect towards HUVEC cells (cell viability >75 percent). Thus, it can be resulted that D-10 is a non-toxic polymer which was supported by the HC_{50} results. Additionally, the MTS assay results of the other DABCO double-charge salt and pyridinium salt bearing homo- and copolymers can be found in Appendix C. They were also found to be non-toxic as well as non-hemolytic polymers.

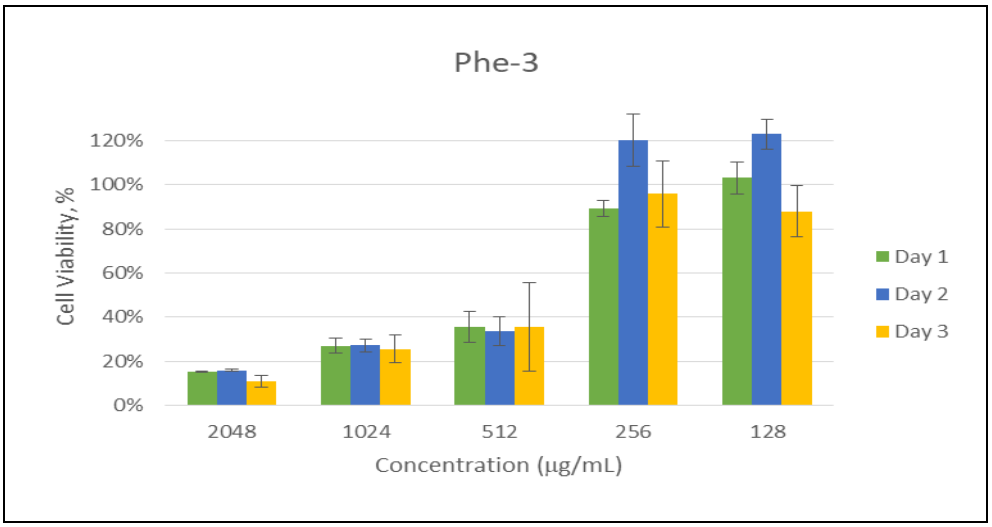

Figure 5.34. MTS results of Phe-3

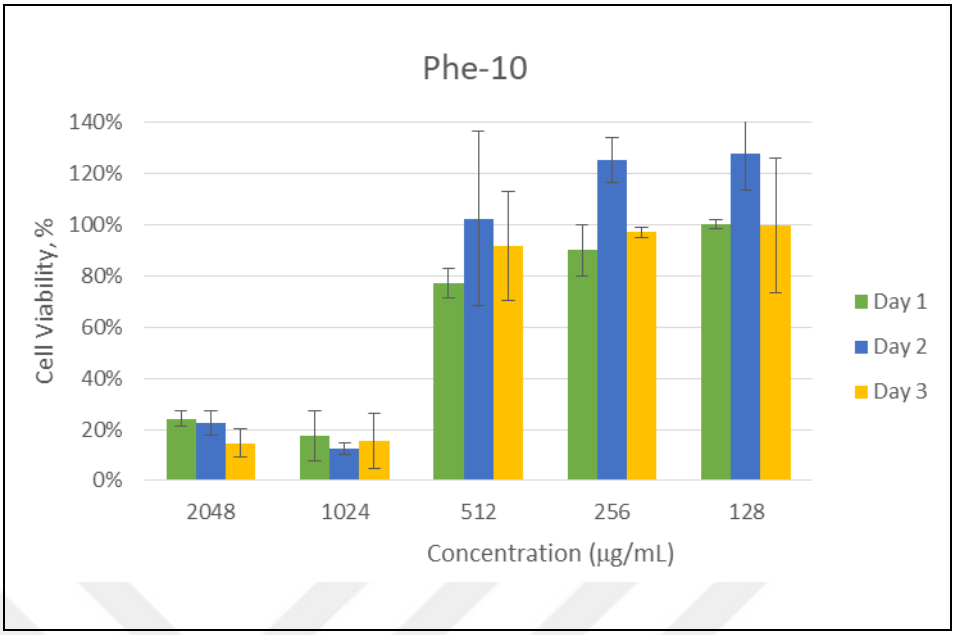

Figure 5.35. MTS results of Phe-10

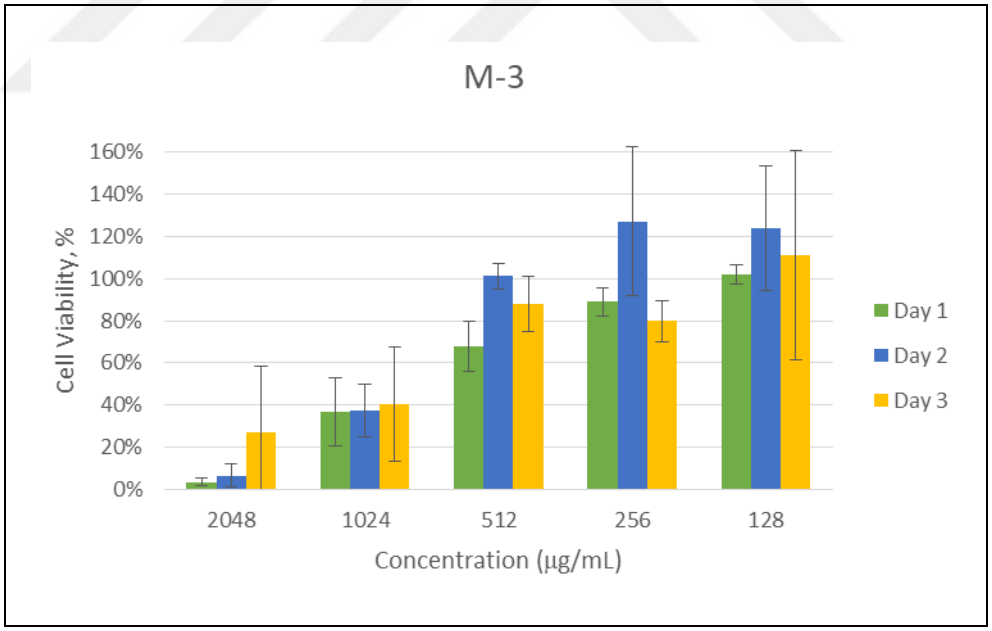

Figure 5.36. MTS results of M-3

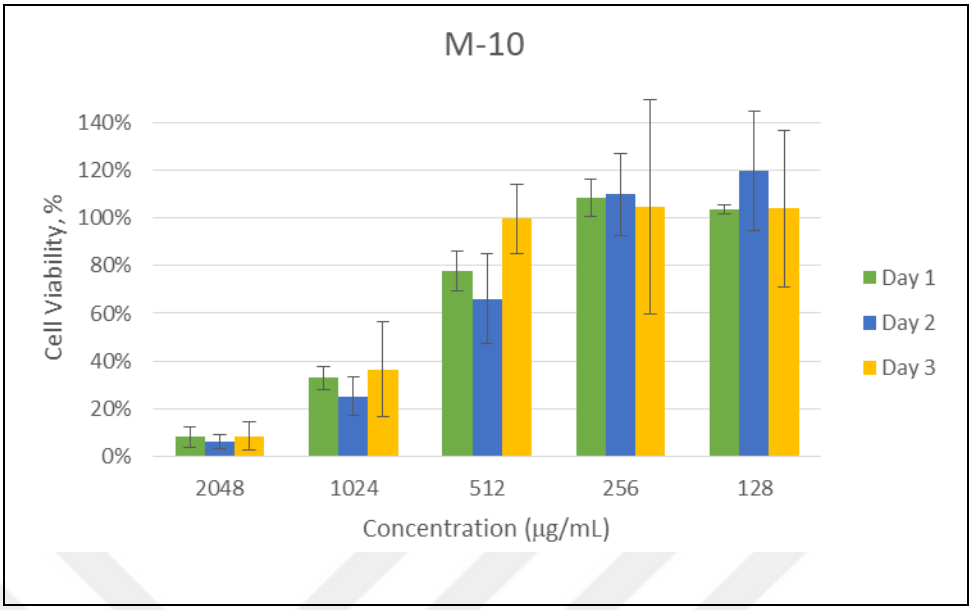

Figure 5.37. MTS results of M-10

Figure 5.34-Figure 5.37 represent the MTS assay results of triphenyl phosphonium (Phe-3 and Phe-10) and trimethoxyphenyl phosphonium (M-3 and M-10) bearing homopolymers. According to Figure 5.34, Phe-3 polymer was found to be toxic at 512 µg/mL, and higher concentrations (<40 percent). Phe-10 polymer (Figure 5.35) was found to be toxic at 2048 µg/mL and 1024 µg/mL (<30 percent). M-3 and M-10 polymers (Figure 5.36 and Figure 5.37, respectively) were found to be toxic at 2048 µg/mL and 1024 µg/mL (<40 percent). However, while the MTS assay was conducted to the triphenyl phosphonium and trimethoxyphenyl phosphonium bearing polymers, the stock solution of those prepared in DMSO were diluted using cell culture medium DMEM, which is a highly aqueous solution. During the dilution process the polymers with the highest two concentrations precipitated in DMEM due to their hydrophobic structures. The microscopic images of the cells were taken while they were treating with these polymers (Figure 5.38). The low cell viability results for triphenyl phosphonium and trimethoxyphenyl phosphonium bearing polymers might be caused by the relatively big polymer particles suppressing the viability of the small cells as they precipitated on them. But, as HC_{50} results triphenyl phosphonium and trimethoxyphenyl phosphonium bearing homopolymers already showed toxic effect on the blood cells, MTS results, whether due to precipitation or not, support the toxicity of these polymers above a certain concentration.

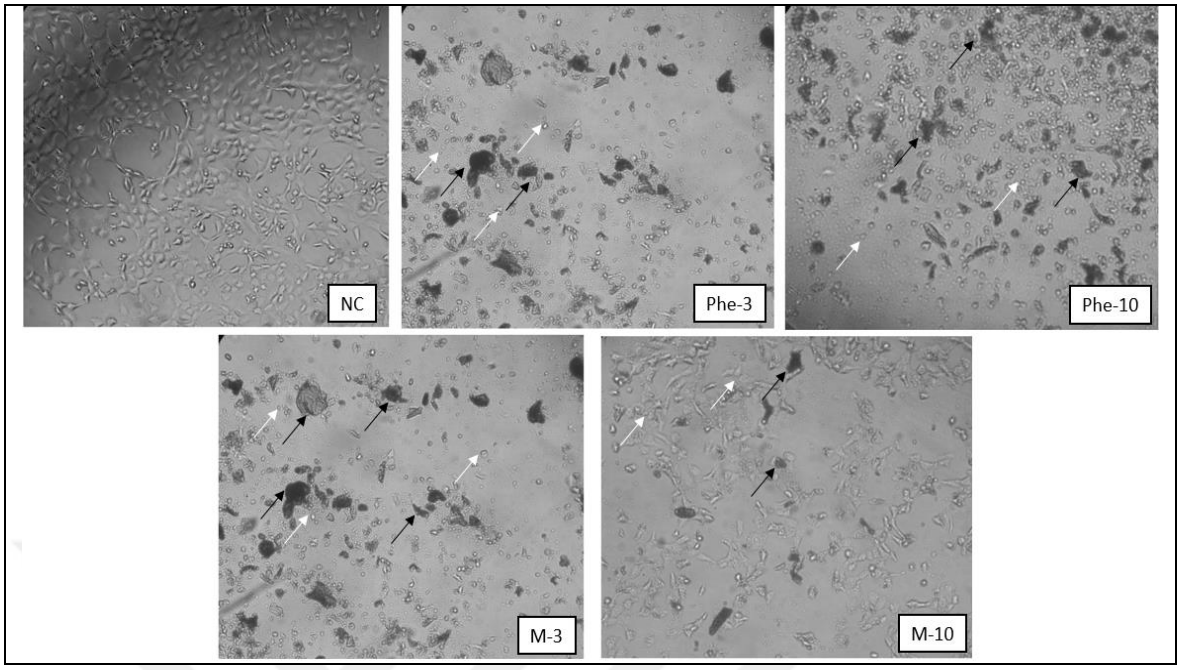

Figure 5.38. Microscopic images of HUVEC vs the synthesized polymer in cell culture medium (NC:Control Cells)

The toxicity of the materials which were synthesized for biological use has a significant importance. However, toxicity is harder to define, due to the different toxicity types that can be measured. The toxicity of synthetic mimics of antimicrobial peptides is typically evaluated by presenting them to erythrocytes to examine the lysis of the cells [165]. In many studies, it was reported that cationic polymers exhibit enhanced antibacterial activities [27, 12, 166, 167, 168]. The quaternary ammonium or phosphonium functionalized polymers are the most common. According to the toxicity of this class of polymers at relatively low concentrations, they are predominately used in solid state as biocidal coatings or filters, potent disinfectants etc [27]. Li *et al.*, reported that a soluble pyrdinium polymer had low acute toxicity towards the skin of test animals [169]. Tew and Coughlin pioneered the field of ROMP-based synthetic analogous of the antimicrobial peptides [27]. A number of poly(norbornene) derivatives with facially amphiphilic repeat units were reported. The ratios of hydrophobic and hydrophilic moieties per repeat unit were gradually varied in this polymer series and they studied the effect of this variation on these polymers' antibacterial and hemolytic activities [27]. They have reported that the norbornene derivatives synthesized via ROMP showed good antibacterial activities and high selectivities for bacteria over RBCs. In this study the cationic pyridinium salt, DABCO double-charge salt

bearing polymers were synthesized individually and also their copolymers were synthesized, and they were found non-hemolytic and non-toxic, in lieu with literature.

Wang *et al*., synthesized quaternary phosphonium salt bearing water soluble chitosan derivatives and pursued cytotoxicity studies using mouse fibroblast cells (L929 cells). They reported that chitosan alone did not exhibit any toxic effect to L929 cells, while the cytotoxicity of quaternary phosphonium salt bearing polymers were slightly increased. Since they introduced small amount of cationic triphenylphosphonium groups comparing to chitosan backbone, the cytotoxicity to L929 cells were low [170]. Megiatto et al., synthesized a water-soluble polyphosphonium polymer and its ammonium analog. They investigated the cytotoxicity of the polymers using human cervical cancer cells (HeLa cells). The cell viability was >90 percent in the presence of phosphonium polymers up to 250 μg/mL) after 48 hours [171]. Trimethoxyphenyl phosphonium salt (M-3 and M-10) and triphenyl phosphonium salt (Phe-3 and Phe-10) bearing polymers were synthesized in this study and they were found hemolytic, however due to their hydrophobicity the MTS assay did not give decent results for higher concentrations (>512 μg/mL), yet the polymers were found non-toxic at lower concentrations (≤512 μg/mL). It was reported by Xue et al. that excessive hydrophobicity tends to increase toxicity [172], which is similar to the results we obtained. Additionally, Carmona-Ribeiro *et al*., reported that the toxicity towards eukaryotic cells correlate to antimicrobial activity and the most active antimicrobials are significantly hemolytic as well [42].

In summary, D-3, D-10, D1-P1, D1-P2 and D2-P1 showed non hemolytic, yet active towards *S.aureus*, all exhibiting high selectivity towards the bacteria. The presence of the double positive charge on the D-3, D-10, D1-P1, D1-P2 and D2-P1 polymers appear not to significantly affect the antimicrobial activity on the negative cell membrane of bacteria, possibly because of the double cell wall that *E.coli* possesses and the lack of hydrophobicity in these polymers. Phe-3, Phe-10, M-3 and M-10, being hydrophobic polymers, showed high activity towards *S.aureus* and *E.coli*, however being not very selective and simultaneously being hemolytic. The antimicrobial ones are those that possess one positive charge but are significantly more hydrophobic.

5.5. CHARACTERIZATION OF VANCOMYCIN-PEG CONJUGATE

Vancomycin-PEG (VP) conjugate was synthesized via michael addition reaction at room temperture which is shown in Figure 5.39.

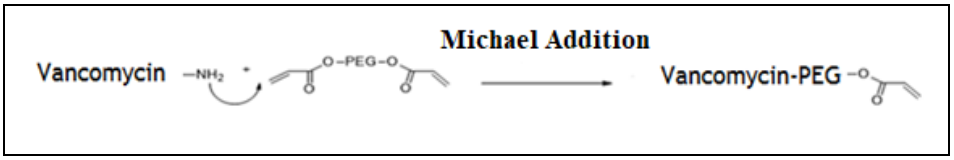

Figure 5.39. Synthetic schema of Vancomycin-PEG acrylate

5.5.1. NMR Analysis of Vancomycin-PEG Conjugate

The excess amount of PEG-diacrylate was used to ensure that only one of the two acrylates of PEG was bound to the amine group of vancomycin. The unreacted components were removed via purification process. The ^{1}H NMR spectra of vancomycin, (Figure 5.40), PEG-dicarylate (Figure 5.41) and VP conjugate (Figure 5.42) are shown below.

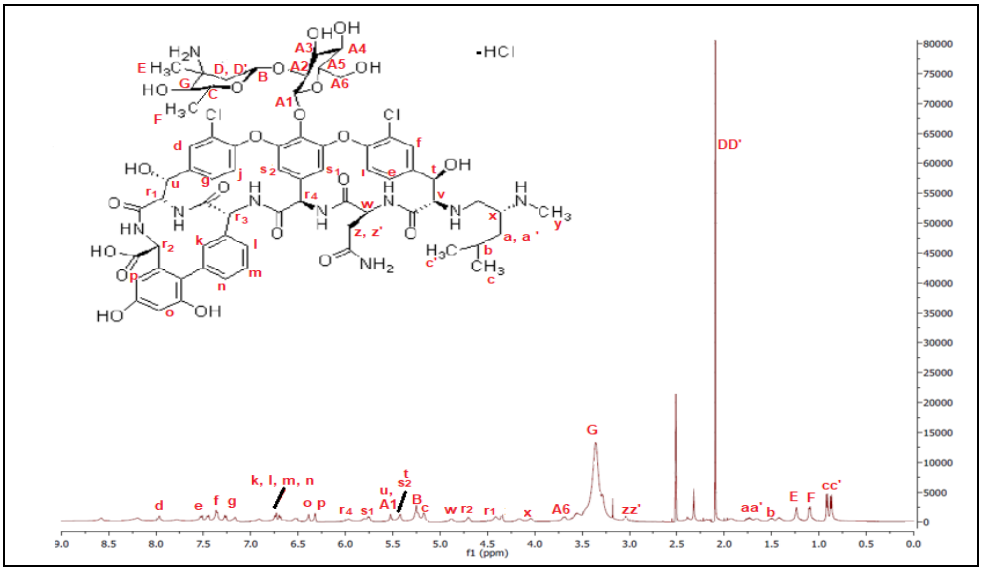

Figure 5.40. ^{1}H NMR spectrum of Vancomycin-HCl [173, 174]

The structure asssignment of vancomycin is given in Figure 5.34. ^{1}H NMR spectrum of vancomycin matches with the data which was reported by Swiatek *et al.(*2005) [173], and Pearce *et al.* (1995) [174].

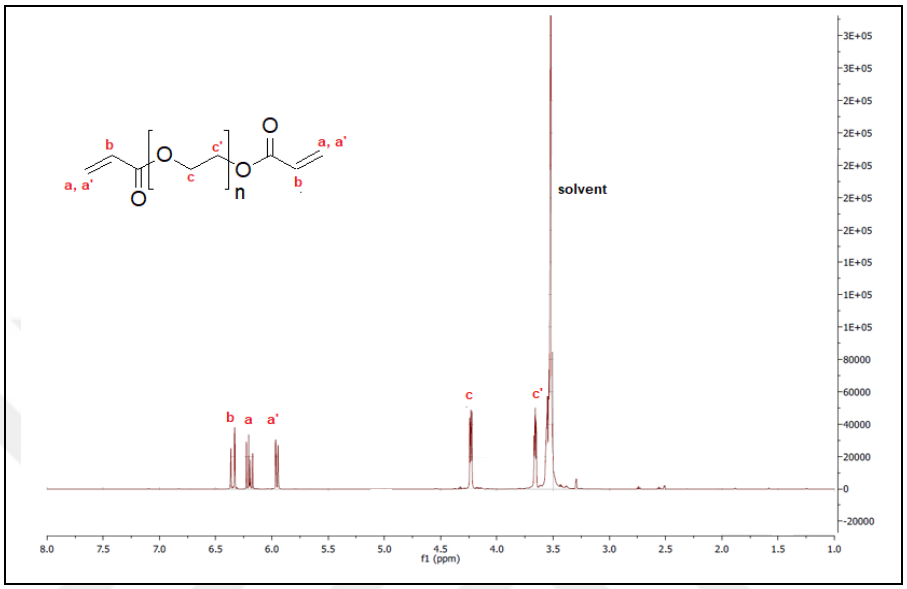

Figure 5.41. ^{1}H NMR spectrum of PEG-diacrylate

The peaks between 5.7 ppm- 6.5 ppm on ^{1}H NMR spectrum of PEG-diacrylate represent the protons of diacrylate of the structure.

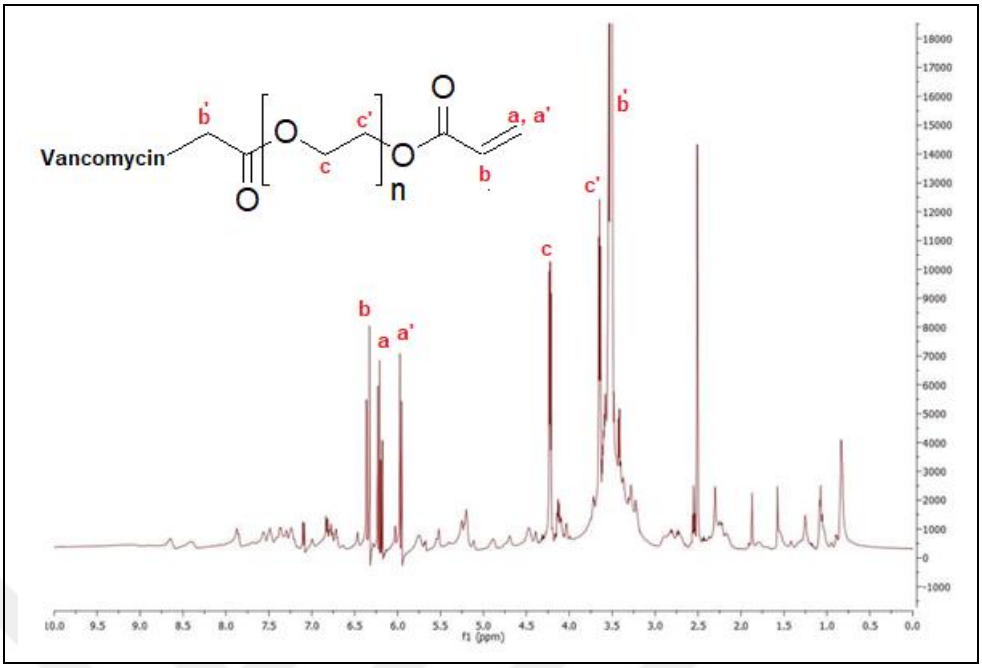

Figure 5.42. ^{1}H NMR spectrum of Vancomycin-PEG Conjugate

When the ^{1}H NMR Spectrum of Vancomycin-PEG Conjugate is compared with the spectra of vancomycin and PEG-diacrylate it is seen that the conjugate has all the peaks corresponding to those structures, and the peaks between 5.7 ppm-6.5 ppm which are corresponding to the protons of diacrylate remaining in the conjugate's structure. Furthermore, TLC analysis was applied to the NMR sample of the VP conjugate and it was found that there were not any unreacted PEG-diacrylate left in the VP conjugate sample.

5.5.2. HPLC Analysis of Vancomycin-PEG Conjugate

A HPLC-UV method was modified from Toi *et al.*'s study [175], and the same method was applied to vancomycin, PEG-diacrylate and VP conjugate sample. The conditions of HPLC method are shown in Table 4.1. The stock solutions of 1mg/mL for the standards were prepared using diH_2O for vancomycin and PEG-diacrylate, and diluted further in 1:10, 1:25, 1:50, 1:100 and 1:200 fractions for vancomycin standards, 1:2, 1:5, 1:10, and 1:25 fractions for PEG-diacrylate standards.

The HPLC spectrum of PEG-diacrylate (Figure 5.42) showed that the peak corresponding to PEG-diacrylate occured between 14-15 minutes of retention time, and the intensities of the

peaks that were belong to different concentrations were changing proportional to the concentrations generating a fit with R^2=0.9989. In the HPLC spectrum of vancomycin (Figure 5.43) the vancomycin peak was seen between 24-27 minutes of retention time. Same with PEG-diacrylate standards; the intensities of the vacomycin peaks were proportional to the related concentrations, generating a fit with R^2=0.9983. VP conjugate was purified using dialysis cassettes (2000 MWCO) for 15 days, after the synthesis via Michael Addition reaction. For the pupose of investigating the successfulness of the purification process, 1 mg/mL and 0.1 mg/mL of VP conjugate solutions in diH_2O were prepared. In the HPLC spectrum of VP conjugate (Figure 5.44) the related peak occured between 13-14 minutes of retention time, and there were not any peaks belonged to vancomycin or PEG-diacrylate, thus the purification was conducted succesfully. For further analysis, the calibration curves of vancomycin and PEG-diacrylate standarts were built (Figure 5.44) and the remaining vancomycin and PEG-diacrylate amounts within VP conjugate were calculated. Residual vancomycin was calculated as $0.24x10^{-4}$ mg/mL and PEG-diacrylate was calculated as $0.25x10^{-6}$ mg/mL, which are negligible amounts.

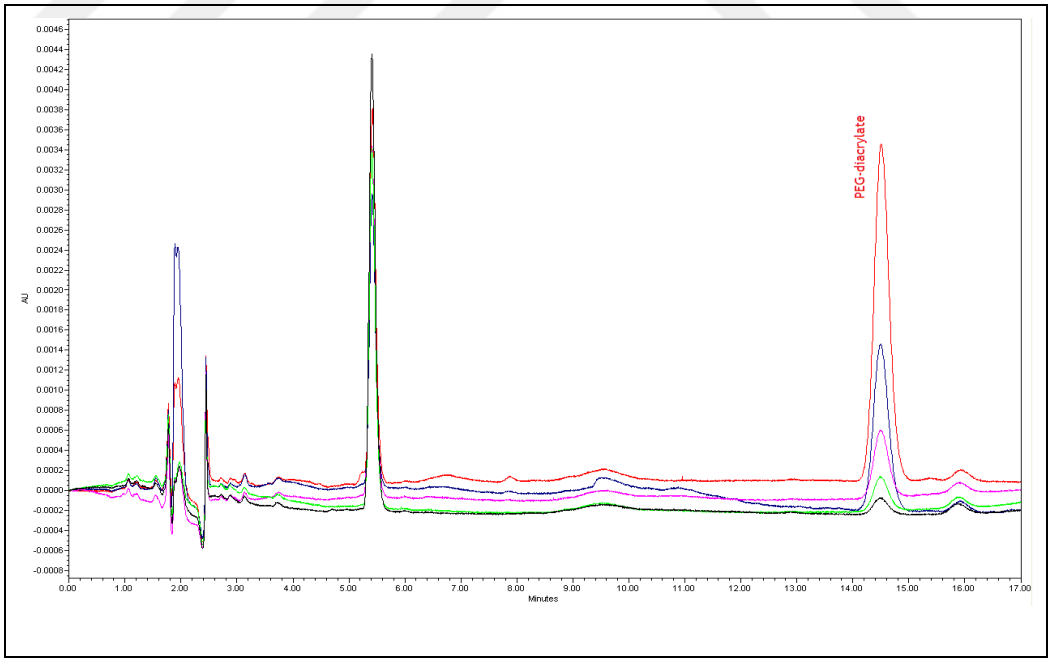

Figure 5.43. HPLC spectrum of PEG-diacrylate standarts

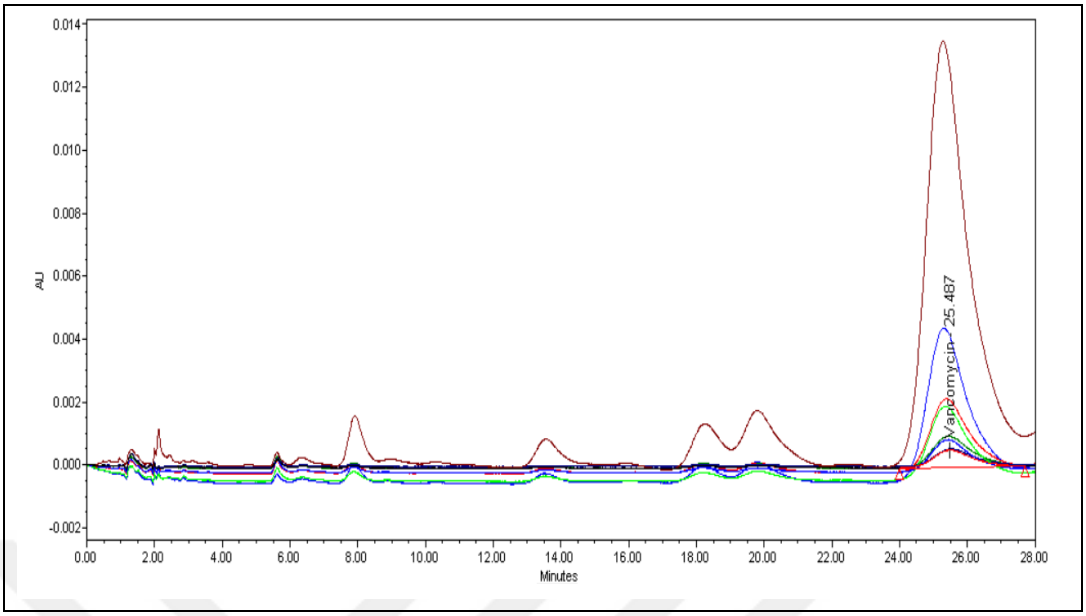

Figure 5.44. HPLC spectrum of Vancomycin standarts

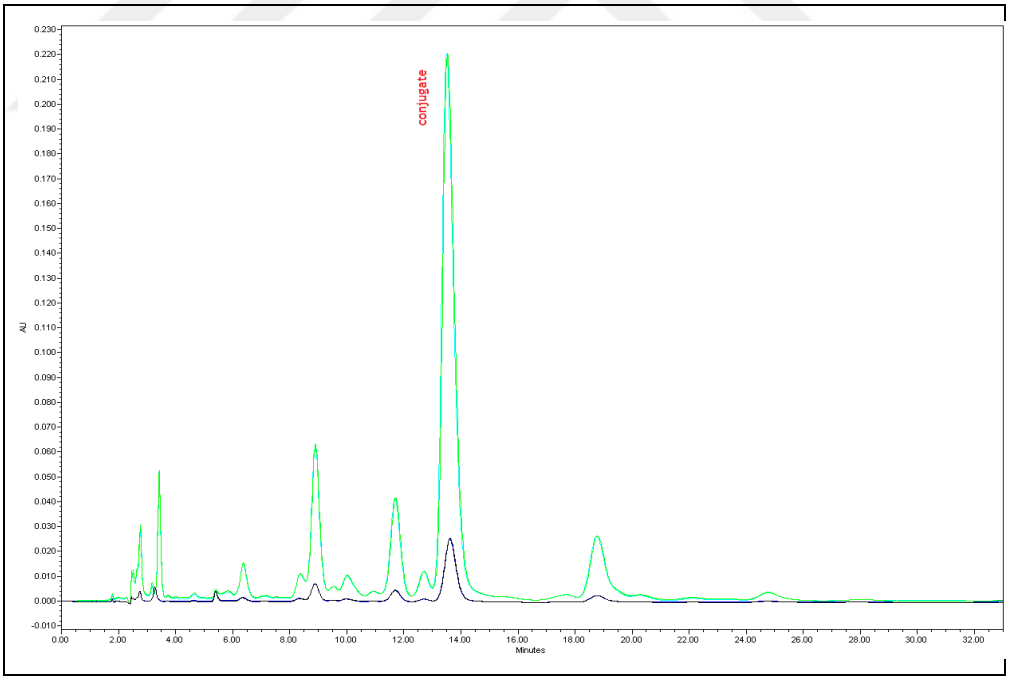

Figure 5.45. HPLC spectrum of VP conjugate

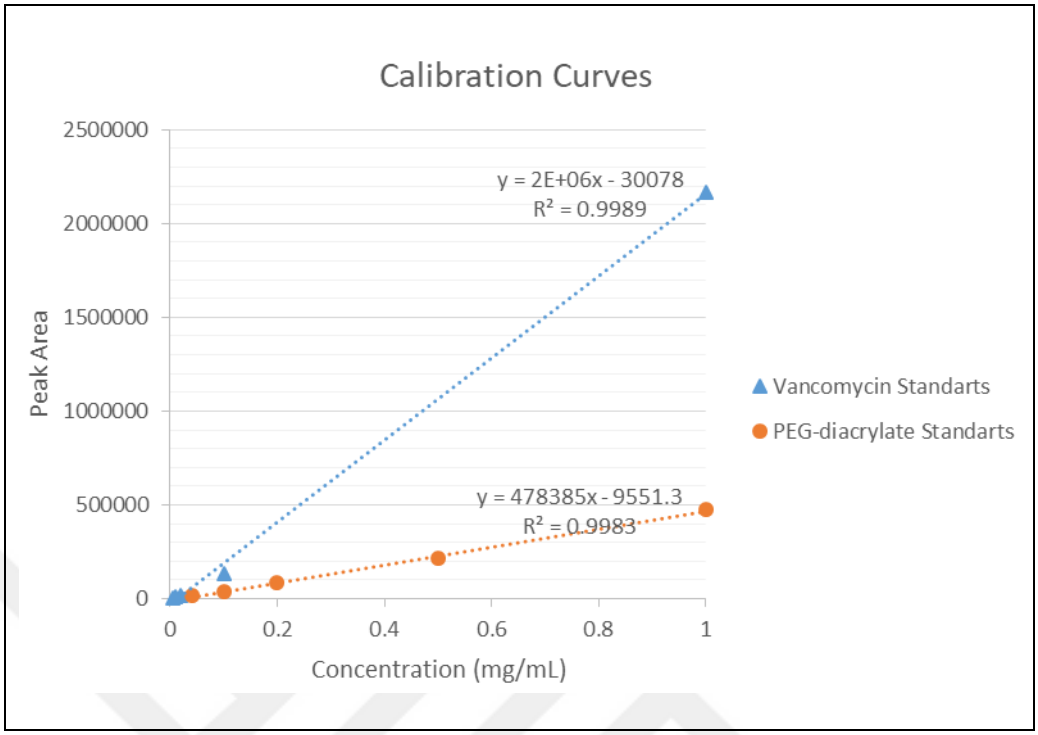

Figure 5.46. Calibration curve of standarts

5.5.3. FTIR Analysis of Vancomycin-PEG Conjugate

VP conjugate was dried using lyophilization after purification process. The conjugate in aqueous medium was frozen using liquid N_2 and freeze dried for 2 days, and white powder product (VP conjugate) was obtained. FTIR spectroscopy was used to analyze vancomycin, PEG-diacrylate, and their conjugation product VP conjugate (Figure 5.47). In vancomycin and VP conjugate spectra, the broad bands at 3281 and 3296 cm^{-1} are due to the N-H and O-H bonds vibration and the residual moisture in the structures. In PEG-diacrylate and VP conjugate spectra, the bands around 2860 to 2870 cm^{-1} are regarding to the C-H stretching and the peaks around 1650 to 1720 cm^{-1} are attributed to the stretching vibrations of C=O bonds, which is not seen on vancomycin's spectra. The peaks around 1300-1460 cm^{-1} are regarding to the stretching vibrations of C-O bonds on VP conjugate and PEG-diacrylate spectra. Additionally, one of the characteristic peaks of PEG-diacrylate, C=C stretching is seen on PEG-diacrylate's and VP conjugate's spectra at 810 cm^{-1}, contrarily, this peak is not seen on vancomycin's spectrum.

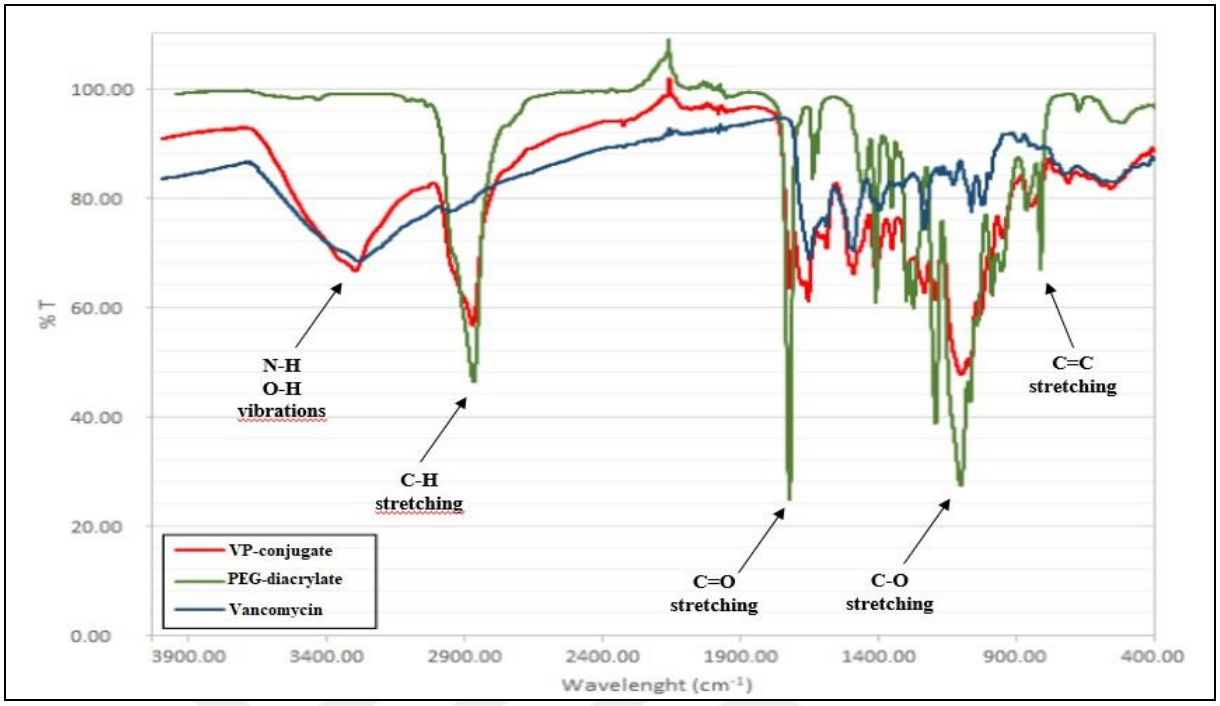

Figure 5.47. FTIR spectra of Vancomycin, PEG-diacrylate and VP Conjugate

In this section the VP conjugate was characterized using ^{1}H NMR, FTIR and HPLC techniques. VP conjugate was synthesized using excess amount of PEG-diacrylate in order to ensure that only one of the two acrylates of PEG-diacrylate was consumed during michael addition reaction. Keeping one of the two acrylates in VP conjugates structure has a great importance, because in cross metathesis reactions double bonds between carbon atoms are broken and bind from these carbons in the prescence of Grubbs catalysts. In our study, we conjugated vancomycin with PEG-diacrylate and obtain VP conjugate in order to bind the newly synthesized polymers to vancomycin from the acrylate part of the VP conjugate via cross metathesis pathways in the prescence of Grubbs catalysts. The structural assignment and analysis were performed using ^{1}H NMR. According to ^{1}H NMR results analysis, VP conjugate had the characteristic peaks of vancomycin and PEG-diacrylate. FTIR analysis supported the ^{1}H NMR analysis, as both analysis showed that VP conjugate was formed and the prescence of the acrylate group in the VP conjugate. For further analysis HPLC was used and it was found that a new peak occurred in HPLC spectrum for VP conjugate which was not seen either on vancomycin's or PEG-diacrylate's spectra and the negligible amount of PEG-diacrylate and vancomycin residue amounts were calculated from HPLC results. Thus, it was seen that the VP conjugate was synthesized and purified successfully.

5.6. CHARACTERIZATION OF POLYMER-VANCOMYCIN CONJUGATES

The remaining mono acrylate of VP conjugate (C=C) was bound to the double bonds of ROMP polymers using different Grubbs catalysts, via cross metathesis reaction. For the conjugation of VP conjugate with the synthesized polymers, the cross metahesis reaction was held at different conditions. Grubbs catalysts are higly active catalysts and they are used widely in cross metathesis reactions [153]. In this study, the cross metathesis reactions were catalysed using 3 different types of Grubbs catalyts (Grubbs catalysts 1st generation, Grubbs catalysts 2nd generation and Hoveyda-Grubbs catalyst 2nd generation) were used for the purposes of comparing and contrasting in order to find most effective one. VP conjugate and polymers ratios were varied as 1:1, 5:1, 10:1 and 20:1 on molar basis. The reactions were conducted at different temperatures as 40 ^{o}C and 100 ^{o}C for different reaction times as 4 hours and 24 hours. The synthetic schema of the polymer-VP conjugates are given in Figure 5.47 and Figure 5.48.

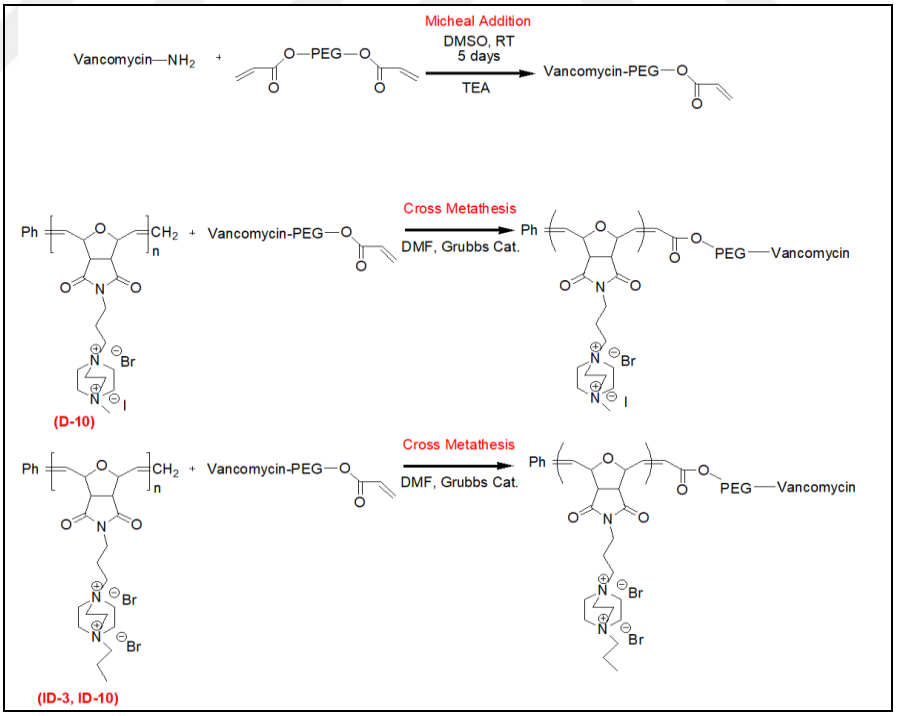

Figure 5.48. Cross metathesis reactions of VP conjugate with DABCO double-charge bearing polymers (D-10, ID-3 and ID-10)

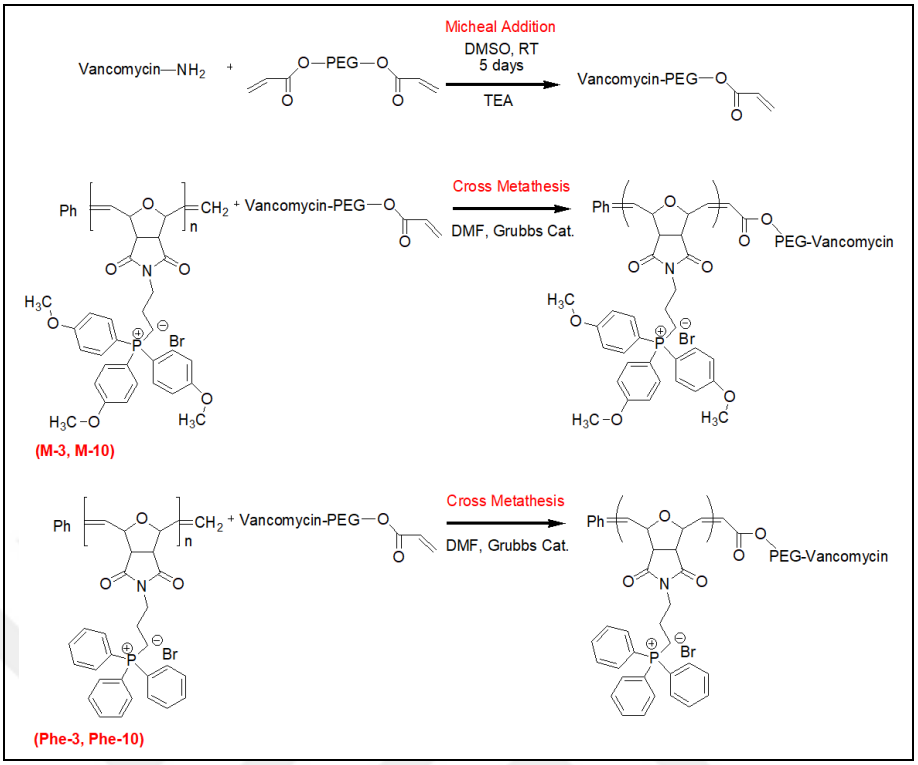

Figure 5.49. Cross metathesis reactions of VP conjugate with Trimethoxyphenyl Phosphonium and Triphenyl Phosphonium bearing polymers (M-3, M-10, Phe-3 and Phe-10)

5.6.1. NMR Analysis

The ^{1}H NMR analysis was applied to the VP-polymer conjugates in order to determine if vancomycin and the polymers were succesfully conjugated (Figure 5.50-Figure 5.56). Appendix D (Figure D.1-Figure D.13) shows the ^{1}H NMR spectra for all the conjugates.

Figure 5.50 shows the ^{1}H NMR spectrum of the D10(DMF)-M1 conjugate compared to VP conjugate and D-10(DMF) polymer. D10(DMF)-M1 conjugate was synthesized from the cross metathesis between DABCO double-charge salt bearing (via methyl iodate) polymer (MW: 10000 g/mol) syntesized using DMF as solvent and 24 hours of reaction time, and VP conjugtate with the ratio of 1:1 (D10(DMF):VP conjugate). Hoveyda Grubbs 2nd generation catalyst was used and the cross metathesis reaction was conducted using DMF as solvent at 40 ^{o}C for 24 hours under $N_{2(g)}$ atmosphere. The peaks at 4 ppm on D-10(DMF) represent the methylene protons of DABCO ring (-N-CH_2-CH_2-N-), which was also seen after cross-

metathesis reactions on D10(DMF)-M1conjugate's spectrum. The peaks at 7-7.50 ppm correspond to aromatic groups of vancomycin, and the peaks at 3.5 ppm represent the protons of ethylene glycol (–O-CH_2CH_2-O-), which might be overlaped with the O-H protons of vancomycin. These characteristic peaks are seen on D10(DMF)-M1 conjugate's spectrum, meaning the conjugation was conducted succesfully.

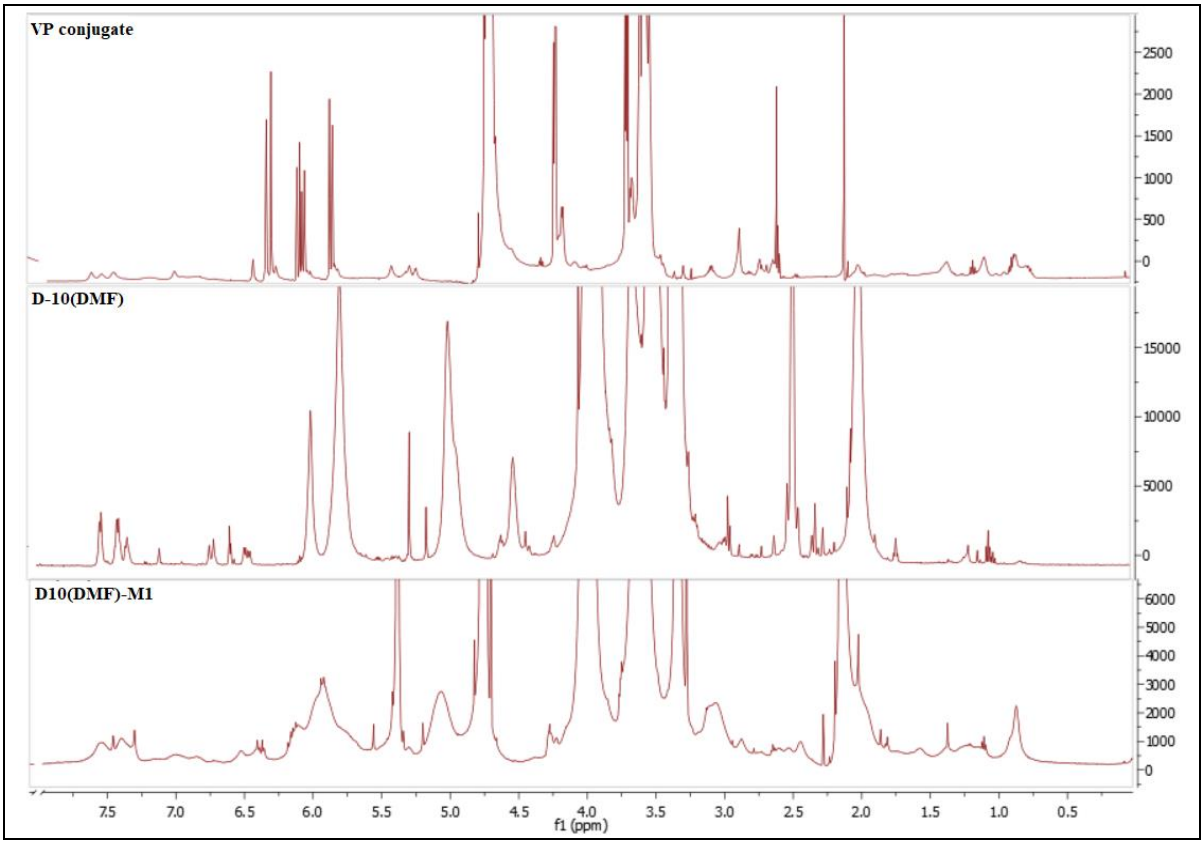

Figure 5.50. ^{1}H NMR spectrum of D10(DMF)-M1 conjugate

Figure 5.51 represents the ^{1}H NMR spectrum of the D10-M1 conjugate compared to the VP conjugate and D-10 polymer. D10-M1 conjugate was synthesized from the cross metathesis between DABCO double-charge salt bearing (via methyl iodate) polymer (MW: 10000 g/mol) synthesized using TFE as solvent with reaction time of 3.5 hours, and VP conjugtate with the ratio of 1:1 (D-10:VP conjugate). The cross metathesis reaction was conducted using DMF as solvent and Hoveyda Grubbs 2nd generation catalyst at 40 ^oC for 4 hours under $N_{2(g)}$ atmosphere. The peaks of methylene protons at 4 ppm is seen on D-10 and D10-M1 conjugate's spectra, however the peaks corresponding to aromatic groups of vancomycin (7-7.5 ppm) has very low intensity as well as the peaks corresponding to protons of ethylene

glycol. Thus, D10-M1 was not used for further analysis as well as D10-M3, D10-M5 and D10-M7 (See Appendix D).

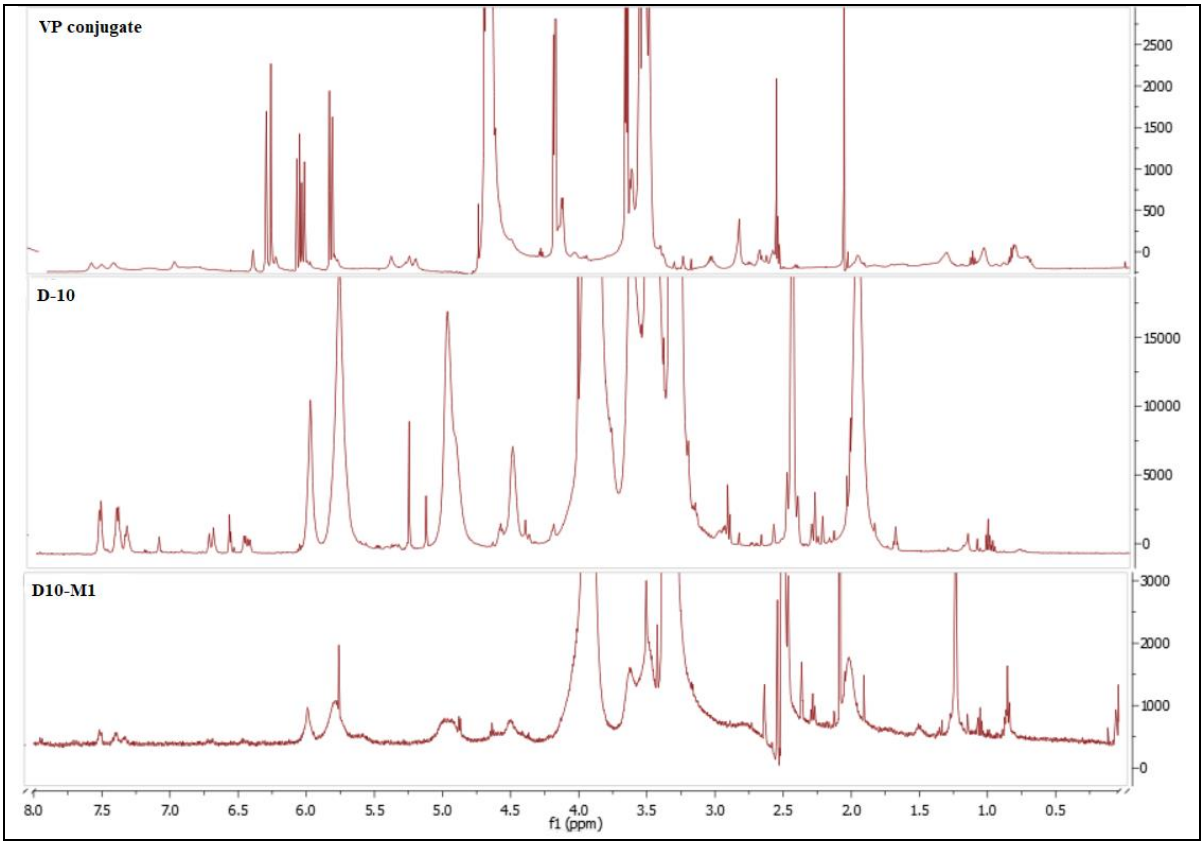

Figure 5.51. ^{1}H NMR spectrum of D10-M1 conjugate

The D10(DMF)-M1, D10-M3 and D10-M7 conjugates mentioned above were synthesized using Hoveyda 2nd generation Grubbs, Grubbs 2nd generation and Grubbs 1st generation catalysts, respectively under same reaction contiditions (D-10 as polymer with VP conjugate:polymer ratio 1:1, at 40 ^{o}C and for 24 hours). The ^{1}H NMR spectrum of D10(DMF)-M1 is shown in the Figure 5.50, when it was compared to Figure D.1 (spectrum of D10-M3) and Figure D.5 (spectrum of D10-M7) it is clearly seen that the peaks corresponding to protons of ethylene glycol has much higher intensity as well as the peaks corresponding to D-10 polymer especially the characteristic peak of DABCO ring's protons (-N-CH_2-CH_2-N-) at 4 ppm (^{1}H NMR (500 Mhz, d_6-DMSO, ppm): δ 6.58, 5.16, 3.83, 3.49, 3.26, 2.97, 1.94.). Thus, using the Hoveyda 2nd generation catalysts resulted with higher

yield and the Hoveyda 2nd generation Grubbs catalyts was used for the continued cross metathesis reactions.

Figure 5.52 shows the ^{1}H NMR spectrum of the D10-M2 conjugate compared to VP conjugate and D-10 polymer. D10-M2 conjugate was synthesized from the cross metathesis between DABCO double-charge salt bearing (via methyl iodate) polymer (MW: 10000 g/mol) synthesized using TFE as solvent and 3.5 hours of reaction time, and VP conjugate with the ratio of 1:5 (D10:VP conjugate). The cross metathesis reaction was conducted using DMF as solvent and Hoveyda Grubbs 2nd generation catalyst at 40 ^{o}C for 24 hours under $N_{2(g)}$ atmosphere. The peaks of methylene protons at 4 ppm is seen on D-10 and D10-M2 conjugate's spectra, and the peaks at 3.5 ppm represent the protons of ethylene glycol (–O-CH_2CH_2-O-). These characteristic peaks are seen on D10-M2 conjugate's spectra, meaning the conjugation was conducted succesfully D10-M2 spectrum is similar to D10-M4, D10-M6, D10-M8, D10-M9, D10-M11 and D10-M12 conjugates (See Appendix D).

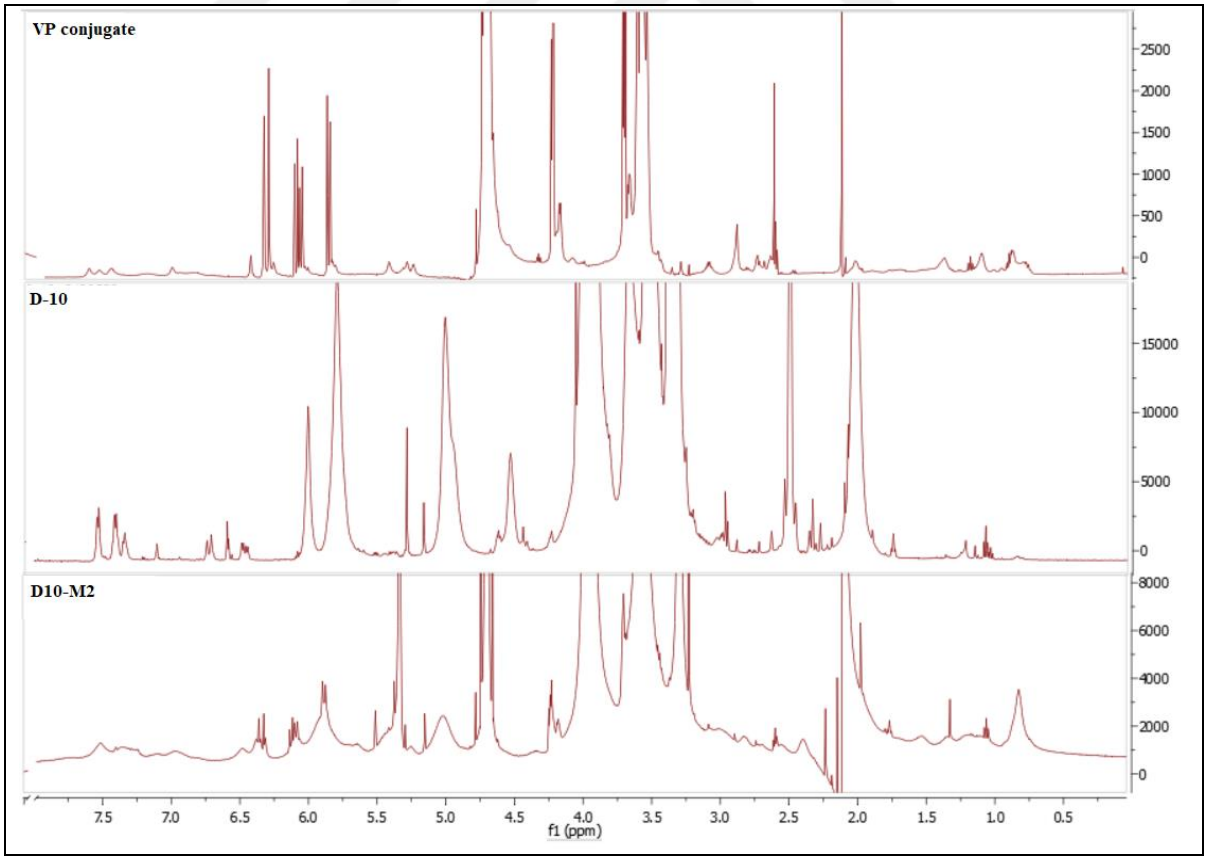

Figure 5.52. ^{1}H NMR spectrum of D10-M2 conjugate

Figure 5.53 shows the ^{1}H NMR spectrum of the ID3-M1conjugate compared to VP conjugate and ID-3 polymer. ID3-M1 was synthesized from the cross metathesis between DABCO double-charge salt bearing (via propyl bromide) polymer (MW: 3000 g/mol) synthesized using MeOH:DCM (1:1, v:v) as solvent and 6 hours of reaction time, and VP conjugate with the ratio of 1:10 (ID-3:VP conjugate). The cross metathesis reaction was conducted using DMF as solvent and Hoveyda Grubbs 2nd generation catalyst at 100 ^{o}C for 4 hours under $N_{2(g)}$ atmosphere. The peaks representing proton of aromatic groups of vancomycin are seen around 7.00-7.50 ppm on VP conjugate's, ID3-M1 conjugate's spectra. Additionally, the peak regarding to methylene group protons of DABCO structure seen at 4.00 ppm is seen on spectrum of ID3-M1 spectum as well as the peak regarding the protons of ethylene glycol at 3.5 ppm. ID3-M2 conjugate was synthesized with the same conditions but with higher VP conjugate ratio (1:20, ID-3:VP conjugate) had similar results (see Appendix D).

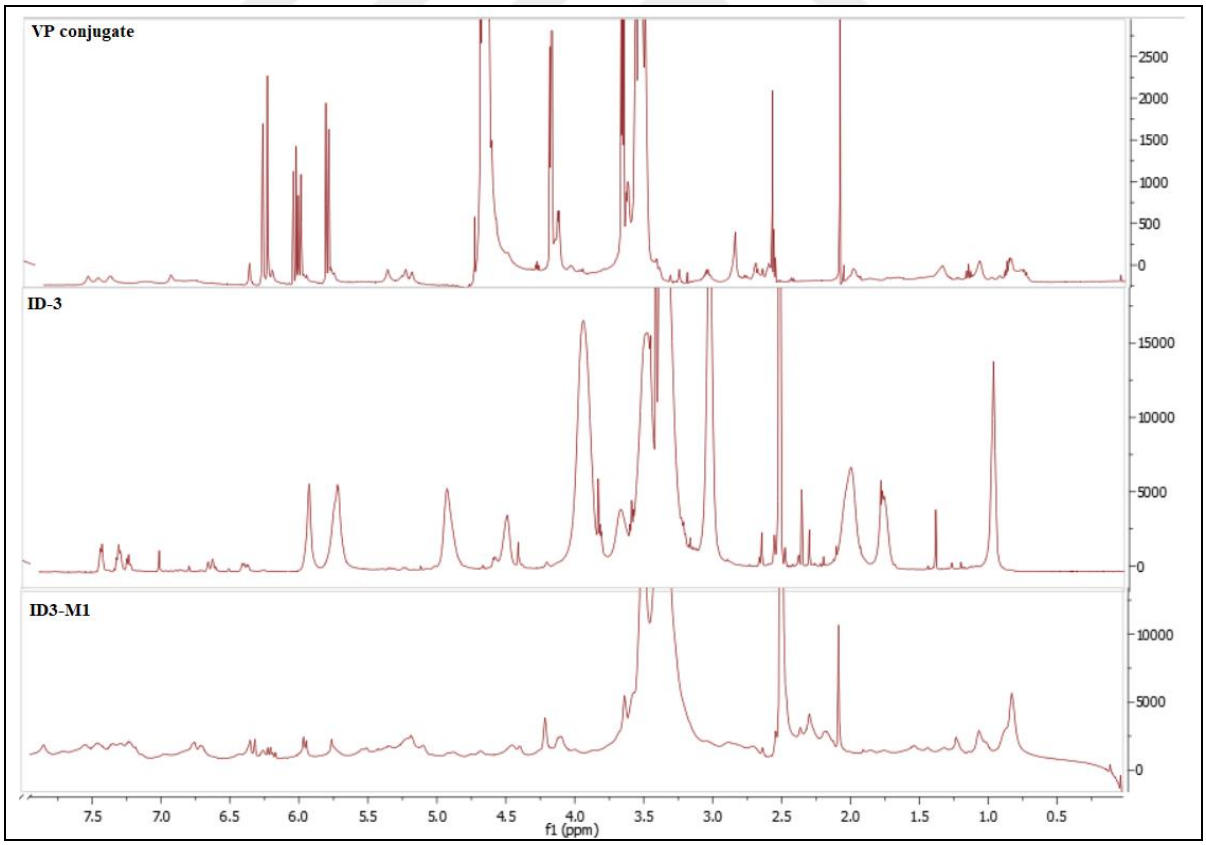

Figure 5.53. ^{1}H NMR spectrum of ID3-M1 conjugate

Figure 5.54 shows the ^{1}H NMR spectrum of ID10-M1 conjugate comparing with VP conjugate and ID-10 polymer. ID10-M1 was synthesized from the cross metathesis between DABCO double-charge salt bearing (via propyl bromide) polymer (MW: 10000 g/mol), MeOH:DCM (1:1, v:v) as solvent and 6 hours of reaction time, and VP conjugate with the ratio of 1:10 (ID-10:VP conjugate). Hoveyda Grubbs 2nd generation catalyst was used and the cross metathesis reaction was conducted at 100 ^{o}C for 4 hours under $N_{2(g)}$ atmosphere. The ^{1}H NMR spectrum of the ID10-M1 conjugate does not exhibit any characteristic peaks of VP conjugate, thus, the conjugation was not successful and this conjugate was used for further analysis.

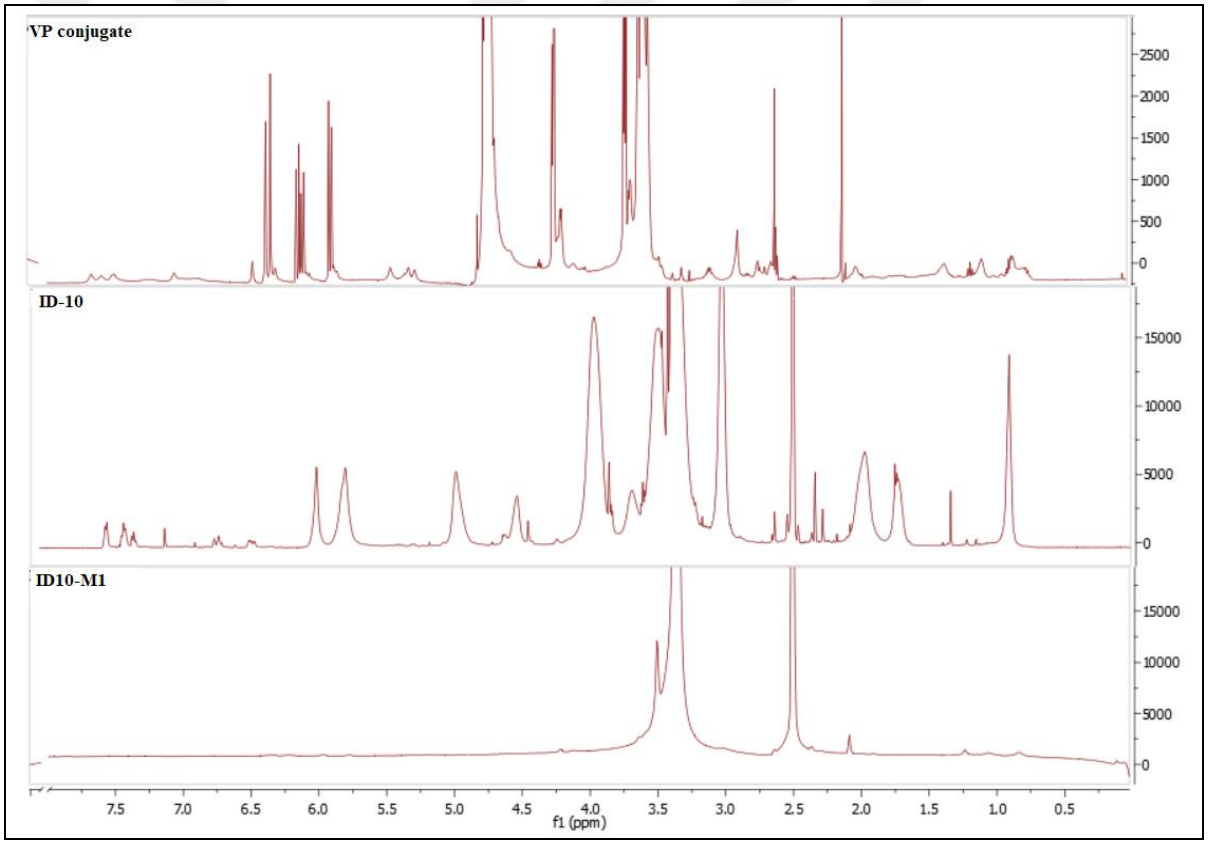

Figure 5.54. ^{1}H NMR spectrum of ID10-M1 conjugate

Figure 5.55 shows the ^{1}H NMR spectrum of the Phe3-M1conjugate compared to VP conjugate and Phe-3 polymer. Phe3-M1 conjugate was synthesized from the cross metathesis between triphenyl phosponium salt bearing polymer (MW: 3000 g/mol). The cross metathesis reaction of Phe3-M1 conjugate was conducted using DMF as solvent and Hoveyda Grubbs 2nd generation catalyst at 100 ^{o}C under $N_{2(g)}$ atmosphere for 4 hours with

the Phe-3:VP conjugate the ratio of 1:5. The peaks of phenyl rings protons around 8.00 ppm is seen on Phe-3 and Phe3-M1 conjugate's spectra. The peaks corresponding to aromatic groups of vancomycin are seen at 7-7.5 ppm on VP conjugate's and Phe3-M1 conjugate's spectra. The peaks at 3.5 ppm represent the protons of ethylene glycol (–O-CH_2CH_2-O-) are seen on the Phe3-M1 conjugate's spectrum as well as VP conjugate's spectrum. These characteristic peaks are seen on Phe3-M1 conjugate's spectra, meaning the conjugation was conducted succesfully. Phe10-M1 conjugate's (which was synthesized with the same conditions but using 10000 g/mol of triphenyl phosphonium bearing polymer, Phe-10) spectra is smilar to Phe3-M1 conjugate's spectra (see Appendix D).

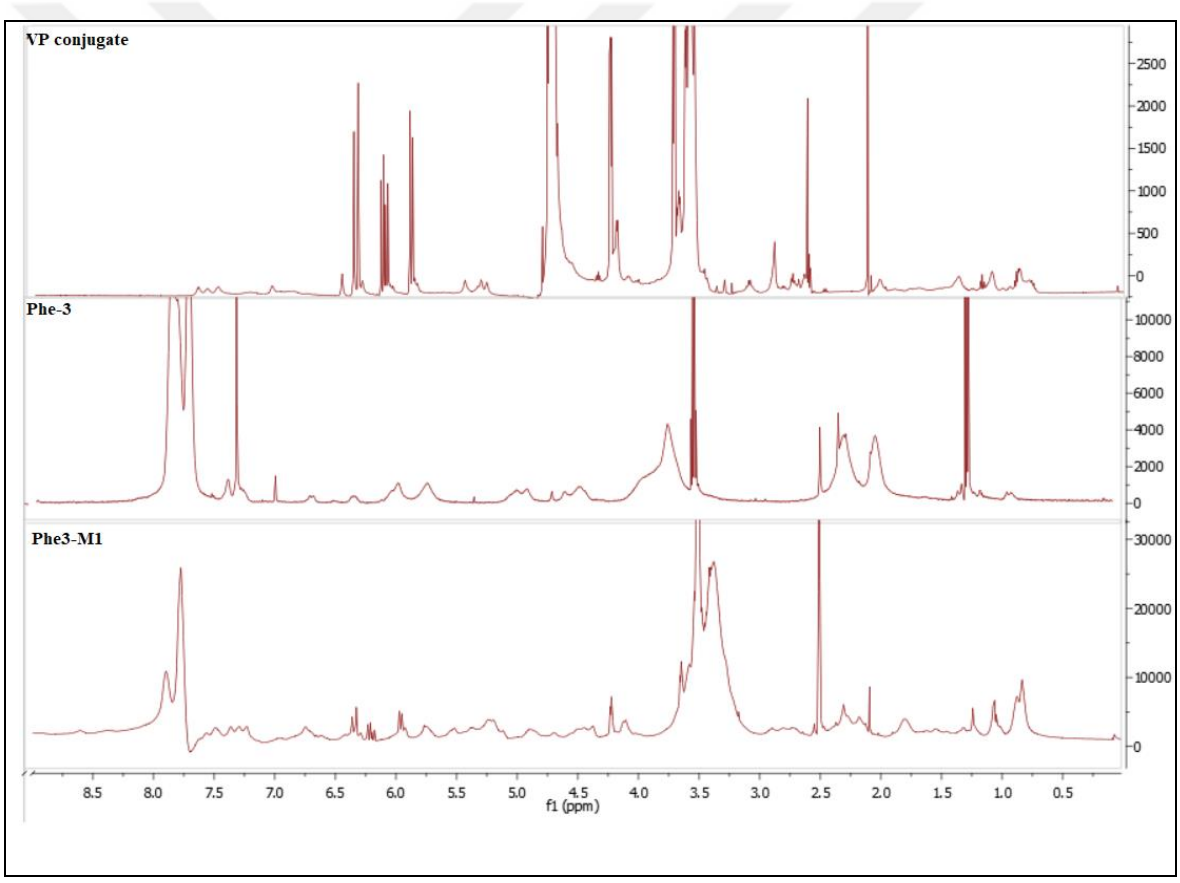

Figure 5.55. ^{1}H NMR spectrum of Phe3-M1 conjugate

Figure 5.56 shows the ^{1}H NMR spectrum of M3-M1conjugate compared to VP conjugate and M-3 polymer. M3-M1 conjugate was synthesized from the cross metathesis between trimethoxy phosponium salt bearing polymer (MW: 3000 g/mol). The cross metathesis reaction was held using DMF as solvent and Hoveyda Grubbs 2nd generation catalyst at 100

^{o}C under $N_{2(g)}$ atmosphere for 4 hours. The peaks of phenyl rings protons around 8.00 ppm is seen on M-3 spectrum and also is seen on M3-M1 conjugate's spectrum with lower intensity. The peaks regarding the aromatic groups of vancomycin are seen at 7-7.5 ppm on VP conjugate's and M3-M1 conjugate's spectra. The peaks corresponding to protons of ethylene glycol are seen at 3.5 ppm on VP conjugate's and M3-M1 conjugate's spectrum. M10-M1 conjugate, which was synthesized with the same conditions but using 10000 g/mol of trimethoxyphenyl phosphonium bearing polymer (M-10), had similar results with M3-M1 conjugate (see Appendix D).

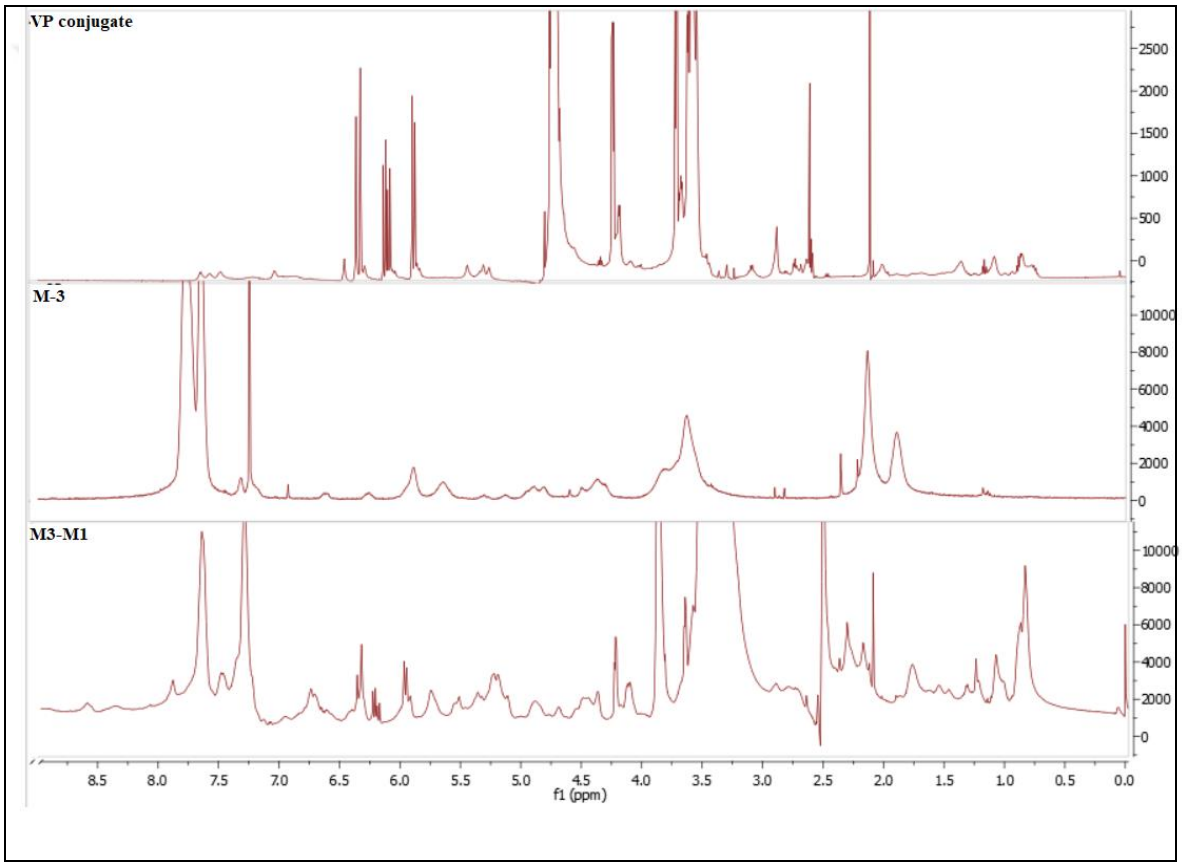

Figure 5.56. ^{1}H NMR spectrum of M3-M1 conjugate

5.6.2. FTIR Analysis

According to ^{1}H NMR results, the successfully conjugated VP-polymer conjugate samples were chosen and FTIR analysis was applied for further investigation of the structure. Figure

5.57 shows the FTIR spectrum of D10(DMF)-M1 and Figure 5.58 shows the spectrum of Phe3-M1 conjugates compared to VP conjugate and the polymers. The characteristic peaks are marked on the spectra. The characteristic peak of VP conjugate at 810 cm^{-1} does not exist on D10(DMF)-M1 and Phe3-M1 conjugates' spectra. After cross metathesis reaction between monoacrylate functional VP conjugate and polymers, the synthesized polymers bond to the VP conjugate from the monoacrylate and the FTIR results of VP-polymer conjugates supported the consumption of monoacrylate of the VP conjugate. From FTIR spectra of the VP-polymer conjugates, it is seen that the VP-polymer conjugates had the characteristic peaks of the polymers and VP conjugate, additionally the peak corresponding to acrylate disappeared, thus, the cross metathesis reactions were succesfully performed and VP-polymer conjugates were succesfully synthesized.

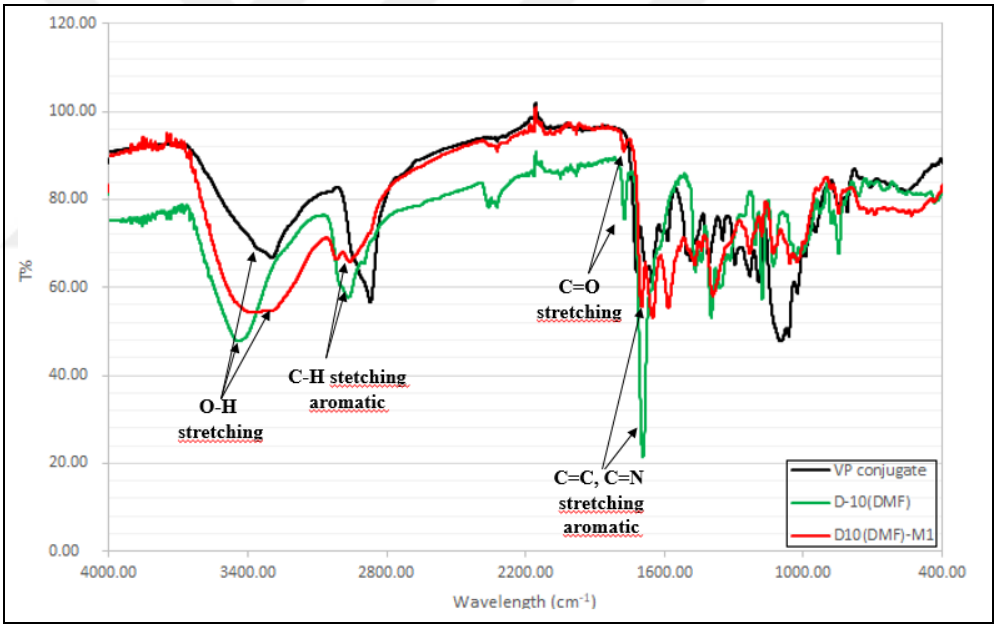

Figure 5.57. FTIR spectrum of D10(DMF)-M1 conjugate

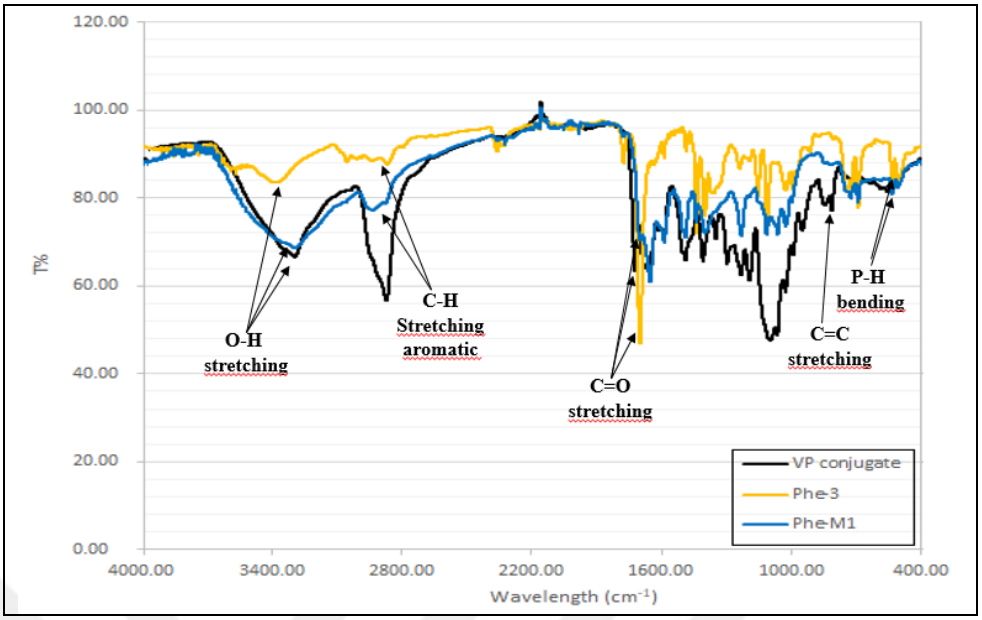

Figure 5.58. FTIR spectrum of Phe3-M1 conjugate

5.6.3. HPLC analysis

The HPLC analysis was applied to the polymers and VP-polymer conjugates. Retention time is the time between the sample input and the maximum signal of the compound given in detector, and it is characteristic for specific a compound in the analysis [176]. Thus, the retention time is critical identifying analytes. In Figure 5.59, the HPLC spectrum of D-10(DMF) and its conjugate D10(DMF)-M1 are shown. The HPLC analysis was conducted using same conditions which were explained in "5.2.2. HPLC Analysis of Vancomycin-PEG Conjugate".

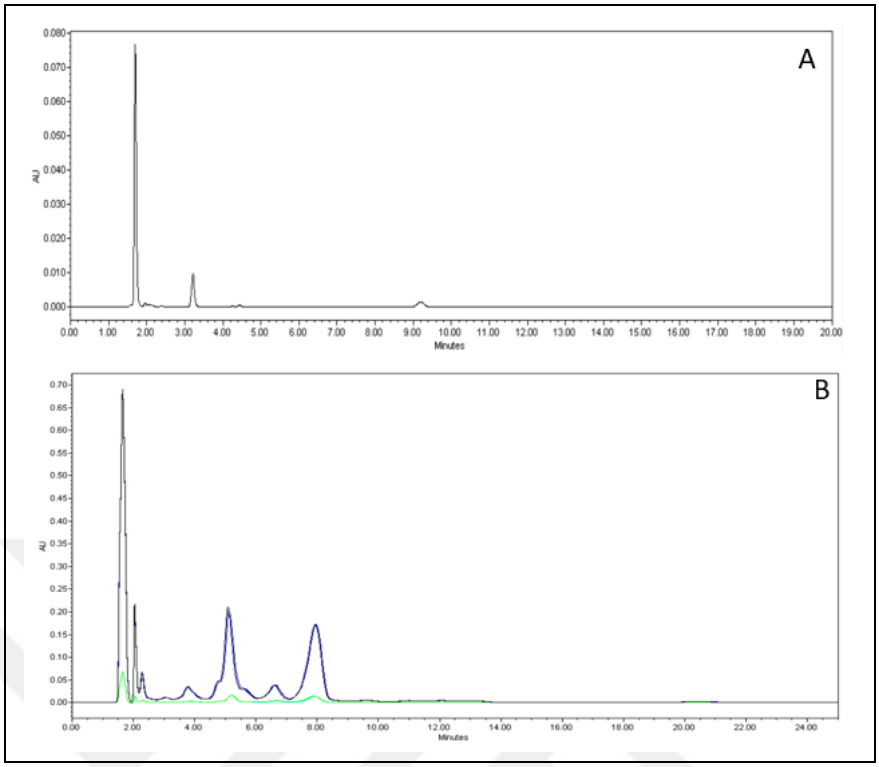

Figure 5.59. HPLC spectra of A:D-10 (DMF), B: D10(DMF)-M1

1 mg/mL of D-10(DMF) and D10(DMF)-M1 solutions in diH_2O were prepared for the HPLC analysis. In Figure 5.59.A shows that the retention time of D-10(DMF) polymer alone was around 2 minutes. The same peak is also seen on D10(DMF)-M1 conjugate's spectrum, shows the remaining unreacted polymer in the conjugate. It is thought that the peaks at 6 minutes and 8 minutes were belonged to the D10(DMF)-M1 conjugate. Additionally, when the D10(DMF)-M1 conjugate's spectrum compared to the VP conjugate's HPLC spectrum (Figure 5.45), the signals (14-18 minutes) corresponding to VP conjugate did not exist on the D10(DMF)-M1 conjugate's spectrum.

In this section the VP-polymer conjugates were characterized using ^{1}H NMR, FTIR and HPLC techniques. VP-polymer conjugates were synthesized via cross metathesis under different reaction conditions. According to ^{1}H NMR results Hoveyda 2nd generation grubbs catalysts was chosen for the continued synthesis and also ^{1}H NMR provided the information about the success of the cross metahtesis reactions. FTIR analysis was also applied to the VP-polymer conjugates and the results were supported the NMR analyses. After cross metathesis reactions, VP-polymer conjugates were purified using dialysis cassettes (3500

MWCO). For further analysis HLPC was applied to the polymers and succesfully conjugated VP-polymer conjugates. HPLC results of VP conjugates were compared with the related polymers and VP conjugate in order to point the new peaks different than VP conjugate and the polymers. HPLC spectrum of D10(DMF)-M1 conjugate was given as representative. According to HPLC analysis it was found that the new peaks occurred which is the new conjugate, however there remained peaks assigned to the unreacted polymers, showing some insufficiency in the purification process. After characterization of the VP-polymer conjugates the antimicrobial analysis and cytotoxicity analysis were conducted to the successfully formed conjugates.

5.7. VANCOMYCIN RELEASE FROM VP-POLYMER CONJUGATES

HPLC analysis was used in order to determine the vancomycin release from VP-polymer conjugates. 1 mg/mL of D10(DMF)-M1 and Phe3-M1 conjugates' solutions were prepared using 1x PBS, as three parallels each. The solutions were replaced in an orbital shaker at 100 rpm and at 37 ^{o}C for 15 days. The samples were colected for HPLC measurements in every two days (t= Day 0, 1, 3, 5, 7, 9, 11, 13 and 15). The vancomycin standarts were fresly prepared at various concentrations (0.1 mg/ml, 0.04 mg/ml, 0.02 mg/ml, 0.01 mg/ml and 0.005 mg/ml) for each analysis.

Ozalp *et al*., studied on vancomycin loaded PLA and its copolymers PLGA 90:10 and PLGA 70:30. They examined the vancomycin release behaviour from these polymeric complexes for ~2 months in a static system. It was observed that ~50 percent vancomycin was released from all the polymers at Day 7. They also synthesized polymer-PEG-vancomycin complexes and reported that, the prescence of PEG increases the release rate almost two times higher, however, the molecular weight did not exhibit any effect on release rate. Ozalp *et al.* suggested that, in the prescence of PEG, it absorbs significant amount of water due to its hydrophilic structure, and thus channels are forming for vancomycin to be released [177].

Figure 5.60 represents the vancomycin release profile from VP-polymer conjugates. According to release profile of D10(DMF)-M1 conjugate, it is seen that, vancomycin did not release for the first 7 days, the relase started after 7 days. It was thought that the ester bonds

within the structure were hydrolysed and broken, thus allow the release of vancomycin from the structure. However, Phe3-M1 conjugate exhibited completely different release profile than D10(DMF)-M1 which might be due to the different structures of the polymers. The most of the vancomycin was released in the first 5 days, afterwhich a plateau was reached. It is not possible to exactly calculate the amount of vancomycin in the polymer-vancomcin conjugate. Assuming all the unreacted polymer and unreacted vancomycin are removed via purification, a 1:1 molar ratio of vancomycin:polymer can be assumed to be present after purification.

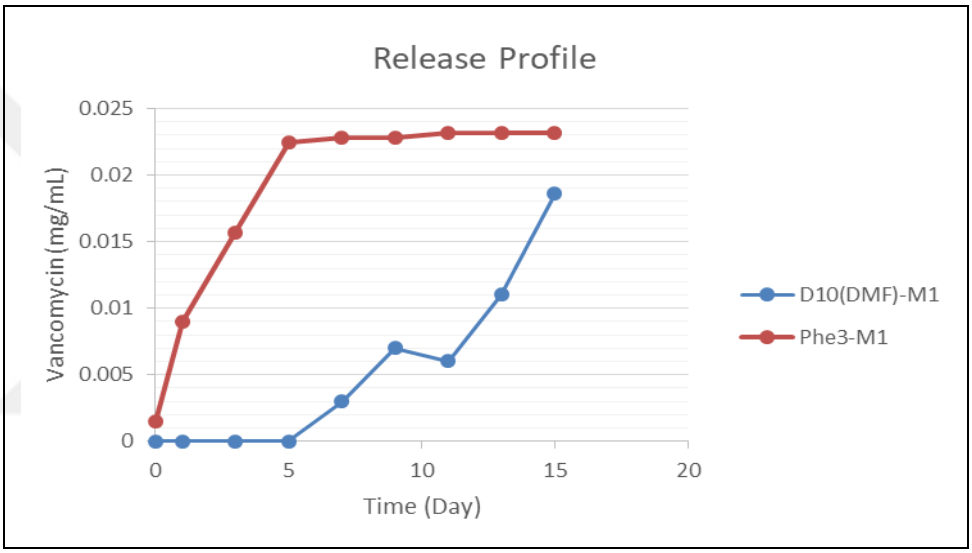

Figure 5.60. Release profiles of Vancomycin

5.8. ANTIMICROBIAL ACTIVITY OF THE VP CONJUGATE AND VP-POLYMER CONJUGATES

MIC analysis of the VP and the VP-polymer conjugates' were conducted using the same method which was explained under the "4.6. ANTIMICROBIAL ACTIVITY (MIC ANALYSIS)". MIC analysis of VP-polymers conjugates were investigated using E.coli (ATCC25922) as Gram (-) bacteria and *S.aureus* (ATCC29213) as Gram (+) bacteria.

Table 5.3 shows the MIC values of the vancomycin-polymer conjugates. The Gram (-) active Tobramycin and Gram (+) active Vancomycin were used as control agents. In Table 5.3, the

MIC values of VP-polymer conjugates and the polymers are shown for comparison. Among all DABCO double-charged salt and pyridinium salt bearing polymers D-10 showed the highest activity towards *S.aureus* (8 μg/mL), thus D-10 polymer was used for conjugation with vancomycin. It is seen from the table that VP-D10 conjugates were found to have low activity towards *E.coli* and the activity towards *S.aureus* was decreased after conjugation with vancomycin. D10(DMF)-M1 exhibit the highest activity towards *S.aureus* among all the VP-D10 conjugates (MIC: 64 μg/mL). Additionally, it is seen that the activity towards *S.aureus* of VP-ID3 conjugates were enhanced from >512 μg/mL to 128 μg/mL, yet they remained inactive against *E.coli* (>512 μg/mL).

Table 5.3. MIC values of the VP-polymer conjugates vs. synthesized polymers

Conjugate	***S.aureus* (μg/mL)**	***E.coli* (μg/mL)**	***Polymer***	***S.aureus* (μg/mL)**	***E.coli* (μg/mL)**
D10(DMF)-M1	64	>512	D-10	8	>512
D10-M2	>512	>512			
D10-M4	>512	>512			
D10-M6	>512	>512			
D10-M8	>512	>512			
D10-M9	128	>512			
D10-M10	128	>512			
D10-M11	128	>512			
D10-M12	>512	>512			
ID3-M1	128	>512	ID-3	512	>512
ID3-M2	128	>512			
Phe3-M1	32	>512	Phe-3	8	16
Phe10-M1	>512	>512	Phe-10	16	32
Phe10-M2	>512	>512			
M3-M1	32	>512	M-3	8	64
M10-M1	32	>512	M-10	8	32
VP conjugate	256	>512	-	-	-
Positive Controls					
Vancomycin	0.5	-			
Tobramycin	-	1			

The triphenyl phosphonium and trimetoxhy phenyl phosphonium salt bearing polymers were found highly active towards both *S.aureus* and *E.coli*. However, their conjugates with vancomycin showed lower activity towards *S.aureus* (MIC:32 μg/mL), and their activity against *E.coli* has worsened (MIC>512 μg/mL). It was reported in literature that the antimicrobial activity of polymers is increasing with the increasing molecular weight due to increasing repeating unit of the polymer [25, 57, 58, 178]. Eventhough, the polymers Phe-3, Phe-10, M-3 and M-10 were found active towards *E.coli*, their conjugates with vancomycin became inactive against *E.coli*. It was thought that the low activity towards *E.coli* might be due to the insufficient polymer content of the vancomycin-polymer conjugates, and vancomycin might comuflage the polymer structure and disable the biochemical interactions between the polymers and *E.coli*. In order to investigate this theory further research should be carried out with using the polymers with higher molecular weights.

5.9. CYTOTOXICITY OF THE VP-POLYMER CONJUGATES

MTS analysis of the VP and the VP-polymer conjugates, which exhibit the highest antimicrobial activity towards *S.aureus,* D10(DMF)-M1 and Phe3-M1 (MIC: 64 μg/mL and 32 μg/mL, repectively) were conducted using the same method which was explained in Chapter 4 (4.7.2. MTS Assay). In vitro cytotoxicity of VP conjugate, D10(DMF)-M1 and Phe3-M1 were tested at 5 different concentrations. Figure 5.61, Figure 5.62 and Figure 5.63 show the MTS assay results of VP-conjugate, D10(DMF)-M1 and Phe3-M1, respectively.

In Figure 5.61, it can be seen that VP conjugate was found cytotoxic towards HUVEC cells at the concentration of 2048 μg/mL. Although VP conjugate affected cell viability slightly negatively at the concentration of 1024 μg/mL on the first day (>60 percent), there were not any significant cytotoxic effects. VP conjugate was found to be non-cytotoxic towards HUVEC cells at concentrations of 1024 μg/mL and lower. Drouet *et al*., pursued a study in order to find out the toxicity of clinical dosage of vancomycin on HUVEC cells over a 24 h-72 h period using invasion method. They have reported that, vancomycin was significantly toxic towards HUVEC cell at 2500 μg/mL concentration and higher concentrations (4000, 5000 and 7500 μg/mL). In their study, vancomycin at 500, 1000 and 1500 μg/mL of concentrations did not exhibit any noticible toxicity on HUVEC cells, however, cell viabiliy

was decreased proportional to the concentration and treatment time [179]. In this study, vancomycin-PEG acrylate conjugate found to be non-toxic at 1024 µg/mL and lower concentration, thus, the PEG acrylate addition to vancomycin structure did not exhibit a significant toxicity towards HUVEC cells.

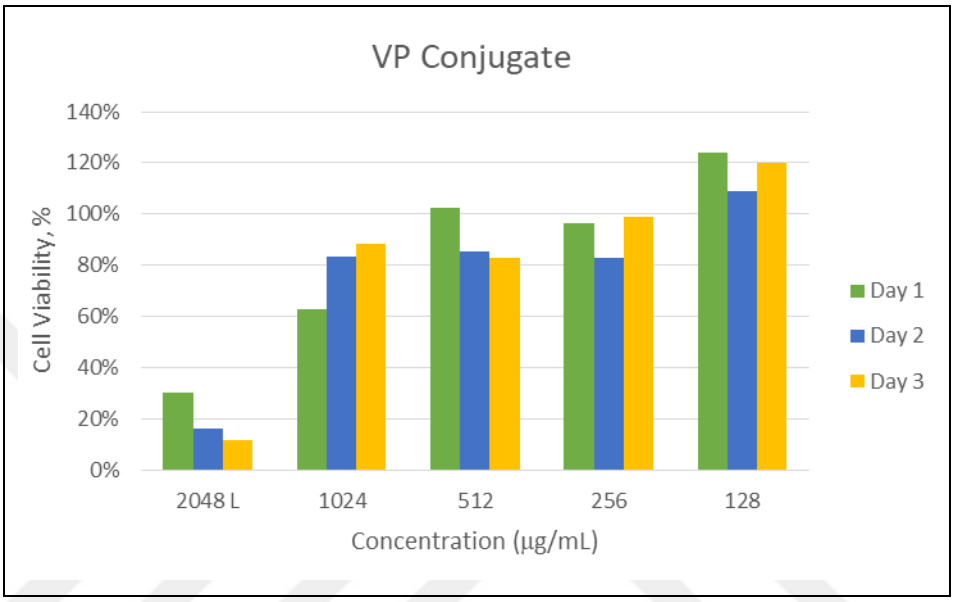

Figure 5.61. MTS results of VP conjugate

Figure 5.62 represents MTS assay results of D10(DMF)-M1 conjugate. D-10 polymer was found non-toxic at the concentration of 2048 µg/mL and lower, however VP conjugate was found cytotoxic at that concetration of 2048 µg/mL. D10(DMF)-M1 conjugate effected cell viability negetively at the concentration of 2048 µg/mL (<40 percent), however, it was found to be non-toxic at concentrations of 1024 µg/mL and lower.

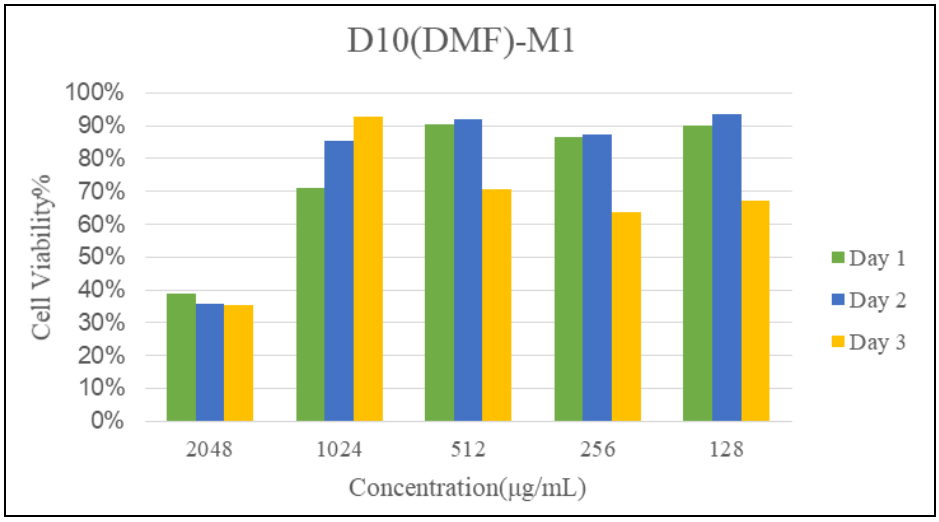

Figure 5.62. MTS result of D10(DMF)-M1

Figure 5.63 shows MTS assay results of Phe3-M1 conjugate. According to hemeolytic concentration (HC_{50}) results, Phe-3 polymer was found hemolytic and for further analysis MTS assay was applied to the polymer, however, due to the hydrophobicity of the polymer a sufficient results could not be obtained for the concentration of 512 µg/mL and higher, in order to support HC_{50}, yet it was found non-toxic at lower concentrations than 512 µg/mL. It can be seen from the Figure 5.63 that Phe3-M1 affected cell viability relatively negative at the concentration of 2048 µg/mL for all treatment days as well as VP conjugate, however it was found to be non-toxic at concentration of 1024 µg/mL and below.

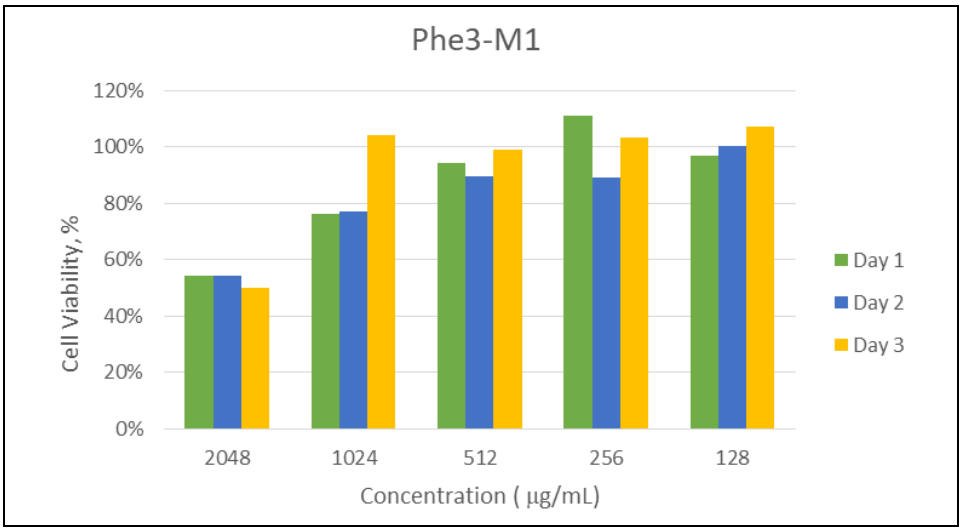

Figure 5.63. MTS result of Phe3-M1

For further investgation hemolytic concentrations of VP-polymer conjugates were found (Table 5.4). Both conjugates (D10(DMF)-M1 and Phe3-M1 were non-hemolytic (HC_{50}: >2000 μg/mL).

Table 5.4. HC_{50} and selectivity values of VP-polymer conjugates

Conjugate	**HC_{50} (μg/mL)**	**SI (HC_{50}/MIC*)**	
		S.aureus	***E.coli***
D10(DMF)-M1	>2000	31.25	3.90
Phe3-M1	>2000	62.50	3.90

Based on these results, it is seen that Phe-3 polymer that was toxic, once conjugated with vancomycin-PEG, became non-toxic, possibly due to becoming more hydrophillic. At the same time, this polymer after conjugation became less effective towards *S.aureus* and the activity towards *E.coli* had significantly lowered (from MIC:16 μg/mL to MIC:>512 μg/mL). The remaining activity towards *S.aureus* may be due to the presence of vancomycin in the structure, which is still much lower than that of vancomycin alone. However, Phe3-M1 conjugate showed good selectivity towards *S.aureus*, two times more than D10(DMF)-M1 (Table 5.4). D-10 polymer conjugate was non-hemolytic but showed antimicrobial activity predominantly towards *S.aureus*, remained non-hemolytic but became less active towards *S.aureus* and lost its antimicrobial activity towards *E.coli*. As in the case of Phe-3-vanomycin-PEG conjugate, the remaining activity towards *S.aureus* maybe be due to the presence of vancomycin in the structure.

5.10. MORPHOSTRUCTURAL DAMAGE ANALYSIS OF VP-POLYMER CONJUGATES

The morphostructural activity of D10(DMF)-M1and Phe3-M1 conjugates against *S.aureus* were monitored using SEM. *S.aureus* cells alone were prepared in LB broth as control group. In Figure 5.64.a represents SEM image of the control cells (untreated *S.aureus*). The untreated S.aureus cells exhibits their characteristic shape as grape-like cluster, they were found approximately 1 μm in diameter each. It can be seen from the image that they exhbit smooth spherical shapes, intact surfaces and distinct boundaries. After treatment with sub-

MIC concentrations of D10(DMF)-M1 (Figure 5.64.b) and Phe3-M1 (Figure 5.64.d), some *S.aureus* cells remained their original shape, while some exhibited dimples and deformations on their surfaces. However, after treatment with supra-MIC concentrations of D10(DMF)-M1 (Figure 5.64.c) and Phe3-M1 (Figure 5.64.e), vital morphological changes were formed in *S.aureus*. It can be observed that the VP-conjugates damaged bacterial membranes made bacteria cells shrink and ruptured, resulting in effective killing.

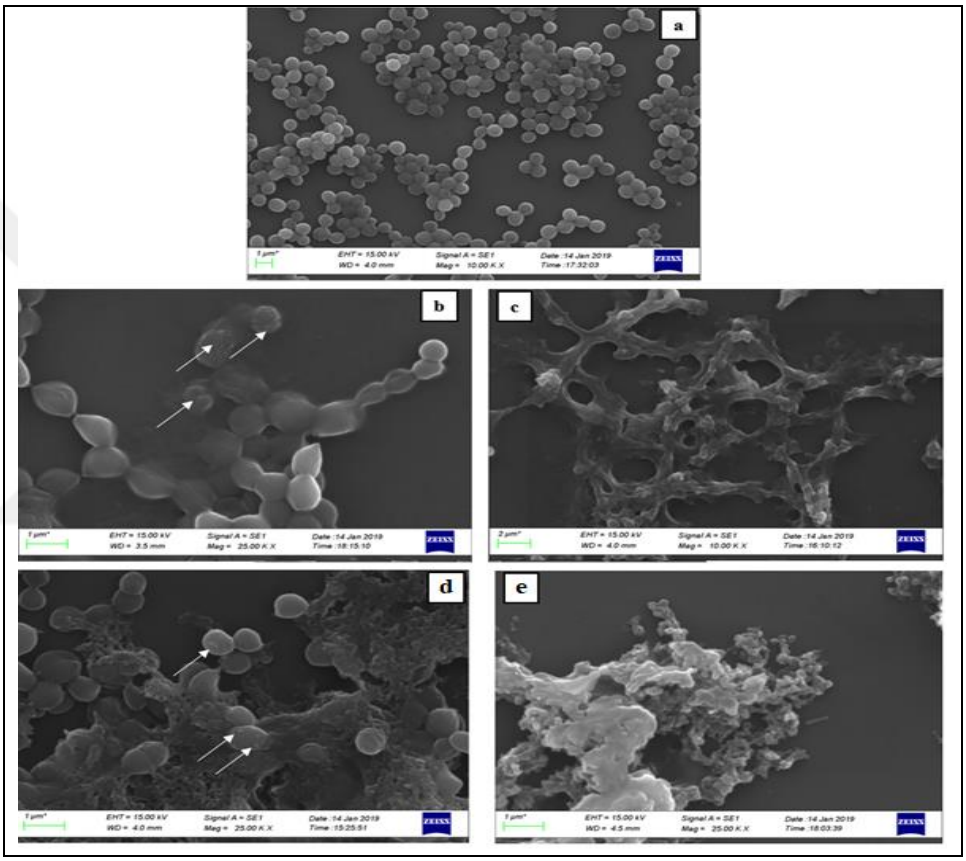

Figure 5.64. SEM of VP-polymer conjugates a) control *S.aureus*, b) Sub-MIC concentration of *S.aureus* treated with D10(DMF)-M1, c)Supra-MIC concentration of *S.aureus* treated with D10(DMF)-M1, d) Sub-MIC concentration of *S.aureus* treated with Phe3-M1, e) Supra-MIC concentration of *S.aureus* treated with Phe3-M1

6. CONCLUSION

Infectious diseases are critically important in healthcare globally. Especially, the increase rate of bacterial resistant, even to the strongest antibiotics, is at an alarming rate. Hospitals are the origin and primary source of MDR bacteria, and patients thus infected, have clinical practises requiring prolonged treatments. Every year, 648 thousands to almost 2 million hospitalized patients are affected by HAIs in USA alone. In Turkey, the mortality rate of people due to infectious diseases is on the rise. In the Ministry of Health decleration against infection based diseases, it is emphasized that R&D funding should be increased for the development of antibacterial and antiviral medicines.

Vancomycin is a Gram (+) bacteria effective antibiotic and is approved by the FDA for its bactericidal action towards Gram (+) bacteria, however, it is inactive towards Gram (-) bacteria. There are some limitations of use of vancomycin. Vancomycin has nephrotoxicitiy when it is used longer than 7 days and/or high doses (20 mg/L or 4 g/day). The short half-life and the labile structure of vancomycin cause severe problems on formulations, which brings the need to combine vancomycin with a polymer or a carrier system. In this study, we conjugated vancomycin with well-designed cationic polymers which were expected to be active towards *S.aureus* and *E.coli,* due to their structures. Then, the synergistic activity against Gram (+) and Gram (-) bacteria of the combinations were investigated. The cationic polymers which were used in this study, were synthesized using a controlled polymerization method, ROMP polymerization with the well-designed polymer structures and molecular weight distributions.

Firstly, DABCO and pyridinium salt bearing homopolymers and copolymers were synthesized using ROMP method with different hydropobicities and molecular weights. The cationic charges were obtained via quaternization of the ammonium groups. The homopolymers were sythesized with two different molecular weights as 3000 g/mol and 10000 g/mol and the copolymers were synthesized with the molecular weight of 5000 g/mol. The structural characterization of all monomers and polymers were determined using NMR techniques (^{1}H NMR and ^{13}C NMR), and FTIR analysis also applied to the synthesized polymers, and these analyses showed that the polymers were synthesized succesfully. After succesful syntheses of the polymers, the antimicobial activities and cytotoxicities were

investigated. According to MIC analysis; among all DABCO and pyridinium based homopolymers and copolymers, DABCO double-charge salt bearing homopolymer D-10 (10000 g/mol) had the highest activity and highest selectivity towards Gram (+) *S.aureus* (MIC: 8 μg/mL and SI: 250) and highest activity towards Gram (-) *E.coli* (MIC: 128 μg/mL and SI:15.62). It is widely known that the cationic charge and the hydrophobicity of the polymers has significant importance in antimicrobial activity. Positively charged polymers adhere to the negatively charged cell surface of the bacteria due to the sufficient cationic charges, and the hydrophobicity is required in order to provide the insertion to cell membrane. In order to increase the hydrophobicity of the DABCO double-charged polymers, propyl bromide was used instead of methyl iodate which provides longer alkyl chains in the synthesis and ID-3 (MW: 3000 g/mol) and ID-10 (MW:10000 g/mol) were obtained. Among the biocidal activities of new DABCO double-charged polymers, it was observed that they had high MICs suggesting low activity against both *S.aureus* and *E.coli*. Furthermore, trimethoxyphenyl phosphonium (M-3 and M-10) and triphenyl phosphonium salt bearing (Phe-3 and Phe-10) polymers were synthesized which were highly hydrophobic and their antibacterial activities and cytotoxicities were also investigated. The cationic charge was obtained via quaternization of phosphonium group in their structures. In literature it was pointed in several studies that quaternary phosphonium salt bearing polymers have higher antibacterial activities. Our findings were supported that the quaternary phosphonium salt bearing polymers exhibit higher activities towards *S.aureus* and *E.coli* than quaternary ammonium salt bearing polymers (D-3, D-10, P-3, P-10, D1-P1, D1-P2 and D2-P1). Among the quaternary phosphonium salt bearing polymers, Phe-3 had the highest activity against *S.aureus (*MIC: 8 μg/mL) and *E.coli* (MIC: 16 μg/mL). The cytotoxicities of the synthesized polymers were determined via the hemolytic concentration (HC_{50}) and MTS assay. DABCO and pyridinium salt bearing polymers had high HC_{50} values (>1000 μg/mL) shows they were non-hemolytic towards red blood cells and the MTS assay showed that they were non-toxic towards HUVEC cells as well. However, phosphonium salt bearing homopolymers were found very hemolytic (HC_{50}<250 μg/mL) due to their overly aromatic structure and hydrophobicity thus their selectivity towards bacteria were also low. It is known that, generally most of the strong antibacterial polymers are hemolytic as well. While the MTS assay was performed with phosphonium salt bearing homopolymers, they precipitated in highly aqueus DMEM at highest two concentrations (2048 and 1024 μg/mL), thus reliable

data were not able to collected at these concentration. This problem did not occur at lower concentrations (≤512 μg/mL) and they were found non-toxic towards HUVEC cells at lower concetrations.

Second step of the project was conjugation of vancomycin with PEG-diacrylate via Michael Addition reaction. This step was the preperation of vancomycin for cross metathesis reaction, in order to synthesize the vancomycin-polymer conjugates. After michael addition reaction between vancomycin and PEG-diacrylate, the monoacrylate functional vancomycin-PEG acrylate (VP conjugate) molecule was obtained and purified, and characterized using proton NMR, FTIR and HPLC techniques. These analyses showed that the conjugation between vancomycin and PEG-diacrylate was succesfully achieved. In the conjugation of vancomycin with PEG-diacrylate, keeping one of the two acrylates was important for cross metathesis reactions. Cross metathesis is a type of olefin metathesis and, olefin metatheses mechanism consist of breaking carbon-carbon double bond in order to form a new carbon bond. In order to ensure keeping one of the acrylates of PEG unit, excess amount of PEG-diacrylate was used in Michael Addition reaction. In ^{1}H NMR analysis the protons corresponding to acrylate were seen between 5.7-6.5 ppm and furthermore, FTIR analysis also supported that finding with the presence of the peak at 810 cm^{-1} which corresponds to the C=C stretching of acrylate group. After succesful synthesis and purification of VP conjugate, the next step of the project was the cross metathesing of the polymers with VP conjugate. The polymers with highest activities towards bacteria were chosen (D-10, Phe-3, Phe-10, M-3 and M-10). Cross metathesis reactions were conducted with different parameters such as: using different Grubbs catalysts (Grubbs 1st generation, Grubbs 2nd generation and Hoveyda Grubbs 2nd generation catalysts), at different temperatures (40 ^{o}C and 100 ^{o}C) and for different reaction times (4 hours and 24 hours). The Hoveyda Grubbs 2nd generation catalyst provide the succesfull cross metathesis, however, varying the temperature and reaction times did not influence the synthesis significantly. Thus, it is not possible to make such a decision about reaction temperatures and reaction times. In our study the most active VP-polymer conjugates were D10(DMF)-M1 and Phe3-M1, both conjugates were synthesized using Hoveyda Grubbs 2nd generation catalysts however, the reaction temperatures and times differ as 40 ^{o}C and 100 ^{o}C, 24 hours and 4 hours, respectively. According to MIC values of the polymers, D-10 showed high activity towards *S.aureus* with a MIC of 8 μg/mL and tolerable activity against *E.coli* with

a MIC of 128 μg/mL. After conjugation with vancomycin, an increase in MIC values which means a decrease in antimicrobial activity was observed in all conjugates. Among them, D10(DMF)-M1 showed the highest activity towards *S.aureus* (MIC: 64 μg/mL), however the activity towards *E.coli* was lost completely (MIC: >512 μg/mL). The quaternary phosphonium salt bearing polymers (Phe-3, Phe-10, M-3 and M-10 were found highly active towards both *S.aureus* and *E.coli*, however, after they were conjugated with vancomycin, activity towards *S.aureus* were worsened and completely lost towards *E.coli*. Phe-M1 showed the highest activity towards *S.aureus* (MIC: 32 μg/mL), however it also became inactive against *E.coli* (MIC: >512 μg/mL). The reason for conjugates to lost their activity might be due to the vancomycin-polymer structure become hydrophilic because of addition of hydrophilic VP-conjugate to the structure. Another reason might be due to the nature of the cross metathesis reaction. In cross metathesis reaction, the metathesis catalysts break the carbon-carbon double bond which leads several possibilities. The polymers might be break from any C=C bonds, which means a lost might be occur in the number of repeating units. It is known that increasing repeating unit of the antmicrobial polymers resulted with an increase in the activity. During the cross metathesis of polymers with VP conjugate, the number of repeating unit of the polymers might decrease and resulted with a decrease in their activity towards *S.aureus*, and lost their activity towards *E.coli* completely. The toxicity of VP-conjugate was investigated against HUVEC cells via MTS assay. VP conjugate was found to be non-toxic towards HUVEC cells at the concentration of 1024 μg/mL and lower. In literature, it is reported that vancomycin is non-toxic towards HUVEC cells at lower concetrations than 2500 μg/mL, thus it can be concluded that the addition of PEG acrylate to the structure of vancomycin did not exhibit any significant difference on toxicity towards HUVEC cells. The cytotoxicities of Phe3-M1 and D10(DMF)-M1 were determined applying HC_{50} and MTS assay. Phe3-M1 and D10(DMF)-M1 were found to be non-toxic at the concentration of 1024 μg/mL and lower towards HUVEC cells. HC_{50} results were also showed that these conjugates were not hemolytic (>2000 μg/mL). D-10 polymer was already found non-hemolytic, however, it was observed that Phe-3 became non-hemolytic after conjugation with vancomycin, which is thought to be due to the increasing hydrophilicity of the structure. Furhermore, Phe3-M1 had good and higher selectivity towards S.aureus than D10(DMF)-M1 (SI: 62.5 and 31.25, respectively). For further biocidal analysis, the biophysical techniques were applied to D10(DMF)-M1 and Phe3-M1. The morphostructural

activity of D10(DMF)-M1 and Phe3-M1 conjugates against *S.aureus* were monitored using SEM, and it was seen in SEM images that the conjugates broke the cell integrity of the cell membrane of *S.aureus* even at sub-MIC and especially at supra-MIC concentrations.

The vancomycin release from these conjugates was monitored using HPLC analysis for 15 days. Phe3-M1 and D10(DMF)-M1 conjugates had different release profile which might be caused by the differences in the structures. While D10(DMF)-M1 did not release any vancomycin at first 7 days then the release started at 9^{th} day and continued, Phe3-M1 released most of the vancomycin in the first 5 days, afterwhich a plateau was reached.

In this study, synthesis of double charged and single charged cationic polymer were synthesized and some of them were found effective towards Gram (-) *E.coli* and Gram (+) *S.aureus*. Amongst these polymers, two were chosen to be conjugated with an antibiotic, vancomycin which is highly active towards Gram (+) bacteria. The polymer what was originally effective against *E.coli* was found to be no longer effective. This can be linked with its increased hydrophilicity which was the predominant reason for this polymer to be antimicrobial. As conjugation with vancomycin-PEG with any polymer would increase the hydrophilicity, it appears that it will remain a challenge to form a conjugate that will be effective towards both Gram (-) and Gram (+) bacteria. In order to enhance the activities of these conjugates further studies should be pursued.

The need of new trends in antibiotic is due to the bacterial resistance. It is known that, bacteria become resistant to antibiotics when they used mutliple times with high doses and/or for long times. However, contrary of antibiotics, even multiple uses of polymers do not lead to drug resistance. The antibiotic in this study was vancomycin, and it has some limitations in its clinical use. Vancomycin has a adverse effect which it can be ototoxic or nephrotoxic when it is used without a carrier. In this study, we synhesized newly designed cationic ROMP polymers which were not used as drug carrier before, and conjugated vancomycin with these cationic polymers. We found that the vancomycin-polymer conjugates remained active and selective towards *S.aureus*, which is a promising result in the fight against resistant bacteria. We also found that these vancomycin-polymer conjugates released vancomycin in small doses with different release profiles, further studies should be achieved, however this might be a solution to combat with the adhere effects of vancomycin in clinical use. All in all, this study can be a pathway for the development of new

antimicrobial cationic polymers and new generation antibiotics and due to their high activity and selectivity against Gram (+) bacteria, they can be used in implant materials (such as; plasters, compression bandages, etc.), in coating of medical surfaces such as catheters, implants, etc.

7. FUTURE WORK

In this project, newly designed cationic ROMP polymers were synthesized, which were not used as drug carrier before, and covalently bind to vancomycin using cross metathesis pathways. The bactericidal activity of these polymers and vancomycin-polymer conjugates were investigated towards Gram (+) *S.aureus* and Gram (-) *E.coli*. Among the vancomycin-polymer conjugates; D10(DMF)-M1 and Phe3-M1 had the highest activity against *S.aureus* (64 μg/mL and 32 μg/mL, respectively), however, they were inactive against *E.coli* (>512 μg/mL). In order to provide the activity towards *E.coli* and enhanced the activity towards *S.aureus*, there are some conditions which can be study as future work. It is known that, sufficient cationic charge and hydrophobicity have significant importance on antibacterial activity. The hydrophobicity of the polymers should be increased in order to provide higher activity. Thus, the alkyl chain length could be increase which increases the hydrophobicity of the structure. We have used methyl iodate and propyl bromide in the synthesis of DABCO double-charge polymers. The alkyl chain might be extended adding hexyl, decyl or octyl groups to the polymers structures. Quaternary phosphonium salt bearing polymers were found highly active towards Gram (+) and Gram (-) bacteria, however, after conjugation with vancomycin, their activity was decreased towards Gram (+) bacteria and they became inactive against Gram (-) bacteria. In literature it was reported that the antimicrobial activity increases with the increasing molecular weight, which is due to the increasing repeating unit of the polymers. Thus, quaternary phosphonium bearing polymers can be synthesized with higher molecular weights such as: 200000 g/mol and 300000 g/mol, then conjugated with vancomycin. Hence, the effect of increasing repeating unit of polymers on antimicrobial activity can be investigated. Furthermore, PEG-diacrylate is water soluble compound as well as vancomycin. The addition of PEG-diacrylate to the vancomycin-polymer structure might lower the hydrophobicity. In order to remove this effect of PEG-diacrylate, a vancomycin based monomer can be synthesized via binding vancomycin covalently to the amphilic bromooxanorbornene (Compound 2), and copolymerize with hydrophobic monomers such as: tripheylmethoxy phosphonium and triphenyl phosphonium salt bearing monomers.

REFERENCES

1. Trubiano JA, Padiglione AA. Nosocomial infections in the intensive care unit. *Anaesthesia Intensive Care Medicine*. 2015;16(12):598–602.

2. Carter EJ, Pouch SM, Larson EL. Common infection control practices in the emergency department: a literature review. *American Journal of Infection Control*. 2014;42(9):957–62.

3. Khan HA, Baig FK, Mehboob R. Nosocomial infections: epidemiology, prevention, control and surveillance. *Asian Pacific Journal of Tropical Biomedicine*. 2017;7(5):478–82.

4. Breathnach AS. Nosocomial infections and infection control. *Medicine (Baltimore)*. 2013;41(11):649–53.

5. Muller MP, MacDougall C, Lim M, Armstrong I, Bialachowski A, Callery S, Ciccotelli W, Cividino M, Dennis J, Hota S, Garber G, Johnstone J, Katz K, McGeer A, Nankoosingh V, Richard C, Vearncombe M. Antimicrobial surfaces to prevent healthcare-associated infections: a systematic review. *Journal of Hospital Infection*. 2016;92(1):7–13.

6. Van Boeckel TP, Gandra S, Ashok A, Caudron Q, Grenfell BT, Levin SA, Laxminarayan R. Global antibiotic consumption 2000 to 2010: an analysis of national pharmaceutical sales data. *Lancet Infectious Diseases*. 2014;14(8):742–50.

7. Goossens H, Guillemot D, Ferech M, Schlemmer B, Costers M, Van Breda M, Baker LJ, Cars O, Davey PG. National campaigns to improve antibiotic use. *European Journal of Clinical Pharmacology*. 2006;62(5):373–9.

8. Prigitano A, Romanò L, Auxilia F, Castaldi S, Tortorano AM. Antibiotic resistance: Italian awareness survey 2016. *Journal of Infections and Public Health*. 2018;11(1):30–4.

9. Szekeres E, Baricz A, Chiriac CM, Farkas A, Opris O, Soran ML, Andrei AS, Rudi K, Balcazar JL, Dragos N, Coman C. Abundance of antibiotics, antibiotic resistance genes and bacterial community composition in wastewater effluents from different Romanian hospitals. *Environmental Pollution*. 2017;225:304–15.

10. Allegranzi B. *Report on the burden of endemic health care-associated infection worldwide*. Geneva: World Health Organization Production Services. 2011.

11. Khair HN, VanTassell P, Henderson JP, Warren DK, Marschall J. Vancomycin resistance has no influence on outcomes of enterococcal bacteria. *Journal of Hospital Infections*. 2013;85(3):183–8.

12. Steinmetz T, Eliakim-Raz N, Goldberg E, Leibovici L, Yahav D. Association of vancomycin serum concentrations with efficacy in patients with MRSA infections: A systematic review and meta-analysis. *Clinical Microbiology and Infections*. 2015;21(7):665–73.

13. Su X, Wang M, Ouyang H, Yang S, Wang W, He Y, Fu Z. Bioluminescent detection of the total amount of viable Gram positive bacteria isolated by vancomycin-functionalized magnetic particles. *Sensors Actuators B: Chemical*. 2017;241:255–61.

14. Jung HM, Kim SY, Moon HJ, Oh DK, Lee JK. Optimization of culture conditions and scale-up to pilot and plant scales for vancomycin production by Amycolatopsis orientalis. *Applied Microbiology and Biotechnology*. 2007;77(4):789–95.

15. Estes K, Derendorf H. Camparison of the pharmacokinetic properties of vancomycin, linezolid, tigecyclin, and daptomycin. *European Journal of Medical Research*. 2010;15:533–43.

16. Nagarajan R. Antibacterial activities and modes of action of vancomycin and related glycopeptides. *Antimicrobial Agents of Chemotheraphy*. 1991;35(4):605–9.

17. Meng X, Li F, Li F, Xiong Y, Xu H. Vancomycin modified PEGylated-magnetic nanoparticles combined with PCR for efficient enrichment and detection of Listeria monocytogenes. *Sensors Actuators B: Chemical*. 2017;247:546–55.

18. Bailie GR, Neal D. Vancomycin ototoxicity and nephrotoxicity a review. *Journal of Medical Toxicology*. 1988;3:376–86.

19. Yousry C, Elkheshen SA, El-laithy HM, Essam T, Fahmy RH. Studying the influence of formulation and process variables on Vancomycin-loaded polymeric nanoparticles as potential carrier for enhanced ophthalmic delivery. *European Journal of Pharmaceutical Sciences*. 2017;100:142–54.

20. Broome L, So TY. An evaluation of initial vancomycin dosing in infants, children, and adolescents. *International Journal of Pediatrics*. 2011;2011:1–4.

21. Kaymaz AP, Acaroğlu-Degitz İ, Yapaöz MA, Sezer AD, Malta S, Aksu B, Eren T. Synthesis of 1,4-diazabicyclo[2.2.2]octane and pyridinium based cationic polymers via ROMP technique and examination of their antibacterial activity and cytotoxicity. *Materialia*. 2019;5:1-34.

22. Antibiotic Resistance Threaths in the United States, 2013 [cited 2018 Oct 30]. The Treath of Antibiotic Resistance. Available from: www.cdc.gov/drugresistance/pdf/ar-threats-2013-508.pdf

23. He M, Zhou Y, Xiao H, Lu P. Amphiphilic cationic copolymers with ciprofloxacin: Preparation and antimicrobial activities. *New Journal of Chemistry*. 2016;40(2):1354–64.

24. Castonguay A, Ladd E, van De Ven TGM, Kakkar A. Dendrimers as bactericides. *New Journal of Chemistry*. 2012;36(2):199–204.

25. Albert M, Feiertag P, Hayn G, Saf R, Hönig H. Structure-activity relationships of oligoguanidines-influence of counterion, diamine, and average molecular weight on biocidal activities. *Biomacromolecules*. 2003;4(6):1811–7.

26. Felczak A, Wrońska N, Janaszewska A, Klajnert B, Bryszewska M, Appelhans D, Voit B, Rózalska S, Lisowska K. Antimicrobial activity of poly(propylene imine) dendrimers. *New Journal of Chemistry*. 2012;36(11):2215–22.

27. Ilker MF, Nüsslein K, Tew GN, Coughlin EB. Tuning the hemolytic and antibacterial activities of amphiphilic polynorbornene derivatives. *Journal of the American Chemical Society*. 2004;126:15870–5.

28. Hancock R, Patrzykat A. Clinical development of cationic antimicrobial peptides: from natural to novel antibiotics. *Current Drug Target-Infectious Disorders*. 2002;2(1):79–83.

29. Hancock REW, Lehrer R. Cationic peptides: a new source of antibiotics. *Trends in Biotechnology*. 1998;16(2):82–8.

30. Hancock REW. Peptide antibiotics. *The Lancet Journal*. 1997;349:418–22.

31. Hancock REW, Sahl HG. Antimicrobial and host-defense peptides as new anti-infective therapeutic strategies. *Nature Biotechnology*. 2006;24(12):1551–7.

32. Wade D, Boman A, Wåhlin B, Drain CM, Andreu D, Boman HG, Merrifield RB. All-D amino acid-containing channel-forming antibiotic peptides. *Proceedings of the National Academy of Science of the U.S.A*. 1990;87(12):4761–5.

33. Nilsson MF, Sandstedt B, Sørensen O, Weber G, Borregaard N, Ståhle-Bäckdahl M. The human cationic antimicrobial protein (hCAP18), a peptide antibiotic, is widely expressed in human squamous epithelia and colocalizes with interleukin-6. *Infection and Immunity*. 1999;67(5):2561–6.

34. Dathe M, Wieprecht T. Structural features of helical antimicrobial peptides: their potential to modulate activity on model membranes and biological cells. *Biochimica et Biophysica Acta - Biomembranes*. 1999;1462(1–2):71–87.

35. Fosgerau K, Hoffmann T. Peptide therapeutics: current status and future directions. *Drug Discovery Today*. 2015;20(1):122–8.

36. Zubris DL, Minbiole KP, Wuest WM. Polymeric quaternary ammonium compounds: versatile antimicrobial materials. *Current Topics in Medicinal Chemistry*. 2017;17(3):305–18.

37. Scott RW, Tew GN. Mimics of host defense proteins; strategies for translation to therapeutic applications. *Current Topic in Medicinal Chemistry*. 2017;17(5):576–89.

38. Kenawy ER, Worley SD, Broughton R. The chemistry and applications of antimicrobiaş polymers: a state-of-the-art review. *Biomacromolecules*. 2007;8(5):1359–84.

39. Tew GN, Liu D, Chen B, Doerksen RJ, Kaplan J, Carroll PJ, Klein ML, DeGrado WF. De novo design of biomimetic antimicrobial polymers. *Proceedings of the National Academy of Sciences*. 2002;99(8):5110–4.

40. Timofeeva L, Kleshcheva N. Antimicrobial polymers : mechanism of action, factors of activity, and applications. *Applied Microbiology and Biotechnology*. 2011;89(3):475–92.

41. Tew GN, Scott RW, Klein ML, Degrado WF. De novo design of antimicrobial polymers, foldamers, and small molecules: from discovery to practical applications. *Accounts of Chemical Research*. 2010;43(1):30–9.

42. Carmona-Ribeiro AM, de Melo Carrasco LD. Cationic antimicrobial polymers and their assemblies. *International Journal of Molecular Sciences*. 2013;14(5):9906–46.

43. Jain A, Duvvuri LS, Farah S, Beyth N, Domb AJ, Khan W. Antimicrobial polymers. *Advanced Healthcare Materials*. 2014;3(12):1969–85.

44. Takahashi H, Nadres ET, Kuroda K. Cationic amphiphilic polymers with antimicrobial activity for oral care applications : eradication of S.mutans biofilm. *Biomacromolecules*. 2017;18(1):257–65.

45. Kuroda K, Caputo GA. Antimicrobial polymers as synthetic mimics of host-defense peptides. *Wiley Interdisciplinary Reviews: Nanomedicine and Nanobiotechnology*. 2013;5:49–66.

46. Palermo EF, Kuroda K. Structural determinants of antimicrobial activity in polymers which mimic host defense peptides. *Applied Microbiology and Biotechnology*. 2010;87:1605–15.

47. Tian J, Zhang J, Yang J, Du L, Geng H, Cheng Y. Conjugated polymers act synergistically with antibiotics to combat bacterial drug resistance. *American Chemical Society: Applied Materials and Interfaces*. 2017;9:18512–20.

48. Walsh C. Molecular mechanisms that confer antibacterial drug resistance. *Nature*. 2000;406:775–81.

49. Cal PMSD, Matos MJ, Bernardes GJL. Trends in therapeutic drug conjugates for bacterial diseases: a patent review. *Expert Opinion on Therapeutic Patients*. 2017;27(2):179–89.

50. Smith D, Pentzer EB, Nguyen ST. Bioactive and therapeutic ROMP polymers. *Polymer Reviews*. 2007;47:419–59.

51. Kalhapure RS, Suleman N, Mocktar C, Seedat N, Govender T. Nanoengineered drug delivery systems for enhancing antibiotic therapy. *Journal of Pharmaceutical Sciences*. 2015;104:1–33.

52. Ng VWL, Tan JPK, Leong J, Voo ZX, Hedrich JL, Yang YY. Antimicrobial polycarbonates: investigating the impact of nitrogen-containing heterocycles as quaternizing agents. *Macromolecules*. 2014;47(4):1285–91.

53. Lienkamp K, Madkour AE, Musante A, Nelson CF. Antimicrobial polymers prepared by ROMP with unprecedented selectivity : a molecular construction kit approach. *Journal of the American Chemical Society*. 2008;130(30):9836–43.

54. Al-Badri ZM, Som A, Lyon S, Nelson CF, Nüsslein K, Tew GN. Investigating the effect of increasing charge density on the hemolytic activity of synthetic antimicrobial polymers. *Biomacromolecules*. 2008;9(10):2805–10.

55. Eren T, Som A, Rennie JR, Nelson CF, Urgina Y, Nu K, Coughlin EB, Tew GN. Antibacterial and hemolytic activities of quaternary pyridinium functionalized polynorbornenes. *Macromolecular Chemistry and Physics*. 2008;209(5):516–24.

56. Altay E, Altıkatoğlu-Yapaöz M, Keskin B, Yucesan G, Eren T. Influence of alkyl chain length on the surface activity of antibacterial polymers derived from ROMP. *Colloids and Surfaces B: Biointerfaces*. 2015;127:73–8.

57. Süer NC, Demir C, Unubol NA, Yalcin O, Kocagoz T, Eren T. Antimicrobial activities of phosphonium containing polynorbornenes. *Royal Society Chemistry Advances*. 2016;6(89):86151–7.

58. Lawson MC, Shoemaker R, Hoth KB, Bowman CN, Anseth KS. Polymerizable vancomycin derivatives for bactericidal biomaterial surface modification: Structure-function evaluation. *Biomacromolecules*. 2009;10:2221–34.

59. 2015 Annual Report for the Emerging Infections Program for Clostridium difficile Infection. [cited 2018 Oct 21]. Available from: https://www.cdc.gov/hai/eip/Annual-CDI-Report-2015.html

60. Elliott C, Justiz-vaillant A. Nosocomial infections: a 360-degree review. *International Biological and Biomedical Journal*. 2018;4(2):72–81.

61. Klevens RM, Edwards JR, Richards CL, Horan TC, Gaynes RP, Pollock DA, Cardo DM. Estimating health care-associated infections and deaths in U.S. Hospitals, 2002. *Public Health Reports*. 2007;122(2):160–6.

62. Vincent J, Rello J, Marshall J, Silva E, Anzueto A, Martin CD, Moreno R, Lipman J, Gomersall C, Sakr Y, Reinhart K. International study of prevalence and outcomes of infection in intensive care units. *The Journal of the American Medical Association.* 2009;302(21):2323–9.

63. Shukla P, Garg RK, Dahiya AK. Role of technology to combat nosocomial infections. *Apollo Medical*. 2016;13(1):71–3.

64. Joshi SG. Acinetobacter baumannii: an emerging pathogenic threat to public health. *World Journal of Clinical Infectious Disseases*. 2013;3(3):25.

65. Warren JW. Catheter-associated urinary tract infections. *International Journal of Antimicrobial Agents*. 2001;17(4):299–303.

66. Most Common Healthcare-Associated Infections. [cited 2018 Oct 24]. Available from]: https://www.beckershospitalreview.com/quality/most-common-healthcare-associated-infections-25-bacteria-viruses-causing-hais.html

67. Aitken C, Jeffries DJ. Nosocomial spread of viral disease nosocomial spread of viral disease. *Clinical Microbiology Reviews*. 2001;14(3):528–46.

68. Ducel JF, Fabry J, Nicolle L. *Prevention of hospital-acquired infections: a practical guide*. Geneva: World Health Organization Production Service; 2002.

69. Shalini S, Vidyasree MD, Abiselvi A, Gopalakrishnan S. Impact and effect of nosocomial infections: a review. *Research Journal of Pharmaceutical, Biological Chemical Sciences*. 2015;6(1):947–51.

70. Keller M a, Stiehm ER. Passive immunity in prevention and treatment of infectious diseases. *Clinical Microbiology Reviews*. 2000;13(4):602–14.

71. Erbay H, Yalcin AN, Serin S, Turgut H, Tomatir E, Cetin B, Zencir M. Nosocomial infections in intensive care unit in a Turkish university hospital: a 2-year survey. *Intensive Care Medicine*. 2003;29(9):1482–8.

72. Anderson DJ. Surgical site infections. *Infectious Disease Clinics of North America*. 2011;25(1):135–53.

73. Owens CD, Stoessel K. Surgical site infections: epidemiology, microbiology and prevention. *Journal of Hospital Infections*. 2008;70(2):3–10.

74. Koenig SM, Truwit JD. Ventilator-associated pneumonia: diagnosis, treatment, and prevention. *Clinical Microbiology Reviews*. 2006;19(4):637–57.

75. Li N, Sheng GP, Lu YZ, Zeng RJ, Yu HQ. Removal of antibiotic resistance genes from wastewater treatment plant effluent by coagulation. *Water Research*. 2017;111:204–12.

76. Salih ZH. Evaluation of antibacterial effect of pistacia vera l. nut pericarp extract against clinical isolates of methicillin-resistant Staphylococcus aureus (MRSA) and vancomycin resistant Enterococcus (VRE). University of Gaziantep; 2015.

77. Favor L, Baum M. *Germs: disease-causing organisms bacteria*. New York: The Rosen Publishing Group, Inc; 2016.

78. Bakteriler Hakkında Bilgi. [cited 2018 Oct 30]. Available from: http://www.nkfu.com/bakteriler-hakkinda-bilgi/

79. Cell Wall - Gram Positive vs Negative Bacteria. [cited 2018 Oct 30]. Available from: https://www.easybiologyclass.com/difference-between-the-cell-wall-of-Grampositive-and-Gramnegative-bacteria/

80. Kango N. *Textbook of microbiology*. New Delhi: IK International Pvt Ltd; 2010.

81. Gram Staining: Principle, Procedure and Results. [cited 2018 Oct 30]. Available from: https://microbeonline.com/gram-staining-principle-procedure-results/

82. Werkman CH, Wilson PW. *Bacterial physiology*. New York: Academis Press Inc.; 1951.

83. Yalçin AN, Hayran M, Unal S. Economic analysis of nosocomial infections in a Turkish university hospital. *Journal of Chemotheraphy*. 1997;9(6):411–4.

84. Khan MM, Celik Y. Cost of nosocomial infection in Turkey: an estimate based on the university hospital data. *Health Service Management Research*. 2001;14(1):49–54.

85. Levy SB. Factors impacting on the problem of antibiotic resistance. *Journal of Antimicrobial Chemotherapy*. 2002;49:25–30.

86. Alsaimary IE. Efficacy of some antibacterial agents on Staphylococcus aureus isolated from various burn cases. *International Journal of Medical Sciences*. 2009;1(4):110–4.

87. Argenziano M, Banche G, Luganini A, Finesso N, Allizond V, Gulino GR, Khadjavi A, Spagnolo R, Tullio V, Giribaldi G, Guiot C, Cuffini AM, Prato M, Cavalli R. Vancomycin-loaded nanobubbles: a new platform for controlled antibiotic delivery against methicillin-resistant Staphylococcus aureus infections. *International Journal of Pharmaceutics*. 2017;523(1):176–88.

88. Leman R, Alvarado-Ramy F, Pocock S, Barg N, Kellum M, McAllister S, Cheek J, Kuehnert M. Nasal carriage of methicillin-resistant staphylococcus aureus in an american indian population. *Infection Control and Hospital Epidemiology*. 2004;25(2):121–5.

89. Soju C, Dawn MS, Jeffrey CH, Matthew LB, Fred CT, Frances, Pouch D, Sandip S, James TR, Guy RP, William JB, Denise C, Scott KF. Infection with vancomycin-resistant. The *New England Journal of Medicine*. 2003;348:1342–7.

90. Carmeli Y, Eliopoulos G, Mozaffari E, Samore M. Health and economic outcomes of vancomycin-resistant Enterococci. *American Medical Association*. 2002;162:2223–8.

91. Cetinkaya Y, Falk P, Mayhall CG. Vancomycin-resistant Enterococci. *Clinical Microbiology Reviews*. 2000;13(4):686–707.

92. Ellis B, Smith R. *Polymers: a property database*. Boca Rayton: CRC Press; 2008.

93. Fried JR. *Polymer science and technology*. Massachusetts: Pearson Education; 2014.

94. Zhou H, Lawrence JG, Bhaduri SB. Fabrication aspects of PLA-CaP/PLGA-CaP composites for orthopedic applications: a review. *Acta Biomaterialia*. 2012;8(6):1999–2016.

95. Kankılıç B. Analysis of the effects of vancomycin containing bioceramic/polymer composites on biofilm prevention, biocompatibility and osteogenic modification of mesenchymal stem cells. Middle East Technical University; 2015.

96. Wade LG. *Organic chemistry*. 8th ed. New York: Pearson Education; 2012.

97. Sacak M. *Polimer kimyası*. 4th ed. Ankara: Gazi Kitabevi; 2008.

98. Addition Polymers. [cited 2018 Oct 31]. Available from: http://preparatorychemistry.com/Bishop_Addition_Polymers.htm

99. Rodriguez F, Cohen C, Ober CK, Archer L. *Principles of polymer systems*. Mischigan: CRC Press; 2014.

100. Ravve A. *Principles of polymer chemistry*. New York: Springer Science and Business Media; 2013.

101. Stevens MP. *Polymer chemistry*. New York: Oxford University Press; 1990.

102. Szwarc M. Living polymers: their discovery, characterization, and properties. *Journal of Polymer Sciences Part A: Polymer Chemistry*. 1997;36:9–15.

103. Bielawski CW, Grubbs RH. Living ring-opening metathesis polymerization. *Progress in Polymer Science*. 2007;32(1):1–29.

104. Matyjaszewski K. *Controlled/living radical polymerization: progress in RAFT, DT, NMP and OMRP*. In: American Chemical Society Symposium Series. 2009.

105. Grubbs RH. *Handbook of metathesis*.Weinheim: Wiley-VCH. 2003.

106. Trost BM. The atom economy: a search for synthetic efficiency. *Science*. 1991;254(5037):1471–7.

107. Forbes MDE, Myers TL, Maynard HD, Schulz GR, Patton JT, Smith DW, Wagener KB. Solvent-free cyclization of linear dienes using olefin metathesis and the thorpe-ingold effect. *Journal of the American Chemical Society*. 1992;114(27):10978–80.

108. Finkel'shtein ES, Ushakov NV, Portnykh EB. Metathesis of silicon-containing olefins. *Journal of Molecular Catalysis*. 1992;76:133–44.

109. Hilf S, Kilbinger AFM. Functional end groups for polymers prepared using ring-opening metathesis polymerization. *Nature Chemistry*. 2009;1(7):537–46.

110. Endo T. General mechanisms in ring-opening polymerization. *Handbook of ring-opening polymerization*. 2009:53–63.

111. Schwab P, Grubbs RH, Ziller JW. Synthesis and applications of $RuCl_2(=CHR')(PR_3)_2$: The influence of the alkylidene moiety on metathesis activity. *Journal of the American Chemical Society*. 1996;118(1):100–10.

112. Wu Z, Nguyen SBT, Grubbs RH, Ziller JW. Reactions of ruthenium carbenes of the type $(PPh_3)_2(X)_2Ru=CH-CH=CPh_2$(X=Cl and CF_3COO) with strained acyclic olefins and functionalized olefins. *Journal of the American Chemical Society*. 1995;117(20):5503–11.

113. Kim SJ, Matsuoka S, Patti GJ, Schaefer J. Vancomycin derivative with damaged d-ala-d-ala binding cleft binds to cross-linked peptidoglycan in the cell wall of staphylococcus aureus. *Biochemistry*. 2008;47(12):3822–31.

114. Sakoulas G, Moise-broder PA, Schentag J, Forrest A, Moellering RC, Eliopoulos GM. Relationship of MIC and bactericidal activity to efficacy of vancomycin for treatment of methicillin-resistant staphylococcus aureus bacteremia. *Journal of Clinical Microbiology*. 2004;42(6):2398–402.

115. Elyasi S, Khalili H, Dashti-Khavidaki S, Mohammadpour A. Vancomycin-induced nephrotoxicity: Mechanism, incidence, risk factors and special populations. A literature review. *European Journal of Clinical Pharmacology*. 2012;68:1243–55.

116. Minejima E, Choi J, Beringer P, Lou M, Tse E, Wong-Beringer A. Applying new diagnostic criteria for acute kidney injury to facilitate early identification of nephrotoxicity in vancomycin-treated patients. *Antimicrobial Agents Chemotheraphy*. 2011;55(7):3278–83.

117. Zang L, Gallo RL. Antimicrobial peptides. *Current Biology Magazine*. 2016;26:R14–9.

118. Diamond G, Beckloff N, Weinberg A, Kisich KO. The roles of antimicrobial peptides in innate host defense. *Current Pharmaceutical Design*. 2009;15(21):2377–92.

119. Ataman M. Antimikrobiyal peptidlerin çeşitli enfeksiyon etkenlerine karşı in vitro antibakteriyel aktivitelerinin araştırılması. Istanbul University; 2016.

120. Scott MG, Gold MR, Hancock REW. Interaction of cationic peptides with lipoteichoic acid and Grampositive bacteria. *Infection and Immunity*. 1999;67(12):6445–53.

121. Matsuzaki K. Control of cell selectivity of antimicrobial peptides. *Biochimica et Biophysica Acta*. 2009;1788:1687–92.

122. Matsuzaki K. Why and how are peptide-lipid interactions utilized for self-defense? Magainins and tachyplesins as archetypes. *Biochimica et Biophysica Acta*. 1999;1462:1–10.

123. Rocca PL, Biggin PC, Tieleman DP, Sansom MSP. Simulation of the interaction of antimicrobial pepdites and lipid bilayers. *Biochimica et Biophysica Acta*. 1999;1462:185–200.

124. Moghaddam MM, Aghamollaei H, Kooshki H, Barjini KA, Mirnejad R, Choopani A. The development of antimicrobial peptides as an approach to prevention of antibiotic resistance. *Reviews in Medical Microbiology*. 2015;26:98–110.

125. Siedenbiedel F, Tiller JC. Antimicrobial polymers in solution and on surfaces: overview and functional principles. *Polymers-Basel*. 2012;4(1):46–71.

126. Konai MM, Bhattacharjee B, Ghosh S, Haldar J. Recent progress in polymer research to tackle infections and antimicrobial resistance. *Biomacromolecules*. 2018;19(6):1888–917.

127. Chen A, Peng H, Blakey I, Whittaker AK. Biocidal polymers: a mechanistic overview. *Polymer Reviews*. 2017;57(2):276–310.

128. Brogden KA. Antimicrobial peptides: pore formers or metabolic inhibitors in bacteria? *Natıre Reviews Microbiology*. 2005;3:238–50.

129. Yeaman MR, Yount NY. Mechanisms of antimicrobial peptide action and resistance. *Pharmacological Reviews*. 2003;55(1):27–55.

130. Yang L, Harroun TA, Weiss TM, Ding L, Huang HW. Barrel-stave model or toroidal model? A case study on melittin pores. *Biophysical Journal*. 2001;81:1475–85.

131. Shai Y, Oren Z. Form “carpet” mechanism to de-novo designed diastereomeric cell-selective antimicrobial peptides. *Peptides*. 2001;22:1629–41.

132. Li S, Dong S, Xu W, Tu S, Yan L, Zhao C, Ding J, Chen X. Antibacterial hydrogels. *Advanced Sciences*. 2018;5:1–17.

133. Marr AK, Gooderham WJ, Hancock RE. Antibacterial peptides for therapeutic use: obstacles and realistic outlook. *Current Opinion in Pharmacology*. 2006;6(5):468–72.

134. Giuliani A, Pirri G, Nicoletto SF. Antimicrobial peptides: an overview of a promising class of therapeutics. *Center European Journal of Biology*. 2007;2(1):1–33.

135. Papo N, Shai Y. Host defense peptides as new weapons in cancer treatment. *Cellular and Molecular Life Sciences*. 2005;62:784–90.

136. Riedl S, Zweytick D, Lohner K. Membrane-active host defense peptides-challenges and perspectives for the development of novel anticancer drugs. *Chemistry and Physics of Lipids*. 2011;164:766–81.

137. Haag R, Kratz F. Polymer therapeutics: concepts and applications. *Angewandte Chemie-International Edition*. 2006;45(8):1198–215.

138. Larson N, Ghandehari H. Polymeric conjugates for drug delivery. *Chemistry of Materials*. 2012;24:840–53.

139. Ringsdorf H. Structure and properties of pharmacologically active polymers. *Journal of Polymer Science: Polymer Symposia*. 1975;51:135–53.

140. Arimoto H, Nishimura K, Kinumi T, Hayakawa I, Uemura D. Multi-valent polymer of vancomycin: enhanced antibacterial activity against VRE. *Chemical Communications*. 1999;1361–2.

141. McClure CK. *Structural chemistry using NMR spectroscopy, organic molecules*. Massachusetts: Elsevier; 2010.

142. Lindon JC, Tranter GE, Koppenaal D. *Encyclopedia of spectroscopy and spectrometry*. Virginia: Academic Press; 2016.

143. Rouessac F, Rouessac A. *Chemical analysis: modern instrumentation methods and techniques*. Chichester: John Wiley and Sons; 2013.

144. Gerwert K, Kötting C. *Fourier transform infra-red (FTIR) spectroscopy*. Chichester: John Wiley and Sons LTd; 2010.

145. Perkin Elmer Technical Note. *FT-IR spectroscopy attenuated total reflectance (ATR)*. 2005.

146. Mirabella FMJ. Internal reflection spectroscopy:theory and applications. *Analytica Chimica Acta*. 1993;276(2).

147. FTIR Sample Techniques: Attenuated Total Reflection (ATR). [cited 2018 Nov 12]; Available from: https://www.thermofisher.com/tr/en/home/industrial/spectroscopy-elemental-isotope-analysis/spectroscopy-elemental-isotope-analysis-learning-center/molecular-spectroscopy-information/ftir-information/ftir-sample-handling-techniques/ftir-sample-handling-techniques-attenuated-total-reflection-atr.html

148. Sundaram H, Vijayalakshmi N, Srilatha KP. High performance liquid chromatography and its role in identification of mycobacteriae: an overview. *National Informatics Centre Bulletin*. 2009;45:1–4.

149. Hamilton RJ, Sewell PA. *Introduction to high performance liquid chromatography*. Dortrecth:Springer; 2011.

150. Scanning Electron Microscopy (SEM). [cited 2018 Nov 15]. Available from: https://serc.carleton.edu/research_education/geochemsheets/techniques/SEM.html

151. Flegler SL, Heckman JW, Klomparens KL. *Scanning and transmission electron microscopy: an introduction*. Oxford: Oxford University Press *1993*.

152. Bazzi H SHF. Adenine-containing block copolymers via ring-opening metathesis polymerization: synthesis and self-assembly into rod morphologies. *Macromolecules*. 2002;35(26):9617–20.

153. Love JA, Morgan JP, Trnka TM, Grubbs RH. A practical and highly active ruthenium-based catalyst that effects the cross metathesis of acrylonitrile. *Angewandte Chemie International Edition*. 2002;114(21):4207–9.

154. Movassagh B, Shaygan P. Michael addition of thiols to α,β-unsaturated carbonyl compounds under solvent-free conditions. *Archive for Organic Chemistry*. 2006;12(12):130–7.

155. Herigstad B, Hamilton M, Heersink J. How to optimize the drop plate method for enumerating bacteria. *Journal of Microbiological Methods*. 2001;44:121–9.

156. Lambert RJW, Skandamis PN, Coote PJ, Nychas GJE. A study of the minimum inhibitory concentration and mode of action of oregano essential oil, thymol and carvacrol. *Journal of Applied Microbiology*. 2001;91(3):453–62.

157. Malich G, Markovic B, Winder C. The sensitivity and specificity of the MTS tetrazolium assay for detecting the in vitro cytotoxicity of 20 chemicals using human cell lines. *Toxicology*. 1997;124(3):179–92.

158. Tiller JC, Liao C, Lewis K, Klibanov AM. Designing surfaces that kill bacteria on contact. *Proceedings of the National Academy Sciences*. 2001;98(11):5981–5.

159. Shai Y. Mode of action of membrane active antimicrobial peptides. *Peptide Sciences*. 2002;66:236–48.

160. Zhang L, Rozek A, Hancock REW. Interaction of cationic antimicrobial peptides with model membranes. The *Journal of Biological Chemistry*. 2001;276(38):35714–22.

161. Sarapas JM, Backlund CM, deRonde BM, Minter LM, Tew GN. ROMP- and RAFT-based guanidinium-containing polymers as scaffolds for protein mimic synthesis. *Chemistry-A European Journal.* 2017;23(28):6858–63.

162. Buchmeiser MR. Metathesis-based monolithic supports: synthesis, functionalization and applications. *Macromolecular Rapid Communications*. 2001;22(14):1081–94.

163. Kröll RM, Schuler N, Lubbad S, Buchmeiser MR. A ROMP-derived, polymer-supported chiral Schrock catalyst for enantioselective ring-closing olefin metathesis. *Chemical Communications*. 2003;2742–3.

164. Dathe M, Wieprecht T, Nikolenko H, Handel L, Maloy WL, MacDonald DL, Beyermann M, Bienert M. Hydrophobicity, hydrophobic moment and angle subtended by charged residues modulate antibacterial and haemolytic activity of amphipathic helical peptides. *Federation of European Biochemical Societies Letters*. 1997;403:208–12.

165. Lienkamp K, Tew GN. Synthetic mimics of antimicrobial peptides- a versatile ring-opening metathesis polymerization based platform for the synthesis of selective. *Chemistry-A European Journal*. 2009;15(44):11784–800.

166. Thorsteinsson T, Loftsson T, Masson M. Soft antibacterial agents. *Current Medicinal Chemistry*. 2003;10:1129–36.

167. Kenawy E, Mahmoud YA. Biologically active polymers, a synthesis and antimicrobial activity of some linear copolymers with quaternary ammonium and phosphonium groups. *Macromolecular Bioscience*. 2003;3(2):107–16.

168. Lim S, Hudson SM. Review of chitosan and its derivatives as antimicrobial agents and their uses as textile chemicals. *Journal of Macromolecular Science Part C: Polymer Reviews.* 2003;C43(2):223–69.

169. Li G, Shen J, Zhu Y. Study of pyridinium-type functional polymers: antibacterial activity of soluble pyridinium-type polymers. *Journal of Applied Polymer Science*. 1998;67:1761–8.

170. Wang L, Xu X, Guo S, Peng Z, Tang T. Novel water soluble phosphonium chitosan derivatives: synthesis, characterization and cytotoxicity studies. *International Journal of Biological Macromolecules*. 2011;48:375–80.

171. Ornelas-Megiatto C, Wich PR, Fréchet JMJ. Polyphosphonium polymers for siRNA delivery: an efficient and nontoxic alternative to polyammonium carriers. *Journal of the American Chemical Society*. 2012;134:1902–5.

172. Xue Y, Xiao H, Zhang Y. Antimicrobial polymeric materials with quaternary ammonium and phosphonium salts. *International Journal of Molecular Sciences*. 2015;16:3626–55.

173. Świątek M, Valensin D, Migliorini C, Gaggelli E, Valensin G, Jezowska-Bojczuk M. Unusual binding ability of vancomycin towards Cu^{2+} ions. *Dalton Transactions*. 2005;(23):3808–13.

174. Pearce CM, Williams DH. Complete assignment of the ^{13}C NMR spectrum of vancomycin. *Journal of the Chemical Society, Perkin Transactions*. 1995;2:153–7.

175. Toi PV, Tho NDK, Phuong PN, Thao HP, Quynh TT, Thuy HTM, Hanh DTH, Chau N, Thwaites GE, Hien TT. High performance liquid chromatography method for implementation of therapeutic drug monitoring of vancomycin at hospital for tropical diseases -ho chi minh city vietnam. *Madihol University Journal of Pharmaceutical Sciences*. 2015;42(2015):186–94.

176. Avans N V. Qualitative analysis. [cited 2019 Mar 20]. Available from: https://chem.libretexts.org/Bookshelves/Analytical_Chemistry/Supplemental_Modules_(Analytical_Chemistry)/Chromedia/01Gas_Chromotography_(GC)/Gas_Chromotography percent3A_Basic_Theory/25Qualitative_analysis percent3A_identification

177. Özalp Y, Özdemir N, Hasirci V. Vancomycin release from poly(D,L-lactide) and poly(lactide-co-glycolide) disks. *Journal of Microencapsulation*. 2002;19(1):83–94.

178. Lienkamp K, Madkour AE, Musante A, Nelson CF, Nüsslein K, Tew GN. Antimicrobial polymers prepared by ROMP with unprecedented selectivity: a molecular construction kit approach. *Journal of the American Chemical Society*. 2008;130(30):9836–43.

179. Drouet M, Chai F, Barthélémy C, Lebuffe G, Debaene B, Décaudin B, Odou P. Influence of vancomycin infusion methods on endothelial cell toxicity. *Antimicrobial Agents Chemotheraphy*. 2014;59(2):930–4.

APPENDIX A: ^{1}H NMR SPECTRA OF THE POLYMERS

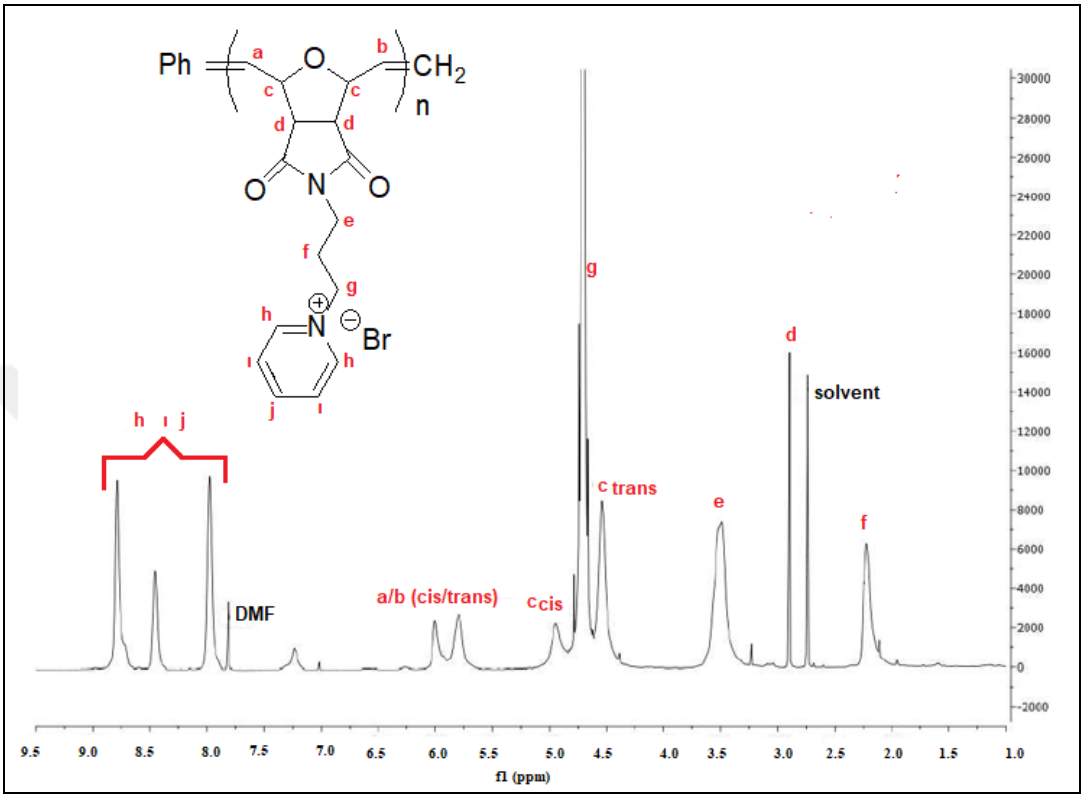

Figure A.1. The proton NMR spectrum of P-3

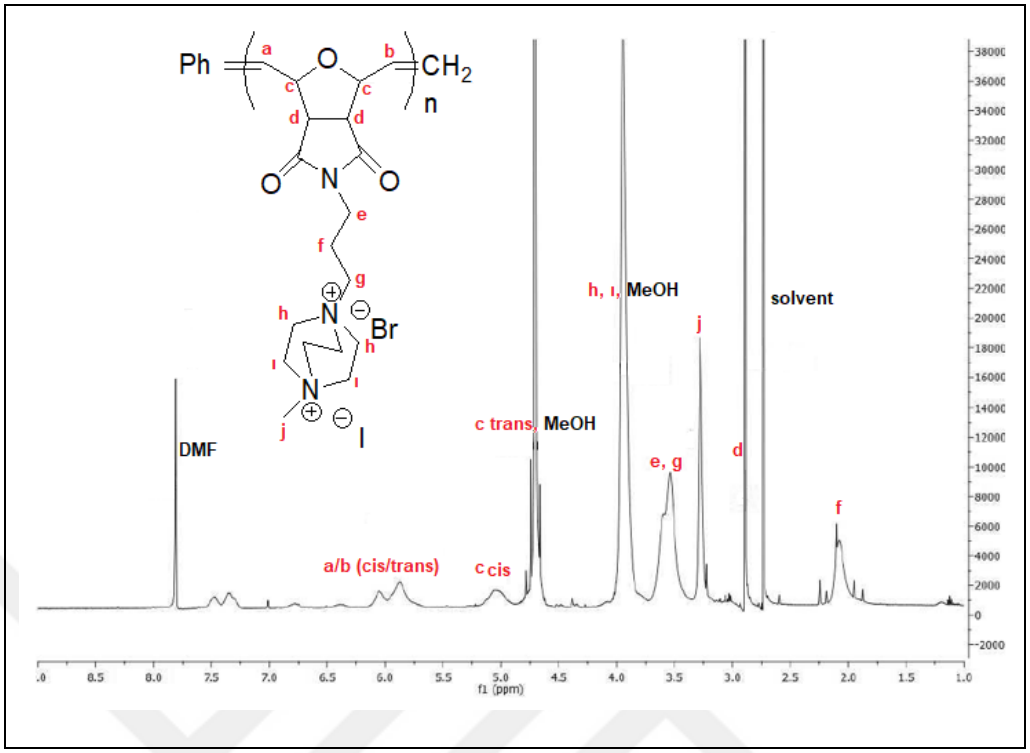

Figure A 2. The proton NMR spectrum of D-3

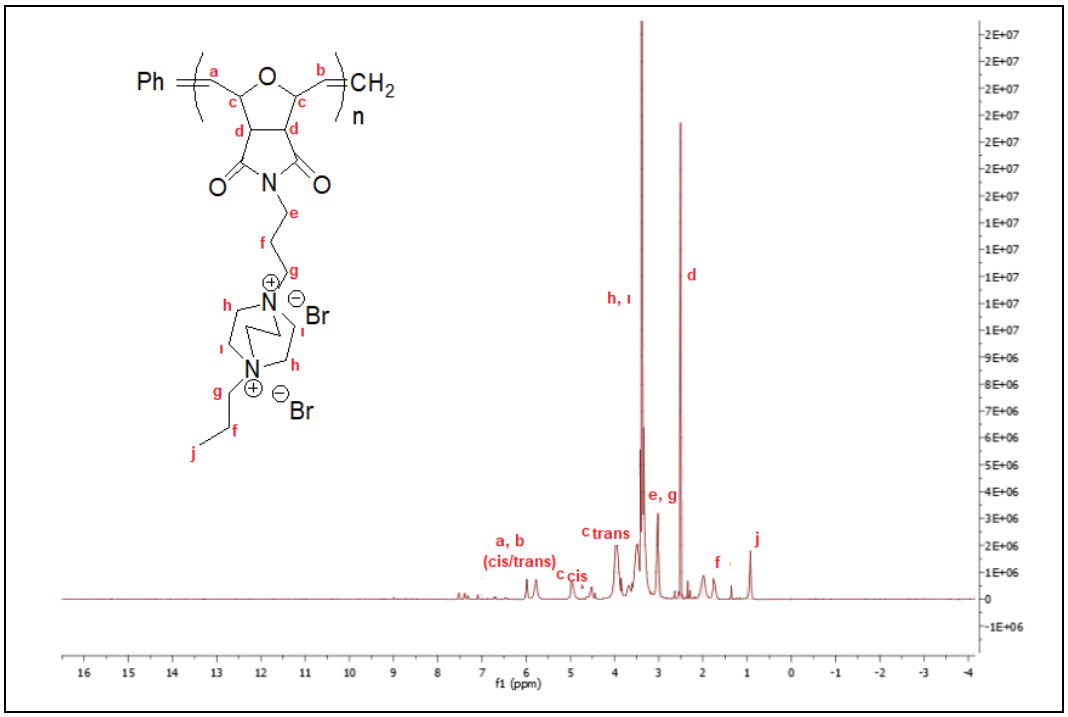

Figure A.3. The proton NMR spectrum of ID-3

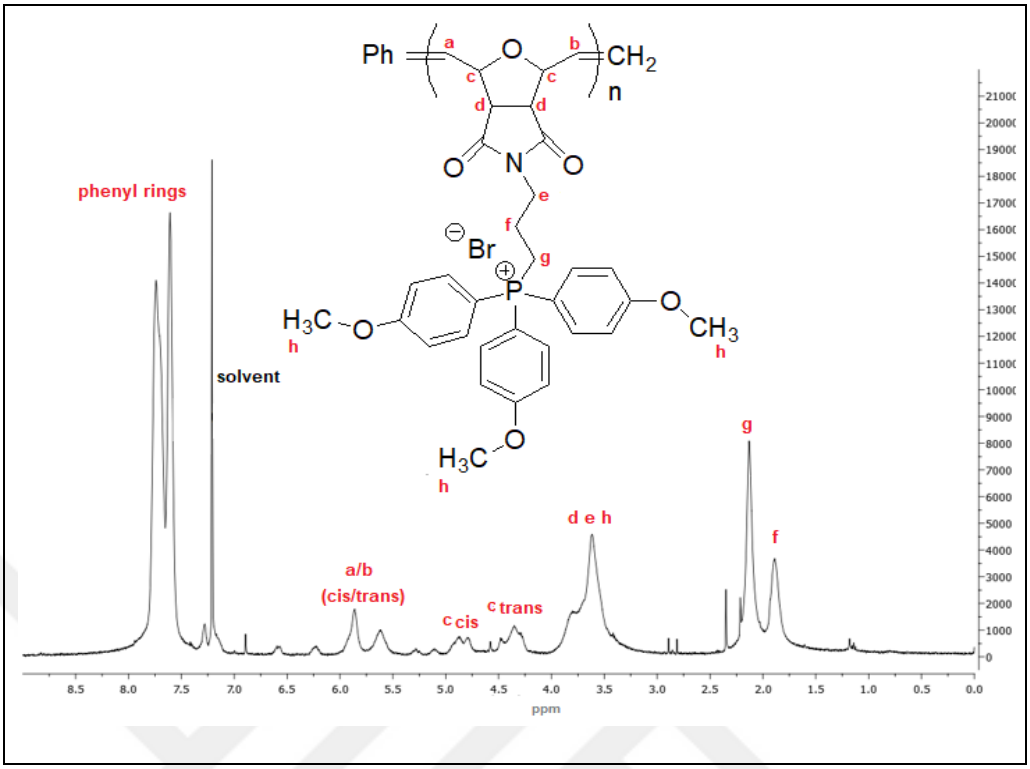

Figure A.4. The proton NMR spectrum of M-10

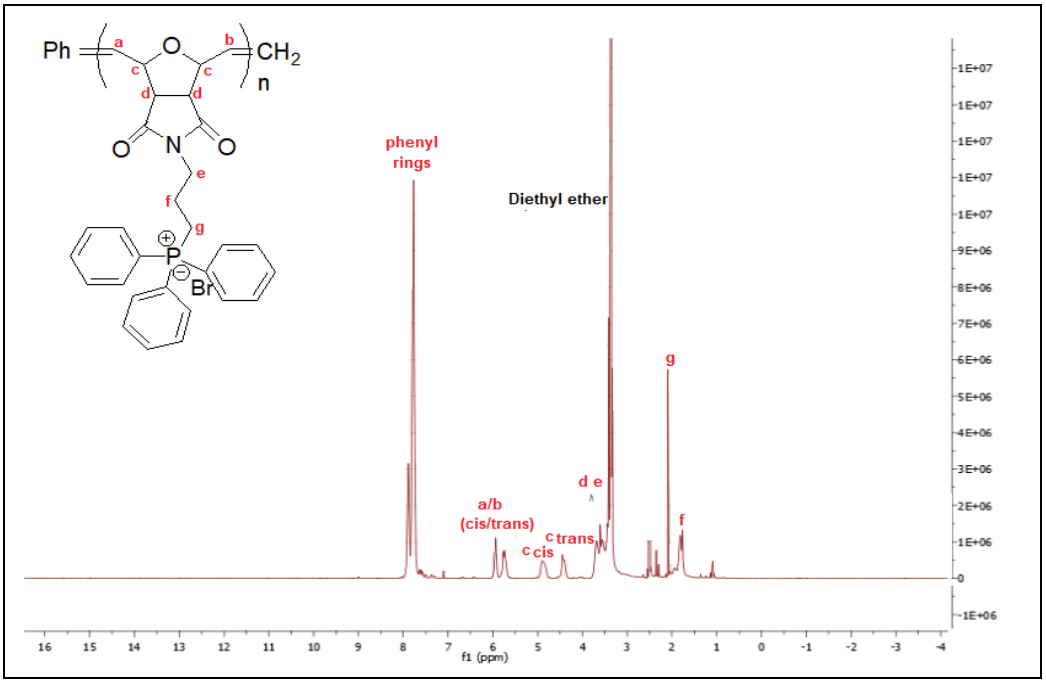

Figure A.5. The proton NMR spectrum of Phe-10

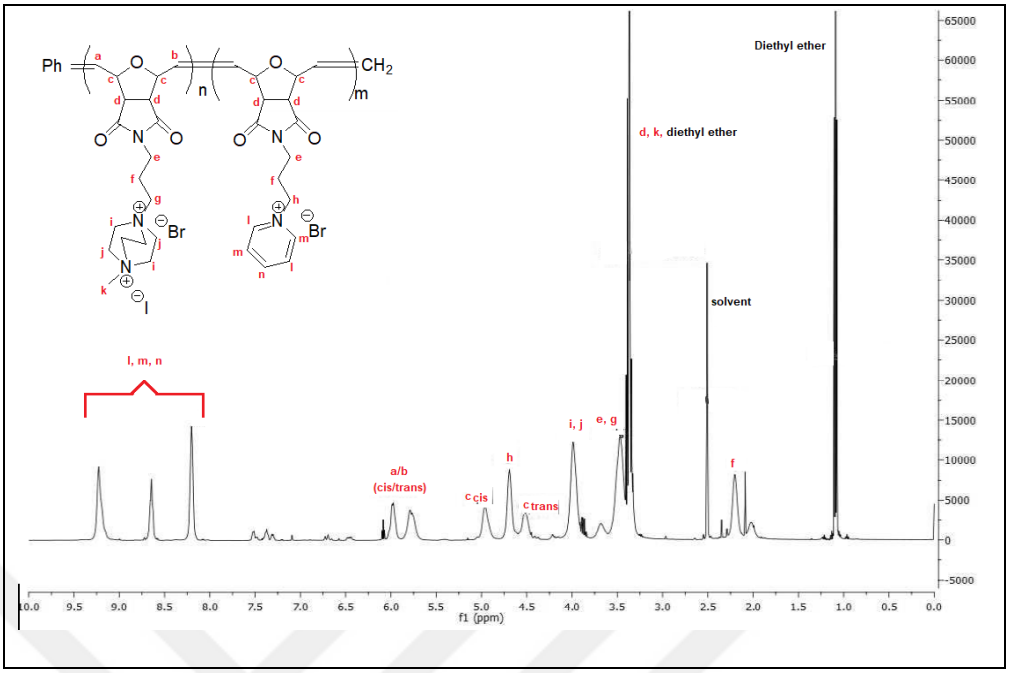

Figure A 6. The proton NMR spectrum of Copolymer D1-P2

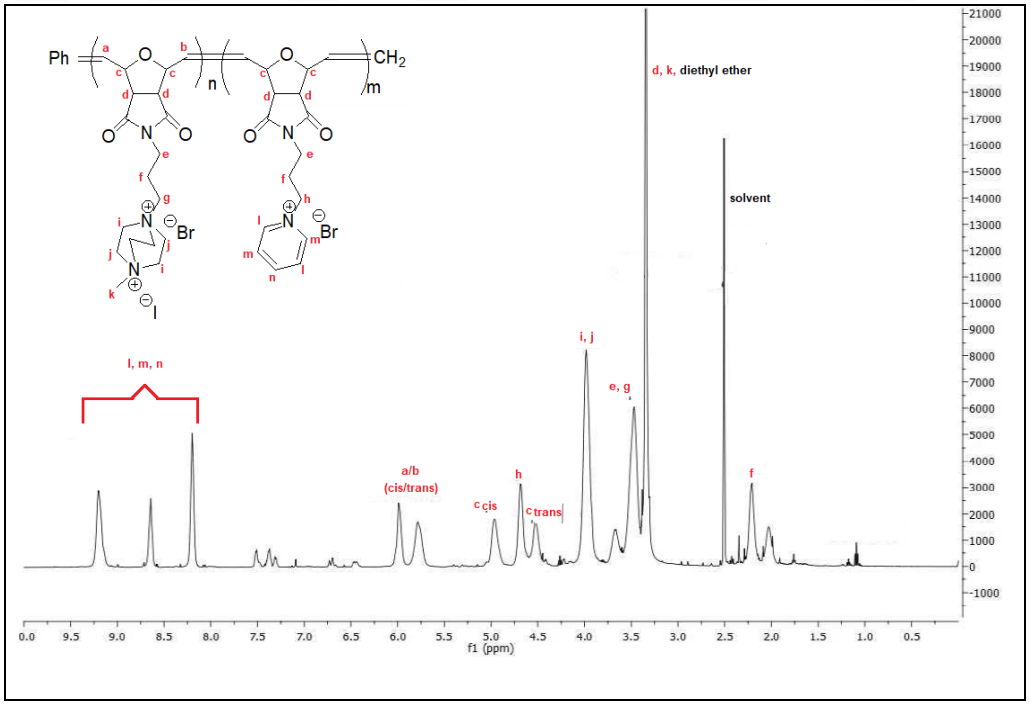

Figure A.7. The proton NMR spectrum of Copolymer D2-P1

APPENDIX B: FTIR ANALYSIS OF THE POLYMERS

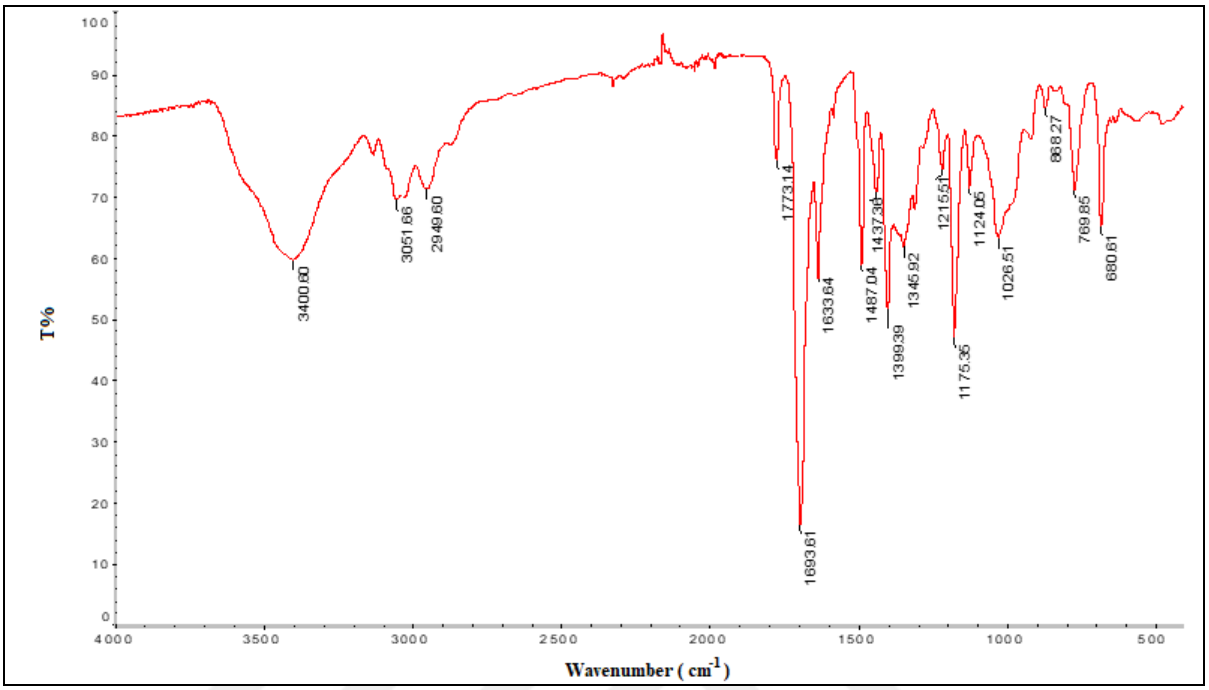

Figure B.1. FTIR spectrum of P-3

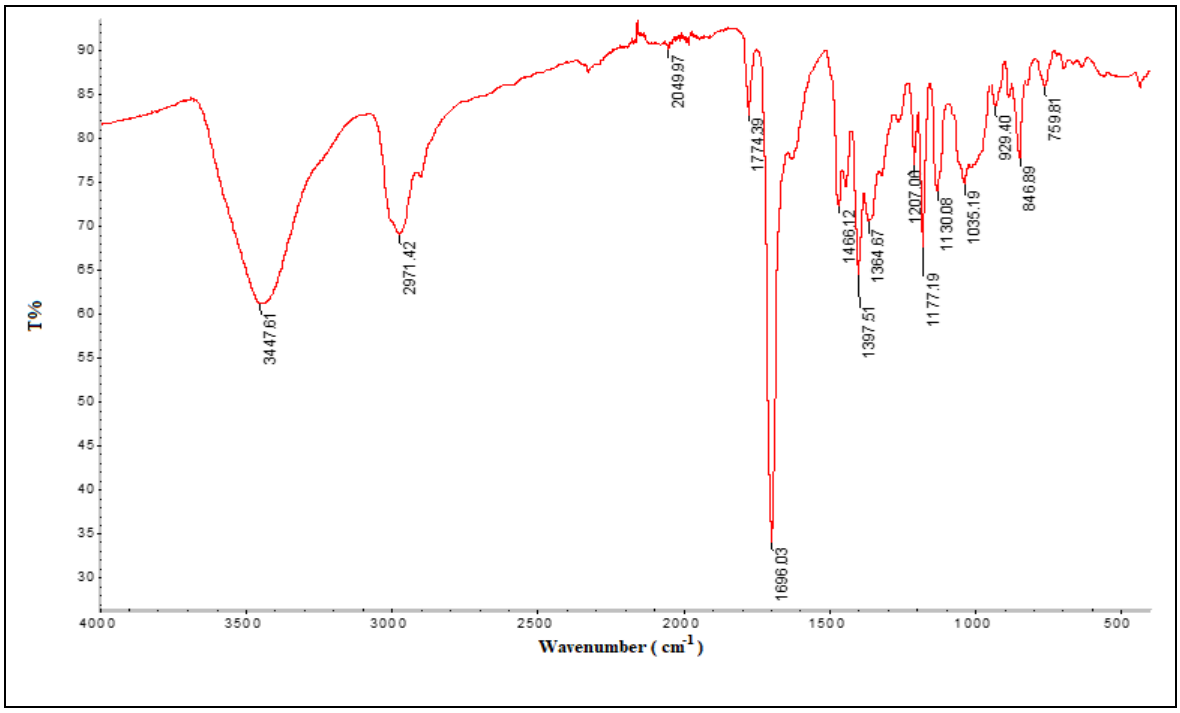

Figure B.2. FTIR spectrum of D-3

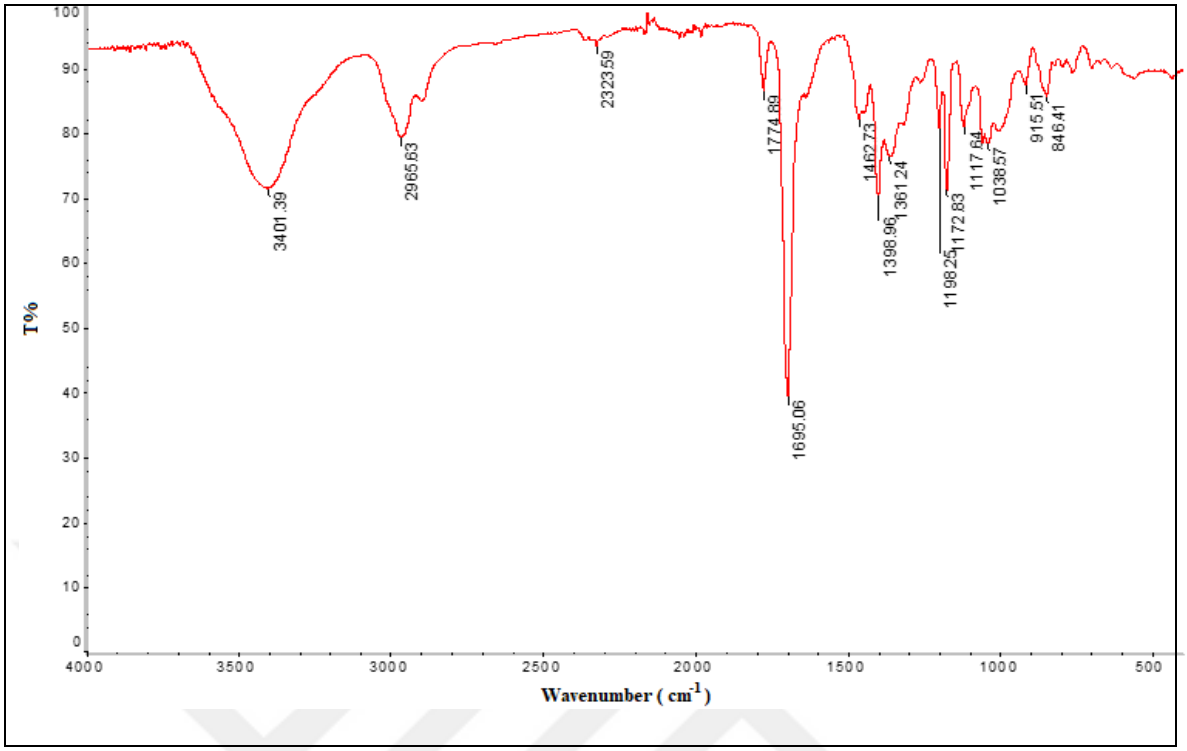

Figure B.3. FTIR spectrum of ID-3

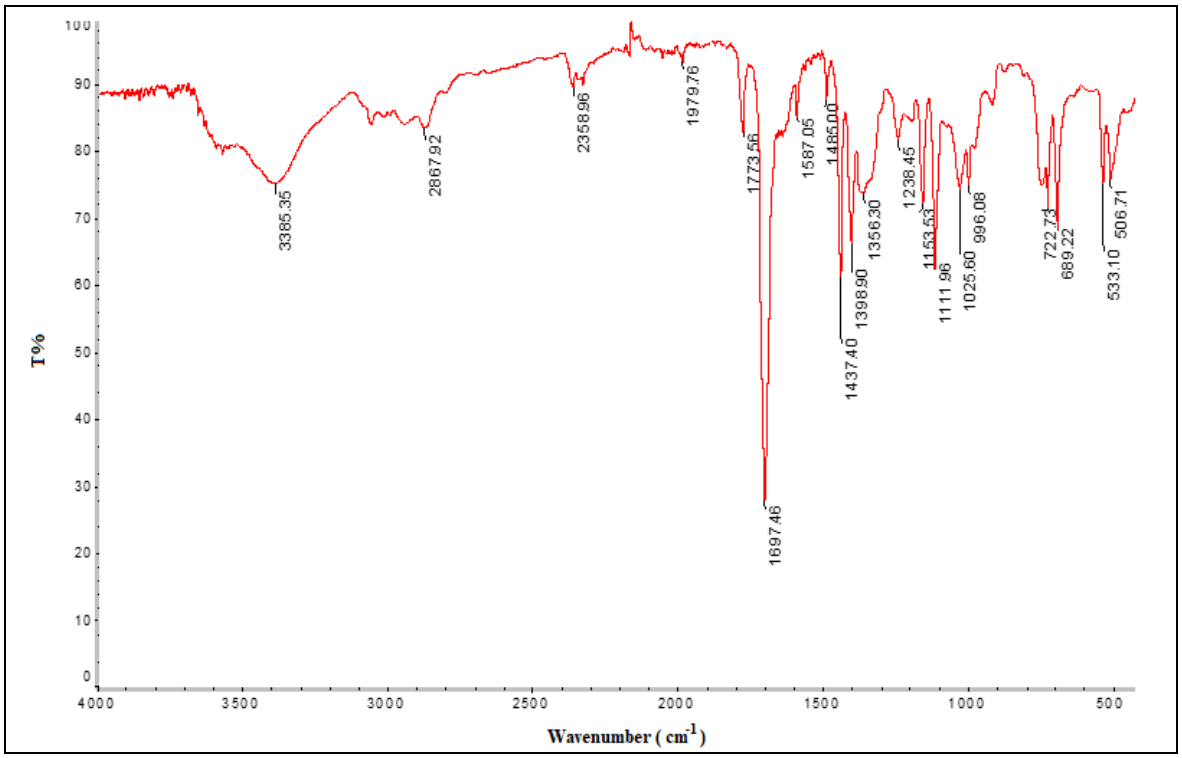

Figure B.4. FTIR spectrum of Phe-10

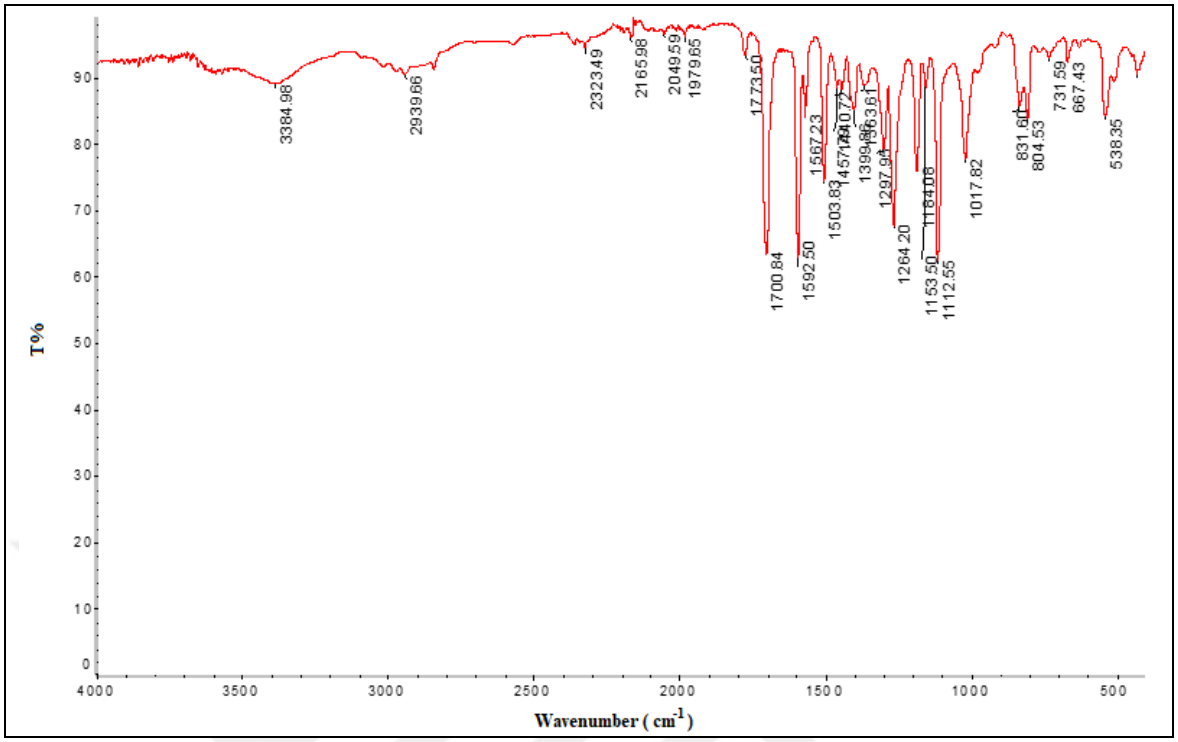

Figure B.5. FTIR spectrum of M-3

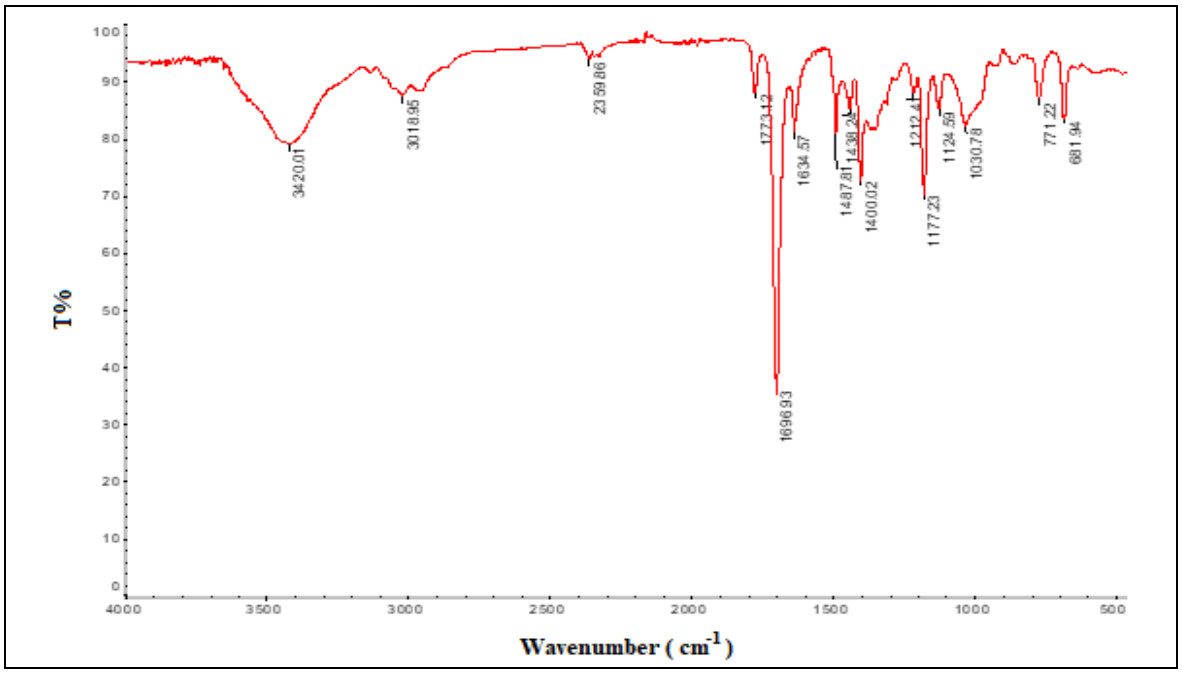

Figure B.6. FTIR spectrum of D1-P2

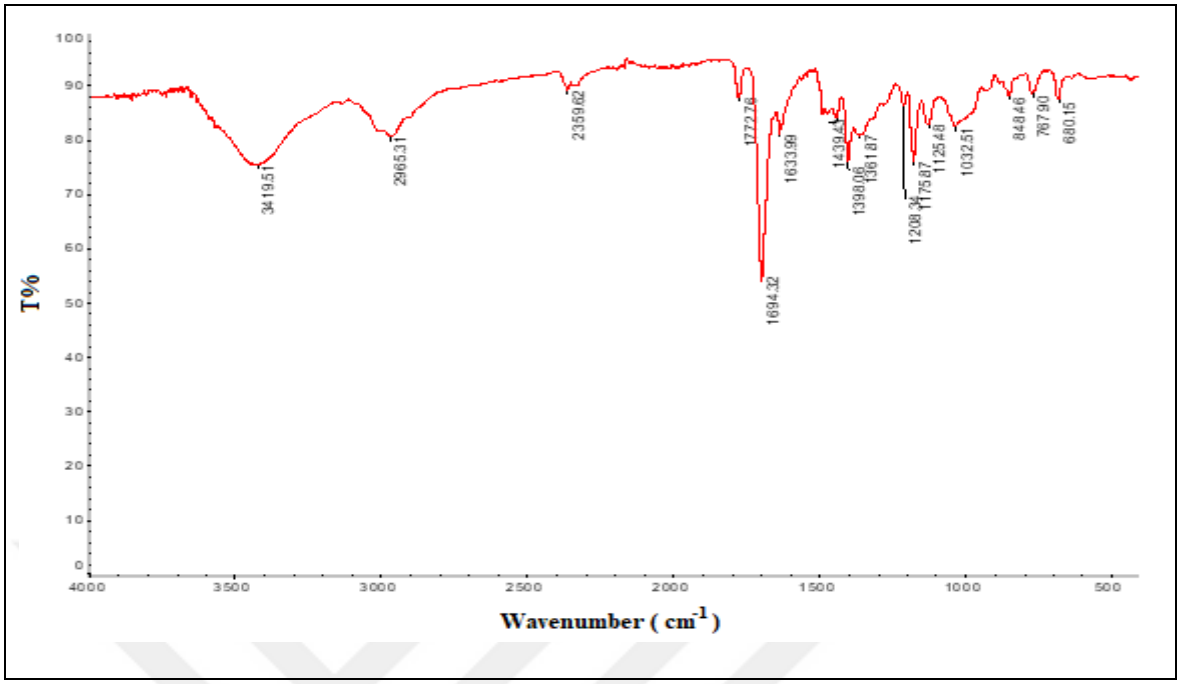

Figure B.7. FTIR spectrum of D2-P1

APPENDIX C: MTS ASSAY RESULTS OF THE POLYMERS

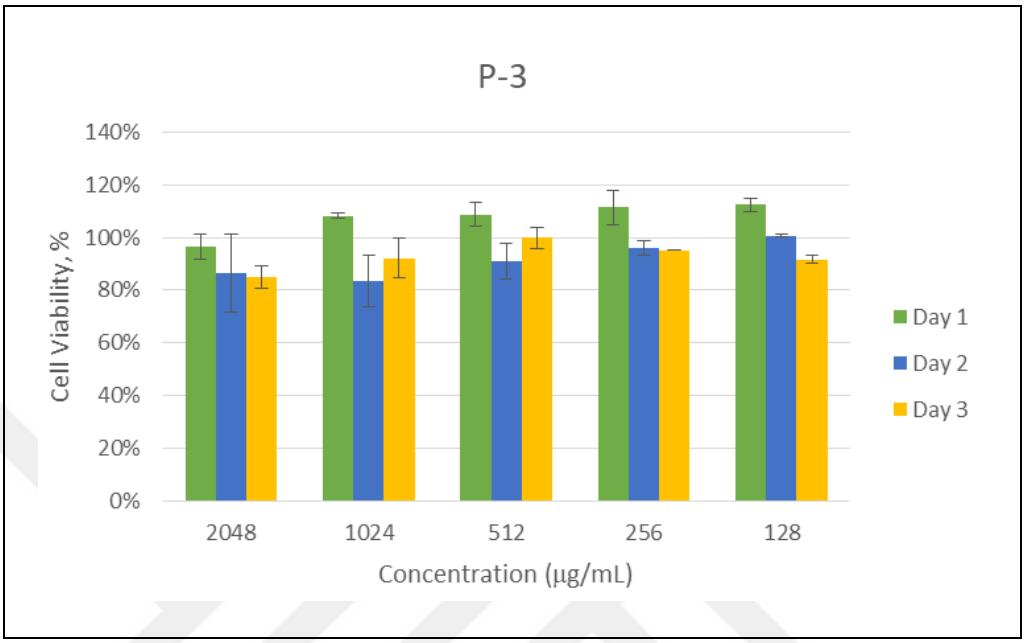

Figure C.1. Cell viability results of P-3 Homopolymer

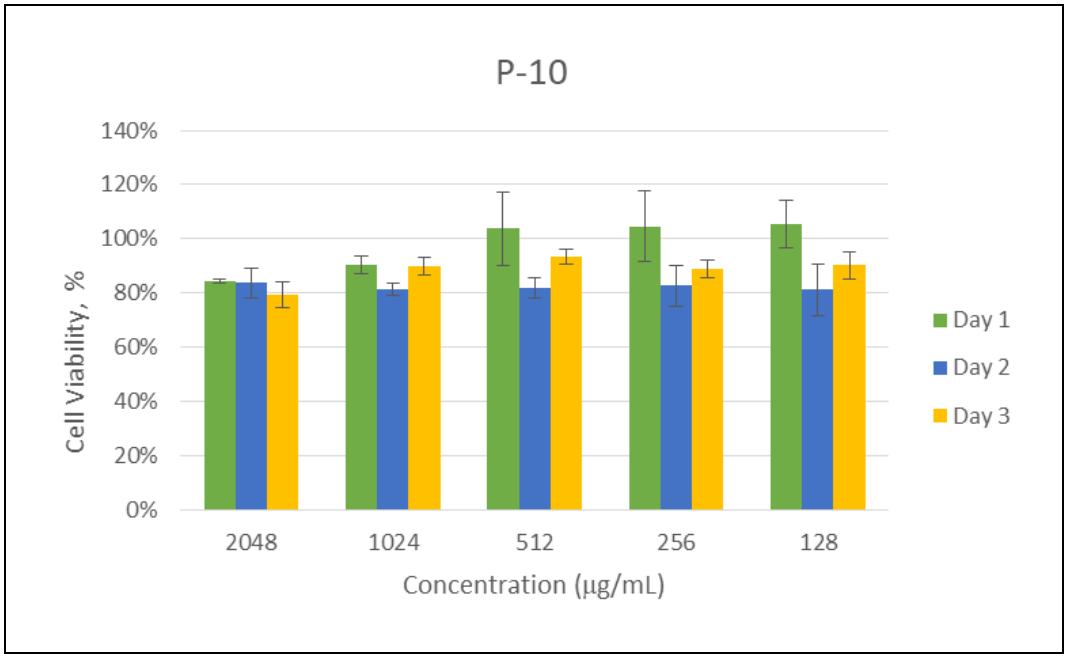

Figure C.2. Cell viability results of P-10 Homopolymer

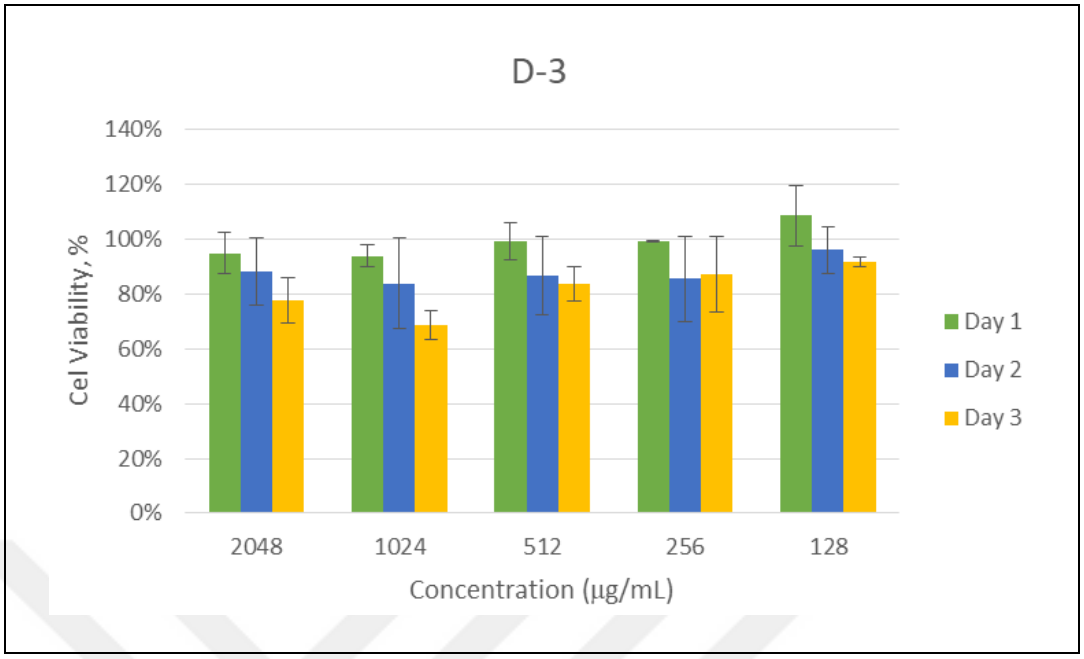

Figure C.3. Cell viability results of D-3 Homopolymer

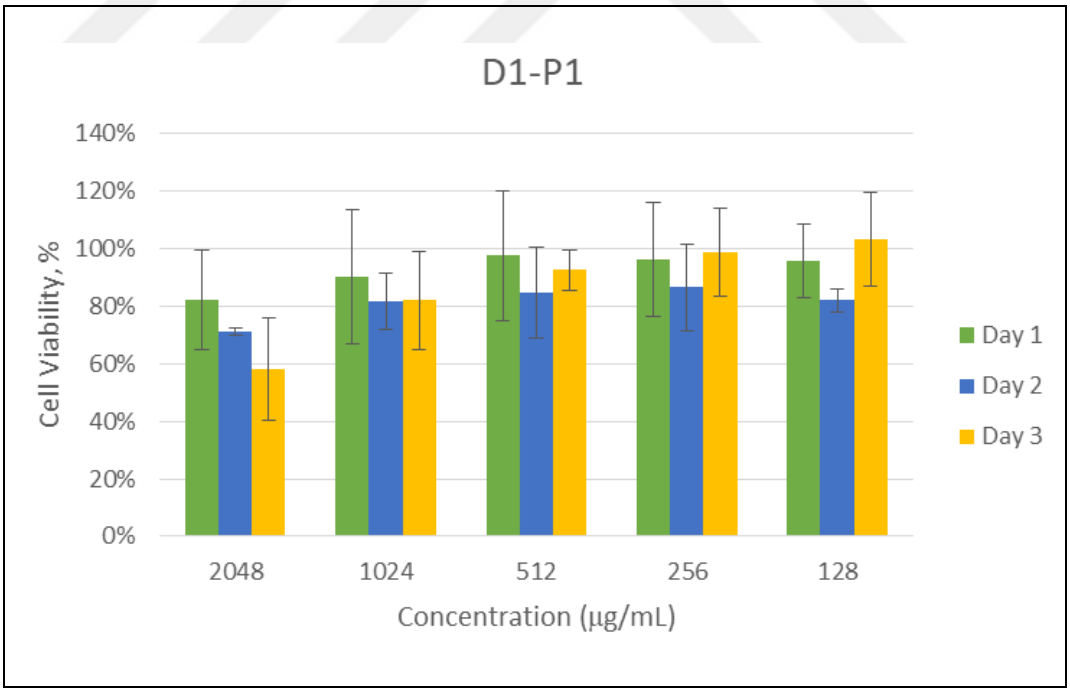

Figure C.4. Cell viability results of D1-P1 Copolymer

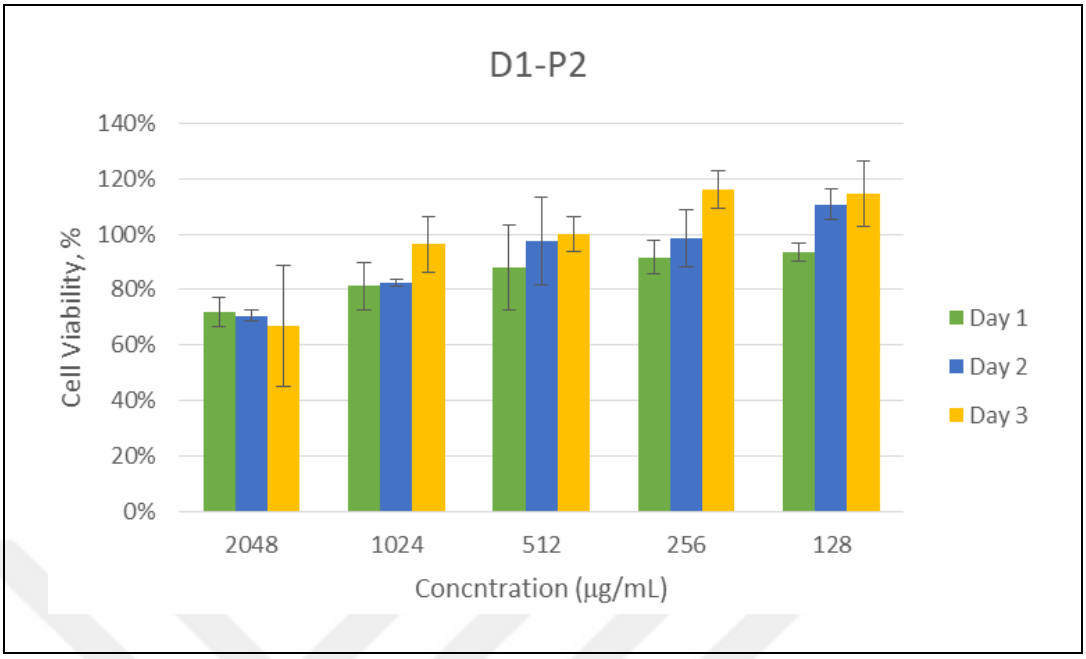

Figure C.5. Cell viability results of D1-P2 Copolymer

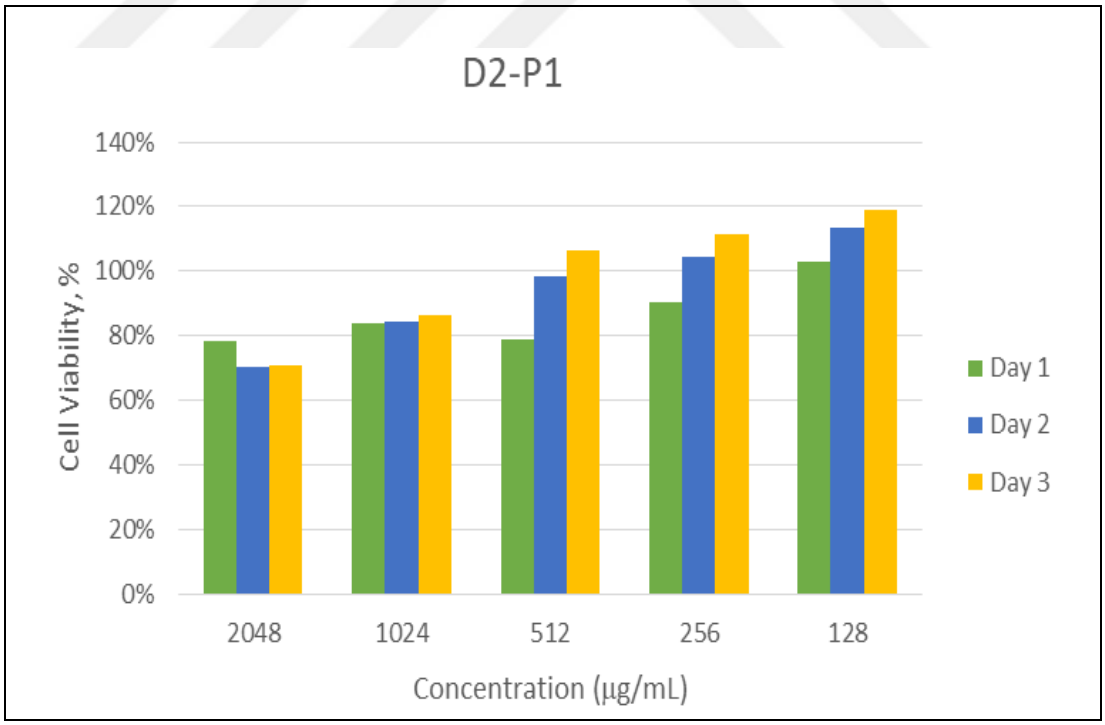

Figure C.6. Cell viability results of D2-P1 Copolymer

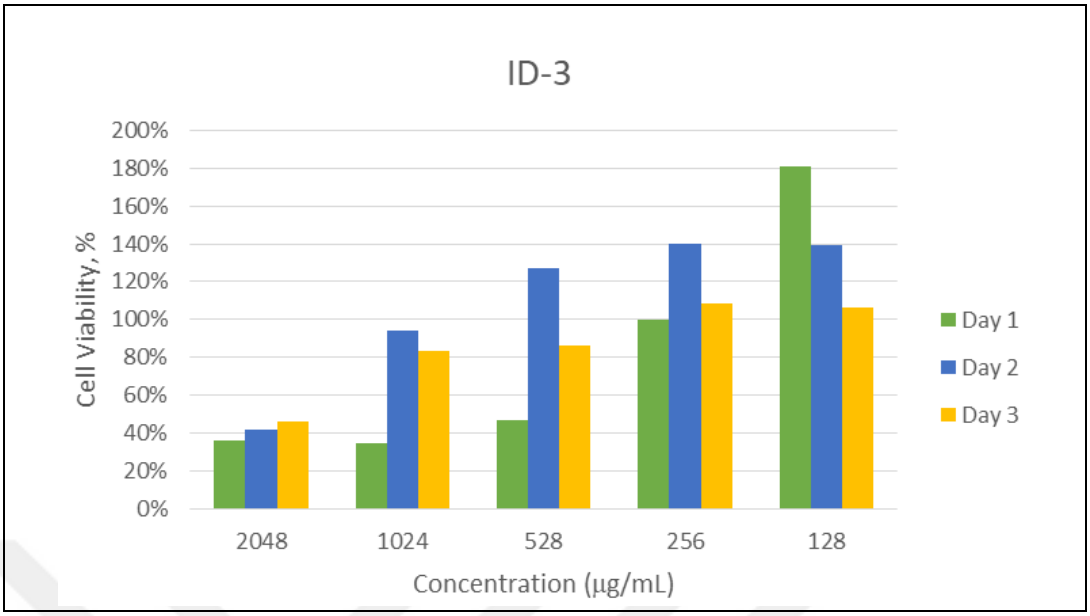

Figure C.7. Cell viability results of ID-3 Homopolymer

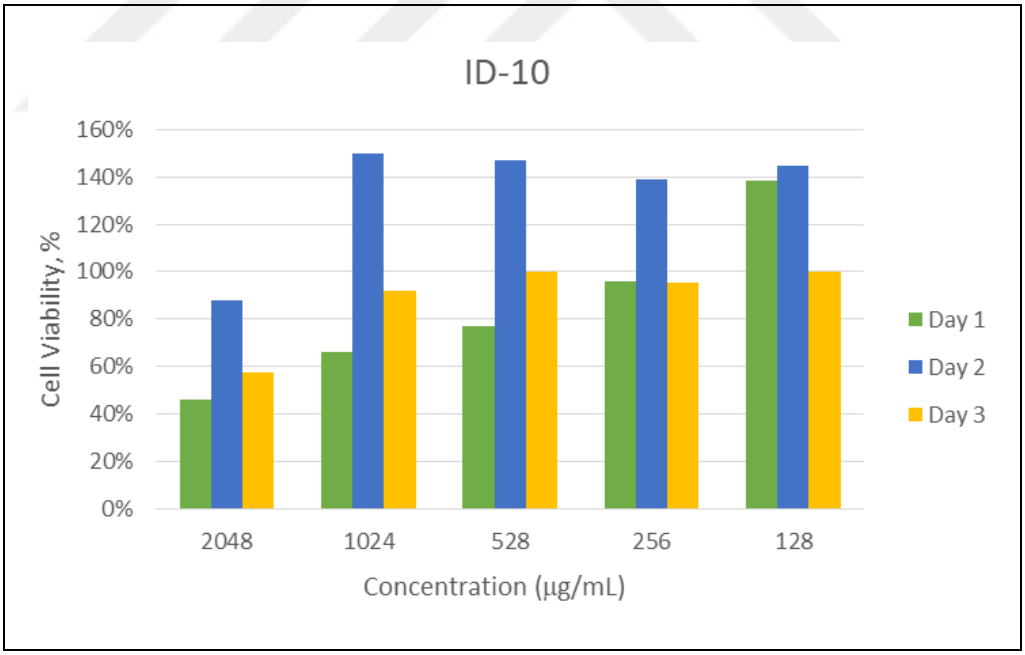

Figure C.8. Cell viability results of ID-10 Homopolymer

APPENDIX D: ^{1}H NMR SPECTRA OF THE VP-POLYMER CONJUGATES

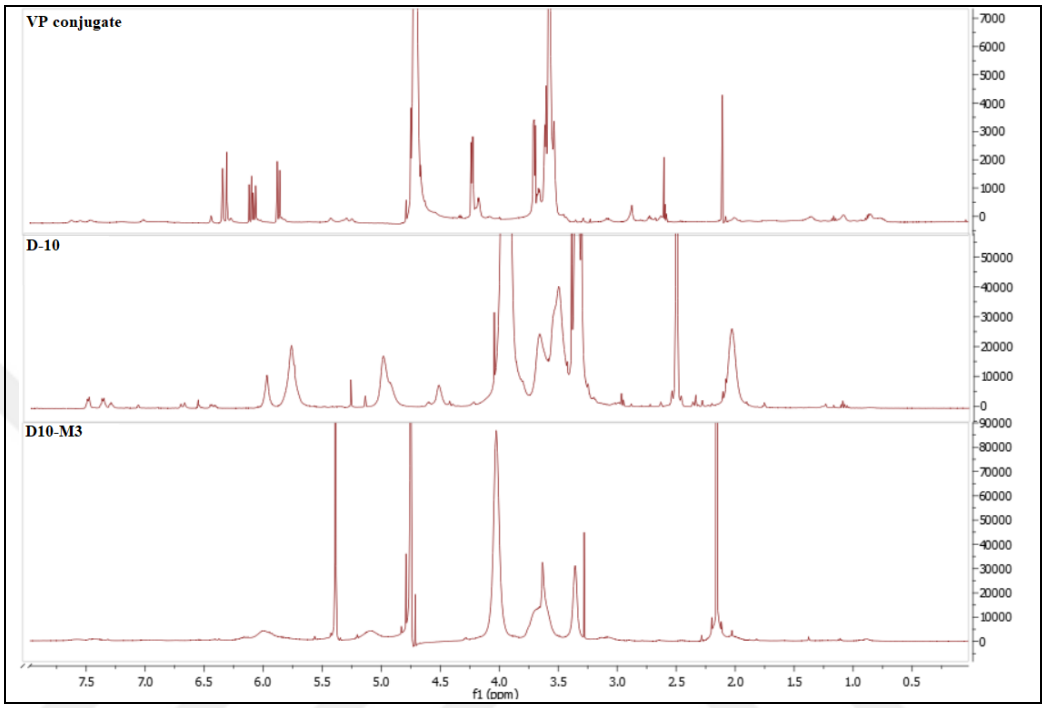

Figure D.1 The proton NMR spectrum of D10-M3 conjugate

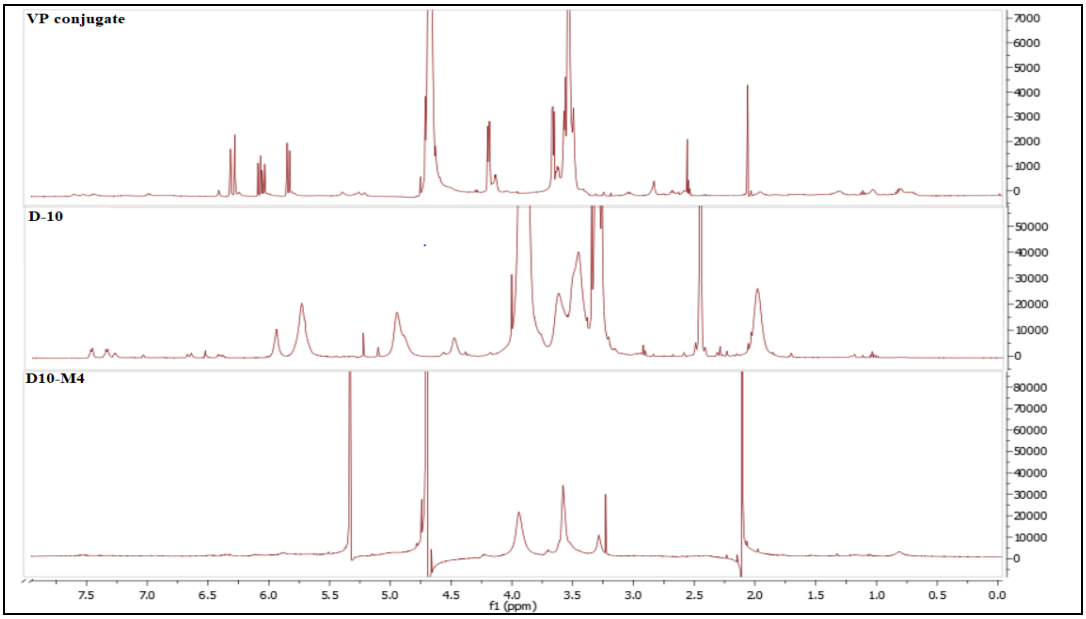

Figure D.2. The proton NMR spectrum of D10-M4 conjugate

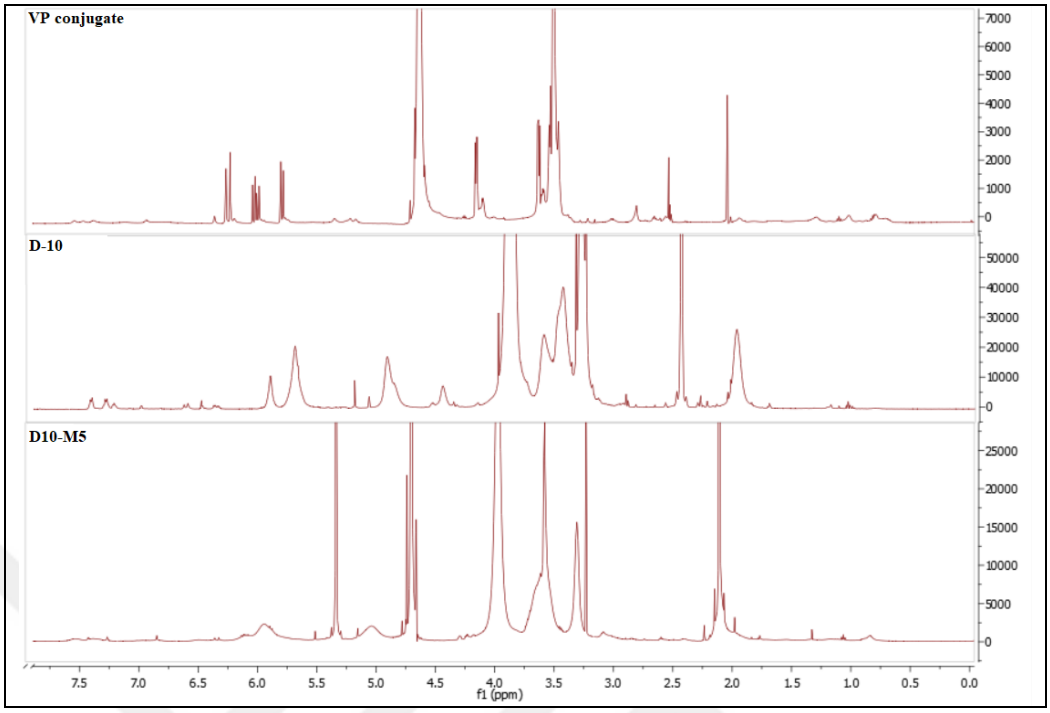

Figure D.3. The proton NMR spectrum of D10-M5 conjugate

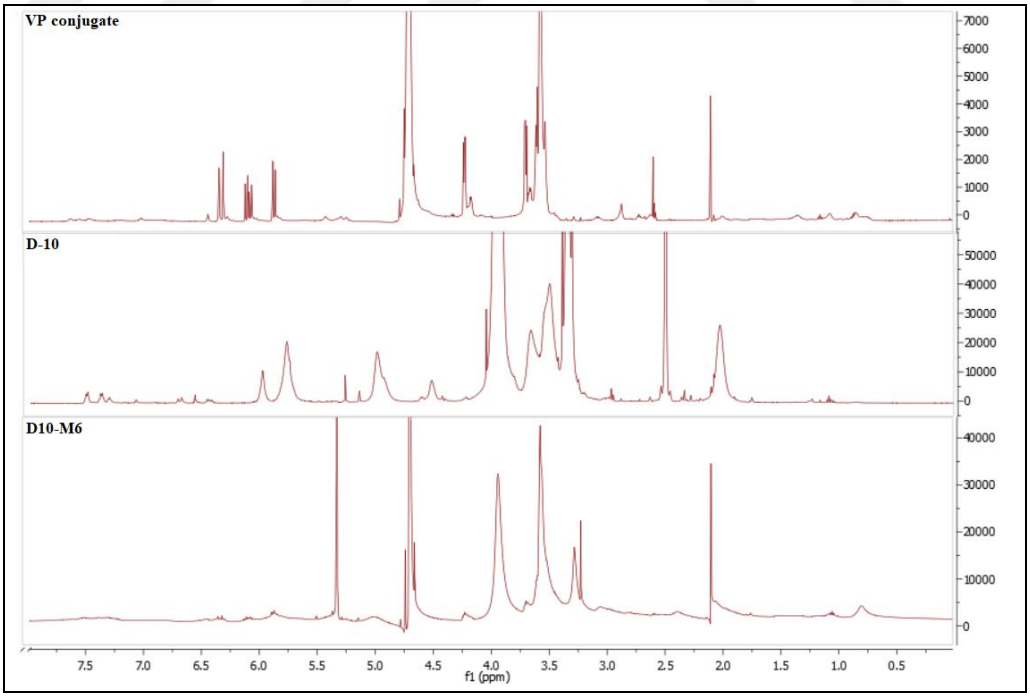

Figure D.4. The proton NMR spectrum of D10-M6 conjugate

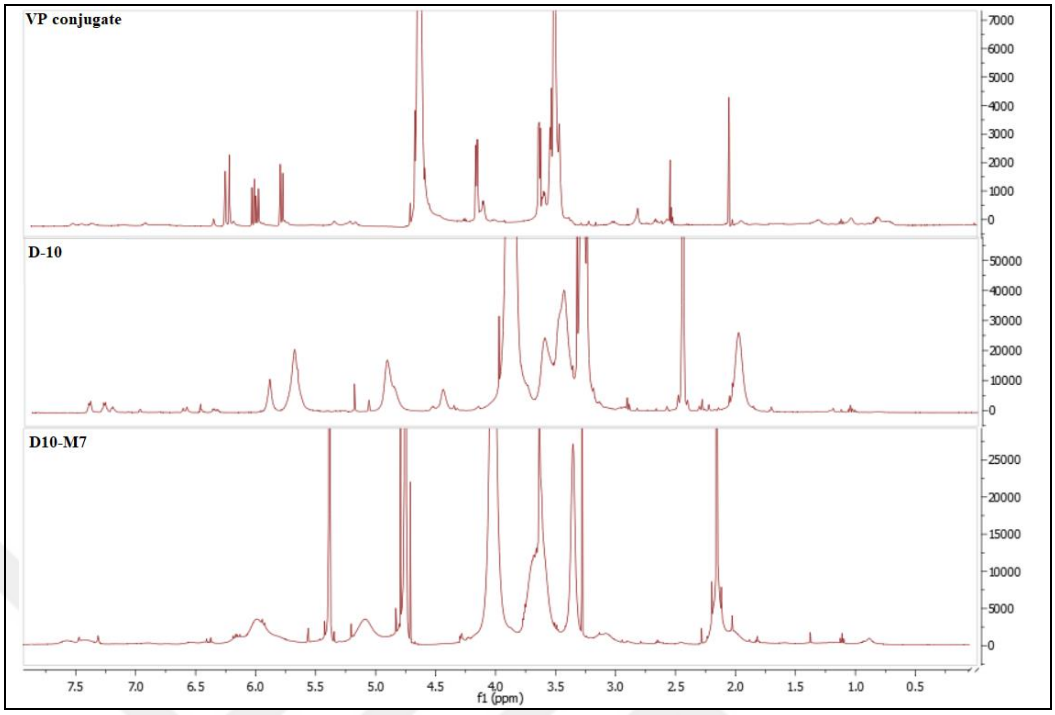

Figure D.5. The proton NMR spectrum of D10-M7 conjugate

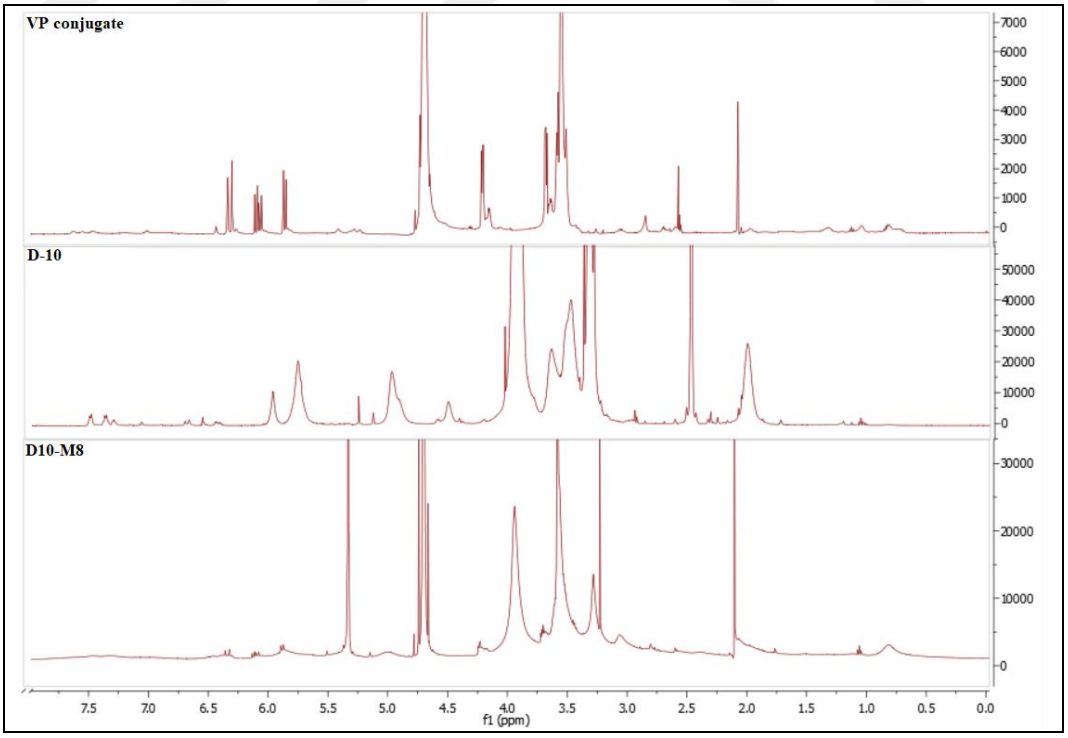

Figure D.6. The proton NMR spectrum of D10-M8 conjugate

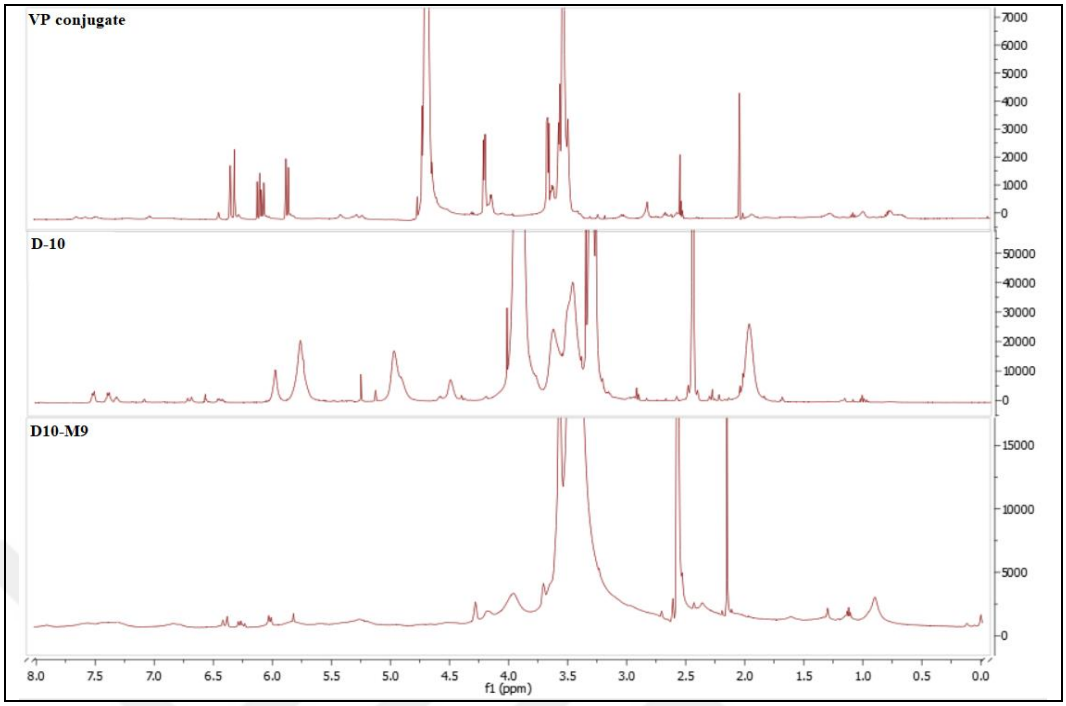

Figure D.7. The proton NMR spectrum of D10-M9 conjugate

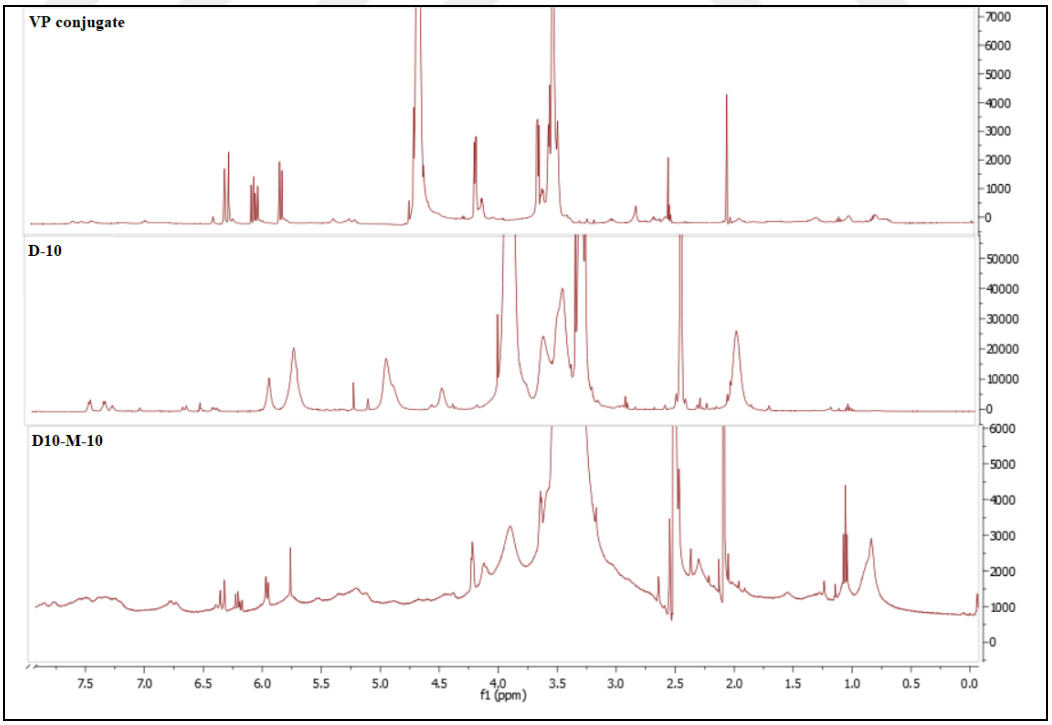

Figure D.8. The proton NMR spectrum of D10-M10 conjugate

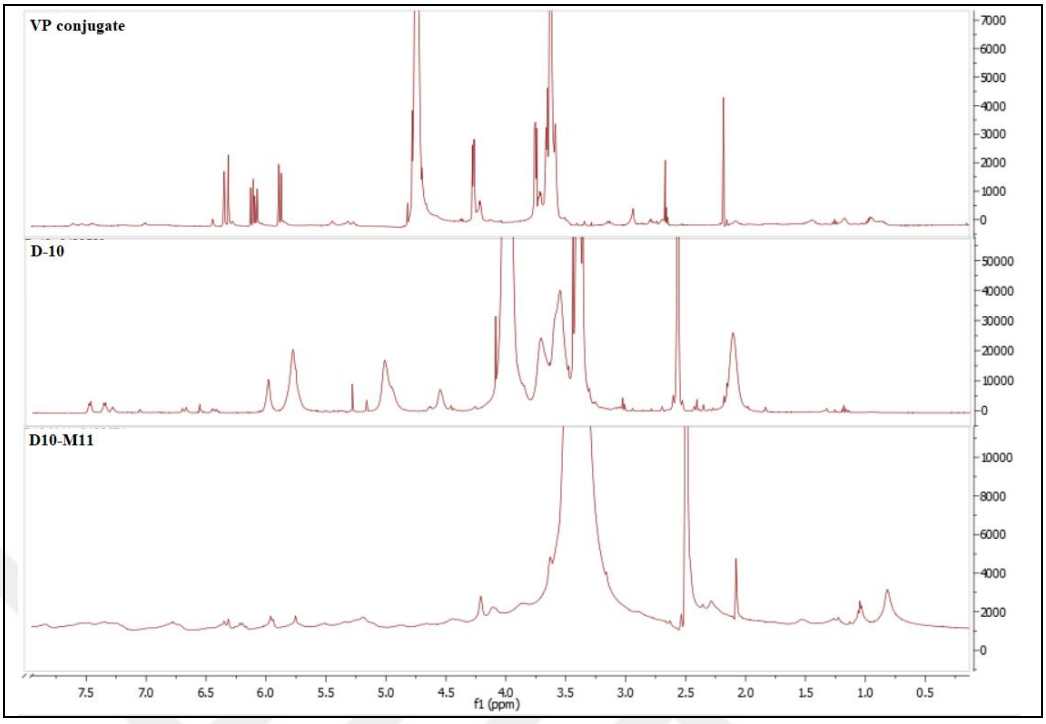

Figure D.9. The proton NMR spectrum of D10-M11 conjugate

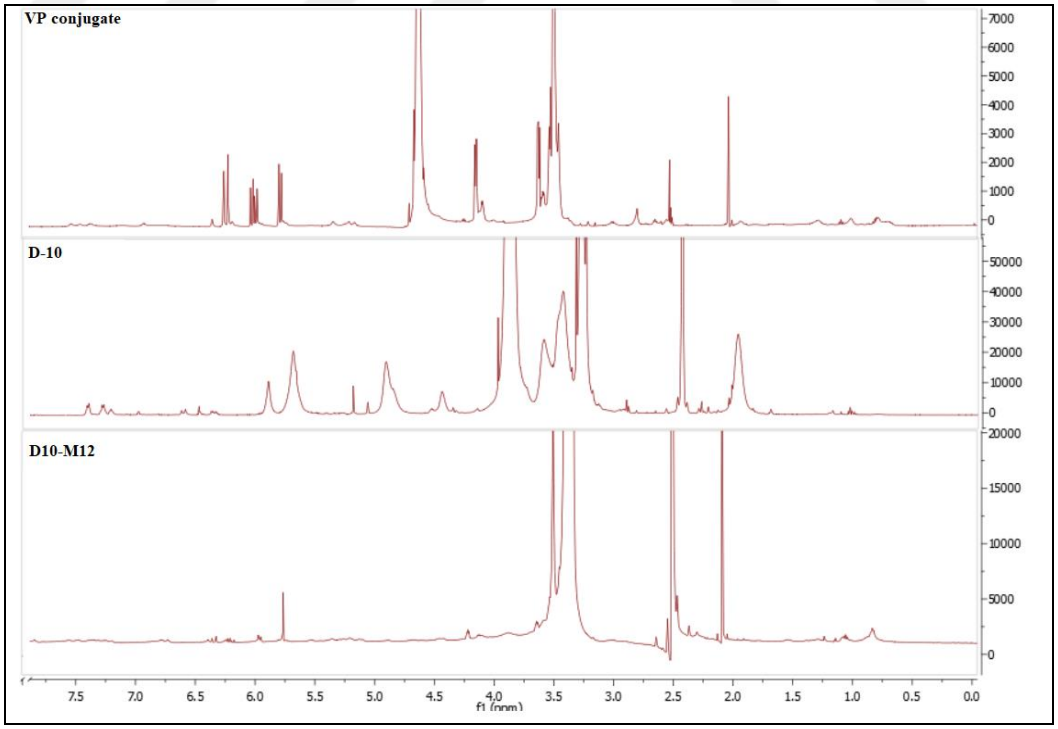

Figure D.10. The proton NMR spectrum of D10-M12 conjugate

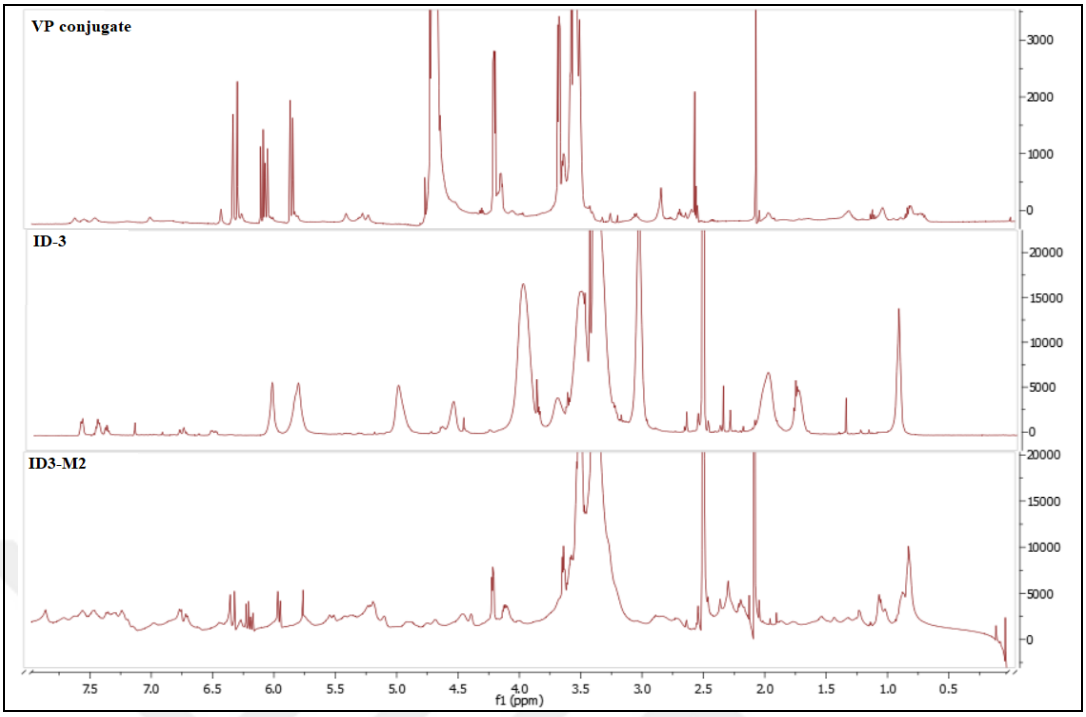

Figure D.11. The proton NMR spectrum of ID3-M2 conjugate

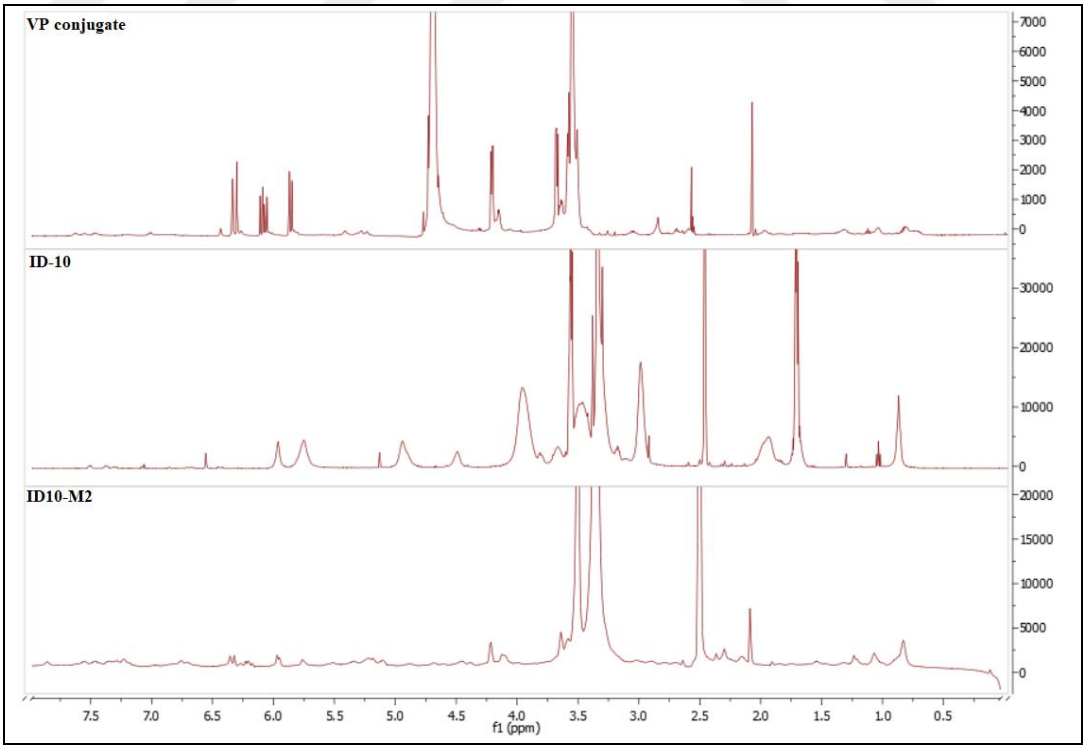

Figure D.12. The proton NMR spectrum of ID10-M2 conjugate

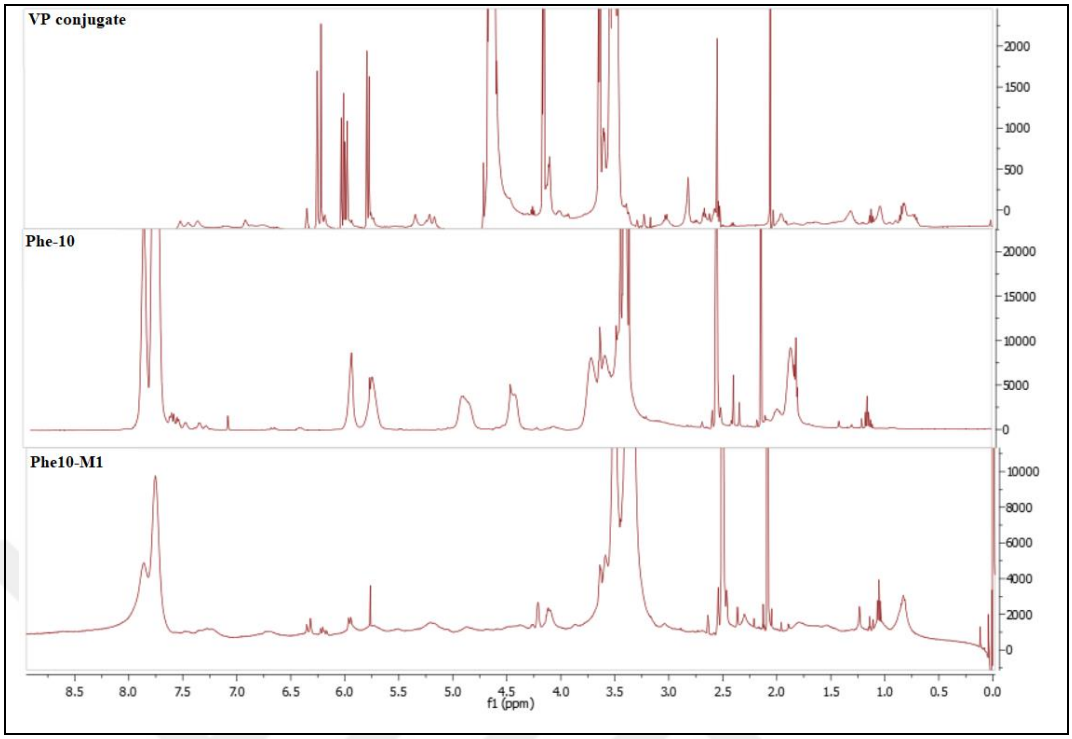

Figure D.13. The proton NMR spectrum of Phe10-M1 conjugate

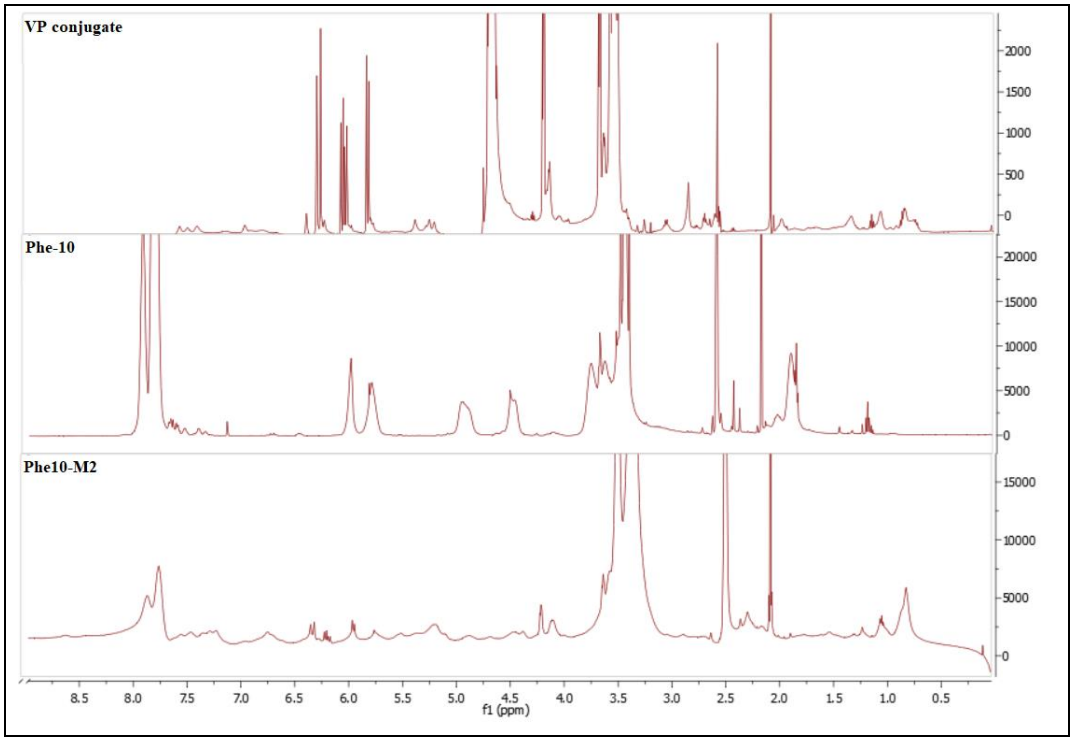

Figure D.14. The proton NMR spectrum of Phe10-M2 conjugate

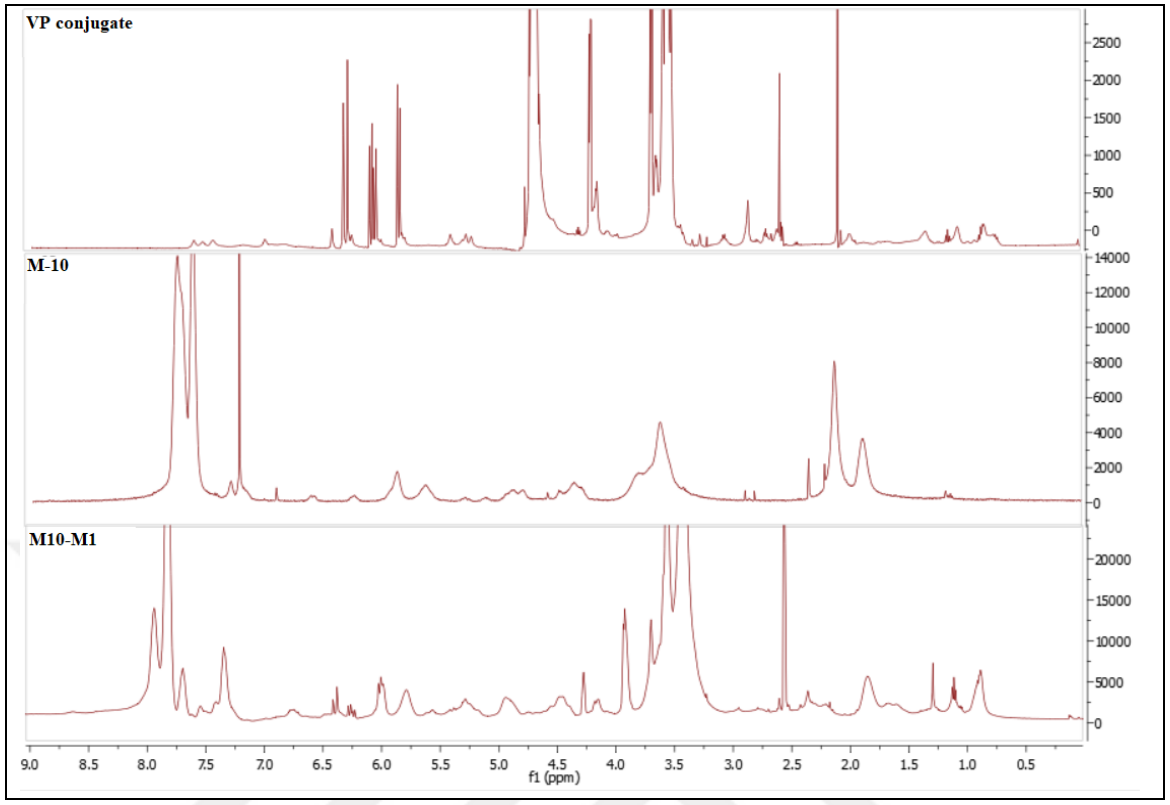

Figure D.15. The proton NMR spectrum of M10-M1 conjugate